Multimeric Protein Structures of African Horsesickness Virus and their use as Antigen Delivery Systems

By

Francois Frederick Maree

A thesis submitted to the University of Pretoria in the Faculty of Biological and Agricultural Sciences (Department of Genetics) in fulfilment of the requirements for the degree of

PHILOSOPHY DOCTORALES

Pretoria

August 2000

Ek gee nuwe krag aan dié wat moeg is,
Ek maak die moedelose weer vol moed. *Jer. 31:25*

Hy gee die vermoeides krag,
Hy versterk dié wat nie meer kan nie.
Selfs jongmanne word moeg en raak afgemat,
selfs manne in hulle fleur struikel en val,
maar dié wat op die Here vertrou,
kry nuwe krag.
Hulle vlieg met arendsvlerke,
hulle hardloop en word nie moeg nie,
hulle loop en raak nie afgemat nie. *Jes. 40:29-31*

Die Here my God gee vir my krag.
Hy maak my voete soos dié van 'n ribbok
op hoë plekke laat Hy my veilig loop. *Hab. 3:19*

ACKNOWLEDGEMENTS

I wish to express my sincere appreciation to the following people:

Prof **H. Huismans** for his guidance, support and criticism throughout this study.

Dr **A.A. van Dijk** and Mrs **S. Maree** for their support, advice and assistance in the collaboration on the particle project.

Dr **Wade-Evans** for her idea on the use of VP7 crystals as peptide delivery systems.

The staff and students in the Department Genetics, especially Mrs **P. de Waal** and Mrs **M. van Niekerk**, for their useful discussions and encouragement.

Dr **J. Theron** and Dr **F. Joubert** for their interest and useful advice. Dr **F. Joubert** also assists with software regarding computer modelling.

Mr **A.N. Hall** and Mr **C. van der Merwe** for their assistance with electron microscopy.

The Foundation of Research and Development (**FRD**) for providing the necessary funding.

My wife, **Sonja Maree**, also a molecular biologist, for her valuable input in this study and continuing support and encouragement as well as proof reading of this document.

My family who supported me on so many levels throughout this study.

CONTENTS

CHAPTER 4

EFFECT OF SITE DIRECTED INSERTION MUTATION ON THE CRYSTAL FORMATION, SOLUBILITY AND CLP FORMATION OF AHSV-9 VP7

LIST OF FIGURES

SUMMARY

African horsesickness virus (AHSV), a member of the genus *Orbivirus* in the family *Reoviridae*, is the aetiological agent of African horsesickness, a highly infectious non-contagious disease of equines. The AHSV virion is composed of seven structural proteins organised into a double layered capsid, which encloses ten double-stranded RNA segments. The double stranded (ds) RNA genome of AHSV encodes, in addition to the seven structural proteins, at least three non-structural proteins (NS1 to NS3). The assembly of viral proteins in AHSV-infected cells results in at least three characteristic particulate structures. The first of these structures are the complete virions and viral cores. Empty virions or particles that simulate the virion surface can be produced synthetically by the co-expression of various combinations of AHSV structural genes in insect cells. Apart from the core particles and complete virions, there are two additional structures observed in AHSV-infected cells. Unique virus-specified tubular structures, composed of NS1, are observed in the cytoplasm of all orbivirus-infected cells. The second structure, distinctive hexagonal crystals, is unique to AHSV and is composed entirely of VP7, the major core protein. The assembly of all these particles can be produced synthetically when expressed individually in an insect cell expression system. The aim of this investigation was first of all to investigate the structure and assembly of these structures and secondly to evaluate their use as vehicles for foreign immunogens.

The NS1 gene of AHSV-6 was cloned as a complete and full-length cDNA fragment from purified dsRNA genome segment 5 and the complete nucleotide sequence determined. The gene was found to be 1749 bp in length with one major open reading frame (ORF) of 1645 bp, encoding a protein comprising 548 amino acids. The 5' and 3' termini of the gene were found to contain the conserved terminal hexanucleotide sequences of AHSV RNA fragments, followed by inverted heptanucleotide repeats. The deduced amino acid sequence was analysed and found to define a hydrophobic protein of 63 kDa. Antigenic profile analysis indicated a hydrophilic domain with relative high antigenicity in the C-terminus of the protein. This represents a possible insertion site for immunogenic epitopes. The cloned NS1 gene of AHSV-6 was modified at the 5' and 3' terminal ends to facilitate expression of the gene. *In vitro* expression yielded a protein corresponding to the predicted size of NS1. The gene was also expressed in insect cells, using a recombinant baculovirus and yields of approximately 1.0mg NS1 protein/10^6 cells were obtained. Expression of NS1 in insect cells resulted in the intracellular formation of tubular structures with diameters of 23 ±2 nm. Biophysical analysis of the AHSV tubules suggests that they are more fragile and unstable than BTV NS1 tubules.

To gain more insight into the structure, assembly and the biochemical characteristics of AHSV cores and virions, a number of baculovirus multigene expression vectors have been developed and utilised to co-express various combinations of AHSV genes. Cells infected with a dual-recombinant baculovirus, expressing AHSV-9 VP3 and VP7 genes, contained high levels of VP7 and low levels of VP3. The simultaneous expression of the two proteins resulted in the spontaneous intracellular assembly of empty multimeric core-like particles (CLPs) with a diameter of approximately 72 nm. These particles structurally resembled authentic AHSV cores in size and appearance. The yield of CLP production was low as a result of the insolubility of VP7, which aggregates preferably into large hexagonal crystal as well as the low yield of VP3. The interaction of CLPs with either VP2 or VP5 was investigated by co-infection of the VP3 and

VP7 dual recombinant baculovirus with a VP2 or VP5 single recombinant baculovirus. Each of the outer capsid proteins interacted separately with CLPs. Co-expression of all four major structural proteins of AHSV, using two dual recombinant baculoviruses one expressing VP2 and VP3, the other VP5 and VP7, resulted in the spontaneous assembly of empty virus-like particles with a diameter of 82 nm. Although co-expression of the different combinations of AHSV proteins was obtained, the levels of expression were low. This low levels of the AHSV capsid proteins and the aggregation of VP7 downregulated the assembly process.

In order to investigate the possibility of the use of CLPs and VP7 crystals as particulate delivery systems, insertion analysis of VP7 was used to identify certain sequences in the VP7 protein that are not essential for the assembly of CLPs or trimer-trimer interactions in the crystals. Two insertion mutants of VP7 (mt177 and mt200) were constructed. In each case three unique restriction enzyme sites were introduced that coded for six amino acids. In mt177 these amino acids were added to the hydrophilic RGD loop at position 177 - 178 and for mt200 to amino acid 200 - 201. Both regions were located in the top domain of VP7. Insertion mt177 increased the solubility of VP7, but did not abrogate trimerisation and CLP formation with VP3. The yield of mutant CLPs was significantly higher than the normal CLPs, possibly due to the increased solubility and availability of VP7 trimers. Evidence about the size of an insert that can be accommodated by VP7 was provided by the insertion of a 101 amino acid region of VP2, containing a previously identified immunodominant region of VP2. The two chimeric VP7/TrVP2 proteins were investigated for their ability to form crystal structures and CLPs. The chimeric proteins did not produce the typical hexagonal crystal structure, but rather small ball-like structures.

This investigation yielded valuable information regarding the structure and assembly of AHSV tubules, CLPs and VLPs. These findings also have practical value, since the multimeric structures can be utilised as delivery systems for immunogens, like the AHSV VP2 immunodominant epitopes.

LIST OF ABBREVIATIONS

AcNPV	-	*Autographa californica* nuclear polyhedrosis virus
AHS	-	African horsesickness
AHSV	-	African horsesickness virus
AHSV-9	-	African horsesickness virus serotype 9
ATP	-	adenosine-5'-triphosphate
amp	-	ampicillin
BHK	-	Baby hamster kidney cells
bp	-	base pairs
BRDV	-	Broadhaven virus
BSA	-	bovine serum albumin
BT	-	bluetongue
BTV	-	bluetongue virus
°C	-	degrees Celcius
ca.	-	approximately
cDNA	-	complementary DNA
ccc	-	covalently closed circular
CF	-	complement fixation
Ci	-	Curie
CIP	-	calf intestinal alkaline phosphatase
CLP	-	core-like particle
cm^2	-	square centimetre
cpm	-	counts per minute
CsCl	-	cesium chloride
Da	-	dalton
ddH_2O	-	deionized distilled water
DEPC	-	deithylpyrocarbonate
dATP	-	2'-deoxyadenosine-5'-triphosphate
dCTP	-	2'-deoxycytidine-5'-triphosphate
dGTP	-	2'-deoxyguanosine-5'-triphosphate
dTTP	-	2'-deoxythymidine-5'-triphosphate
dNTP	-	deoxyribonucleoside-triphosphate
ddATP	-	2',3'-dideoxyadenosine-5'-triphosphate
ddCTP	-	2',3'-dideoxycytidine-5'-triphosphate
ddGTP	-	2',3'-dideoxyguanosine-5'-triphosphate
ddTTP	-	2',3'-dideoxythymidine-5'-triphosphate
DNA	-	deoxyribonucleic acid
DNAse	-	Deoxyribonuclease
ds	-	double stranded
DTT	-	1,4-dithiothreitol
EDTA	-	ethylenediaminetetra-acetic acid
EEV	-	Equine encephalosis virus
e.g.	-	*exempli gratia* (for example)

EHDV	-	epizootic haemorrhagic disease virus
et al.	-	*et alia* (and others)
etc.	-	*et cetera* (and so forth)
EtBr	-	ethidium bromide
FCS	-	fetal calf serum
FESEM	-	Field emission scanning electron microscopy
Fig.	-	figure
g	-	gram / gravitational acceleration
GTP	-	guanosine-5'-triphosphate
GST	-	glutathione S-transferase
h	-	hour
HPRI	-	human placental RNase inhibitor
IgA	-	immunoglobulin class A
IgG	-	immunoglobulin class G
IPTG	-	isopropyl-β-D-thiogalactopyranoside
kb	-	kilobase pairs
kDa/kd	-	kilodalton
l	-	litre
LB	-	Luria-Bertani
log	-	logarithmic
M	-	Molar
mA	-	milliampere
MAb	-	monoclonal antibody
MCS	-	multiple cloning site
mg	-	milligram
min	-	minute
ml	-	millilitre
mM	-	millimolar
mmol	-	millimole
MMOH	-	methylmercuric hdroxide
MOI	-	multiplicity of infection
M_r	-	molecular weight
mRNA	-	messenger ribonucleic acid
m/v	-	mass per volume
N	-	normal
NaAc	-	sodium acetate
nm	-	nanometre
NS	-	non-structural
OD_{550}	-	optical density at 550 nm
OD_{260}	-	optical density at 260 nm
ORF	-	open reading frame
OVI	-	Onderstepoort Veterinary Institute

PAGE	-	polyacrylamide gel electrophoresis
PCR	-	polymerase chain reaction
p.f.u.	-	plaque forming units
p.i.	-	post infection
pmol	-	picomole
PSB	-	protein solvent buffer
PSV	-	perdesiekte virus
RE	-	restriction endonuclease
RNA	-	ribonucleic acid
RNAse	-	ribonuclease
rpm	-	revolutions per minute
RT	-	room temperature
RT-PCR	-	reverse transcriptase PCR
s	-	second
S	-	Svedberg unit
S 1-10	-	segment 1-10
SDS	-	sodium dodecyl sulphate
SEM	-	Scanning electron microscopy
Sf9	-	*Spodoptera frugiperda*
ss	-	single stranded
T_{An}	-	annealing temperatures
TC	-	transcriptase complex
TdT	-	terminal deoxynucleotidyl transferase
TEM	-	Transmission electron microscopy
TEMED	-	N,N,N',N'-tetramethylethylenediamine
tet	-	tetracycline hydrochloride
TFB	-	Transformation buffer
Tris	-	Tris(hydroxymethyl)-aminomethane
TSB	-	Transformation suspension buffer
TSBG	-	Transformation suspension buffer with glucose
TX-100	-	Triton X-100
U	-	units
µCi	-	microcurie
µg	-	microgram
µl	-	microlitre
UV	-	ultraviolet
V	-	volts
v	-	volume
VIB	-	viral inclusion body
VLP	-	virus-like particle
VP	-	viral protein
VT	-	viral tubules

v/v	-	volume per volume
W	-	watt
X-gal	-	5-bromo-4-chloro-3-indolyl-β-D-galactopyranoside

CHAPTER ONE

LITERATURE REVIEW

1.1. INTRODUCTION

African horsesickness (AHS) is an infectious, but non-contagious arthropod transmitted viral disease that causes high mortality in horses. In naive populations of horses, the mortality rate commonly exceeds 80% and may be as high as 95%. The disease occurs regularly in most countries in sub-Saharan Africa and is regarded as one of the major scourges of the continent. AHS was already present in South Africa in natural reservoir hosts at the time the first Dutch settlers had arrived in the Cape of Good Hope in 1652. Following the import of horses, major epidemics occurred approximately every 20 to 30 years prior to 1953. Although the virus has not maintained itself outside sub-Saharan Africa, occasional outbreaks have occurred in Egypt, Saudi-Arabia, Afghanistan, Pakistan, India as well as the relative recent outbreak in the western Mediterranean region (Coetzer & Erasmus, 1994).

The first pioneering research on AHS was carried out by Sir Arnold Theiler. He established that the causative agent was filterable through Chamberland filters capable of retaining bacteria. He concluded that the agent was a virus capable of inducing a variety of anthrax and biliary symptoms in horses. His research also indicated that immunologically distinct strains of AHS virus (AHSV) may exist, seeing as immunity acquired against one strain of virus did not always protect the horse when challenged against infection by a heterologous strain (reviewed in Coetzer & Erasmus, 1994). Theiler, together with Pitchford-Watkins, ascertained in 1903 that AHSV may be transmitted by biting insects, thereby establishing the groundwork for future research on the epidemiology, pathogenesis and aetiology of the AHS. In 1921, Theiler reported the first detailed descriptions of the clinical signs and gross lesions produced by infection with AHSV (Theiler, 1921). Alexander and co-workers were the first to succeed in propagating AHSV in chicken embryos and demonstrated that the virus became attenuated during passage in embryonated eggs (Coetzer & Erasmus, 1994). Characterisation of the AHSV structure and morphology occurred in the 1960s and early 1970s (Els & Verwoerd, 1969; Verwoerd, 1969; Oellerman *et al.*, 1970; Verwoerd *et al.*, 1970). During this time, AHSV was classified as belonging to the *Orbivirus* genus within the family *Reoviridae* (Oellerman *et al.*, 1970; Bremer, 1976).

The prevention of AHS and the spread of AHSV are of great economic importance to all affected countries, as serious losses in both the horse racing and show jumping industry could rapidly occur

if the disease is not kept under control. The export and transfer of horses from affected countries is also severely hampered due to stringent quarantine regulations, affecting the competitiveness of the horses (Coetzer & Erasmus, 1994). South Africa is considered enzootic for AHS, therefore several European and other countries prohibit the import of horses from countries like South Africa where the disease occurs or where active vaccination with live attenuated virus takes place. In order to control the disease, the following guidelines have been developed: restriction of animal movement during outbreaks of the disease, quarantine and slaughter of infected animals, control of the insect vectors (biting midges of the *Culicoides* species) and vaccination. These exercises are costly and labour intensive.

1.2. CLASSIFICATION OF THE GENUS *ORBIVIRUS*

The aetiological agent of AHS is *African horsesickness virus* (AHSV), a member of the genus *Orbivirus* in the family *Reoviridae* (Oellerman *et al.*, 1970; Bremer, 1976; Verwoerd *et al.*, 1979; Holmes, 1991; Murphy *et al.*, 1995). Other genera in the family include *Orthoreovirus*, *Rotavirus*, *Aquareovirus*, *Phytoreovirus*, *Fijivirus*, *Cypovirus, Coltivirus*, and *Oryzavirus* (Matthews, 1982; Francki *et al.*, 1991; Gorman, 1992; Calisher & Mertens, 1998). The main characteristic of viruses within the *Reoviridae* family is that they possess a segmented, linear, double-stranded (ds) RNA genome (generally 10-12 segments) enclosed within a double-layered capsid, and contain no lipoprotein (Matthews, 1982; Joklik, 1983; Francki *et al.*, 1991; Gorman, 1992). The virus particle or virion is icosahedral with a diameter of 60-80 nm.

AHSV is similar in morphology, physicochemical attributes and immunological properties to other orbiviruses such as *Epizootic haemorrhagic disease virus* (EHDV) of deer, *Equine encephalosis virus* (EEV) and *Bluetongue virus* (BTV), with BTV being the prototype virus of this genus (Verwoerd *et al.*, 1979; Spence *et al.*, 1984). Orbiviruses share similar physicochemical properties and morphological appearance (Borden *et al.*, 1971), although no common antigen has been found. Like the rotaviruses and orthoreoviruses, the orbiviruses are non-enveloped viruses with a diameter of 60-80 nm. Orbiviruses can be distinguished morphologically from the other genera by the presence of a characteristic diffuse outer capsid layer, surrounding the inner nucleocapsid which consists of 32 ring-shaped capsomeres arranged with icosahedral symmetry (Verwoerd *et al.*, 1969; Borden *et al.*, 1971; Murphy *et al.*, 1971; Murphy *et al.*, 1995). The genus name is derived from this characteristic ring-like structure of the capsomeres (*orbis* being Latin for ring or circle). Unlike other members of the family *Reoviridae*, orbiviruses replicate in insects and in vertebrates (Gorman & Taylor, 1985), show a greater sensitivity to lipid solvents and detergents, and virus-infectivity is lost in mild acid conditions (Murphy *et al.*, 1971; Gorman, 1978; Verwoerd *et al.*, 1979). The physicochemical properties of orbiviruses versus those of other *Reoviridae* are summarised in table 1.

Members of the genus *Orbivirus* are subdivided into serogroups based on the cross-reactivity of their antigens in complement fixation (CF), immunodiffusion and immunofluorescence tests (Gorman, 1979 & 1983; Knudson & Monath, 1990; Brown *et al*., 1991). Orbiviruses are grouped into 19 distinct serological groups (Gorman & Taylor, 1985; Calisher & Mertens, 1998)(as summarised in Table 2). Serotypes within a serogroup are recognised by distinct reactivities in serum neutralisation tests (Gorman, 1979,1983 & 1985) and with gene reassortment sometimes occurring between the closely related viruses (Samal *et al.*, 1987; Brown *et al.*, 1988; Cowley *et al.*, 1989). The serotypes are determined by the outer capsid proteins, VP2 and VP5, encoded by genome segments 2 and 5, respectively (Calisher & Mertens, 1998). To date, nine different serotypes of AHSV have been identified with little, if any, cross-neutralisation between them (McIntosh *et al.*, 1958; Howell *et al.*, 1962; Calisher & Mertens, 1998).

The genus *Orbivirus* includes a number of viruses, which are of agricultural importance such as the pathogenic agents of native and domestic animals. Important pathogens include AHSV, *Bluetongue virus* (BTV), *Epizootic haemorrhagic disease virus* (EHDV) of deer and *Equine encephalosis virus* (EEV) (Verwoerd *et al.*, 1979; Spence *et al.*, 1984). Other than BTV, the prototype virus of this genus, a limited amount of information is available on other orbiviruses such as AHSV. Due to similarities between BTV and AHSV many of the features of BTV can be extrapolated to AHSV. This chapter therefore mainly reviews findings with BTV, although relevant studies on AHSV are also included.

TABLE 1: *Physicochemical properties of orbivirus versus orthoreoviruses (Adopted from Verwoerd et al., 1979; Gorman, 1978; Knudson & Monath, 1990).*

Property	**Orbivirus**	**Orthoreovirus**
Acid sensitivity	Sensitive	Resistant
Detergent lability	Partial instability	Stable
Temperature stability	Reasonable thermostable	Thermostable
Portal of entry	Skin via vector	Oral
Tissue tropism	Hemopoietic	Intestinal tract
Invertebrate vector	Culicoid midges, mosquitoes, phlebotomines and ticks	none

TABLE 2: *Viruses of the genus Orbivirus by serogroups, serotypes, hosts and principle vector (Gorman & Taylor, 1985; Gorman, 1992; Holmes et al., 1995; Calisher & Mertens, 1998).*

Species	Number of Serotypes	Host species	Principle vector
Bluetongue virus (BTV)	24	Cattle, sheep, goats, camels, ruminants	*Culicoides*
African horsesickness virus (AHSV)	9	Equids, camels, dogs, cattle, sheep, elephants	*Culicoides*
Epizootic haemorrhagic disease (EHDV)	10	Cattle, sheep, deer, etc.	*Culicoides*
Equine encephalosis virus (EEV)	7	Equids	*Culicoides*
Eubanangee virus (EUBV)	4	Unknown (isolated from insects)	*Culicoides* and mosquitoes
Palyam virus (PALV)	11	Cattle, sheep	*Culicoides* and mosquitoes
Umatilla virus (UMAV)	4	Birds	mosquitoes
Changuinola virus (CGLV)	12	Humans, rodents, sloths	Plebotomine flies and mosquitoes
Corriparta virus (CORV)	3	Humans, rodents	Culicine mosquitoes
Chenuda virus (CNUV)	7	Seabirds	Ticks
Chobar Gorge virus (CGV)	2	Bats	Ticks
Ieri virus (IERIV)	3	Birds	*Culex* mosquitoes
Great island virus (GIV)	36	Seabirds, rodents, humans	Ticks
Lebombo virus (LEBV)	1	Humans, rodents	Culicine mosquitoes
Orungo virus (ORUV)	4	Humans, camels, cattle, monkeys	Culicine mosquitoes
Warrego virus (WARV)	3	Marsupials	*Culicoides* and mosquitoes
Wallal virus (WALV)	3	Marsupials	*Culicoides*
Wongorr virus (WGRV)	8	Cattle, macropods	*Culicoides* and mosquitoes
Wad Medani virus (WMV)	2	Domestic animals	Ticks
St Croix River virus (SCRV)	1	Unknown (deer)	Ticks
Unassigned viruses within species	8		

1.3. EPIDEMIOLOGY, TRANSMISSION AND PATHOGENESIS OF AHSV

AHS is endemic to sub-Saharan Africa (Howel, 1963; Brown & Dardiri, 1990; House *et al.*, 1992a; Mellor, 1994), although severe epizootics have occurred in North Africa, the Middle East, Asia and in certain European countries (McIntosh, 1958; Mellor, 1993, Coetzer & Erasmus, 1994). The most recent outbreaks have been reported in Spain, Portugal, Morocco and Saudi Arabia (House *et al.*, 1992a; Rodriguez *et al.*, 1992; Mellor, 1993; House *et al.*, 1994). Problems with clinical recognition, pathological diagnosis and vector traffic make AHSV a very difficult disease to control and eradicate.

AHS manifests as an acute, peracute, subacute or mild infectious disease of *Equidae* (Tomori *et al.*, 1992; Mellor, 1993). The virus is transmitted between susceptible animals, in the same manner as BTV, by biting haematophagous midges of the *Culicoides* species (Du Toit, 1944; Tomori *et al.*, 1992). *Culicoides imicola* is the major AHSV vector and is also responsible for the spread of BTV (Mellor & Boorman, 1995). An adult *Culicoides* midge becomes infective 8 days after feeding on a viraemic animal and stays infective until death. Mosquitoes of the Aedes, Anopheles and Culex species, as well as the brown dog tick, *Rhipicephalus sanguineous*, have also been reported to transmit the disease to susceptible animals (Lubroth, 1988 & 1992; Tomori *et al.*, 1992; Mellor, 1993). However, their role in natural transmission is not known. The distribution of AHS is limited by the requirement for susceptible vertebrate hosts and the relevant arthropod vectors and usually disappears abruptly after the first frost (Mellor, 1993).

AHSV infects horses, ponies, mules, donkeys and zebras and occasionally dogs (Brown & Dardiri, 1990; Mellor, 1994; Barnard, 1997). Horses are the most susceptible and the mortality rates commonly exceed 80%. In a naive population, AHS can kill up to 95% of horses that become infected. Mules and donkeys appear to have some natural resistance to development of severe disease and zebras are even less susceptible and may serve as inapparent carriers (Davies & Otieno, 1977; Erasmus *et al.*, 1978; Brown & Dardiri, 1990; Lubroth, 1992; Mellor, 1994; Barnard *et al.*, 1994). Various natural reservoirs exist for the disease and antibodies against AHSV have been identified in camels, goats, sheep, cattle, buffalo dogs and elephants (Tomori *et al.*, 1992; Lubroth, 1992; Barnard *et al.*, 1995). A single incident of AHSV infection in humans by neuroadapted strains of the virus (serotypes 1 and 6) has also been reported (Swanepoel *et al.*, 1992) and was confirmed by inoculation of primates with these strains (Taylor *et al.*, 1992).

Initial virus replication occurs in the lymph nodes of the animal following transfer by the bite of an infected insect. After this initial replication phase, viruses are transported throughout the body where they replicate in certain endothelial cells (Lubroth, 1992; Laegreid *et al.*, 1992). In

experimentally induced cases, the incubation period varies between five and seven days, but the more virulent the virus and the larger the infectious dose, the shorter the incubation period becomes (Burrage & Laegreid, 1994; Coetzer & Erasmus, 1994). Classically, the disease presents in four clinopathological syndromes in horses, which vary in the organs affected, the severity of the lesions, the time of onset of clinical signs and mortality rates. These 4 forms, in decreasing order of severity, are the pulmonary or peracute form, the cardio-pulmonary or mixed form, the cardiac of subacute form and mild horsesickness fever (Theiler, 1921; Erasmus, 1973; Brown & Dardiri, 1990; Mellor, 1993).

The clinical form of disease expressed has been shown to be a function of the viral virulence phenotype (Laegreid *et al.*, 1993; Burrage & Laegreid, 1994), but is not serotype dependent. According to Laegreid (1996) the immune status of horses can also influence the form of disease they develop. McIntosh (1958) stated that differentiation of disease forms appears to be related to variation in susceptibility as a result of immunity from previous infection, rather than any viral property. Erasmus (1973) reiterated this view, suggesting that the cardiac and febrile forms of AHS are usually observed in immune animals that have been infected with a heterologous virus type. However, the existence of attenuated vaccine strains of each AHSV serotype, demonstrates that viral properties can also dramatically affect the severity of the disease caused by each of the AHSV serotypes, even in serologically naive animals. Laegreid *et al.* (1993) clearly indicated that in naive horses, the clinical form of the disease is a property of the specific AHSV strain used as inoculum. Recent studies (Laegreid *et al.*, 1995; O'Hara *et al.*, 1998) of AHSV reassortants between virulent and avirulent strains have indicated that genome segments 2, 6 and 10, coding for the outer capsid proteins VP2 and VP5 and the non-structural, cell release protein NS3, appeared to have a controlling influence on the determination of AHSV virulence.

1.4. THE MOLECULAR BIOLOGY AND STRUCTURE OF ORBIVIRUSES

Profound research on the molecular biology of AHSV started in the 1980s, therefore little information is available on the structure-function relationships of genes and gene products of AHSV. However, electron microscopic and physicochemical studies indicate a close morphological and biochemical relationship to BTV, the prototype orbivirus (Oellerman *et al.*, 1970; Bremer, 1976), which has been thoroughly investigated. Much of the current knowledge and research on AHSV is based on findings from studies of BTV.

1.4.1. The virion

Orbiviruses are complex non-enveloped viruses with seven structural proteins, organised into two concentric protein shells, which displays icosahedral symmetry. Early electron microscopic studies found the diameter of most orbiviruses to be 65-70 nm (Verwoerd *et al.*, 1972; Martin & Zweerink, 1972; Verwoerd *et al.*, 1979). The icosahedral virion consists of an indistinct outer layer, which surrounds a well-defined core-particle (Els & Verwoerd, 1969; Oellerman *et al.*, 1970; Verwoerd *et al.*, 1972), which encloses ten double-stranded RNA genome segments each encoding at least one viral protein (Oellerman *et al.*, 1970; Huismans, 1979; Grubman & Lewis, 1992) (*Figure 1.1*). Three morphologically distinct particles have been identified in orbivirus-infected cells, including virions, cores and subcores. These particles have been obtained, for BTV, by stepwise removal of specific structural proteins of the virus (Huismans *et al.*, 1987; Huismans & Van Dijk, 1990). More recently, core-like and virus-like particles (CLPs & VLPs) containing no nucleic acid have been produced by the co-expression of the relevant BTV and AHSV structural proteins in expression systems (Belyaev & Roy, 1993; Maree *et al.*, 1998). In the fully infectious BTV virion, the outer capsid is composed of two major proteins (VP2 and VP5), while the core particle consists of two major [VP3(T2)and VP7(T13)] and three minor [VP1(Pol), VP4(Cap) and VP6(Hel)] components, as well as the dsRNA genome (Verwoerd *et al.*, 1972; Martin *et al.*, 1973; Els 1973; Bremer, 1976; Huismans, 1979; Huismans *et al.*, 1979).

The purified BTV virion is composed of approximately 88% protein and 12% dsRNA (Huismans & Van Dijk, 1990; Knudson & Monath, 1990; Mertens *et al.*, 1996)) and contains no single-stranded adenine rich component as is found in reovirus (Martinez-Torrecuadrada, 1994), while the core contains approximately 19.5% RNA (Stuart *et al.*, 1998; Grimes *et al.*, 1998; Gouet, *et al.*, 1999). Infectivity for mammalian cells is lost if one of the proteins in the outer capsid layer is removed (Verwoerd *et al.*, 1979), although purified core particles do have infectivity, comparable to that of intact virus, for cells of the insect vector species (*Culicoides*) (Mertens *et al.*, 1996). The virions are stable in lipid solvents (Verwoerd *et al.*, 1979) and non-ionic detergents such as Triton X-100 (Huismans *et al.*, 1987; Mertens *et al.*, 1987). The virus is sensitive to acid pH, but is relatively resistant to pH changes on the alkaline side of neutrality (Stanley, 1967; Huismans *et al.*, 1987). Recent advances in cryo-electron microscopy and computer imaging, as well as the ability to synthesise BTV core-like particles (CLPs) and virus-like particles (VLPs) using baculovirus expression vectors, have greatly facilitated an understanding of the BTV virion architecture. The structure and assembly of the virus is discussed in more detail in section 2.3.

1.4.2. The viral genome

BTV was the first orbivirus found to contain a dsRNA genome (Verwoerd, 1969). Since then the segmented dsRNA nature of the genome of other orbiviruses have also been confirmed (Oellerman, 1970; Huismans *et al.*, 1979; Knudson *et al.*, 1984; Kusari and Roy, 1986). The genomic RNA contains 5' terminal Cap 1 structures (7mGpppG$^{(2\text{-}Om)}$...). The genome of AHSV is, like that of BTV, composed of 10 linear ds RNA segments that are packaged in exactly equimolar ratios, one of each segment per particle. There is no evidence for short ssRNA oligonucleotides in intact virions. The size of the ten AHSV genome segments range from 3965 to 756 bp, with a total size and total molecular weight of 19.5 kbp and 13,2 x 10^6 dalton, respectively (Vreede & Huismans, 1997). This is in agreement with the BTV genome of 19.2 kbp and total M_r of 13.1 x 10^6 (Fukusho *et al.*, 1989; Roy, 1992). The molecular weights reported for the ds RNA genomes of orbiviruses vary between 11.0 x 10^6 and 13 x 10^6 (Verwoerd *et al.*, 1972; Schnagl and Holmes, 1975; Bremer, 1976; Gorman *et al.*, 1977), which does not differ significantly from the molecular weights of the other members of the *Reoviridae* family (18.8 kbp for rotavirus-A). The RNA segments are numbered 1 to 10 in order of their migration on agarose gels or polyacrylamide gel electrophoresis (PAGE) and are grouped as three size classes, namely large, medium and small segments (designated L1-3, M4-6 and S7-10). When compared with other members of the *Reoviridae* family, the orbiviral dsRNA profiles are distinctive (*Figure 1.1*).

Each viral segment encodes at least one viral-specific polypeptide (Huismans, 1979; Gorman *et al.*, 1981; Grubman *et al.*, 1983; Mertens *et al.*, 1984; Pedley *et al.*, 1988; Van Dijk & Huismans, 1988), but the smallest segment encodes two related proteins from in-phase AUG initiation codons (Van Staden & Huismans, 1991; Van Staden *et al.*, 1995). The largest genome segment, S1, is 3965 bp long, while segment 10 is only 756 bp in length. All ten genome segments share some common features. These include, like other viruses belonging to the family *Reoviridae*, 5' and 3' terminally conserved hexanucleotides on each segment which are species specific (Rao *et al.*, 1983). In the AHSV species the terminal sequences are not always identical and may not be conserved in all 10 segments. In addition, the orbiviruses, contain an inverted repeat, adjacent to the conserved termini, which differs in sequence for each segment (Roy, 1989; Nel *et al.*, 1990; Moss *et al.*, 1992; Mizukoshi *et al.*, 1993). It is postulated that these termini are involved in sorting and assembly of the genome during viral replication, due to their ability to form mRNA secondary structures (Anzola *et al.*, 1987).

The coding assignment of each dsRNA segment is summarised in *Figure 1.1* and the protein characteristics and functions are summarised in Table 3. The structural proteins VP1(Pol), 2, 3(T2), 4(Cap) and 7(T13) are encoded by segments 1, 2, 3, 4 and 7 respectively and VP5 and 6(Hel) by segments 6 and 9 (O'Hara *et al.*, 1993; Burroughs *et al.*, 1994). Segments 5 and 8 encode the non-

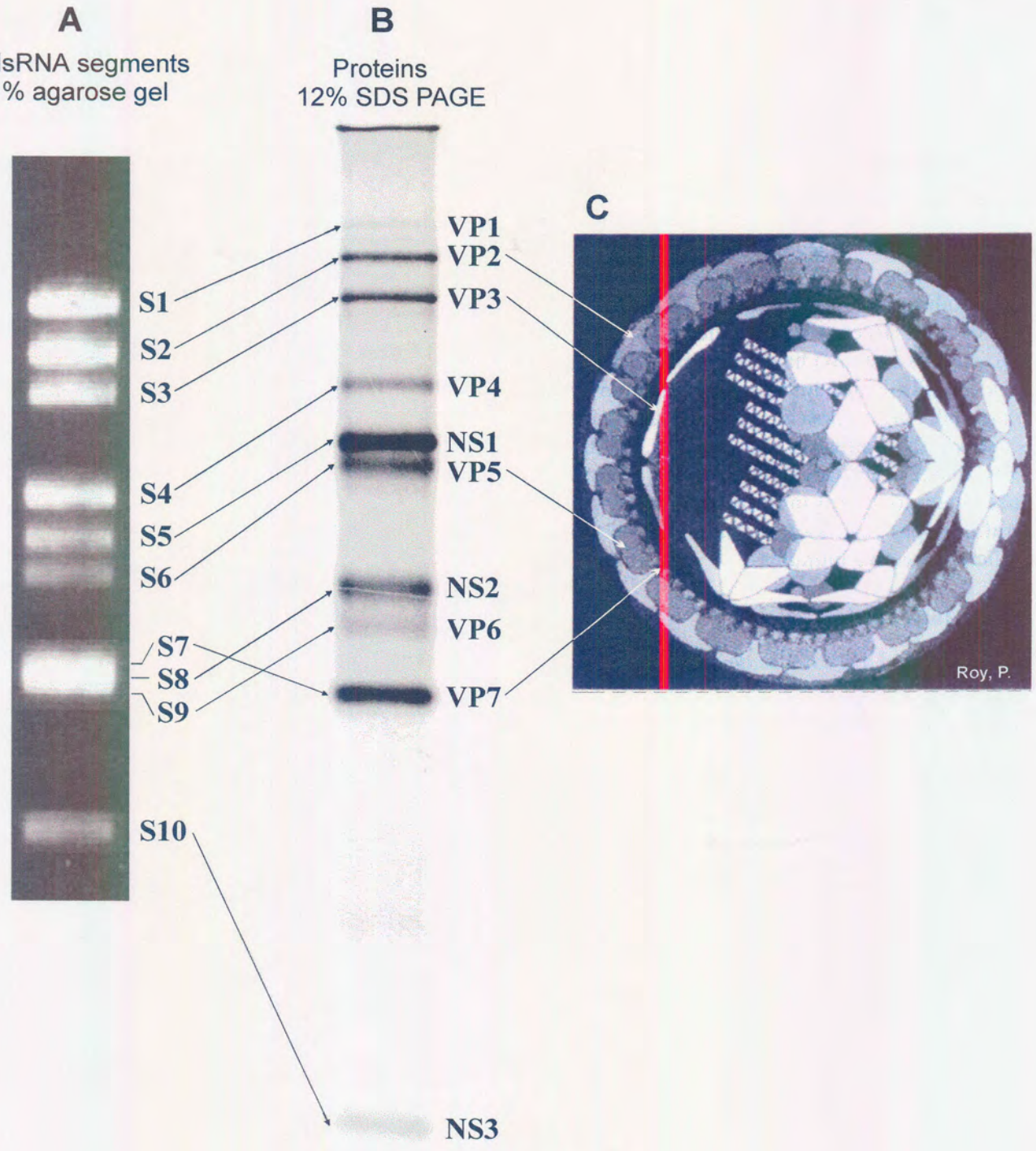

Figure 1.1: AHSV coding assignments: (a) represent gel electrophoretic separation of the dsRNA segments of AHSV-6 (adopted from Grant Napier, 1999), (b) represents the size distribution of the polypeptides, encoded by the ten dsRNA segments, on polyacrylamide gel (kindly provided by Michelle van Niekerk) and (c) a schematic diagram of the orbivirus particle (adopted from Roy, 1998). All orbiviruses share some basic morphological features with BTV, the prototype orbivirus.

TABLE 3: *AHSV genome segments and their encoded proteins. Adopted from Vreede & Huismans (1997).*

dsRNA Segm.	Sero	Segment length (bp)	Protein	Number of aa (Predicted M_r)	Function or property
1	9	3965	VP1	1305 (150 292)	Minor core structural protein; possible dsRNA-dependent ssRNA polymerase
2	3	3221	VP2	1057 (123 063)	Outer capsid structural protein; cell attachment protein; serotype specific; highly variable; protective neutralising antigen; determination of virulence
3	4	2795	VP3	905 (103 269)	Major core structural protein; subcore scaffold layer; T=2 symmetry; serogroup specific; control overall size and organisation of capsid structure
4	4	1978	VP4	642 (75 826)	Minor core structural protein; dimer; transmethylase 1 and 2; Guanylyltransferase activity (capping enzyme)
5	9	1566	VP5	505 (56 771)	Outer capsid structural protein; intra-serogroup variable gene; glycosylated; trimer
6	9	1748	NS1	548 (63 377)	Major non-structural protein; virus-specified tubular structures
7	9	1167	VP7	349 (37 916)	Major core surface structural protein; ring-like capsomeres; trimers with T=13 symmetry; serogroup specific; involved in cell entry
8	9	1166	NS2	365 (41 193)	Non-structural protein; binds ss RNA; phosphorylated; viral inclusion body (VIBs) matrix protein
9	3	1169	VP6	369 (38 464)	Minor core structural protein; possible helicase and NTPase; binds ss & ds RNA
10	9	756	NS3/ NS3A	217 (23 659) 206 (22 481)	Minor non-structural proteins; glycosylated; membrane associated; involved in virus release; determination of virulence

structural proteins NS1 and NS2, while segment 10 encodes NS3 and NS3A. These coding assignments and protein nomenclature are consistent with that of BTV.

The recent availability of nucleotide sequences of a number of different orbiviruses has made detailed comparisons of genes and gene products possible. In addition, the information to enables analysis of the structural, functional and biochemical characteristics of the proteins in an attempt to understand the molecular biology of the orbiviruses. To date, the nucleotide sequences of all ten AHSV RNA segments have been determined, although not all from the same serotype (Table 3) and their similarities with the analogous genes of BTV or other orbiviruses documented by Roy *et al.*, 1991; Van Staden and Huismans, 1991; Van Staden *et al.*, 1991; Iwata *et al.*, 1992; Mizukoshi *et al.*, 1992.

1.4.3. The viral proteins

The structural proteins are numbered VP1(Pol) to VP7(T13) in order of decreasing size based on electrophoretic migration in polyacrylamide gels, and the non-structural proteins are designated NS1, NS2 and NS3 (Huismans & Van Dijk, 1990)(*Figure 1.1*).

1.4.3.1. The outer capsid polypeptides

The outer capsid proteins, VP2 and VP5, are encoded by RNA segments 2 and 6 respectively in the case of BTV, EHDV and AHSV (Mertens *et al.*, 1984; Bremer *et al.*, 1990; Le Blois *et al.*, 1991; Iwata *et al.*, 1992; Vreede & Huismans, 1994). Of the two outer capsid proteins, VP2 is the more variable and exhibits the least conservation between serotypes and serogroups (Fukusho *et al.*, 1987; Iwata *et al.*, 1992; Vreede & Huismans, 1994). VP2 is the main determinant of serotype-specificity (Huismans & Erasmus, 1981; Kahlon *et al.*, 1983; Roy *et al.*, 1990), is the viral haemagglutinin (Cowley & Gorman, 1987; French *et al.*, 1990; Loudon *et al.*, 1991) and elicit neutralising antibodies (Mecham *et al.*, 1986; Huismans *et al.*, 1987a; Inumaru & Roy, 1987; White & Eaton, 1990; Huismans & Van Dijk, 1990; Burrage *et al.*, 1993). The protein is also associated with cell adsorption in virus infection since removal of VP2 eliminates binding of the virus to the cell (Eaton & Crameri, 1989; Van Dijk & Huismans, 1990).

VP2 seems to be a candidate for the production of a subunit vaccine. VP2 has been shown to induce serotype-specific neutralising antibodies in sheep, where BTV VP2 inoculates were protected against subsequent challenge with the corresponding virus serotype (Huismans & Erasmus, 1981; Kahlon *et al.*, 1983; Huismans *et al.*, 1987; Inumaru & Roy, 1987; Gould *et al.*, 1988; White & Eaton, 1990). In AHSV it was also found that VP2 has neutralising properties, as the neutralising epitopes of AHSV-4 were found to be located on VP2 (Burrage *et al.*, 1993). Martinez-

Torrecuadrada *et al.* (1994) have shown that antibodies raised to AHSV VP2 in rabbits neutralise a virulent strain of AHSV-4, while Stone-Marchat *et al.* (1996) have also shown that horses can be immunised using a vaccinia-based construct containing the VP2 gene of AHSV-4. The regions on VP2 that are involved in eliciting protective immune response and determination of serotype specificity have not as yet been fully identified.

In contrast to VP2, very little is known about the function of VP5 other than its close association with the core particle. The protein is less variable than VP2 (Gould & Pritchard, 1988; Wade-Evans *et al.*, 1988; Oldfield *et al.*, 1991; Iwata *et al.*, 1991; Du Plessis & Nel, 1997), suggesting a high degree of restraint on the structural variability of VP5. Although the protein is located in the outer capsid, it is mostly unexposed (Hewat *et al.*, 1992; Iwata *et al.*, 1992) and it does not appear to have any distinct neutralising ability on its own (Mertens *et al.*, 1989). Antisera raised against baculovirus expressed VP5 protein do not demonstrate any neutralising activity *in vitro* (Marshall & Roy, 1990), however there are indications that VP5, in the combination with VP2, does contribute to the induction of neutralising antibodies in BTV infection (Mertens *et al.*, 1989; Roy *et al.*, 1990). It is postulated that although VP5 does not elicit neutralising antibodies on its own, it may enhance the immune response to VP2 by affecting the conformation of VP2, and hence the serological properties of the protein (Roy *et al.*, 1996). It is thought that these proteins stabilise each other in the virion outer capsid during virus morphogenesis (Liu *et al.*, 1992).

1.4.3.2 The core polypeptides

In virus-infected cells, BT or AHS virions are converted to core particles with the removal of the outer capsid proteins, VP2 and VP5 (Verwoerd *et al.*, 1972; Els 1973). The diameter of the core particles is in the order of 73 nm (Mertens *et al.*, 1987; Hewat *et al.*, 1992; Grimes *et al.*, 1998). The VP3(T2) and VP7(T13) proteins are the two major components of the core (Verwoerd & Huismans, 1972, Huismans *et al.*, 1987), VP7(T13) being the more abundant. These two major core proteins are highly conserved between orbiviruses (Iwata *et al.*, 1992; Roy *et al.*, 1991; Bremer *et al.*, 1994) and are associated in a highly ordered, three-dimensional manner in the core, resulting in icosahedral symmetry (Grimes *et al.*, 1998).

VP7(T13), the major serogroup-specific antigen, is located on the surface of the core (Huismans & Erasmus, 1981; Oldfield *et al.*, 1990; Chuma *et al.*, 1992). This major component of the core is highly conserved among serotypes (Bremer *et al.*, 1990; Roy *et al.*, 1991; Iwata *et al.*, 1992). It is an extremely hydrophobic protein, and has been demonstrated to form trimers (Kowalik *et al.*, 1990; Roy, 1992). This hydrophobicity is particularly evident in AHSV VP7(T13) where it self-assembles to form disc shaped, hexagonal crystalline structures of various sizes (Chuma *et al.*, 1992; Burroughs *et al.*, 1994). Such crystals have so far never been observed for other orbiviruses. AHSV-4

VP7(T13) has an estimated M_r of 38.0 kDa (Roy *et al.*, 1991). The VP7(T13) protein of different orbiviruses contains a conserved Arg-Gly-Asp (RGD) tripeptide motif, which has been suggested as a possible determinant for attachment of VP7(T13) to a cell surface receptor. This tripeptide is present on almost all known orbivirus VP7(T13) proteins and is situated in an exposed position of the viral core (Eaton *et al.*, 1991; Grimes *et al.*, 1995).

The third largest RNA segment encodes VP3(T2), which is, like VP7(T13), also hydrophobic in nature and contains group specific antigens (Iwata *et al.*, 1992; Inummaru *et al.*, 1987). Sequence data previously obtained for the VP3(T2) gene and deduced protein of BTV, AHSV and EHDV, indicates that of the four major capsid proteins, VP3(T2) is the most conserved (Iwata *et al.*, 1992). VP3(T2) plays an important role in the structural integrity of the virus core and has been proposed to form the protein scaffold on which the capsomers, of which VP7(T13) are the main component, are arranged (Huismans *et al.*, 1987a). AHSV-4 VP3(T2) is composed of 905 amino acids with a predicted size of 103.27 kDa (Iwata *et al.*, 1992) and the amino acid content and size is similar to the BTV and EHDV VP3(T2) proteins (Le Blois *et al.*, 1991). VP3(T2) has also been shown to have an affinity for ssRNA (Loudon & Roy, 1992).

Inside the subcore, VP3(T2) acts as a framework for interaction with the minor proteins VP1(Pol), VP4(Cap) and VP6(Hel). The core particles are transcritionally active and are associated with an RNA-dependent RNA polymerase activity (Van Dijk & Huismans, 1980; Verwoerd & Huismans, 1972). This enables the virus to synthesise mRNA from the virion dsRNA templates. Based on its size (M_r = 150 kDa), location and molar ratio (estimated at 10 molecules per virion) (Stuart *et al.*, 1998), VP1(Pol) is the prime candidate for the RNA polymerase. BTV VP1(Pol) has also shown homology with a vaccinia virus DNA-dependent RNA polymerase subunit (Roy *et al.*, 1988; Urakawa *et al.*, 1989; Vreede & Huismans, 1998), as well as several other prokaryotic and eukaryotic RNA polymerases (Kowalik et al., 1990; Kowalik & Li 1989). VP4(Cap) is thought to be responsible for the guanylyl transferase activity based on results indicating that VP4(Cap) of BTV binds GTP. VP4(Cap) has therefore been associated with mRNA 5' capping and methylation during transcription. (Le Blois *et al.*, 1992; Roy, 1992; Mizokoshi *et al.*, 1993; Ramadevi *et al.*, 1998). However, VP1(Pol) and VP4(Cap) are thought to have a co-operative enzymatic function in RNA transcription and/or RNA replication (Huismans & Van Dijk, 1990). It has recently been shown that BTV VP4(Cap) has nucleoside triphosphate phosphohydrolase activity with specific substrate preference, viz. GTP>ATP>UTP>CTP (Ramadevi & Roy, 1998) and has capping activity (Ramadevi *et al.*, 1998). The VP6(Hel) protein of BTV, is rich in charged amino acids and is reported to possess single and double stranded RNA binding properties (Roy *et al.*, 1990; Hayama & Li, 1994) and sequence analysis has revealed a motive common to several helicases (Roy, 1992; Turnbull *et al.*, 1996). Such an activity may be involved in unwinding the dsRNA prior to transcription and

replication. VP6(Hel) may also have a role in the encapsidation of the RNA (Roy, 1992). All three minor proteins are closely associated with the ten dsRNA segments.

1.4.3.3. The non-structural proteins

At least four non-structural viral proteins are synthesised in orbivirus-infected cells. NS1 and NS2 are both synthesised abundantly in orbivirus-infected cells, while only small amounts of NS3 and NS3a are produced (Bremer *et al.*, 1976; Huismans, 1979; Mertens *et al.*, 1984; Van Dijk & Huismans, 1988; Mecham & Dean, 1988; Whistler & Swanepoel, 1990; Grubman & Lewis, 1992; O'Hara *et al.*, 1993). Little is known about the roles of the non-structural proteins in orbivirus replication cycle, although it is believed that these proteins are involved in the process of viral morphogenesis, leading to viral assembly and release. The two major non-structural proteins (NS1 and NS2) coincide with the appearance of two virus specific structures, namely tubules and virus inclusion bodies (VIBs), which characterise the cytoplasm of cells infected with orbiviruses (Lecatsas, 1968; Cromack *et al.*, 1971; Murphy *et al.*, 1971; Huismans, 1979).

The synthesis of NS2 in orbivirus-infected cells coincides with the synthesis of granular viral inclusion bodies (Roy *et al.*, 1990; Roy, 1992). VIBs have both granular and fibrillar characteristics and are found throughout the cell, but predominantly in proximity to the nucleus (Eaton *et al.*, 1990). NS2 is the major component of the VIBs observed in BTV-infected cells (Eaton *et al.*, 1987; Thomas *et al.*, 1990; Brookes et al., 1993). In addition to NS2, these VIBs also contain ssRNA, dsRNA, NS1, structural proteins as well as both complete and incomplete viral particles (Eaton & Hyatt, 1988; Eaton *et al.*, 1990; Hyatt *et al.*, 1992; Brookes *et al.*, 1993). These observations have led to the recognition of these inclusion bodies as the sites in which the viral assembly process occurs. The NS2 protein of various orbiviruses has been reported to bind ssRNA (Huismans & Basson, 1983; Huismans *et al.*, 1987; Thomas *et al.*, 1990; Theron *et al.*, 1994; Uitenweerde *et al.*, 1995) and forms a complex in the presence of virus mRNA. It has been suggested that NS2 may play a role in the selection and condensation of the 10 viral ssRNA species into precursor subviral particles, prior to dsRNA synthesis. A distinctive feature of NS2 is that it is the only orbivirus-encoded phosphoprotein (Huismans & Basson, 1983; Huismans *et al.*, 1987; Devaney *et al.*, 1988; Theron *et al.*, 1994), but its significance in NS2 activity is unknown. The phosphorylation of NS2 seems to down regulate its ssRNA binding ability (Theron *et al.*, 1994).

The two smallest and closely related non-structural proteins NS3 and NS3A are synthesised in low abundance in orbivirus-infected cells (French *et al.*, 1989; Wu *et al.*, 1992; Van Staden *et al.*, 1995). NS3 and NS3A proteins are co-linear products encoded by the genome segment 10 and the two proteins are translated from different in-frame initiation codons (Mertens *et al.*, 1984; Lee & Roy, 1987; Van Dijk & Huismans, 1988; French *et al.*, 1989; Van Staden & Huismans, 1991; Wu *et al.*,

1992). Thus, it is possible that NS3A is essentially a truncated form of NS3. Both NS3 and NS3A are glycosylated, contain two conserved hydrophobic regions implicated to act as transmembrane regions and are involved in virus release from infected cells (Wu *et al.*, 1992; Hyatt *et al.*, 1991; Hyatt *et al.*, 1993; Van Staden *et al.*, 1995).

NS1:

Virus tubules are present in large numbers predominantly in peri- or juxtanuclear locations. These morphological structures are believed to be attached to the intermediate filament components of the cytoskeleton of the cell (Eaton *et al.*, 1987; Eaton *et al.*, 1988; Eaton & Hyatt, 1989) and are presumed to be involved in some way in the virus replication or transportation process. The unique virus-specified tubular structures observed in the cytoplasm of orbivirus-infected cells are composed of NS1 subunits (Murphy *et al.*, 1971; Huismans & Els, 1979, Urakawa & Roy 1988; Nel & Huismans., 1991). NS1 is encoded by RNA segment 5 (Urakawa & Roy, 1988; Nel & Huismans, 1991). This 64K non-structural protein is expressed more abundant than any other BTV protein in infected cells, comprising about 25% of the virus-specified protein complement (Huismans & Els, 1979). In a number of different orbiviruses investigated, it has been found that the ten different mRNA species are not synthesised in equimolar amounts. Instead, the dsRNA genome segment encoding NS1 is transcribed at a higher rate than the other genome segments (Huismans & Verwoerd, 1973; Venter *et al.*, 1991). During virus infection the NS1 protein is synthesised in large excess over the other viral proteins, but very little soluble NS1 is observed in the cytoplasm. The NS1 polymerises very rapidly into high molecular weight tubular structures (Huismans, 1979; Huismans & Bremer, 1979; Huismans & Els, 1979).

The NS1 proteins are highly ordered structures, most likely due to the large number of conserved cysteine residues and the major hydrophilic and hydrophobic regions scattered throughout the protein (Fukusho *et al.*, 1989, Nel *et al.*, 1990). Monastyrskaya *et al.* (1994) have revealed several conserved elements in the protein which are necessary for tubule formation, with cysteine residues at positions 337 and 240 and the conserved carboxyl- and amino-terminals shown to be of particular importance. The assembly of NS1 in tubular structures and the function of the tubules in orbivirus replication are unknown. Some virions and inner core particles have been observed in association with tubules in the cytoplasm of BTV-infected cells (Eaton *et al.*, 1988). Brookes *et al.* (1993) have reported that BTV NS1 is present within distinct areas of the VIBs and that these areas correlated with the presence of virus particles of different size dimensions (i.e. particles in different stages of morphogenesis), indicating that NS1 is involved in the early stages of morphogenesis. Another hypothesis is that NS1 may be involved as molecular chaperons to prevent the core particles from assembling before the correct minor core proteins [VP1(Pol), VP4(Cap) and VP6(Hel)] and/or genome have been incorporated (Hewat *et al.*, 1992).

1.5. ORBIVIRUS MORPHOGENESIS AND VIRAL REPLICATION

Following infection of a susceptible animal, BTV binds to a receptor in the cell membrane and the virus is believed to enter the cells by receptor-mediated endocytosis. No information is available on the nature of the cell receptor to which BTV or AHSV binds. The adsorption of the viruses to mammalian cells is mediated by VP2. Huismans *et al.* (1983) demonstrated that particles of BTV lacking VP2, but containing the other outer coat protein VP5, were unable to adsorb to cells in suspension. Although core particles of BTV bind to mammalian cells, they show very low infectivity, perhaps because these cells cannot correctly internalise them. The outer capsid proteins are therefore important for mammalian cell infection. Cores however, are highly infectious for cells of the insect vector *Culicoides variipennis,* which suggests infection of these cells, is via a different mechanism (Mertens *et al.*, 1996).

After endocytosis, the clathrin-coated vesicles are transported to the vicinity of the nucleus where they fuse to form endosomes (Eaton *et al.*, 1990), and BTV probably enters the cytoplasm by penetration of the endosomal membrane. Shortly after infection, BTV virions are converted to core particles, which have an active RNA transcriptase, and then to subcore particles, containing VP3(T2) and the three minor core proteins (Huismans *et al.* 1987). The conversion of BTV to core particles by removal of both outer capsid proteins VP2 and VP5 may occur in the endosome, which has an acid pH, or may be completed in the cytoplasm after partial uncoating in the endosome (Huismans *et al.*, 1987; Eaton *et al.*, 1990). Removal of both capsid proteins is required to activate the virion transcriptase and mRNA synthesis (Van Dijk & Huismans, 1980), by a currently unknown mechanism. The most likely explanation is that this modification allows free access of the NTPs to the genome and the unimpaired extrusion of the newly synthesised mRNA (Huismans & Van Dijk, 1990).

Because the dsRNA would trigger host defence mechanisms if released into the cytoplasm, dsRNA viruses retain their genomes within a protein core that contains active dsRNA-dependent ssRNA polymerases (transcriptases) and for most eukaryotic dsRNA viruses, capping enzymes (Furuichi *et al.*, 1975; Gouet *et al.*, 1999). The core particle is therefore vital for function, acting as an enzyme complex that produces full-length, capped mRNA copies simultaneously from each of the genome segments it contains.

Following release from endosomes, the transcriptionally active core particles in the cytoplasm rapidly become associated with a matrix and transcription of the viral RNA occurs. This matrix is similar in structure, but less dense, than that found in mature VIBs (Hyatt *et al.*, 1991; Fu *et al.*, 1995). Presumably the viral mRNA transcripts which are transported to the cytoplasm, and the

proteins which are translated from the viral mRNA, condense around the parental cores to form VIBs (Brookes *et al.*, 1993). The transcripts, function not only to encode proteins, but also as a template for production of minus strands to form the dsRNA genome segments encapsidated in the progeny virions (Furuichi *et al.*, 1976). The interaction of NS2 with ssRNA, the predominant form of RNA within VIBs, probably leads to the formation of VIBs. In addition to this selection and condensation of virus-specific mRNA, among cellular RNAs, there has to be a segment specific recognition, which allows the encapsidation of only one copy of each segment into the progeny virion (Hyatt *et al.*, 1988; Eaton *et al.*, 1990). It is not yet clear which proteins are involved in this process, and what the exact mechanisms of recognition and selection are. Structural proteins are translated on neighbouring ribosomes and condense predominantly at the VIB periphery to form subcores and cores. Once these structures have been formed, the ssRNA is copied to form dsRNA.

Proteins VP3(T2), VP5, VP7(T13), VP6(Hel) and NS1 have also been identified in association with VIBs. Core-like and subcore-like particles are observed within VIBs, although double-shelled virions are only detected at the periphery of VIBs (Huismans *et al.*, 1987; Gould *et al.*, 1988; Hyatt & Eaton, 1988; Brookes *et al*, 1993; Fu *et al.*, 1999). The NS1 protein is not uniformly distributed throughout the inclusion bodies, but is present within distinct areas which correlate with the presence of core and virus particles (Eaton *et al.*, 1988). This led Hyatt *et al.* (1992) to speculate that the addition of NS1 to the core particles may prevent transcription of virion RNA by progeny particles lacking their complement outer capsid proteins, hindering the release of immature virions. The addition of NS1, alternatively, may facilitate the efficient addition of VP2 and/or VP5 to the core particles at the periphery of the VIB. Since the outer capsid protein VP2 is only present on structurally complete viruses at the periphery of VIBs, it could be reasoned that virus particles are assembled at the edge of VIBs and are released into the cytoplasm upon addition of VP2 (Gould *et al.*, 1988; Brookes *et al.*, 1993).

Immediately following the addition of these outer coat proteins, the virus particles appear to associate with the intermediate filaments of the cells' cytoskeleton. VIBs, virus-specified tubules, and virus particles are associated with the cytoskeleton in BTV-infected cells (Eaton *et al.*, 1987). The viruses can be present singly, in groups, or in linear arrays (Eaton *et al.*, 1987). Both outer coat proteins VP2 and VP5 are required for stable virus-cytoskeleton interaction (Hyatt *et al.*, 1993). It is unlikely that the progeny viral particles of 65 nm in diameter can diffuse through the cytoplasm of a viable cell from the site of synthesis to the cell surface. The intermediate filaments enclosing the viral particles may provide a route whereby the progeny viruses are transported through the cell to the regions of the plasma or intracellular membranes containing NS3. These viruses are then released from the infected cells in a number of different ways. The virus might be spontaneously released as a result of cell death and subsequent cell lysis. Viruses are also released both as

enveloped particles by budding through the plasma membrane, and as non-enveloped particles by extrusion through the membrane (Hyatt *et al.*, 1989). It may also be postulated that BTV bound to the cytoskeleton filaments could facilitate interaction with NS3/NS3A manifested in smooth-surfaced vesicles, which may be transported to the plasma membrane. Here they may fuse with the membrane and facilitate the localised release of viruses from the cell (Hyatt *et al.*, 1993). The release of virions is accompanied by the removal or conformational change of VP2, resulted in the increased accessibility of VP7(T13) (Hyatt *et al.*, 1992). The following superinfection of BTV-infected cells by progeny virions effectively increases the multiplicity of infection and enhances the kinetics of BTV replication (Hyatt *et al.*, 1989).

1.6. ORBIVIRUS ASSEMBLY

BTV, the prototype orbivirus, has been the subject of extensive molecular and genetic studies, to resolve the mechanisms involve in the intracellular assembly process and the stoichiometry of the virus components in the morphogenic pathways of virions. Until recently, the mechanism by which an architecturally complex virus such as BTV is synthesised, the temporal order of virion construction and the specific interaction of the protein components to produce the icosahedral core particle were not known. Significant advances in orbivirus research have been made in recent years using gene manipulation techniques and by employing baculovirus expression system combined with 3D image reconstruction of virion particles and cores, and the X-ray crystallographic structure of certain proteins. Considerable insight has been gained into the intricate organisation and topography of the individual viral components.

1.6.1. Three-dimensional structure of orbivirus cores and core-like particles

The 3D structure of BTV core particles has been determined to a resolution of 3 nm using cryo-electron microscopy and computer image reconstruction (Hewat *et al.*, 1992; Prasad *et al.*, 1992). The particles are 69 nm (690 Å) in diameter and exhibit an icosahedral symmetry. The main morphological feature of the core particle is the presence of 32 distinct morphological units or capsomeres with a circular configuration which are organised with a triangulation number of 13 (Els & Verwoerd, 1969; Prasad *et al.*, 1992; Grimes *et al.*, 1997). The core structure is divided into two concentric layers of protein enclosing the inner core, containing the genomic dsRNA and minor proteins [VP1(Pol), VP4(Cap) and VP6(Hel)]. The surface layer of the core comprises rings or clusters of VP7(T13) trimers (Basak *et al.*, 1992; Grimes *et al.*, 1995) providing 260 prominent knob-like protrusions (780 VP7(T13) molecules; M_r 38K) organised into pentameric and hexameric units with channels in between. The 780 molecules of VP7(T13) are the main components of the virion

and are located in 260 trimeric units as a middle layer bridging the outer capsid and the inner subcore. These trimers are the basis from which the complex surface lattice of the viral core is built (Grimes *et al.*, 1995; Stuart *et al.*, 1998) and appear as triangular columns with distinct inner and outer domains, forming the attachment sites for the two surface proteins. The trimers extend outwards to a radius of 34.5 nm, from an inner radius of 30 nm. The VP7(T13) clusters are arranged so that there are 132 channels into the core interior, involving all the threefold axes and with dimensions approximately 70 Å deep and 80 Å wide at the surface. Some of the channels penetrate through the inner layer and are probably the pathways for metabolites to reach the sites of viral mRNA transcription and for the transportation of nascent mRNA molecules out of the cores to the cell cytoplasm to initiate viral protein synthesis. (French & Roy, 1990; French *et al.*, 1990; Le Blois *et al.*, 1991; Loudon and Roy, 1991; Hewat *et al.*, 1992; Liu *et al.*, 1992; Prasad *et al.*, 1992; Roy 1996).

The underlying scaffold (*Figure 1.2*) upon which the clusters of VP7(T13) trimers are arranged, consists of the second major core protein, VP3(T2) (M_r 100K). This inner layer or subcore particles has a radius of between 21.5 and 28 nm, is composed of 120 copies of VP3(T2) arranged as 12 closely bonded decamers, and has a relative smooth outer surface for attachment of the VP7(T13) trimers (Prasad *et al.*, 1992; Stuart, *et al.*, 1998). It appears that the VP3(T2) molecules form the building blocks for the icosahedral structure. The 120 molecules of VP3(T2) per virion are organised with a triangulation number of T = 2 (Burroughs *et al.*, 1995; Grimes *et al.*, 1998) forming two sets (A and B) of 60 subunits each (Grimes *et al.*, 1998). Thus, the ratio of VP7(T13) to VP3(T2) has been estimated to be 13:2 (Burroughs *et al.*, 1995) which is not in agreement with the earlier estimation of 13:1 (Hewat *et al.*, 1992). Until recently it was not understood, how 120 subunits of VP3(T2) molecules of dsRNA viruses, build an icosahedral shell, an ability that is inexplicable within the current conceptual framework (Caspar & Klug, 1962). The VP3(T2) subcore can retain its structure if the outer VP7(T13) core layer is lost (Huismans *et al.*, 1987; Loudon & Roy, 1991). Inside the subcore, VP3(T2) acts as a framework for interaction with the minor proteins VP1(Pol), VP4(Cap) and VP6(Hel). It is currently not known how the other viral components are organised with respect to each other, or to VP3(T2) and VP7(T13).

The images of baculovirus-synthesised CLPs revealed a similar icosahedral configuration (T = 13 for the surface layer) and an identical diameter (approximately 70 nm) to that of BTV cores. Some of the synthetic particles lacked the full complement of VP7(T13) and, as a consequence, the shapes of VP7(T13) trimers were more clear (Hewat *et al.*, 1992). The trimers have tripod-like shapes (8.0 nm in height) and each consists of an upper (outermost) and lower (innermost) domain. The shapes and structures of VP7(T13) trimers have recently been confirmed by X-ray crystallographic data. It appears that the VP3(T2) molecules are organised into unique plate-like structures and that

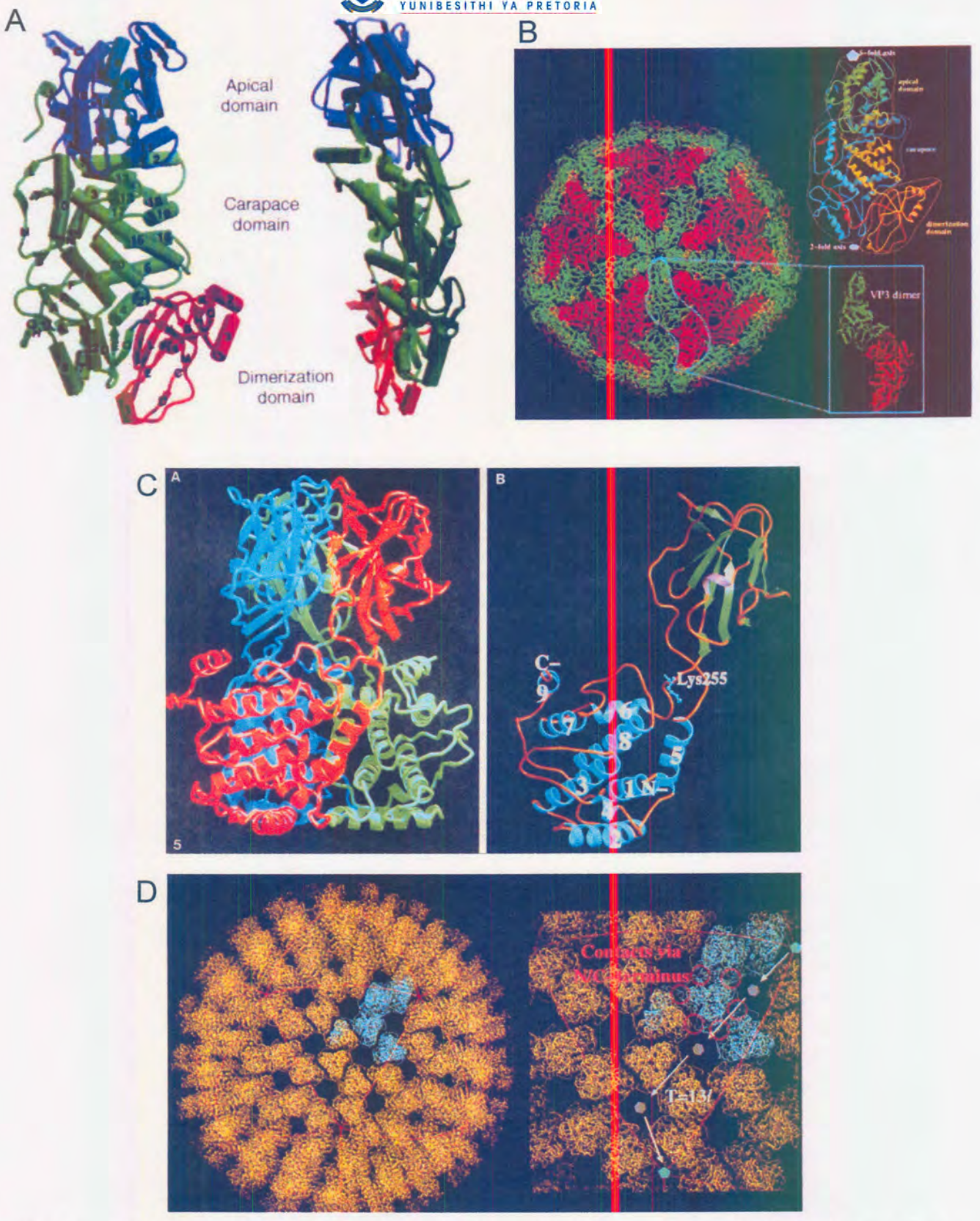

Figure 1.2: (A) A representation of the secondary structural elements of the BTV VP3(T2)B molecule (standard view left and orthogonal view right). The apical domain (residues 297-588) is colored blue, the carapace (residues 7-297, 588-698 and 855-901) is green and the dimerisation domain (residues 698-855) is red (adopted from Grimes *et al.*, 1998). (B) The architecture of the VP3 layer of the BTV core particle. The A and B subunits are shown in green and red respectively. The VP3(T2) is arrange as decamers (adopted from Stuart *et al.*, 1998). (C) A trimer and a monomer of orbivirus VP7 (T13). The protein from BTV is shown, although AHSV VP7 was found to be virtually indistinguishable (adopted from Basak *et al.*, 1997). (D) The architecture of the VP7 (T13) layer of BTV. The trimers are shown in yellow. The icosahedral 5-fold axes is joined by red lined. The right hand panel shows a close-up: The organisation of the trimers over the surface of the core is clarified in blue (adopted from Stuart *et al.*, 1998).

decamers of VP3(T2) form the building blocks for the icosahedral structure. The subcore-like particle is noticeably thicker around the fivefold axes. The disk-shaped configuration of VP3(T2) is clearly visible in the case of the CLP, due to the fact CLPs appear to be empty, so that the contrast between the inner shell and the interior is greater than that in virus-derived cores (Hewat *et al.*, 1992). In isolation, VP3(T2) will self-assemble to form particles (Moss & Nuttal, 1994; Grimes *et al.*, 1998), it binds RNA and the smallest viral particles containing RNA are VP3(T2) subcores (Loudon & Roy, 1991; Fu *et al.*, 1999). VP3(T2) seems to play a fundamental role in the early stages of BTV core assembly.

The ability of VP7(T13) trimers to interact with VP3(T2) subcores and form CLPs has been used to identify the regions of VP7(T13) necessary for the formation of particles. A number of site specific mutants and deletion or extension mutants of VP7(T13) were generated and expressed in the presence of VP3(T2). The data indicated that the intact carboxyl terminus of the BTV VP7(T13) molecule is critical for CLP formation and that the amino terminus can be modified by the addition of foreign sequences without compromising the ability to form the CLP structures. However, the CLPs that were formed were physically less stable than those formed with unmodified VP7(T13) and VP3(T2). A hydropathic plot of VP7(T13) indicates the existence of hydrophobic domains involving the last 50 amino acid residues of VP7(T13). Such domains may be involved in intra- and intermolecular interactions important for the function of the protein in particle formation (Belyaev & Roy, 1992; Le Blois & Roy, 1993).

1.6.2. Three-dimensional atomic structure of core particles

The BTV core represent the puzzle of how a large complex containing mismatched symmetry, can assemble. Results obtained by Grimes *et al.* (1998) and Gouet *et al.* (1999) from the X-ray crystallographic structure of *Bluetongue virus* core particles greatly facilitated an understanding on the assembly of bluetongue and other orbiviruses.

The outer layer of the core is built up of 13 icosahedrally independent copies of the VP7(T13) protein, in the form of four trimers in general positions and one situated with its molecular threefold axis aligned with the icosahedral threefold axis. These trimers are arranged on a pseudo-hexagonal T = 13 lattice and are all very similar to each other and are almost indistinguishable from the structure observed in monoclinic crystals of the recombinant VP7(T13) protein. Thus the T = 13 lattice follows the precept of classical quasi-equivalence (Caspar & Klug, 1962; Johnson & Speir, 1997) to an extraordinary degree. The quasi-equivalent trimers build up the core surface layer, such that they are arrange in pairs related by almost exact, local twofold symmetry axes, which are perpendicular to the surface of the virus particle. The contact regions between the different

VP7(T13) trimers are located in a thin band within the lower α-helical domain and are essentially 1-dimensional in nature. This region is formed in large part by a short hydrophobic α-helix, which seems to act as a hinge, about which the trimers are able to roll, as they pack down onto the surface of the inner core of VP3(T2). This rolling enables the same modes of interaction to be used between the different trimers, with minimal distortion (Grimes *et al.*, 1998; Stuart *et al.*, 1998).

VP3(T2) is highly unusual being organised into a structure that resembles a triangular wedge (13 Å by 75 Å) (*Figure 1.2*). The 901 amino acids of VP3(T2) are organised into a unique plate-like structure of three domains: an apical domain that sits nearest to the icosahedral 5-fold axis, a carapace domain which forms a rigid plate, and a dimerization domain that is involved in forming the quasi-2-fold interaction between the different molecules of VP3(T2). None of these domains resembles any other protein structure yet seen. The icosahedral building block of the subcore-like particle contains two molecules of VP3(T2) which perform different structural roles. The 60 VP3(T2)A subunits define the size of the subcore by forming a continuous scaffold of pairs, which span icosahedral 2-fold axes and link adjacent 5-fold axes. This scaffold is sealed off by the 60 VP3(T2)B subunits, which cluster at the icosahedral 3-fold axes to form triangular plugs. A tightly packed shell is achieved by distortion of these VP3(T2) molecular building blocks. The conformational changes occur primarily at two places in the VP3(T2) molecules: the dimerisation domain, which is intimately involved in forming the quasi-2-fold interface between molecules A and B, and between the carapace and apical domains. Ten of the VP3(T2) subunits are arranged around each five-fold axis, in the form of a decamer. The subtle rotation of the dimerisation domains is such that there is an almost exact local 2-fold relationship between dimerisation domains of the A and B molecules in adjacent decamers, so that an A molecule clips onto a B molecule in the neighbouring decamer and vice versa (Grimes *et al.*, 1998; Stuart *et al.*, 1998). This fragile internal scaffold carries the information that defines the size of the virus. This minimum possible conformation distortion, achieved by geometrical quasi-equivalent contacts, explains how 120 triangular subunits of VP3(T2) can build an icosahedral shell.

The VP7(T13) and VP3(T2) layers interact through flattish, predominantly hydrophobic surfaces (*Figure 1.2*). As a direct consequence of the symmetry mismatch between the two layers of the core there are 13 different sets of contacts between the 13 copies of VP7(T13) packed onto the 2 copies of VP3(T2) (*Figure 1.2*). Both VP3(T2)A and VP3(T2)B molecules make completely different yet extensive contacts with the various VP7(T13) molecules, whose structures are virtually identical to one another. The VP7(T13) subunits form themselves into trimers, which may then assemble into flat sheets of hexameric rings. The outer core layer is being completed by the crystallisation of 260 preformed essentially identical VP7(T13) trimers onto a fragile subcore made up of 120 molecules of VP3(T2). The driving force for this assembly of the outer core layer would be the interaction of

the relatively flat surfaces of each trimer with the underlying VP3(T2) layer, with the relative orientation of adjacent trimers of VP7(T13) determined by their side-to-side interaction with each other (Grimes *et al.*, 1998; Stuart *et al.*, 1998). This two dimensional crystallisation model avoids the need for conformational switching in the VP7(T13) layer, a mechanism used by less complex viruses for controlled capsid assembly (Liddington *et al.*, 1991; Johnson & Speir, 1997).

1.6.3. X-ray crystallographic structure of VP7(T13) trimers

The atomic structure of both AHSV and BTV VP7(T13) has recently been resolved to a 2.3 Å resolution (Grimes *et al.*, 1995; Basak *et al.*, 1996) and was found to be very similar. VP7(T13) has a unique molecular architecture not seen previously among viral proteins. The X-ray crystallographic structure of BTV VP7(T13) (*Figure 1.2*) has revealed that the three molecules of VP7(T13) interact extensively to form tightly assembled trimers with relative flat bases which can be oriented unambiguously onto the VP3(T2) subcores (Grimes *et al.*, 1995; Stuart *et al.*, 1998). The three-fold axis of the trimer (85 Å) is perpendicular to the core surface and the broader base (65 Å) of the trimer contacts the internal network of VP3(T2) of the subcore. The base of BTV VP7(T13), which is in contact with VP3(T2) in the virus, is more hydrophobic, while its upper part, which is in contact with the VP2 or VP5 outer capsid in the virus, is slightly more hydrophilic. These changes may reflect complementary changes on the other proteins involved in these interactions (Basak *et al.*, 1996).

In both BTV and AHSV each VP7(T13) subunit of the trimeric structure consists of two distinct domains, the upper or outer and the lower or inner domain, and are twisted such that the top domain of one monomer rests upon the lower domain of the related subunit (*Figure 1.2*). The relative disposition of these domains is such that they wrap around the molecular three-fold axis in a right-handed sense. The crystal structure of BTV VP7(T13) (Grimes *et al.*, 1995) exhibits an anti-parallel β-sandwich structure for the upper domain, resembling the jelly roll motif of the influenza virus haemagglutinin (Wilson *et al.*, 1981) and many other viral capsid proteins. The smaller upper domain of VP7(T13) forms the outer surface of the core and contains the central one third of the polypeptide chain of the molecule. The lower domain of VP7(T13), which contains both the N-terminus and the C-terminus of the molecule, is composed entirely of α-helices (nine in total) and long extended loops. The α-helical bottom domain is not commonly observed among viral capsid proteins. The α-helical and β-sheet domains of VP7(T13) fold independently involving specific amino acid interactions within these domains. The lower part of the bottom domain is composed of the N-terminal helices 1 to 5. The crystallographic data have implicated the lower domain, especially the flat hydrophobic area on helix 2 and the adjoining loops at the base of the VP7(T13) trimers are involved in the interaction with the underlying VP3(T2) molecules (120 VP3(T2) molecules,

arranged as dimers)(Burroughs *et al.*, 1995; Monastyrskaya *et al.*, 1997; Basak *et al.*, 1996; Grimes et al., 1998). The trimers also form side-to-side interactions with adjacent VP7(T13) trimers. Each VP7(T13) has a short C-terminal arm, which involve helix 9, and may tie trimers together during capsid formation. The deletion of five amino acids at the C-terminus of VP7(T13) abolishes CLP formation, presumably due to lack of trimer-trimer interactions (Le Blois & Roy, 1993; Belyaev & Roy, 1992).

The characteristics of the molecular surface of BTV and AHSV VP7(T13) suggest why AHSV VP7(T13) is less soluble than BTV VP7(T13) and indicate the possibility of attachment to the cell via an Arg-Gly-Asp (RGD) motif in the top domain of VP7(T13), to a cellular integrin. The top domain of AHSV VP7(T13), like BTV, involves amino acids 121-249. These amino acids are arranged as β-sheets, which are connected to each other by β-turns. The β-turns contains hydrophilic amino acids and are exposed to the surface of the trimers. Based on the available crystallographic data, the alanine at position 167 and phenylalanine at 209 are two strong candidates for mutations to increasing the solubility of AHSV VP7(T13), and therefore could demolish the crystal formation of AHSV VP7(T13). The C-terminal helix 9 might also have an impact on the solubility of VP7(T13), as the C-terminus of AHSV VP7(T13) is more hydrophobic than BTV VP7(T13) (Monastyrskaya *et al.*, 1997). The presence of a large hydrophilic area composed of strand βC and η1 (aa 168-178, including the RGD motif) of the top domain of one monomer, and the C-terminal helix 9 of the adjoining monomer on the surface of VP7(T13) trimers (BTV and AHSV), have been indicated (Basak *et al.*, 1996).

1.6.4. Incorporation of the three minor proteins within CLPs

Co-expression of VP1(Pol) and/or VP4(Cap) and/or VP6(Hel), using baculovirus vectors, together with VP3(T2) and VP7(T13), demonstrated that each of the minor proteins could be encapsidated within the derived BTV CLPs. When VP7(T13) trimers were removed from CLPs containing VP1(Pol), the derived subcores consisted only of VP3(T2) and VP1(Pol), demonstrating that VP1(Pol) interacts with VP3(T2) (Loudon & Roy, 1991). Similar results were obtained with VP4(Cap) and VP6(Hel) and for combinations of all three minor proteins (Le Blois *et al.*, 1991). However, unlike VP1(Pol) or VP4(Cap), VP6(Hel) was only poorly incorporated into the CLPs. Since VP6(Hel) is a highly basic protein and readily associates with ssRNA or dsRNA, it is possible that VP6(Hel) chaperones the incorporation of RNA into particles and is only poorly incorporated in the absence of RNA (Roy *et al.*, 1990; Hayama and Li, 1994).

It seems likely that the proper organisation of the RNA for the efficient transcription requires that it be laid down within a pre-existing protein shell. The limited size of the pores in the assembled

subcore would, however, prevent entry of the enzymes. It therefore seems probable that the enzymatic components attach to VP3(T2), so that upon formation of the complete subcore there is a transcription complex at each of the 12 fivefold axes (Grimes *et al.*, 1998; Gouet *et al.*, 1999). Electron density maps at lower resolution of BTV cores indicated that the minor structural proteins associated with transcription of the viral genome (transcriptase complex or TC), is positioned directly under the icosahedral 5-fold apices (Grimes *et al.*, 1998; Stuart *et al.*, 1998; Gouet *et al.*, 1999). It is therefore considered possible that there could be 10 or 12 copies of VP1(Pol). VP4(Cap) forms dimers (Devi *et al.*, 1998; Ramadevi *et al.*, 1998) and may therefore be present as either 20 to 24 copies per particle. VP6(Hel) may form hexamers (Stauber *et al.*, 1997) and may be present as 60 to 72 copies per particle. In the orbivirus core, derived from the intact virus, ten of these complexes will be intimately associated with one of the ten segments of the genomic dsRNA. This is in agreement with the data for BTV where four layers of electron density line the inside of the VP3(T2) shell and are closely associated with the TC. This demonstrates that genomic RNA is packaged in a rather structured way, which follows, to a considerable extent, the icosahedral symmetry of the core. This order is imposed by the VP3(T2) layer which possesses, on its inner surface, shallow grooves that seem to form tracks along which the dsRNA lie (Grimes *et al.*, 1998; Stuart *et al.*, 1998). Specific RNA/protein interactions are evident at only two points in the icosahedral VP3(T2) unit, which may facilitate the movement of RNA within the core, for example during transcription (Grimes *et al.*, 1998; Gouet *et al.*, 1999).

Stuart *et al.* (1998) suggested a model for the packaging of the ten segments dsRNA genome within the core so that it remains sufficiently fluid for efficient, repeated and independent transcription. They suggested that each dsRNA segment is associated with a TC complex at the 5-fold apices and is wound around this TC, until it hits a neighbouring RNA segment. At this point due to steric hindrance it may flip down and inward to form the next layer, spiralling back towards the TC. Further switching would lay down the third and fourth layers. This model is also in agreement with some recent observations of other members of the family *Reoviridae* made by cryo electron microscopy (Moss & Nuttal, 1994; Prasad *et al.*, 1996).

1.6.5. Three-dimensional structure of virions and virus-like particles

Image analysis of cryo-electron micrographs revealed well-ordered morphology of the complete virion (Hewat *et al.*, 1992) also displaying icosahedral configuration (86 nm in diameter). The reconstruction revealed a well ordered morphology that contrasts sharply with that deduced by conventional negative-staining methods. The two proteins of the outer capsid have distinctive shapes, one is globular and almost spherical, the other is sail-shaped. The globular VP5 proteins, 120 in number (although biochemical data suggest a total of 360 copies of VP5, indicating that they

may be arranged as trimers (Stuart *et al.*, 1998b), sit neatly in the channels formed by each of the six-membered rings of the VP7(T13) trimers of the core. The sail-shaped spikes, which project 4 nm beyond the globular proteins, are located above 180 of the 260 VP7(T13) trimers and form 60 triskelion-type motifs which cover all but 20 of the VP7(T13) trimers. It is likely that these spikes are the VP2 haemagglutinating and neutralisation antigens, and that the globular proteins are VP5. The two proteins appear to form a continuous layer around the core, except for holes on the fivefold axis. This differs markedly from the structure of the rhesus rotavirus and mammalian reoviruses, which have a more porous structure.

For the synthesis of VLPs, a quadruple gene expression vector was used to synthesise the BTV VP2, VP3(T2), VP5 and VP7(T13) proteins. The expressed proteins assembled into virtually homogenous double capsid particles. Three-dimensional reconstruction of VLPs at 55 Å resolution revealed that the structure of the VLP (86 nm in diameter) is comparable to that of authentic virions. The VLPs exhibit essentially the same basic features and full complement of the four proteins (French *et al.*, 1990; Hewat *et al.*, 1994; Roy, 1992; Roy, 1995).

1.7. DISEASE PREVENTION AND CONTROL: VACCINATION FOR PROTECTION AGAINST VIRAL INFECTION

The main objective of orbivirus vaccination is not to prevent virus infection of the individual animals but to prevent the transmission of the pathogen. In order to achieve this, a vaccine needs to display certain prerequisites. An effective vaccine is one that provokes levels of immunity at the appropriate site, of adequate duration, and of relevant nature, i.e. humoral, cytotoxic T cell or T-helper cell reponses (Roitt, 1994).

Protection against viral disease through vaccination can be accomplished by using a live attenuated virus vaccine, an inactivated virus or virus subunits. A subunit vaccine can either be derived from infectious material or produced by genetic engineering involving specific gene expression, or synthetic peptides representing neutralisation epitopes (Roy *et al.*, 1990). Vaccination has played an important role in the diminishing occurrence of AHS in South Africa by reducing the number of susceptible horses. The control of AHSV has thus far been effected by a variety of vaccines (Coetzer & Erasmus, 1994). Annual vaccination of horses is the most practical prophylaxis, with horses that have received three or more courses of immunisation being well protected against the disease (Coetzer & Erasmus, 1994). These vaccines have certain disadvantages, which include a danger of causing the disease it is supposed to protect against.

1.7.1. Conventional live attenuated and inactivated virus vaccines

At present, both BT and AHS are controlled predominantly by annual vaccinations with polyvalent live attenuated vaccines. All AHSV serotypes are distributed throughout South Africa, therefore the use of a polyvalent vaccine is necessary to protect horses in most parts of southern Africa. The current vaccine of choice is one in which live, polyvalent, low virulence, large plaque variants of AHSV are passaged and attenuated (Coetzer & Erasmus, 1994). The AHSV vaccine strains are attenuated by serial passage in Vero (African green monkey kidney) cell cultures (House *et al.*, 1992; House, 1998). These vaccines were based on the finding that those viruses producing large plaques were avirulent (Erasmus, 1972). The vaccine currently in use in South Africa contains 8 distinct serotypes, administered as two quadrivalent doses (one containing serotypes 1,3,4 and 5 and the second serotypes 2,6,7 and 8). The doses are administered 28 days apart and precautions are advised to minimise exposure and stress (House *et al.*, 1992; Onderstepoort Veterinary Institute). Serotype 9 is not included in the vaccines due to the fact that it is afforded some cross-protection resulting from the inclusion of serotype 6 in one of the vaccines. According to Coetzer and Erasmus (1994), cross-neutralisation exists between serotypes 1 and 2, 3 and 7, 5 and 8 and 6 and 9. Annual re-vaccination is recommended because of the inability of the polyvalent mixtures to always generate protection against all serotypes. Full protection against all serotypes is usually expected after 3 to 4 years.

Although these vaccines have been widely and effectively applied, the use of live attenuated polyvalent vaccines does involve risks and inherent deficiencies. Besides the need to identify naturally attenuated strains, or to artificially create attenuation (resulting in high production costs), and the inconvenience of repetitive inoculations, immunological interference between component serotypes in polyvalent vaccines may result in the development of incomplete immunity. In addition, there is the risk of viral reassortment and recombination between attenuated and virulent strains giving rise to new strains, and the potential problem of reversion to virulence (Oberst *et al.*, 1987; Samal *et al.*, 1987; Stott *et al.*, 1987; Katz *et al.*, 1990; Stone-Marschat *et al.*, 1996). The development of viremia has also been reported, with the danger of infection of vectors. Furthermore, modified live vaccines may cause immune suppression and commonly induce latent infections. They have been associated with abortions in late gestation animals, ovarian lesions and infertility (van Drunen Littel-van den Hurk *et al.*, 1993; Yancey, 1993) or foetuses with teratogenic defects (Van Dijk, 1993). Such vaccines have also been implicated in vaccine-induced epizootics (Yancey, 1993; Brown, 1992; Coetzer & Erasmus, 1994). The immune response generated after vaccination with modified live vaccines cannot be distinguished from those elicited by natural infection (House, 1998). Further side-effects may include fatal encephalitis, which is characterised by blindness and neurological disorders (Coetzer & Erasmus, 1994).

Non-replicating vaccines have theoretical advantages over live attenuated virus vaccines due to the absence of active replicating virus, eliminating many of the risks and deficiencies associated therewith. Efforts have thus been made to develop effective inactivated vaccines. Experimental inactivated viral vaccines (IVV) were reported as early as 1966 but the process was never commercialised, although a IVV for AHSV-4 was developed and used experimentally during the 1987-1990 epizootic in Spain. The efficacy of the AHSV-4 IVV as a single dose vaccine was evaluated and indicated that a single dose of IVV would protect horses from severe clinical signs and death but not necessarily from the development of a viraemia. However, vaccination with two doses of IVV not only give full protection but also prevent the infection of insect vectors, which is a critical consideration for eradicating AHSV from non-enzootic countries (Hassanian et al., 1992; House *et al.*, 1994; House, 1998). The production of inactivated vaccines is complex and expensive. These vaccines do not confer long lasting immunity thus require multiple doses. In addition the afforded protection is not always complete and cross-protection of immunised animals is restricted to viruses of the same serotype. In some cases outbreaks have reportedly been caused by escape of virus from the use of improperly inactivated vaccines. However, many procedures for the effective and reliable inactivation of viruses, both chemical and genetic, have been develop, which should eliminate this problem (House & House, 1989; House et al., 1992b; Burrage & Laegreid, 1994). Another major drawback of inactivated vaccines is the hypersensitisation that has been reported when sheep previously vaccinated with inactivated BTV are challenged with virulent virus (Stott et al., 1985).

1.7.2. Recombinant subunit and peptide vaccines

Recent advances in recombinant DNA technology have prompted a new era in vaccine development, offering new possibilities of preparing genetically engineered vaccines without the need to grow the pathogenic organism. This new direction in vaccine development avoids the difficulties and the risks associated with live virus, or preparation of killed virus vaccines. Proposed vaccines based on this new technology include cloning of portions of the viral genome into a vector that can be administered or used to express viral proteins, the formation of empty capsids lacking the ability to replicate, the production of synthetic peptide vaccines and genetic immunisation. Attention has been focussed on identifying the relevant proteins and sequences involved in protective immune responses to viral infection and on systems to produce and present these proteins, or protein sequences, to elicit the required protection.

1.7.2.1. AHSV antigenic outer capsid proteins and neutralisation domains

In the case of BTV, vaccination with baculovirus-derived BTV VP2 was found to fully protect sheep against virulent homologous BTV, with complete absence of clinical signs and post-challenge viraemia (Inumaru & Roy, 1987; Roy *et al.*, 1990). The outer capsid protein, VP2, of BTV and AHSV induces serotype-specific neutralising antibodies that protect animals fully against virulent virus challenge mediated by a humoral immune response (Huismans *et al.*, 1987; Burrage *et al.*, 1993; Martinez-Torrecuadrada & Casal, 1995). Subunit vaccines for AHSV and BTV are being developed as an alternative to the existing live attenuated polyvalent vaccines including VP2, mixtures of VP2 and VP5 and VLPs (Roy *et al.*, 1990; Pearson & Roy, 1993; Van Dijk, 1993; Martinez-Torrecuadrada *et al.*, 1996). Animals vaccinated with these subunit preparations can also be distinguished from naturally infected animals, which would simplify international movement of horses. Since it was demonstrated that VP2 alone is sufficient to protect horses against AHSV, studies aimed at developing a subunit vaccine against AHSV have been focused mainly on VP2 (Roy *et al.*, 1996; Stone-Marchat *et al.*, 1996). High levels of expression could be achieved when recombinant VP2 was expressed in a baculovirus system, and VP2 of AHSV-4 was reported to be able to protect horses when expressed in this manner (Roy *et al.*, 1996). Although, this suggests that a recombinant baculovirus, expressing VP2 of AHSV (like BTV), may be used to produce antigenic protein for a suitable subunit vaccine, vaccination studies using baculovirus expressed VP2 proteins of other serotypes, experienced complications due to protein aggregation (Du Plessis *et al.*, 1998). These include limited protection caused by insufficient immunogenicity of the recombinant proteins despite the high level of expression. It was thought that the insufficient immunogenicity of the proteins could possibly be caused by the insoluble nature of the baculovirus expressed VP2 (Du Plessis *et al.*, 1998; Venter *et al.*, 1999). Vreede & Huismans (1994) and Martinez-Torrecuadrada *et al.* (1994), also proposed that the soluble form of VP2 has a toxic effect on insect cells, which resulted in very low levels of soluble VP2. Since solubility is important for a protein to act as an effective immunogen, the approach of using VP2 as a subunit vaccine is currently prevented by the lack of producing high yields of soluble VP2. Previous studies with BTV indicated that the presence of VP5 together with VP2 enhances the neutralisation antibody and protective responses against virulent BTV challenge. It has been postulated that VP5 improves the conformation of VP2 when administered together (Roy *et al.*, 1990).

An alternative approach is to identify important epitopic regions on VP2 of AHSV by mapping the exact position of the epitopes using overlapping peptides or phage display libraries. A linear neutralising epitopic domain had been identified on VP2 of AHSV-4 by screening overlapping truncated protein fragments of VP2 with neutralising monoclonal antibodies as well as polyclonal neutralising sera, and by using these fragments to elicit neutralising antibodies in mice (Martinez-

Torrecuadrada *et al.*, 1994; Martinez-Torrecuadrada & Casal, 1995). The study revealed that the major antigenic domain of AHSV-4 VP2 is located in the central region of the protein and that several neutralisation sites are located within this domain. A region between amino acids 253 and 413 was able to elicit consistently high titres of neutralising antibodies. However, this recombinant polypeptide was not able to compete with virus particles for binding of neutralising antibodies in serum from infected or vaccinated horses, which indicates that this region is not immunodominant in infected horses (Martinez-Torrecuadrada & Casal, 1995). A similar approach to epitope mapping was applied to VP2 of serotype 9 using baculovirus expression. A region from residues 252 to 486 was recognised to contain a linear epitope of approximately 33 amino acids. This region that stretches from amino acids 369 to 403 is located in the same region as a neutralising linear epitope identified on AHSV-4 VP2 and is implicated in virus neutralisation (Venter *et al.*, 1999; Torrecuadrada & Casal, 1995). The polypeptides identified in each of these studies were insoluble and thus not ideal immunogens.

1.7.2.2. Protection afforded by biosynthetic particulate structures

VLPs synthesised by recombinant baculoviruses mimic the native virion in size and appearance. The VLPs are not only biologically, but also immunologically similar to the virion. VLPs exhibit high levels of haemagglutination activity, similar to those of authentic BTV and are capable of eliciting protective immune response, but are not infectious since the particles lack genetic material. BTV VLPs were investigated for their vaccine potential in sheep and proved to be highly immunogenic. Antibodies raised to the expressed particles contain high titres of neutralising activity against the homologous BTV serotype (French *et al.*, 1990; Roy *et al.*, 1992). Long lasting protection against homologous BTV challenge has been provided by vaccination with VLPs, as well as some preliminary evidence for cross protection, depending on the amount of antigen (Roy *et al.*, 1994). It has been illustrated that BT VLPs are highly immunogenic, even at low doses compared to VP2 alone or mixtures of VP2 and VP5. Assuming that VP2 plays the primary role in humoral protection, the results implied that 25-50 fold less VP2 was sufficient for protection when presented on VLPs compared to its individual effect or in conjunction with VP5 (Roy *et al.*, 1990 & 1992). It has been suggested that the VP3(T2) and VP7(T13) provides the necessary scaffold for the correct conformational presentation of the relevant epitopes on VP2, which elicits humoral immune response and that any of the 4 BTV capsid proteins might have a direct role in eliciting cell-mediated immunity. Furthermore, both VP2 and VP5 are present (Pearson & Roy, 1993; Roy & Sutton, 1998). It is therefore of critical importance to produce AHS VLPs, which may prove to be an effective and safe recombinant subunit vaccine and will also allow differentiation between vaccinated and naturally infected horses.

BTV CLPs have been demonstrated to be formed by the co-expression of VP3(T2) and VP7(T13) in recombinant baculovirus infected insect cells (French & Roy, 1990). Sheep vaccinated with BTV CLPs and challenged with virulent virus developed only limited clinical signs of disease and all recovered fully. Preliminary serological investigations indicated that immunisation with CLPs did not induce neutralising antibodies, nor did it affect the neutralising antibody response to the challenge virus (French *et al.*, 1990). The finding that CLPs can induce protection in the absence of neutralising antibodies suggested the involvement of a cell-mediated response, but this remains to be investigated (Van Dijk, 1993). Vaccination trials with BT CLPs resulted in partial protection in the absence of neutralising antibodies, suggesting the involvement of cell-mediated response (Pearson & Roy, 1993; Roy & Sutton, 1998). Although immunisation with CLPs has not yet been reported in AHSV, it was recently demonstrated that mixtures of VP2, VP5 and VP7(T13) of AHSV conferred protection in horses against virulent AHSV challenge, although only low levels of neutralising antibodies were induced (Martinez-Torrecuadrada *et al.*, 1996). It has been suggested that VP5 and VP7(T13) could possibly contain T-cell epitopes, which could enhance the immune response.

Wade-Evans *et al.*(1997) demonstrated that AHSV VP7(T13) crystals protect mice against lethal, heterologous serotype challenge, not involving antibody-mediated immune response. This correlates with previous suggestions for BTV that cell-mediated immunity may play an important role in the development of a protective immune response. Since VP7(T13) is the major serogroup specific antigen of AHSV, and thus also the serotype cross reactive antigen, these results may indicate that VP7(T13) crystals may be effective as a prophylactic subunit vaccine against all serotypes of AHSV (Wade-Evans *et al.*,1997).

However, the production of AHSV subunit vaccines may become a reality in the not-so-distant future, which would greatly alleviate these problems. An advantage of subunit vaccines will be that they make it possible to distinguish between horses that have been vaccinated and those that have been infected with the virus itself. Increasing use of molecular biological analysis methods and recombinant DNA technology in recent years has accelerated our knowledge of the functions and structures of the orbivirus proteins, including those of AHSV and may thus find direct application in the production of a suitable subunit vaccine and also in the production of virulence or attenuated markers.

1.8. EXPRESSION SYSTEMS FOR RECOMBINANT PROTEINS

Our ability to achieve these objectives depends on high level expression of the relevant heterologous AHSV genes. There are five major expression systems that are commonly available, namely *Escherichia coli*, *Bacillus subtilis*, yeast, baculovirus and mammalian expression systems (Goeddel, 1991). Proteolysis represents one of the most significant barriers to heterologous gene expression in any organism. Another problem results from the expression of certain recombinant proteins that turn out to be toxic to the cell. The only possible solutions are to switch to a different expression system, to target the toxic proteins into an organelle where its toxicity is no longer manifested.

All expression systems have advantages and disadvantages that should be considered when choosing a suitable expression system. Expression in *E. coli* is neither time-consuming, nor expensive and some strains can produce 30% of their total protein as the expressed gene product. However, eukaryotic proteins expressed in *E. coli* are not properly modified. Proteins expressed in large amounts in *E. coli* often precipitate into soluble aggregates or inclusion bodies, from which they can only be recovered in the active form by solubilisation in denaturing agents followed by careful renaturation. The reducing environment present in *E. coli* does not permit cysteine-rich proteins to form the disulphide bonds required for proper conformation. However, intracellular production of heterologous proteins in *E.coli* is possible even for those proteins that must be oxidised for activity (Gold, 1991).

Yeast are unicellular micro-organisms and many of the manipulations commonly used in bacteria can also be readily applied to yeast. Yeast offers many advantages of both prokaryotic and eukaryotic systems. Yeast grow rapidly, achieve high cell densities and are able to perform post-translational modifications. They can be propagated on simple defined media and transformed with a variety of either self-replicating or integrating plasmid vectors. Yeast being eukaryotic, possess much of the complex cell biology typical of multicellular organisms, including high compartmentalised intracellular organisation and an elaborate secretory pathway which mediates the secretion and modification of many host proteins. However, some proteins are rapidly degraded either during or shortly after synthesis. Others are lost during cell breakage and subsequent purification (Emr, 1991).

Progress in mammalian cell expression systems has been astonishing in the last few years. Mammalian expression systems have several advantages for the expression of higher eukaryotic proteins. Expressed proteins are properly modified and they almost always accumulate in the correct cellular compartment. However, mammalian expression systems are expensive, complicated and more time-consuming than any of the other systems described here (Levinson, 1991).

1.8.1. Baculovirus expression vector system (BEVS)

Since its introduction in 1983, the BEVS technology has become one of the most versatile and powerful eukaryotic vector systems for recombinant protein expression. A wide variety of genes from viruses, fungi, plants and animals have been expressed in insect cells infected with recombinant baculoviruses (Luckow & Summers, 1988; Maeda, 1989; Luckow, 1991; King & Posse, 1992). *Autographica californica* nuclear polyhedrosis virus (AcNPV) is a proven vector for high level expression of heterologous genes in insect cells (O'Reilly *et al.*, 1992).

Owing to the large size of the baculovirus genome (about 130 kb), the BEVS relies on *in vivo* recombination to replace a viral allele, usually the dispensable polyhedrin gene of AcNPV, with the gene of interest cloned into a suitable transfer vector. Transfer vectors contain a site for foreign gene insertion, downstream of a proficient promoter of a wild type viral protein expendable for virus replication, and flanked by viral sequences homologous to the part of the baculovirus genome where the gene is to be inserted. Subsequent co-transfection of insect cells with infectious baculoviral DNA and recombinant transfer plasmid DNA allows cell-mediated allelic replacement of the target viral gene with the plasmid-borne foreign gene through homologous recombination. The percentage of recombinant viruses obtained by this recombination event has been reported to constitute 0.1-1% of the progeny viruses (Kitts et al., 1990; Kitts & Possee, 1993; Zuidema *et al.*, 1990; Anderson *et al.*, 1995). Numerous modifications of this system have been made to increase the frequency of recombination and improve the ease with which recombinants can be selected (Davies, 1995; Miller, 1989 & 1993). However, all methods involve repeated rounds of plaque purification to ensure that recombinant virus is not contaminated with wild type baculovirus. This is time consuming and costly.

BEVS has a number of advantages, eg. extremely high rate and duration of the expression of recombinant proteins, the antigenic, immunogenic and functional similarity of the expressed proteins to their authentic counterparts, the applicability of the system to monolayer or suspension culture and the post-translation modification of proteins in a manner similar to those of mammalian cells. Baculoviruses are essentially non-pathogenic to mammals and plants. This system has proven to be successful in expressing genes as non-fusion proteins, therefore, genes using their natural, translation initiation codon and N-terminal sequences. Although N-terminal fusions may increase the stability of some proteins, the biological activity of many proteins is adversely affected by additional sequences at the N-terminal (Miller, 1988; Yong Kang, 1988; O'Reilly *et al.*, 1992).

Glycosylation of proteins in the baculovirus system has been regarded as relatively successful. This is at first sight surprising, as notable differences exist between the glycosylation pathways of insects

and higher eukaryotes (Davies, 1995). Post-translational modifications in BEVS such as phosphorylation and glycosylation mimic those modifications by mammalian cells.

Synthesis of proteins involved in the formation of complex structures, in eucaryotic cells by an expression vector provides an opportunity to investigate macromolecular interactions under more natural, intracellular conditions. The baculovirus expression system has been exploited extensively over the past few years to investigate the assembly of the major BTV capsid proteins into core-like particles and virus-like particles via co-expression of the relevant genes in insect cells (French *et al.*, 1990; French & Roy, 1990). The productivity and flexibility of the insect baculovirus expression vector system and the ability of the baculovirus genome to incorporate and express large amounts of foreign DNA have permitted this system to be used for the simultaneous expression of multiple foreign genes in a single insect cell (Bishop, 1992). The foreign genes are placed under control of the polyhedron or p10 promoters, which are both non-essential for viral morphogenesis and strong and active in the very late phase of infection. The p10 promoter is responsible for the high level synthesis of a non-structural protein in wild type baculoviral infected cells (Balyaev & Roy, 1993). It is activated in the very late occlusion phase of virus replication, and appears to have a similar relative strength to the polyhedrin promoter (Weyer *et al.*, 1990). The function of the p10 protein is unknown, but it may be involved in host cell lysis (Weyer *et al.*, 1989). The promoters are arranged in opposite orientations to minimise the possibility of homologous sequence recombination and excision of the foreign genes.

BAC-TO-BAC™ baculovirus expression:

Recently, Luckow and co-workers (1993) introduced a novel baculovirus expression system (BAC-TO-BAC™) which permits rapid and efficient generation of recombinant viruses by site-specific transposition of a DNA cassette into a baculovirus shuttle vector (bacmid), propagated in *E.coli*, rather than homologous recombination in insect cells.

The bacmid system utilises transposon 7-mediated transposition in *E. coli* to produce recombinant AcNPV (Davies, 1994; Leusch *et al.*, 1995). The bacmid is a recombinant baculovirus genome (AcNPV) containing a mini-F replicon inserted into the polyhedrin locus, a kanamycin resistant marker, and a mini *att*Tn7 (target site for bacterial transposon TN7) inserted within a *lacZα* complementation region. Therefore the bacmid can replicate in *E. coli* as a plasmid and can also infect susceptible insect cells. The donor plasmid contains the polyhedrin promoter to drive expression of the foreign gene, flanked by left and right ends of Tn7, a SV40 poly(A)-sequence and a multiple cloning site downstream of the original ATG of the polyhedrin gene, which has been mutated to ATT. Therefore, to successfully express a protein, the foreign DNA fragment must contain its own ATG followed by an ORF. To generate a recombinant baculovirus, the gene of interest is cloned into the donor vector downstream of the polyhedrin promoter. A dual expression

transfer vector, pFastbac-Dual, which facilitates the introduction of two heterologous foreign genes inserted at unique multiple cloning sites into a single recombinant virus, is also available. Both foreign proteins are then expressed, under control of two strong very late promoters respectively, the polyhedrin and p10 promoters.

The recombinant donor plasmid is then used to transform *E. coli* DH10Bac cells, containing the bacmid and a helper plasmid, which provides transposition functions in *trans*. The transposition event inserts the gene of interest and polyhedrin promoter into the bacmid. Composite bacmid DNA is transfected into insect cells giving rise to recombinant baculoviruses expressing the gene of interest. The characteristics of the BAC-TO-BAC™ system reduce the time to identify and purify a recombinant virus from 4-6 weeks to 7-10 days. This method permits rapid and simultaneous isolation of multiple recombinant viruses and is particular suitable for expression of protein variants for structure/functional studies.

1.9. SUMMARY AND AIMS

As discussed, the current AHS vaccine, although effective, does involve certain risks and has some inherent deficiencies. At least some of these concerns, including the induction of latent infections and the potentially serious problems of reversion to virulence and vaccine induced epizootics, may be overcome through the development of recombinant vaccines. In the development of any recombinant vaccine, it is mandatory to identify and characterise all the antigens required to stimulate a protective immune response. A disadvantage of a recombinant peptide vaccine is the difficulty in presenting the protective protein, protein fragments or small peptides in their correct three-dimensional structure for an effective immune response. Therefore, it may be found essential to use a particulate delivery system for the display of immunodominant epitopes to evoke an immune response. This focuses the attention on the possible use of AHSV particulate structures for the presentation of antigens or neutralising epitopes to the immune system of the recipient animal.

From the literature review, it is clear that AHSV is associated with three characteristic structures, which are highly immunogenic and could be used as particulate delivery systems for immunologically important determinants. The unique virus-specified tubular structures, composed of NS1, observed in the cytoplasm of orbivirus-infected cells, were proven to be an effective carrier for foreign epitopes, in the case of BTV (Mikhailov *et al.*, 1996). Secondly, AHSV VP7(T13) is highly hydrophobic and aggregate into distinctive hexagonal crystals when expressed in the absence of the other AHSV proteins. These crystals elicit a strong humoral immune response in an animal model (Wade-Evans *et al.*, 1997 & 1998). Thirdly, empty virions or particles that simulate the virion surface should provide a safe way of stimulating protective immunological memory.

The long-term aim of this investigation is to obtain more information on the morphology, biochemical and biophysical properties and the factors involved in the polymerisation of these three AHSV-associated structures and their possible use as peptide delivery systems. The foundation of such an investigation is based on the availability of the genes, knowledge about the gene sequences and a system for producing the required amounts of the proteins. The gene segments encoding the major structural proteins were cloned and characterised previously, but no functional DNA copy of the NS1 encoding segment of AHSV was available.

For these reasons this project was focussed on the following short-term objectives:

Primary objectives:

1. Cloning and characterisation of the AHSV-6 NS1 gene, analysis of the morphological and biophysical properties of the deduced protein and identification of epitope insertion sites.

2. Verification of the interaction of the four major structural proteins to form core-like or virus-like particles and analysis of the morphology of the assembled particles.

3. Modification of the hydrophilic regions of the top domain of AHSV-9 VP7(T13) by means of site-directed insertion mutagenesis and investigation of the effect of additional sequences on the trimerisation, solubility, crystal formation and CLP formation of VP7(T13) as well as the length of inserts tolerated by VP7(T13).

The research strategies for obtaining the primary objectives involved the following:

1. Cloning and sequencing of a full-length cDNA copy of the NS1 gene. Identification of hydrophilic regions which may potentially be used for the insertion of foreign epitopes. Expression of the AHSV-6 NS1 gene with a view to obtain large quantities of the NS1 protein, in the absence of the other viral components, for studies regarding NS1 structure and biophysical properties (see chapter 2).

2. The simultaneous expression of the major proteins of the core particle (VP3(T2) and VP7(T13)) or virus particles (VP2, VP3, VP5 and VP7) in insect cells in order to synthesise core-like (CLPs) or virus-like particles (VLPs). Structural analysis, carried out using electron microscopy (see chapter 3).

3. Insertion mutants of AHSV VP7(T13) will be prepared by means of PCR based site-directed insertion mutagenesis. Previously identified neutralising epitopes of AHSV-9 VP2 will be cloned into the modified regions of VP7(T13). The effect these modifications have on trimer, crystal and CLP formation of VP7(T13) was investigated (see chapter 4).

CHAPTER 2

CHARACTERIZATION OF TUBULAR STRUCTURES COMPOSED OF NONSTRUCTURAL PROTEIN NS1 OF AFRICAN HORSESICKNESS VIRUS EXPRESSED IN INSECT CELLS

2.1. INTRODUCTION

Little is known about the exact roles of the three non-structural proteins in the replication cycle of orbiviruses. Data suggest that these proteins are involved in the process of viral morphogenesis, leading to viral assembly and release. There is as yet no evidence for a specific function of NS1 tubules in virus replication, although it has been proposed that NS1 may play a role in the transport of mature virus particles from the virus inclusion bodies to the cell membrane where NS3 is involved in virus release. Studies have shown that the structure, size and biophysical character of the NS1 tubules differ significantly among AHSV, BTV and EHDV (Huismans & Els, 1979). However, the function of the tubules may be conserved because their synthesis is a characteristic feature of the replication cycle of all orbiviruses investigated thus far. NS1 is potentially useful as a diagnostic antigen since the presence of specific antibodies is an indication that the virus has replicated in the host. It is, however, not antigenically unique and cross-reacts serologically with the analogous protein of the related epizootic haemorrhagic disease virus (EHDV) (Richards *et al.*, 1988).

The baculovirus expression system enabled significant biochemical and structural analysis of BTV and EHDV NS1 tubules in the absence of other viral components (Urakawa & Roy, 1988; Nel & Huismans, 1991). BTV NS1 is a highly hydrophobic protein and particularly rich in cysteine residues (Lee & Roy, 1987; Nel *et al.*, 1990). BTV and EHDV NS1 proteins are highly ordered structures, most likely due to the large amount of conserved cysteine residues and the major hydrophilic and hydrophobic regions scattered throughout the protein (Fukusho *et al.*, 1989; Nel *et al.*, 1990). Monastyrskaya *et al.* (1994) have revealed several conserved elements in the protein which are necessary for tubule formation, with cysteine residue at positions 337 and 240 and the conserved carboxyl- and amino-terminals shown to be of particular importance. The amino acid sequence of NS1 and the structure and biophysical character of the tubules differ significantly among AHSV, BTV, EHDV and BRDV (broadhaven virus).

Three dimensional studies of the BTV NS1 tubules indicated that each tubule has a diameter of 52.3 nm and is composed of a coiled ribbon of NS1 dimers with 22 dimers per helix turn (Hewat *et al.*, 1992). Very little is known about the structure of the AHSV tubules except that they appear to be morphologically different from EHDV and BTV tubules (Huismans & Els, 1979). Although the NS1 gene of AHSV-4 and 9 has been sequenced there are no reports on the structure and biochemical/biophysical properties of AHSV tubules. From the literature review it is clear that many of the details of the process of orbivirus replication, morphogenesis and assembly still need to be elucidated. The non-structural proteins are thought to play important roles in these processes. The role of NS1 and of the tubules in these processes is still obscure.

Recently, Mikhailov *et al.* (1996) have shown that NS1 of BTV can be utilised as an immunogen delivery system, as they had succeeded in inserting sequences ranging from 44 to 116 amino acids in length at the C-terminus of BTV-10 NS1. All the chimeric constructs still possessed the ability to form tubular structures while carrying the foreign antigenic sequences when expressed as recombinant baculoviruses. Interestingly, when insect cells were co-infected with three recombinant baculoviruses expressing the NS1 chimeric proteins with different epitopes, they simultaneously assembled into the same tubule. This has important implications for using NS1 tubules for the structured delivery of multiple epitopes. Two unique antigenic regions of BTV NS1 were identified, using a phage display library, one of which could be effectively mimicked by a 28 residue synthetic peptide (Du Plessis *et al.*, 1995). This peptide did not cross-react with an antiserum directed against NS1 of EHDV and was identified to be located at position 474 to 502.

In order to obtain more information on the characteristics of AHSV NS1. This chapter describes the cloning and characterisation of the NS1-encoding gene of AHSV serotype 6, as well as a comparison with the cognate gene and derived amino acid sequence of AHSV-4 and -9, BTV and EHDV. The sequence data will be used to identify regions that could be utilised for the insertion of foreign epitopes. The NS1 protein of AHSV-6 was also expressed by means of a baculovirus recombinant producing AHSV-specific tubules for elucidation of the structure, biochemical character and stability of these tubules.

2.2. MATERIALS AND METHODS

2.2.1. Materials

The pBS cloning and expression vector and pUC18 were obtained from Stratagene and Boehringer Mannheim, respectively. G-tailed *Pst*I cut pBR322 was purchased from GIBCO BRL. The BAC-TO-BAC™ baculovirus expression system was obtained from Life Technologies, Inc. Restriction endonucleases, calf intestinal alkaline phosphatase (CIP), RNase A, T4 DNA ligase, Klenow polymerase, dNTPs, DNA molecular weight marker II (MWII) and T7 RNA polymerase were purchased from Boehringer Mannheim. *Hae*III-digested ϕX 174 DNA, T3 RNA polymerase and Taq polymerase were obtained from Promega. The Geneclean™ DNA purification kit was purchased from Bio 101 Incorporated. United States Biochemical Corporation (USB) supplied the sequenase™ Version 2.0 sequencing kit. The following radioisotopes were supplied by Amersham: [α-^{35}S]dATP (1 mCi/ml; > 6000 Ci/mmol), [α-^{32}P]dCTP (1 mCi/ml; > 400 Ci/mmol), [γ-^{35}S]methionine (15 mCi/ml; 1000 Ci/mmol). Amersham also supplied Hybond™C, N and N^{+} nitrocellulose membranes. Cronex MRF 31 X-ray film was supplied by Protea Medicals. A nick translation kit was supplied by Promega. Rainbow™ protein molecular weight marker (MW 14 300 - 200 000 Da), human placental RNase inhibitor (HPRI) and nuclease treated message dependent rabbit reticulocyte lysate was also purchased from Amersham. The Lipofectin™ and Cellfectin™ reagents were supplied by GIBCO BRL. Onderstepoort Veterinary Research Institute provided Eagle's medium with or without methionine. Grace's insect medium and foetal calf serum were obtained from Highveld Biological. Other chemicals were purchased from Merck, Sigma and Boehringer Mannheim.

2.2.2. Cells and viruses

South African isolates of AHSV serotype 3 and 6 were obtained from the Onderstepoort Veterinary Research Institute (OVI), Onderstepoort, South Africa. AHSV was propagated in monolayers of chicken embryo reticulocyte (CER cells) or baby hamster kidney cells (BHK cells) grown in Eagle's medium supplemented with 5% bovine serum. Wild type and recombinant baculoviruses were propagated and assayed in *Spodoptera frugiperda* (Sf9) cell cultures. The Sf9 cells were supplied by the NERC Institute of Virology and Environmental Microbiology, Oxford, UK. Sf9 cells were grown as monolayers or suspension cultures at 28°C in Grace's medium (Summers & Smith, 1987) supplemented with 10% (v/v) foetal calf serum and antibiotics (penicillin/streptomycin/fungizone).

2.2.3. Partial characterisation of AHSV serotype 9 NS1 gene by *in vitro* expression

A cDNA copy of the segment 5 gene of AHSV-9, encoding the NS1 protein has previously been cloned by Nel and Huismans (unpublished data) by the cloning technique described by Bremer *et al.* (1990). AHSV-9 segment 5 cDNA and PCR gene copies, respectively cloned into pBR322 (pBR-AH9S5cDNA) and the pSPT19 expression vector (T3 orientation; pSPT-AH9NS1) were digested with each of the following restriction enzymes in order to verify the identity of the clones: *Bam*H1, *Hind*III, *Xho*I and *Xba*I. Restriction enzyme digestions were carried out according to the manufacturer's instructions.

Using the original AHSV-9 NS1 cDNA clone (pBR-AH9S5cDNA) and the PCR copy (pSPT-AH9NS1), a NS1 PCR-cDNA chimeric gene was constructed within pSPT19. The restriction enzyme map of the AHSV-9 NS1 gene was used to identify exchange sites close to each terminal, namely *Acc*I (ca. 450 bp from the 5' end) and *Xho*I (ca. 350 bp from the 3' end). To confirm the presence of these sites in both the

cloned cDNA and PCR copies of the gene, each recombinant plasmid was digested with *Acc*I and *Xho*I enzymes, individually and simultaneously. DNA fragments of interest were excised from pBR-AH9S5cDNA and pSPT-AH9NS1, respectively containing the cDNA and PCR-tailored copies of the NS1 gene. pSPT-AH9NS1 was simultaneously digested with *Acc*I and *Xho*I enzymes to generate a 1.1 kb and 3.9 kb fragments. The ca. 1.1 kb segment 5 cDNA sub-fragment was excised from pBRS5cDNA by simultaneous restriction with *Acc*I and *Xho*I. The fragments of interest were recovered from a 1% agarose gel and cloned as described in section 2.2.7. The ends were verified by sequencing.

2.2.4. Cloning of AHSV-6 segment 5 cDNA using homopolymeric dC-tailing

The isolation of AHSV serotype 6 viral dsRNA and the synthesis of cDNA were performed by Grant Napier, using the strategy as described by Bremer *et al.* (1990). The double-stranded cDNA fragment of AHSV-6 segment 5, was cloned by a modification (Huismans & Cloete, 1987) of the method described by Cashdollar *et al.* (1982 & 1984). Homopolymeric dC-tails were added to the 3' ends of the cDNA using terminal deoxynucleotidyl transferase (TdT; Gibco BRL) as described by Deng & Wu (1981). The C-tailing reaction (30 µl) contained 0.1 mM dCTP and 20 µCi α^{32}P dCTP (400 Ci/mmol; Amersham) in $^1/_5$ volume 5x DNA tailing buffer (0.5 M potassium cacodylate pH 7.2, 10 mM $CoCl_2$, 1 mM dithiotreitol (DTT)) and 15 U TdT. The reaction was incubated at 37°C for 15 min and the cDNA was purified by the Geneclean™ procedure (section 2.2.8.2). The dC-tailed product was annealed to the dG-tailed *Pst*I-cut pBR322 in a DNA thermal cycler. The annealing reaction was carried out in a final volume of 30 µl containing the purified dC-tailed cDNA incubated with 200-400 ng dG-tailed *Pst*I-cut pBR322 (Gibco BRL) in annealing buffer (10 mM Tris-HCL pH 8.0, 150 mM NaCl, 2 mM EDTA) for 5 min at 80°C. The mixture was then subjected for 1 h each at 65°C, 56°C, 42°C and RT to allow annealing. This DNA was then used to transform competent *E. coli* HB101 cells.

2.2.4.1 Preparation of *E. coli* competent cells

The calcium chloride method of preparing competent cells, originally described by Cohen *et al.* (1972), was used, whereby exposure to calcium ions renders cells able to take up DNA, or become competent. The technique is described in Sambrook *et al.* (1989). *E. coli* HB101, JM105 or XL1-Blue cells were routinely used for transformations with pBR322, pUC18 and pBS (Bluescript) plasmid DNA, respectively. An overnight culture of *E. coli* was used to inoculate 100 ml of pre-warmed sterile Luria-Bertani (LB) medium (1% (w/v) bacto-tryptone, 0.5% (w/v) yeast extract, 1% (w/v) NaCl, adjusted to pH 7.4 with NaOH) and the cells were grown at 37°C with continuous shaking to logarithmic (log) phase (OD_{550} = 0.5). Cultured cells (20 ml) were collected by centrifugation at 4 000 rpm for 5 min at 4°C and the pellet was gently resuspended in half the original volume (10 ml) of ice cold freshly prepared 50 mM $CaCl_2$ and incubated on ice for 30 min. The cells were collected by centrifugation as above and resuspended in $^1/_{20}$ of the original volume of $CaCl_2$ (1 ml). The cells were kept on ice for at least 1 h before transformation.

2.2.4.2. Transformation of competent cells with plasmid DNA

The annealed cDNA/vector mixture was added to 200 µl of competent *E. coli* HB101 cells and allowed to adsorb for 30 min on ice. The cells were then subjected to a heat-shock of 42°C for 90 s (described by Sambrook *et al.*, 1989), to allow the DNA to enter the cells, and cooled on ice for 2 min. Pre-warmed (37°C) LB-medium (0.8-1.0 ml) was added, and the cells were incubated at 37°C with shaking for 1 h to allow expression of the plasmid-encoded antibiotic resistance. The cells were plated out in aliquots of 100-150 µl onto 1.2% (w/v) LB-agar plates containing the appropriate antibiotic (12.5 µg/ml tetracycline hydrochloride (tet) and/or 100 µg/ml ampicillin (amp)). Plates were incubated overnight at 37°C.

Plates for transformations of recombinant pBR322 plasmids contained 12.5 µg/ml tet. Colonies were replica-plated on amp and tet plates, as ligation of a cDNA insert in the *Pst*I site of pBR322 inactivates the ampicillin resistance gene. Recombinant plasmids were selected on the basis of tetracycline resistance (tet^R) and ampicillin sensitivity (amp^S). Colonies of desired phenotype were picked with sterile toothpicks and grown overnight in 5 ml LB medium with the appropriate antibiotic.

2.2.5. Plasmid DNA extraction and purification

Recombinant plasmid DNA was extracted from liquid cultures of bacterial cells according to the rapid alkaline lysis method (Sambrook *et al.*, 1989) which is a modification of the method originally described by Birnboim & Doly (1979). The following procedure describes mini-prep plasmid purification. A single bacterial colony was inoculated into 3-5 ml LB-medium supplemented with the appropriate antibiotic and incubated overnight at 37°C. Cells in 3 ml of culture were harvested by centrifugation at 12 000 rpm for 2 min in a microcentrifuge. After removing the supernatant the cells were resuspended in 200 µl of ice cold solution 1 (25 mM Tris-HCL pH 8.0, 50 mM glucose and 10 mM EDTA). After 5 min at RT and 2 min on ice, 400 µl of a freshly prepared solution of 0.2 N NaOH, 1% SDS was added, gently mixed and incubated on ice for 5 min, lysing the bacteria and causing denaturation of the proteins as well as the chromosomal and plasmid DNA. To this 300 µl of 3 M sodium acetate (NaAc), or potassium acetate (KAc) pH 4.8 was added and vortexed vigorously, resulting in reannealing of the plasmid DNA and precipitation of the chromosomal DNA and protein. After 10 min on ice, the supernatant was collected by centrifugation at 15 000 rpm for 10 min at 4°C and transferred to a fresh tube for ethanol precipitation of the plasmid DNA. The plasmid DNA was recovered from the supernatants by the addition of two volumes (1.8 ml) 96% ethanol or 0.7 volumes 100% isopropanol (630 µl) and incubated at -20°C for 1 h or at room temperature for 1 h, respectively. The DNA was pelleted by centrifugation and washed once with 500 µl of ice cold 70% ethanol. Pellets were vacuum dried and resuspended in 40 µl 1 x TE buffer (10 mM Tris-HCL, 1 mM EDTA, pH 8.0). The volume of each reagent was adapted to correlate with 200 ml suspension cultures for large scale plasmid extractions. Contaminating low molecular mass RNA was removed by precipitation with half a volume of 7.5 M ammonium acetate and plasmid DNA was finally recovered by ethanol precipitation.

2.2.5.1. Phenol-chloroform purification

Mini-prep samples were deproteinized by phenol-chloroform extraction. TE buffer (1 x) was added to a final volume of 400 µl and mixed with an equal volume of a 25:24:1 solution of phenol:chloroform:iso-amylalcohol followed by centrifugation at 12 000 rpm for 5 min. The upper aqueous phase was removed and extracted twice with a half volume of chloroform. DNA was recovered from the aqueous phase by ethanol precipitation as described earlier, after the addition of 3M Na.acetate pH 7.0 to a final concentration of 0.3 M.

2.2.5.2. RNase-PEG precipitation

Recombinant plasmid DNA obtained from small-scale plasmid extractions were incubated with 1 µl RNase A (10 mg/ml) at 37°C for 20-30 min and then precipitated with 30 µl of 20% PEG 6000 in the presence of 2.5 M NaCl. After incubation on ice for 20 min, the DNA pellet was collected by centrifugation at 15 000 rpm for 15 min, rinsed with 70% ethanol and resuspended in 30 µl 1 x TE. Although highly purified plasmid DNA was obtained, the method differed from that described below in that it does not efficiently separate nicked circular molecules from the supercoiled ccc form of plasmid DNA.

2.2.5.3. CsCl density gradient centrifugation

The volume of the plasmid DNA solution was adjusted to 3.5 ml with 1 x TE buffer and 3.77 g CsCl (1.078 g/ml) was then added to the solution. After the CsCl was dissolved, 350 µl of a 10 mg/ml ethidium bromide solution was added. The gradient was centrifuged for 40 h at 38 000 rpm in a Beckman SW50.1 swing-bucket rotor or for 16 h at 42 000 rpm in a Beckman VTi65 rotor at 20°C. Two bands of DNA could normally be visualised on an UV transilluminator. The top band consists of chromosomal DNA as well as linear and nicked circular plasmid DNA, while the lower band consists of supercoiled ccc plasmid DNA. The lower band was collected using a hypodermic needle attached to a syringe. Ethidium bromide was removed from the solution by repeated extraction (3 or 4 times) with an equal volume water-saturated n-butanol until both the top organic and the lower water phases were colourless. The water phase (containing the purified ccc form) was diluted by the addition of 3 volumes of 1 x TE and the DNA ethanol precipitated at -20°C. DNA pellets were rinsed with 70% ethanol, dried and resuspended in 1 ml 1 x TE.

2.2.6. Characterisation of recombinant plasmids

Plasmids were isolated from colonies which were tet^R and amp^S and were analysed by horizontal electrophoresis in a 1% agarose gel with 1 x TAE electrophoresis buffer (40 mM Tris-acetate, 2 mM EDTA, pH 8.5) using plasmid pBR322 as control. Gels were prepared as described by Ausubel *et al.* (1987), adding EtBr to a final concentration of 0.5 µg/µl. Possible recombinant pBR322 clones (ccc plasmids which appeared larger than control) were further selected by dot blot hybridisation and restriction enzyme digestion with *Pst*I (Boehringer Mannheim). Reactions were performed in 15-20 µl volumes, containing 1-2 µg plasmid DNA, $^1/_{10}$ volume of 10 x restriction buffer, 10 U *Pst*I/µg of DNA and was incubated at 37°C for 3 h. Digestion products were analysed by agarose gel electrophoresis and the sizes of the DNA bands estimated by comparison to standard DNA markers of known molecular weight, eg. *Hind*III-digested λDNA (SMII) and *Hae*III-digested ϕX174 DNA (Promega).. Terminal sequences of all presumed full-length inserts were determined, by sequencing of the pBR recombinants, using primers that flank the pBR322 *Pst*I site (described in section 2.2.8).

2.2.6.1. Preparations of radiolabelled dsDNA probes by nick translation

The AHSV-9 segment 5 *Bam*H1 fragment (1.7 kb) was purified from an agarose gel using the Geneclean™ procedure (section 2.2.7.2). The fragment was labelled radioactively by nick translation (Rigby *et al.*, 1977) which utilises the enzyme DNaseI to produce nicks in the DNA and DNA polymerase I to translate the nicks with a combination of its 5' →3' exonuclease and polymerase functions, incorporating radioactively labelled nucleotides. A typical nick translation reaction (Promega) contained 1 µg linearised DNA, 0.02 mM each of dATP, dGTP and dTTP, 1 µCi/µl α-^{32}P-dCTP (>400 Ci/mmol; Amersham), nick translation buffer (50 mM Tris pH 7.2, 10 mM $MgSO_4$, 0.1 mM DTT), 1 U DNA polymerase I and 0.1 ng DNaseI. The incubation was at 15°C for 60 min and the reaction was terminated by the addition of EDTA, pH8.0 to a final concentration of 25 mM. The labelled probe was separated from the unincorporated nucleotides by chromatography on a Sephadex G-75 column. A column containing pre-swollen Sephadex beads was prepared using a 5 ml Pasteur pipette with a glass bead and equilibrated with 1 x TE buffer containing 0.5% SDS. Sample volumes were adjusted to 100 µl with ddH_2O prior to the addition to the column after which the column was rinsed with 12 x 100 µl buffer (1 x TE, 0.5% SDS) with simultaneous collection of fractions from the bottom of the column. Fractions were counted in a liquid scintillation counter (Beckman, LS 3801) and peak fractions were pooled.

2.2.6.2. Dot-blot hybridisation for the identification of recombinant pBR clones

Recombinant pBR plasmids were diluted to 100 µl in 1 x TE buffer and denatured by adding 5 µl of a denaturing buffer (0.5 M NaOH, 25 mM EDTA). Denatured DNA was spotted onto Hybond^{TM} N^+ nylon membranes (Amersham), pre-wetted in ddH_2O and equilibrated in 10 x SSC buffer (1.5 M NaCl, 0.15 M Na.citrate, pH 7.0), using a dot-blot apparatus coupled to a vacuum pump. Before and after spotting the DNA samples, each well was rinsed with 100 µl 20 x SSC under vacuum. Recombinant plasmid pSPT-AH9NS1 (Section 2.2.3) was included as positive hybridisation control and pBR322 as negative control.

The adsorbed DNA was fixed to the membranes by placing the nylon filters on an UV transilluminator for 5 min on each side. The membranes with fixed DNA were prehybridised in hybridisation buffer containing 5 x SSPE (0.75 M NaCl, 200 mM $NaH_2PO_4.2H_2O$, 20 mM EDTA pH 7.4), 50% deionised formamide, 0.1% fat-free milk powder, 0.2% SDS at 42°C for 30 min. The labelled probes were denatured by the addition of $^1/_{10}$ volume of 1 N NaOH and boiling for 5 min. The probe was placed on ice and neutralised by the addition of $^1/_{10}$ volume of 1 N HCL before being added to the membrane in hybridisation buffer and incubated for 16 h at 42°C. The membrane was washed twice for 10 min in 2 x SSC at RT with mild agitation, once in 2 x SSC, 0.5% SDS at 37°C for 20 min and once in 2 x SSC, 0.5% SDS at 65°C for 15 min. Autoradiography was carried out by exposing the membranes overnight to Cronex MRF-31 X-ray film at -20°C.

2.2.7. Restriction endonuclease mapping of AHSV-6 segment 5 cDNA

Restriction endonuclease mapping of the cloned AHSV-6 segment 5 cDNA (section 2.2.5) was performed by digesting the recombinant plasmid (pBRS5.2) with each of the following restriction enzymes either individually or in combination: *Bam*H1, *Bgl*II, *Eco*R1, *Eco*RV, *Cla*I, *Hind*III, *Hae*III, *Kpn*I, *Pst*I, *Pvu*I, *Sac*I, *Sma*I, *Sal*I, *Sty*I, *Xba*I and *Xho*I. Restriction enzyme digestions of plasmid DNA were carried out in the recommended salt buffer supplied with the enzyme (Boehringer Mannheim) for 1.5 h under the conditions as described in the protocols supplied with the restriction enzymes. Following restriction of the plasmid DNA, restriction fragments were analysed in 1% (w/v) agarose gel electrophoresis in 1 x TAE (40 mM Tris-HCL, 20 mM Na.acetate, 1 mM EDTA, pH 8.5) and sized according to their migration in the gel as compared to that of standard DNA molecular weight markers. The agarose gels were stained with ethidium bromide (0.5 µg/ml) and the DNA fragments visualised by UV fluorescence.

2.2.8. Subcloning of AHSV-6 NS1 gene

The full-length cDNA copy (pBRS5.2) was then recloned and subcloned into the pBS (Bluescript) cloning vector for sequence determination of the complete gene. The strategy for sequencing of the full-length segment 5-specific insert, involved the construction of subclones in pBS which together would span the full-length of the NS1 gene. By making use of the compiled restriction enzyme map, the subclones were constructed as follows: The 5'-terminal region of the cDNA copy (1-503) was excised from pBRS5.2 by *Pst*I and *HindIII* digestion. A subfragment corresponding to the region from nucleotide 503 to 1450 was excised by *HindIII* and *Xho*I digestion. A third subfragment corresponding to the 3' end of the cDNA (1450-1748) was generated by digestion with *Xho*I and *Pst*I. The 500 bp, 900 bp and 350 bp fragments was cloned into the *Pst*I & *Hind*III, *Hind*III & *Xho*I and *Xho*I & *Pst*I sites of the pBS cloning vector.

2.2.8.1. Vector dephosphorilation

In order to suppress recircularisation of linearised vectors, the digested vector DNA was dephosphorylated as described by Davis *et al.* (1986). The restriction enzyme was inactivated by heating the reaction to 65°C for 10 min. Linearised vector DNA (5 µg) was incubated at 37°C for 30 min in a 50 µl reaction volume, containing a 1:10 dilution of 10 x dephosphorylation buffer (50 mM Tris-HCL, 0.1 mM EDTA, pH 8.5), and 1 U calf intestinal alkaline phosphatase (1 U CIP/µl; Boehringer Mannheim). The vector DNA was then recovered by phenol-chloroform extraction and ethanol precipitation or by Geneclean™ II procedure out of agarose gel.

2.2.8.2. Purification of restricted DNA fragments

The restricted DNA fragments were purified either by using commercially available Geneclean™ DNA purification kit, glasswool or phenol-chloroform extraction. The Geneclean™ kit was used according to the instructions of the manufacturer for the purification of DNA fragments recovered from agarose gels. Briefly, the DNA fragment of interest was excised from the agarose gel and mixed with ca. 3 volumes of a NaI solution. The agarose was dissolved at 50°C after which 5 µl glassmilk was added to the suspension. After incubation on ice for 15 min with periodic agitation, the silica-bound DNA was pelleted by brief centrifugation and washed three times with 0.5 ml ice cold NEW wash (NaCl, Tris, EDTA, ethanol, water). The DNA was eluted from the silica at 50°C for 10 min in a final volume of 15 µl ddH_2O or 1 x TE. Alternatively, the gel slice was centrifuged through glasswool packed in an Eppendorf tube, the base of which had been pierced with a needle. The DNA was then collected by ethanol precipitation. As an alternative, the restriction enzyme-digested DNA was deproteinized by phenol-chloroform extraction as described in section 2.2.4.1.

2.2.8.3. Ligation of DNA fragments and transformation

Restricted vector and segment 5-specific fragments were ligated overnight at 15°C (or 4-6 h at 30°C) in 10 µl reaction volume which contained 1 µl of a 10 x ligation buffer (660 mM Tris-HCL, 10 mM DTT, 50 mM $MgCl_2$, 10 mM ATP, pH 7.5) and 1 U T4 DNA ligase (1U/µl; Boehringer Mannheim). The vector:insert molar ratios were typically in excess of approximately 1:3, as estimated by EtBr staining in an agarose gel.

Half the ligation mixture was used to transform competent *E. coli* XL1-Blue cells which were then plated onto amp and tet LB-agar plates containing X-gal substrate (50 µl of a 2% stock solution) and IPTG inducer (10 µl of 100 mM stock solution). Recombinant transformants were selected by blue/white colour selection, based on the inactivation of the *lacZ* gene. Recombinant transformants with Gal^- phenotype (which gave rise to white colonies) were selected for further characterisation and grown overnight at 37°C in 3 ml of LB-broth, supplemented with amp and tet.

2.2.9. DNA Sequencing of the cloned AHSV-6 NS1 gene

Sequencing was performed on phenol-chloroform, RNase-PEG or CsCl-purified double-stranded plasmid DNA templates using the dideoxynucleotide chain-termination method of Sanger *et al.* (1977) as adapted for dsDNA templates (Hatton and Sakaki, 1986; Riley, 1989). Reactions were carried out according to the protocols of the Sequenase™ Version II sequencing kit (United States Biochemical Corporation). The sequenase™ enzyme is a modified form of T7 DNA polymerase and its properties include high processivity, high speed, efficient incorporation of nucleotide analogues and the absence of 3'→5' exonuclease activity (Tabor & Richardson, 1987). Alternative purification methods, e.g. mini-prep

sequencing (Kraft *et al.*, 1986), glassmilk (BIO 101), or Wizard column (Promega) purification were also performed. All reactions were carried out according to the manufacturers' instructions. The concentration of the plasmid DNA was determined by measuring the absorbance at 260 nm (1 OD_{260}= 50 µg/ml dsDNA).

2.2.9.1. Denaturation of template DNA

Double-stranded plasmid DNA has to be denatured to a single-stranded template for sequencing. Plasmid DNA (1-2 µg) was diluted to 18 µl in ddH_2O and denatured by addition of 2 µl of freshly prepared denaturing buffer (2N NaOH; 2mM EDTA). After incubation at RT for 5 min, 3 µl 3 M Na.acetate pH 4.6, 8 µl 1 M Tris-HCL pH 7.4 was added and mixed, followed by 75 µl ice cold 100% ethanol and precipitated for 30 min at -20°C. The precipitated DNA was collected by centrifugation at 15 000 rpm for 10 min, rinsed with 200 µl ice cold 70% ethanol, vacuum-dried and resuspended in 7 µl ddH_2O.

2.2.9.2. Sequencing reactions

The universal M13/pUC sequencing primers 5'-GTTTCCCAGTCACGAC-3' and 5'-GTAAAACGACGGCCAGT-3' (Boehringer Mannheim) were used for forward and reverse priming on pUC based plasmids and pBR322-PstI (+) and (-) oligonucleotide primers (5'- GCTAGAGTAAGTAGTT-3' and 5'-AACGACGAGCGTGAC-3') for sequencing of pBR322 plasmids. In addition, two synthetic internal primers were used to sequence the full 900 bp *HindIII-XhoI* fragment.

To the denatured DNA, 1 µl (1 pmol) of the appropriate sequencing primer, 2 µl 5 x Sequenase buffer (200 mM Tris-HCL pH 7.5, 100 mM $MgCl_2$, 250 mM NaCl) were added in a final volume of 10 µl and incubated at 37°C for 30 min to allow annealing of the primer to take place. Extension and labelling of the DNA was obtained by adding 1µl 0.1 M DTT, 2 µl 1:5 diluted labelling mix (1.5 µM of each of dCTP, dGTP and dTTP), 0.5 µl ^{35}S dATP (1200 Ci/mmol, 10 mCi/ml, Amersham) and 2 µl Sequenase™ enzyme diluted 1:8 in dilution buffer (10 mM Tris-HCL pH 7.5, 5 mM DTT, 0.5 mg/ml bovine serum albumin), mixed and incubated at RT for 5 min. Reaction termination was accomplished by the addition of 3.5 µl of the labelled incubation mix to 2.5 µl of each of the termination mixes ddATP, ddCTP, ddGTP and ddTTP (each containing 80 µM of each dNTP, 50 mM NaCl and 8 µM of the appropriate ddNTP) prewarmed to 37°C in separate microfuge tubes. Termination reactions were incubated at 37°C for 5 min and the reactions were terminated by the addition of 4 µl stop solution (95% formamide, 20 mM EDTA, 0.05% bromophenol blue, 0.05% xylene cyanol).

2.2.9.3. Polyacrylamide gel electrophoresis

The sequencing reactions were electrophoresed in adjacent lanes of a high-resolution, denaturing polyacrylamide gel. The gels contained 6% acrylamide (w/v), 0.3% bisacrylamide (w/v) and 7 M urea as denaturant in 1 x TBE (90 mM Tris-HCL pH 8.3, 90 mM boric acid, 20 mM EDTA) and was polymerised by the addition of TEMED and 10% ammonium persulfate. The gel was pre-electrophoresed for 30 min before loading of the samples. The samples were heated to 95°C for 3 min before being loaded on the gel, and 2.5-3 µl was loaded per lane. Electrophoresis was carried out on a BRL model S2 sequencing apparatus, connected to a LKB 2197 power supply, at a constant power of 75 W (approximately 1800 V, 45 mA) in 1 x TBE. Following electrophoresis, the gel was fixed in 10% glacial acetic acid and 10% methanol to remove the urea, dried in a vacuum gel dryer for 1h at 80°C. Dried polyacrylamide gels with radiolabelled samples were exposed to Cronex MRF31 X-ray film at room temperature for 16 h or longer.

2.2.10. Preparation of AHSV-6 NS1-encoding tailored DNA copy by polymerase chain reaction

The manipulation of the segment 5 cDNA for the purpose of expression by a recombinant baculovirus, is illustrated in Fig. 1. The cDNA copy was modified by removing the 5' and 3' terminal homopolymeric dG/dC-tails (Nel and Huismans, 1990), by means of PCR (Saiki, 1988) using the enzyme Taq polymerase, and introducing two *Bam H1* sites at the 5' and 3' ends of the NS1 gene. Two 28 mer oligonucleotide primers were synthesised to modify and tailor the ends of the cloned segment 5 cDNA:
S5F: 5'-GACGGATCCAAACATGGATAGGTTCTT-3' and
S5R: 5'-GACGGATCCGATCTAATTATGCATGAAATC-3')
The primers were designed so that most of the 5' and 3' untranslated regions were deleted, but the Kozak sequence flanking the AUG was retained. These primers incorporated BamH1 restriction recognition sites at each terminal to facilitate subsequent DNA manipulations.

A PCR mixture was set up as follow. A 99.7 µl reaction mixture was composed containing 50 ng template DNA (pBRS5.2, the pBR322 recombinant containing the full-length NS1 gene), 100 pmol (800 ng) of each oligonucleotide primer (S5F and S5R), 10 µl of a 10 x Taq polymerase buffer (500 mM KCl, 100 mM Tris-HCL pH 8.4, 15 mM $MgCl_2$, 0.1% gelatin), 0.2 mM of each of dATP, dCTP, dGTP, dTTP (1 µl dNTP mix containing 25 mM of each dNTP) and 4 U Taq DNA polymerase (5 U/µl; Amersham). The reaction mixture was overlaid with three drops of liquid paraffin to prevent condensation and subjected to thermal cycling (Hybaid thermocycler). The template DNA was denatured at 94°C for 5 min after which the reaction mix was subjected to five cycles, with each cycle included a denaturation step at 94°C for 60 sec followed by annealing of the primers at 52 °C for 45 sec and DNA chain extension at 72°C for 2 min. The mix was subjected to a further 25 cycles of denaturation (94°C, 60 sec), primer annealing at 58°C for 45 sec and elongation (72°C, 2 min).

The resulting PCR product was then analysed by agarose gel electrophoresis after which it was recovered and purified by the Geneclean™ procedure (section 2.2.7.2). The identity of the purified product was confirmed by restriction with *Hind*III and *Xho*I, before being digested with *BamH1* and then cloned into the dephosphorylated (described in section 2.2.7.1) *BamH1* site of pBS. Recombinant pBS was further characterised by restriction enzyme mapping with *Hind*III and *Xho*I and a representative clone (pBS-S5PCR), containing the PCR copy of the NS1 gene in the correct orientation for transcription of the sense RNA to be directed by the T7 promotor, was selected.

To retain most of the original cDNA copy of the NS1 gene, the central ±1 kb region of the cloned PCR copy was excised by partial digestion with *HindIII* (position 503) and complete digestion with *StyI* (position 1588) and replaced with the corresponding region of the cDNA copy following the same strategy as in section 2.2.3. Partial digestions were performed as described in Ausubel *et al.* (1988). 2-4 µg pBS-S5PCR was diluted to 60 µl in the recommended salt buffer and aliquotted to nine Eppendorf tubes in 1 x 12 µl and 8 x 6 µl quantities. 0.5 µl *Hind*III (10 U/µl) was added to the 12 µl aliquot on ice and then 6 µl of the reaction mix was consecutively transferred to successive tubes in the series. The reactions were incubated for 1 h at 37°C and then analysed by 1% agarose gel electrophoresis. The reaction conditions yielding the greatest percentage of the desired partial digest, i.e. a DNA band corresponding in size to the 4.9 kb linear pBS-S5PCR plasmid, was calculated and the reaction was scaled up as follows: 1-2 µg pBS-S5PCR was incubated with 0.4 units *Hind*III in the recommended salt buffer in a final volume of 18 µl for 1 h at 37°C. The 4.9 kb DNA band representing the linear pBS-S5PCR, was excised from the gel and purified by Geneclean™ extraction. Recombinant pBS containing the complete NS1 chimeric gene was designated pBS-S5Hyb. The sequences of the 5' and 3' PCR ends of this chimeric gene were verified.

2.2.11. *In vitro* expression of the cloned genome segment 5 gene

2.2.11.1. *In vitro* transcription

The AHSV-6 NS1 chimeric gene, inserted into pBS transcription vector under the control of the T7 promotor (pBS-S5Hyb) was transcribed *in vitro* using T7 polymerase (Boehringer Mannheim). The purified DNA template was linearised by *Sall* restriction, which cuts at an unique recognition site downstream of the coding region of the S5 gene. After verifying complete linearisation by agarose gel electrophoresis, the enzyme was removed from the remaining sample by phenol-chloroform extraction, the DNA recovered by ethanol precipitation and resuspended in diethylpyrocarbonate (DEPC) treated ddH_2O. *In vitro* transcription reactions were performed in a 20 µl reaction mixture containing 1 µg of the linearised DNA template, 2 µl of a 10x transcription buffer (0.4 M Tris-HCl pH 8.0, 60 mM $MgCl_2$, 100 mM DTT, 20 mM spermidine), 30 U of human placental RNase inhibitor (Amersham), 3 µl of a rNTP mixture (2.5 mM of each rNTP), 40 U T7 RNA polymerase. The reaction was incubated for 90 min at 37°C. Samples were analysed on a 0.8% agarose gel using RNase free electrophoretic equipment.

Similarly, the AHSV-9 NS1 clones (pSPT-2.4PCR and pSPT-2.4Hyb; section 2.2.3) were linearised by *Eco*R1 digestion and then transcribed. *In vitro* transcription of recombinant pSPT clones was performed in a 50 µl reaction mixture containing 2-3 µg linearised plasmid DNA, 20 U T3 RNA polymerase, 10 µl 5 x transcription buffer, 10 µl of a rNTP mixture (2.5 mM of each rNTP), 5 µl 100 mM DTT and 30 U human placental ribonuclease inhibitor. Each reaction was incubated at 37°C for 90 min and aliquots were analysed as above.

2.2.11.2. *In vitro* translation

The *in vitro* synthesised mRNA transcripts were translated *in vitro* using nuclease treated rabbit reticulocyte lysates (Amersham) according to the manufacturer's instructions. The reaction mixture (50 µl) contained approximately 1 µg of *in vitro* synthesised AHSV-6 S5 mRNA, 4 µl of a 12.5x translation mixture lacking methionine, 2 µl 2.5 M potassium acetate, 1 µl 25 mM magnesium acetate, 20 µl rabbit reticulocyte lysate and 15 µCi of [^{35}S]-methionine. The reaction was incubated for 90-120 min at 30°C. Samples of the reaction mixture were resolved by SDS-PAGE and the translated products visualised by autoradiography. As a control, [^{35}S]-labelled proteins from AHSV-3-infected CER cells were included in the analyses.

Preparations containing 0.8-1.2 µg of purified AHSV-9 S5-specific mRNA transcripts were incubated in 10 mM MMOH at RT for 15 min for denaturation or alternatively incubated for 5 min at 85°C. Denatured mRNA transcripts were translated *in vitro* in a nuclease treated rabbit reticulocyte lysate system (Amersham). Each translation reaction (25 µl) contained 1-2 µg mRNA, 2.0 µl ^{35}S-methionine and 16 µl rabbit reticulocyte lysate and was incubated at 30°C for 90 min prior to SDS-PAGE gel electrophoresis.

2.2.11.3. SDS-polyacrylamide gel electrophoresis (PAGE)

Protein samples were treated with an equal volume of 2 x protein solvent buffer (125 mM Tris-HCL pH6.8, 4% SDS, 20% glycerol, 10% 2-mercaptoethanol), heated to 95°C for 5 min, sonicated and stored at -20°C until used. The samples were then separated by 12% SDS-PAGE as described by Laemmli (1970). The stacking gels contained 5% acrylamide in 1 x stacking buffer (125 mM Tris-HCL pH 6.8 and 0.1% SDS) and the resolving gels 12% acrylamide in 1 x separating buffer (375 mM Tris-HCL pH 8.8 and 0.1% SDS). The gels were polymerised chemically by the addition of 0.008% (v/v) TEMED and 0.08%

(m/v) ammonium persulfate. Electrophoresis was performed with 1 x TGS electrophoresis buffer (25 mM Tris-HCL pH8.3, 192 mM glycine and 0.1% SDS) in the Mighty Small II SE 250 system (Hoefer Scientific Instruments) for 2-2.5 h at 100-120 V or alternatively in the Sturdier SE400 vertical slab gel units (Hoefer Scientific Instruments) for 16 h at 80-90 V. Gels were stained in 0.125% Coomassie blue (Serva blue), 50% methanol and 10% acetic acid and destained in 5% methanol, 5% acetic acid at 50°C or 20% ethanol. Gels were dried on a slab gel-dryer for 1 h at 80°C under vacuum and dried gels exposed to Cronex MRF31 X-ray film for the appropriate lengths of time.

2.2.12. Expression of NS1 in insect cells with the BAC-TO-BAC baculovirus expression system

2.2.12.1. Construction of a recombinant bacmid transfer vector

pFastbac1, the donor vector in which the gene of choice is to be inserted, contains a strong polyhedrin promoter, upstream of an extensive MCS, to drive expression of the foreign gene. The baculovirus transfer plasmid, pFastbac1, was linearised with *Bam*H1, dephosphorylated and ligated to the full-length, tailored form of the segment 5 gene obtained by *Bam*H1 restriction from the pBS recombinant construct, pBS-S5Hyb. After transformation into competent *E.coli* XI1-blue cells and plating out on LB agar plates containing amp, gent and tet, plasmids from a number of the colonies obtained were isolated and characterised by restriction analysis and PCR (section 2.2.10). A recombinant plasmid (pFB-S5Hyb), which contained the NS1 gene in the desired transcriptional orientation relative to the polyhedrin promoter, was selected by *Hind*III and *Xho*I restriction enzyme digestion and PCR using polyhedrin primer and the reverse primer S5R.

2.2.12.2. Transposition and isolation of recombinant bacmid DNA

E.coli DH10BAC™ cells, containing the bacmid genome (baculovirus shuttle vector) as well as a helper plasmid, was transformed with the recombinant transfer plasmid pFB-S5Hyb according to the manufacturer's specifications (Life Technologies). Briefly, 100 µl of competent DH10Bac cells were mixed with 100 ng donor plasmid and incubated on ice for 30 min. The cells were heat shocked at 42°C for 45 sec, 900 µl SOC medium added and incubated for 4 h at 37°C with agitation. Recombinants were selected on LB plates containing kanamycin (50 µg/ml), gentamycin (7 µg/ml), tetracyclin (10 µg/ml), IPTG (40 µg/ml) and X-gal (300 µg/ml). The bacmid genome carries the *lac Zα* gene and when used to transform *lac*⁻DH10BAC™ cells, produces a functional ß-Galactosidase protein. Therefore, cells containing the bacmid genome produce a blue colour on plates containing X-gal and IPTG. Transposition of the *Tn7* element into the bacmid genome by the pFastbac1 plasmid results in the disruption of the *lac Zα* gene resulting in the production of white colonies on plates containing X-Gal and IPTG. The white colonies are therefore bacmid-containing colonies that have undergone successful transposition and are thus selected for isolation of recombinant bacmid DNA. Several white colonies were selected and replica plated onto fresh LB-agar plates containing antibiotics and histochemicals, in order to distinguish true whites. Once a suitable colony was found, a liquid culture for isolation of composite bacmid DNA was set up.

High molecular weight recombinant bacmid DNA was isolated by the rapid alkaline lysis method modified for the isolation of large plasmid DNA (Amemiya *et al.*, 1994). The recombinants were verified by means of PCR of the isolated bacmid DNA, using primers S5F and S5R. One of the recombinant clones were selected randomly and was designated BAC-5.2Hyb.

2.2.12.3. Transfection of Sf9 cells with the recombinant baculovirus shuttle vector

The purified recombinant bacmid DNA (BAC-S5Hyb) was transfected into *S. frugiperda* cells using cellfectin reagent™ (Life Technologies), according to the instructions of the manufacturer. This is a DNA transfection procedure which makes use of a synthetic cationic lipid that forms liposomes which interact spontaneously with DNA, fuse with tissue culture cells and facilitate the delivery of functional DNA into the cell (Felgner *et al.*, 1987; Summers & Smith, 1987). Sf9 cells were seeded in 35 mm wells (1.2 x 10^6cells/well) and following attachment of the cells for 1 h at RT, were rinsed twice with Grace's medium, lacking FCS (serum proteins inhibits lipofection). A further 1 ml FCS-free medium was then added to the cells. The recombinant bacmid DNA (1 µg) was diluted with 100 µl Grace's medium without antibiotic and FCS. In a separate tube, 6 µl of the cellfectin reagent was diluted to 100 µl with Grace's medium. Just prior to transfection, the two solutions were mixed and added dropwise to the monolayers of SF9 cells. After an incubation period of at least 5 h at 28°C under humid conditions, the transfection mixtures were removed and replaced with 2 ml Grace's medium supplemented with 10% FCS. The cells were then incubated at 28°C until evidence of baculovirus-infected cells was obtained (3-4 days). The supernatant, containing the recombinant baculoviruses (BV-NS1), was harvested from transfected cells and used for plaque assays. Viral stocks were prepared from single plaques using standard virological procedures described by Summers and Smith (1987).

2.2.12.4. Virus titration and plaque purification

In order to obtain purified single plaques or to determine virus titre, a method based on the procedures described by Brown and Faulkner (1977), Possee and Howard (1987) and Kitts *et al.* (1990) was used. A dilution series of the transfection supernatant or virus stock was prepared from 1.0 x 10^{-1} to 1.0 x 10^{-9} in 1 ml medium. Sf9 cells were seeded in 35 mm diameter wells at a density of 1.2-1.5 x 10^6 cells/well and after adsorption for 1 h at RT, the medium was replaced with 1 ml of the virus dilutions. The virus was left to adsorb to the cells for 2 h after which the inoculum was removed and the cells gently overlaid with sterile 3% low melting agarose at 37°C diluted 1:1 in Grace's medium. The dishes were incubated at 27°C for 4 days in a humid environment. The cells were then stained with 2 ml Neutral Red (100 µg/ml in Grace's medium) for 5 h at 27°C. The liquid overlay was removed and the dishes were incubated overnight before screening the plaques. Putative recombinant white plaques were removed as an agarose plug with a sterile pasteur pipette, transferred to 1 ml Grace's medium, vortexed and stored at 4°C (approximately 10^4 pfu/plug). High titre viral stocks were prepared by infecting monolayer cultures at a MOI of 0.01 to 0.1 and harvesting the virus at 96 h p.i.

2.2.13. Radiolabelling and SDS-PAGE analysis of recombinant viral proteins

Monolayers of Sf9 cells were infected with wild type or recombinant baculovirus stocks (BV-NS1) at a multiplicity of 10-15 pfu/cell and incubated at 28°C. Cells were harvested at 72 h post-infection, washed with phosphate-buffered saline (1 x PBS) and resuspended in 10 mM Tris (pH 7.4), 1 mM EDTA, 150 mM NaCl (0.15 M STE). Equal volume 2 x protein dissociation buffer was added to the sample and the proteins analysed by 12% SDS-PAGE and the resolved proteins were stained with Coomassie brilliant blue.

For radiolabelling of viral proteins, Sf9 cells were infected as described above. After 2 h, the inoculum was replaced with Grace's medium to ensure synchronised infection, and incubated at 28°C for 36 h. The medium was replaced with 500 µl methionine-free Eagle's medium and incubated at 28°C for 1 h to

deplete intracellular pools of methionine. The met-free medium was replaced with 500 µl fresh methionine-free Eagle's medium supplemented with 15 µCi/ml [^{35}S]-methionine, followed by a labelling period of 3 h with gentle agitation. Cells were harvested and treated as above prior to loading on a SDS-PAGE gel.

For the preparation of radiolabelled AHSV-3 viral proteins, 75 cm^3 monolayers of BHK or CER cells grown in Eagle's medium containing 6% FCS were rinsed with serum-free Eagle's medium and infected with 2-3 ml AHSV-3 inoculum with high titre. After 1 h at 37ºC, 5 ml additional serum-free Eagle's medium was added and incubated overnight at 32ºC. At 16-18 h pi, the virus was removed and replaced with 3.0 ml methionine-free Eagle's medium. After 1 h at 32ºC, the medium was replaced with 3 ml fresh methionine-free Eagle's medium to which approximately 30 µCi/ml [^{35}S]-methionine was added. After a 3 h incubation period at 37ºC, the cells were washed with PBS and then resuspended in 300 µl lysis buffer (50 mM Tris-HCl (pH 7.4), 20 mM EDTA, 150 mM NaCl, 1% Triton X-100, 0.1% SDS). MOCK infected Sf9 and BHK or CER cells were labelled in the same manner for use as controls.

2.2.14. Purification of NS1 tubules

Monolayers of Sf9 cells were infected with the recombinant baculovirus at a MOI of 5 pfu/cell and the infected cells were harvested 3 or 4 days post-infection. The cells were harvested, washed with 1 x PBS, and collected cells were resuspended in 0.15 M STE buffer and the cell membranes mechanically disrupted with a dounce homogeniser. The nuclei was then removed from the cytoplasmic fraction by low speed centrifugation (2000 rpm for 5 min) and the pellet washed once with 0.15 M STE and the supernatant was added to the cytoplasmic fraction. The cytoplasmic extract was loaded onto a 20 to 50% (W/V) sucrose gradient in 0.15 M STE (pH 7.4) buffer. Centrifugation was carried out for 3 h at 40 000 rpm using a SW50.1 rotor. The gradient was fractionated and a portion of each fraction was subjected to gel electrophoresis, following TCA precipitation of the proteins. The fractions containing predominantly the NS1 protein were pooled after which protein complexes were collected by centrifugation for 2 h at 40 000 rpm. The pellet was resuspended in 0.15M STE buffer.

2.2.15. Electron microscopy and biophysical analysis of tubule morphology

The purified NS1 tubules were adsorbed onto carbon-coated copper 400-mesh electron microscopy grids for 1 min, washed with water, and negatively stained with 2% potassium-phosphotungstic acid (pH 6.4 and 7.0) or with 2% (w/v) uranyl acetate. Alternatively, purified NS1 was adsorbed for 10 min on a grid, washed with 1 x PBS and incubated for 30 min in different dilutions of guinea pig anti-AHSV-6 antiserum. The grids were washed with ddH_2O and negatively stained with 2% (w/v) uranyl acetate and observed in a Hitachi H-600 electron microscope at 75 kV. Freeze-dried specimens were prepared on 5 mm diameter carbon discs. Samples of the tubule suspension (5 µl) were applied to the surface of the discs which were blotted with the filter paper for 1-6 s and then rapidly plunged into liquid propane cooled by liquid nitrogen at -170ºC. The frozen specimens were then freeze dried at -80ºC and coated with chromium in a Gatan 681 ion beam coater. The discs were observed in a Jeol 6000 field emission SEM. Monolayers of Sf9 cells infected with the NS1 recombinant baculovirus were fixed with 3% glutaraldehyde 2 days post-infection. Thin sections were prepared as described by Huismans and Els (1979) for microscopy in a Hitachi H-600.

Aliquots of purified NS1 tubules were pelleted for 20 min at 16 000 rpm and the pellets were resuspended in various test solutions for 30 min. Following centrifugation for 5 min at 2000 rpm, the pellets and supernatants were analysed for the presence of NS1 protein by SDS-PAGE. The treated tubules (as described in the results) were also examined by means of electron microscopy after negative staining with 2% uranyl acetate.

2.3. RESULTS

When this study was initiated a cDNA copy of the NS1 gene of AHSV-9 had previously been cloned and the sequence determined. The nucleotide sequence of the cloned gene revealed that it contained the conserved specie specific 5' and 3' sequences present in AHSV and an ORF encoding 548 amino acids, indicative of a full-length copy of the dsRNA genome segment 5 (L. Nel, unpublished data). However, expression of the gene using a recombinant baculovirus failed to produce a protein of the expected size (results not shown).

The cloned AHSV-9 NS1 gene was then further characterised by *in vitro* expression to determine if the ORF had been retained during the PCR manipulations of the NS1 gene. Both a PCR tailored copy and a PCR-cDNA chimeric NS1 gene were cloned into the pSPT-19 *in vitro* expression vector in the correct orientation for transcription of mRNA, under the control of the T7 promoter located upstream from the start codon of the gene. mRNA transcripts, synthesised using T7 RNA polymerase (section 2.2.11.1), were translated *in vitro* before and after denaturation (section 2.2.11.2). The [^{35}S]methionine-labelled translation products were identified by autoradiography following SDS-PAGE. A prominent protein product of approximately 42 kDa was repeatedly found, expressing both the PCR and chimeric genes, with and without denaturation of the mRNA transcripts (*Figure 2.1*). This 42 kDa protein may represent a truncated form of the NS1 protein due to premature translation termination. The

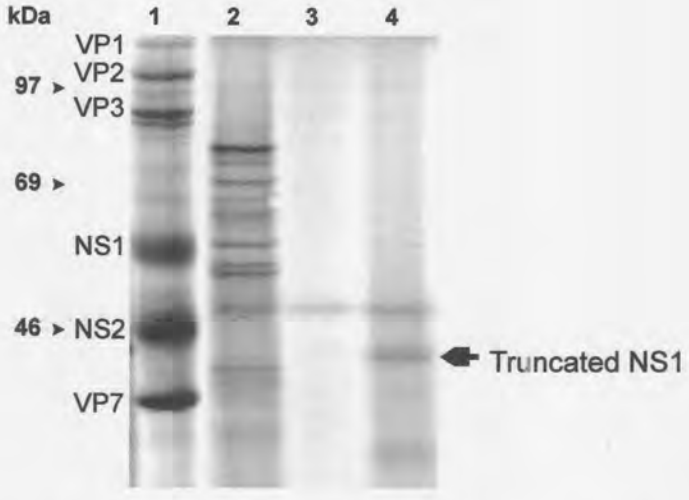

Figure 2.1: Autoradiograph of the ^{35}S-methionine labelled *in vitro* translation product of AHSV-9 NS1 gene separated by SDS-PAGE. Lane 1 represents cell lysates of CER cells infected with AHSV-3. Lanes 2 and 3 represent rabbit reticulocyte translation products in the presence and absence of any input mRNA (provided by the manufacturer) as positive and negative controls, respectively. Lane 4 contains the translation products of mRNA synthesised from the NS1 gene. The position of the truncated translation product is indicated.

truncated protein does not appear to be the result of secondary structures in the mRNA or shortened mRNA, but may be a result of an insertion or deletion mutation, which resulted in a shift in the reading frame and premature translation termination.

Since the existent copy of the NS1 gene resulted in the expression of a truncated protein, it was decided to clone a full-length NS1 gene from a pool of AHSV-6 dsRNA enriched in segments 4, 5 and 6.

2.3.1. Cloning and characterisation of AHSV-6 NS1 gene

AHSV serotype 6 dsRNA was isolated from infected CER cells by Grant Napier using the phenol-SDS method (Huismans & Bremer, 1981) and contaminating ssRNA and tRNA removed by LiCl precipitation and sucrose gradient fractionation, respectively. Double-stranded cDNA was prepared from a pool of medium-sized dsRNA fragments, purified by two successive sucrose gradient fractionation steps, using the methods described by Huismans and Cloete (1987). Since the separation of segment 5-specific cDNA from segments 4 and 6 was impossible, the pool of synthesised cDNA of AHSV-6 medium-sized dsRNA segments, including segment 5, was cloned into the *PstI* site of pBR322 by the dG/dC-tailing cloning method (outlined in *Figure 2.2A*). Plasmid DNA was extracted from the 14 ampicillin-sensitive and tetracycline-resistant recombinants (pBR-S5.1 - pBR-S5.14). All plasmids that appeared to contain inserts after sizing were characterised further. The identity of clones with possible NS1 inserts were verified by means of dot blot hybridisation, using a radiolabelled AHSV-9 NS1 gene (pSPT-2.4PCR) as a probe (*Figure 2.3A*). The size of the inserts was estimated by excision with *Pst*I and comparison of their mobilities to DNA molecular size markers on an agarose gel (*Figure 2.3B*). Of the recombinants obtained, 43% proved to be NS1-specific, for they subsequently hybridised with the probe. In four of the clones the inserts were approximately 1.7 kb in size and was assumed therefore to be full-length NS1 genes, while two other clones (p5.4 and p5.9) contained smaller inserts (1.2 and 1.5 kb) and were probably partial NS1 clones. The other inserts were either VP4 or VP5-specific. Two representative full-length clones of the NS1 gene were selected. The sizes of the inserts in both recombinant plasmids were found to be approximately 1.7 kb and the clones were sequenced in triplicate in both directions. The nucleotide sequences of the 5' and 3' terminal ends revealed the presence of the conserved 5' and 3' hexanucleotides, which proved that the inserts represented full-length clones of the AHSV-6 NS1 gene. The two AHSV-6 segment 5-specific cDNA clones were designated pBR-S5.1 and pBR-S5.2.

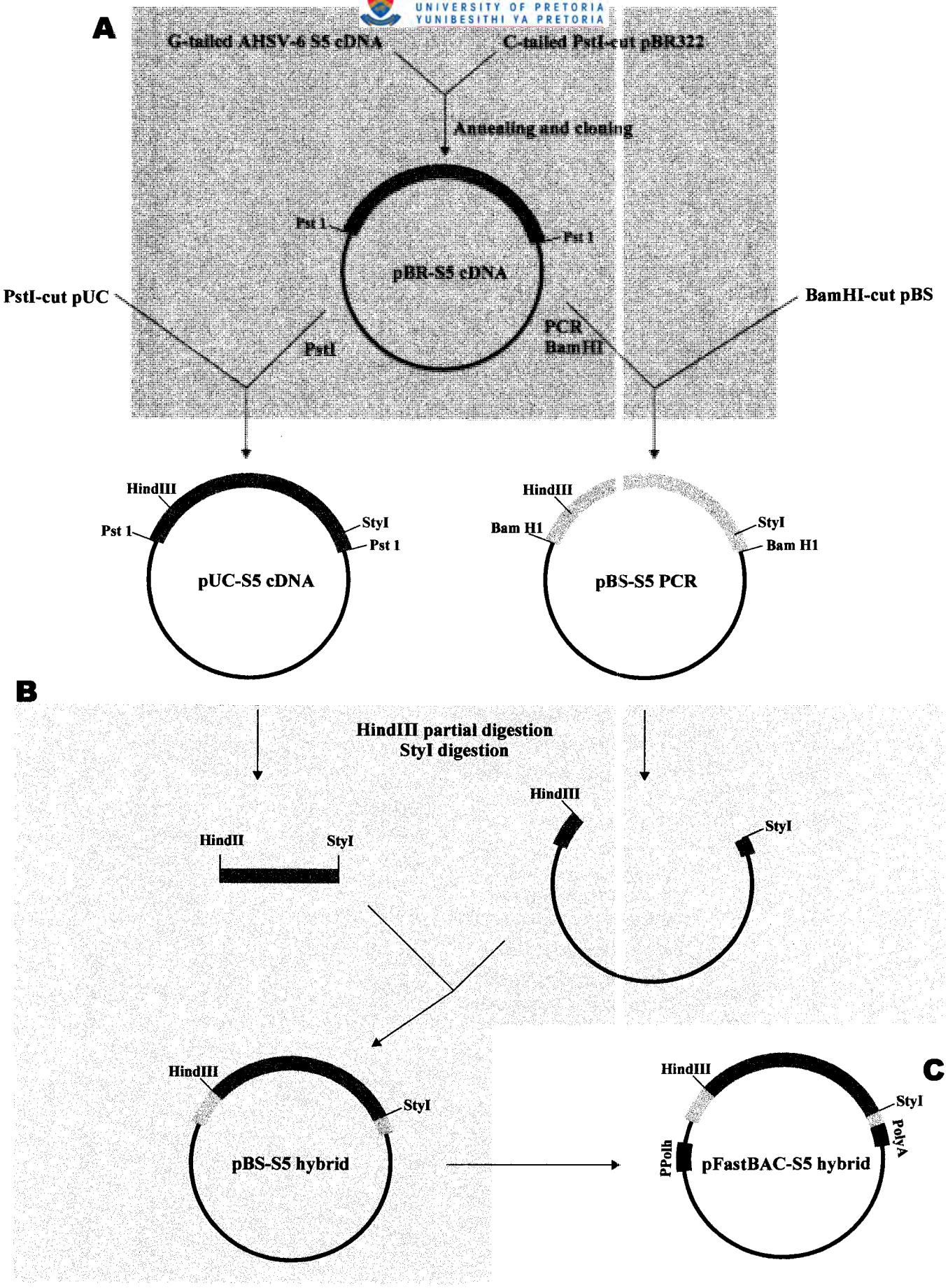

Figure 2.2: Cloning strategy for expression of NS1. A full-length cDNA copy of AHSV-6 NS1 gene was cloned by dG/dC-tailing into pBR322 (A). The cDNA copy of the NS1 gene was cloned into pUC18 for sequencing purposes. The homopolymeric tails were removed by means of PCR and a chimeric gene constructed between the PCR and the original cDNA copy of the NS1 gene (B). Finally a recombinant baculovirus transfer vector, containing the NS1 chimeric gene, was constructed (C). See text for details.

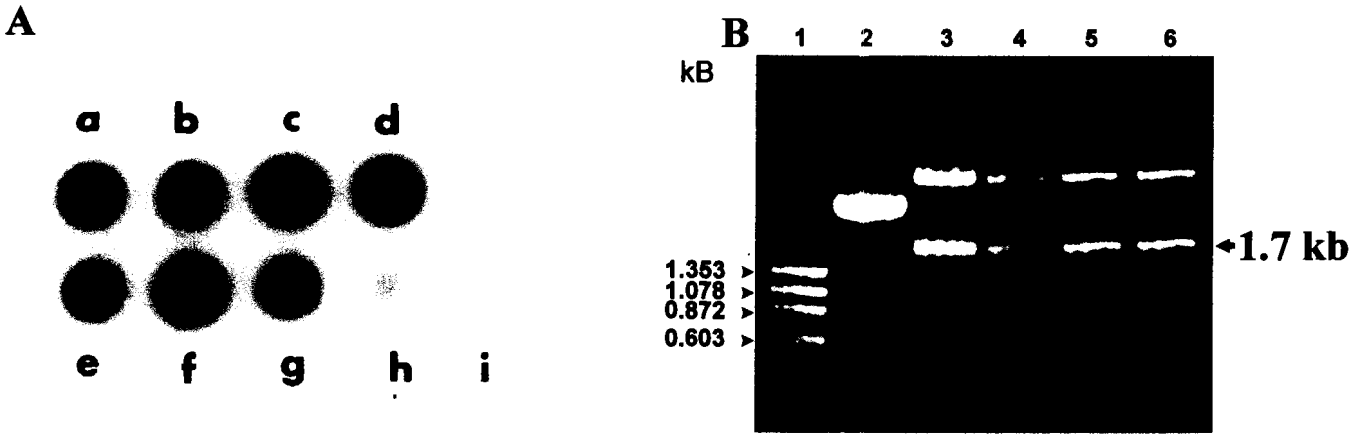

Figure 2.3: (A) An autoradiograph representing dot blot hybridisation of a ^{32}P-labelled AHSV-9 segment 5-specific probe to the recombinant pBR322 plasmids to confirm the identity of the inserts. Controls were plasmid pSPT-AH9NS1 (d), wild type pBR322 (h) and pBS-AH9VP5 (i) The recombinant pBR clones represented in a-c and e-g were p5.1, p5.2, p5.4, p5.7, p5.8 and p5.9. (B) Agarose gel electrophoretic analysis of recombinant plasmids, derived by cloning the cDNA copy of AHSV-6 segment 5 by means of dG/dC-tailing into the *PstI* site of pBR322. The recombinant plasmids p5.1, p5.2, p5.7 and p5.8 after restriction with *PstI* (lanes 3 to 6). The 1.7 kb insert is indicated by an arrow. Lane 1 contains the molecular weight marker and the sizes are indicated to the left of the figures. Lane 2 contains linearised pBR322.

2.3.2. Restriction enzyme mapping and subcloning of AHSV-6 NS1 gene

The strategy for determining the complete sequence of the AHSV-6 NS1 gene necessitated the construction of a series of overlapping restriction endonuclease subclones in pBS. Limited restriction maps of the clones were prepared by individual or combined digestion with various restriction enzymes, described in materials and methods. The restriction enzyme analysis revealed the presence of a *Hind*III site approximately 500 bp from the 5' end, *Xho*I, *Sma*I and *Sty*I sites 300 bp, 40 bp and 150 bp from the 3' end respectively. The compiled restriction enzyme map of the NS1 gene is shown in *Figure 2.4*. The restriction sites were used to prepare the sub-fragments from the full-length NS1 genes (S5.1 and S5.2) which were subcloned into pBS.

Recombinants of interest were purified using different DNA purification methods for sequencing (section 2.2.5). The best sequencing results were obtained with RNA-free CsCl-purified ccc plasmid DNA, although phenol-chloroform purified plasmids also gave consistent good results and were used for most of the sequencing.

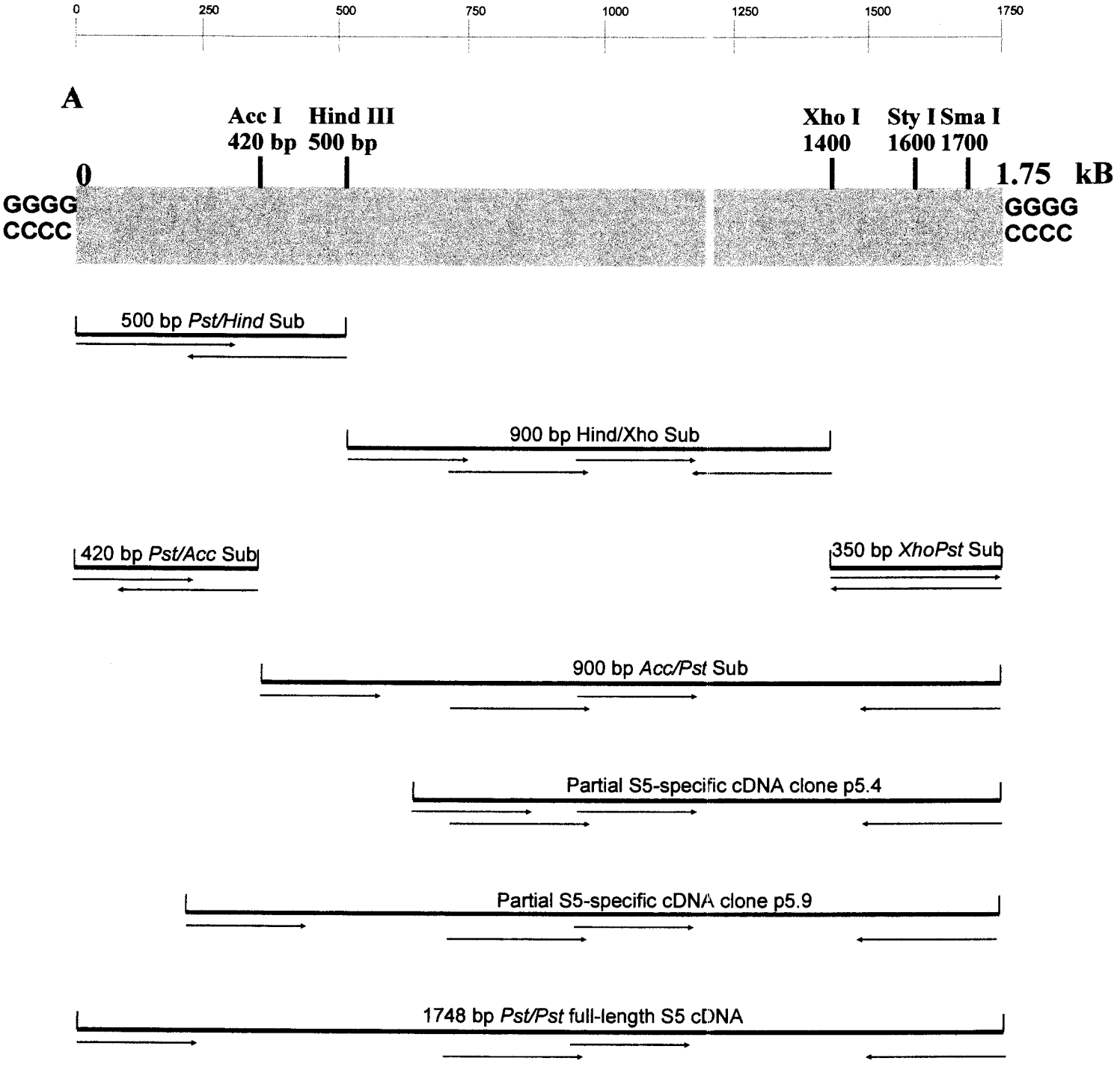

Figure 2.4: NS1 subclones prepared from NS1-specific cDNA clones p5.1 and p5.2 for sequencing, positioned relative to the full-length gene. The subclones are indicated below the NS1 gene, with the position of the restriction sites indicated on the full-length gene as approximate positions in bp from the 5' end of the gene, estimated from gel sizing analysis. Arrows indicate the distance each subclone was sequenced, using M13 primers. Internal NS1-specific primers were used to reach the center of the NS1 gene. Two partial NS1-specific cDNA clones (p5.4 and p5.9) were also used for sequence determination.

2.3.3. Characterisation of the AHSV-6 NS1 gene and deduced amino acid sequence

2.3.3.1. Nucleotide sequence of the AHSV-6 NS1 gene and comparison to the cognate genes of other orbiviruses

The complete nucleotide sequence of AHSV-6 segment 5 gene was determined using different restriction endonuclease subclones, derived from the full-length cDNA copy, in addition to the intact full-length and truncated, overlapping cDNA clones. *Figure 2.4* illustrates the regions of the NS1 gene represented in the different clones and the portion of each clone, which was sequenced. All templates were sequenced at least twice and in both orientations. Sequencing was carried out with the appropriate pBR322-specific primers, M13/pUC forward or reverse primers or with synthetic oligonucleotide primers based on previously determined sequences. By merging the sequences, the complete nucleotide sequence of the NS1 gene of AHSV-6 (*Figure 2.5*) was compiled using the computer program CLUSTAL W (Higgins & Sharp, 1988).

The complete NS1 gene of AHSV-6 (accession number U73658) was found to be 1748 nucleotides in length, with a calculated base composition of 29.98% A, 25.30% G, 28.27% T and 16.45% C. The longest, single open reading frame (ORF) observed contained 1645 base pairs and begins with a translation initiation codon, AUG, at positions 36 to 38. The ORF extended for 548 codons and terminated at nucleotide positions, 1680 to1682 with an UAA codon. The gene was flanked by a 5' and a 3' non-coding region of 35 and 70 nucleotides, respectively. The first 6 nucleotides at the 5' end and the last 6 at the 3' end of the gene are identical to the conserved sequences at the termini of the species AHSV, RNA segments (5'GTT$^{A}/_{T}A^{A}/_{T}$... and ...AC$^{A}/_{T}$TAC3')(Van Staden *et al.*, 1991; Yu *et al.*, 1988). In addition, a near perfect inverted repeat sequence of 11 to 12 bp was identified in the 5' and 3' non-coding regions of the AHSV-6 NS1 gene (see *Figure 2.5*). The flanking sequences of the AUG codon, CAAACATGG, conformed fully to the eukaryotic consensus sequence for initiation of translation (CX$^{A}/_{G}$XCAUGG) proposed by Kozak (1981, 1984 & 1987). The ATG codon is flanked by an A at position -3 and G at position +4 respectively, which is a favourable context for the initiation of protein synthesis according to Kozak's model.

In comparative analyses with analogous orbiviral genome segments (*Table 2.1*), AHSV-6 genome segment 5 was found to be very similar in composition to AHSV-4/9, BTV-10/13/17 and EHDV-2. Homology comparisons of the AHSV-6 segment 5 gene and encoded protein to the cognate genes and proteins of AHSV-4 and 9 were performed at sequence level using the CLUSTAL W and ANTHEPROT (Deléage *et al.*, 1988; Deléage *et al.*, 1989) computer

programs. The nucleotide comparison revealed a 97%, 94% and 93% conservation of nucleotides in type and position between serotypes 4 and 6, 4 and 9, 6 and 9 respectively (*Table 2.2*). Although the 3' non-coding region of the NS1 encoding gene of AHSV-4 was three nucleotides shorter than AHSV-6 and AHSV-9, the non-coding regions were identical among the three AHSV serotypes.

[redacted]gaacctaggcggtttggcaacacacaaac**ATG**GATAGGTTCTTGACTTATTTCCAGGTACGAGGAGAGAGA
GCAAACGCTGTTCGGCTGTTTGGAGAGATTTCCGAACAAATAGATTGCTCACATCTCAAACGAGATT
GCTTTGTAAATGGAATATGTGCAAGACAACACTTTAAAGAATGCTGTAATATTGCTACAGATAATGGC
TCACGCACAAATGCAGATAAACTAGTGGCTTTAGCTTTGCGAGCACTTTTAGATAGACAAACTATTTG
GACTTGTGTCATCAAAAATGCGGATTACGTTAGTCAATATGCTGATGAGCAGATGGAGGAAGAAGTT
AATAAGCTGTATGATGTCTATCTCCAGAGCGGGACGAGAGAGGAATTTGAAGGATTTAGACAGAGG
AATAGACCGAGTAGAGTTGTGATGGATGATAGCTGCTCAATGCTCTCATATTTTTACATTCCAATGAA
TCAAGGGAATCCAGCTCCAGTTGCCAAGCTTAGCCGATGGGGTCAATTTGGAATTTGTTACTATGAT
AGAACAAATGTTGATGGATTGATTCCGTATGATGAGATCGGTTTAGCTCAAGCTATAGACGGCCTAA
AGGATCTGATTGAAGGGCGATTGCCCGTTTGCCCTTATACTGGAGCGAATGGTAGAATTAATGCTGT
TTTACATTTACCATTAGAGATGGAGGTGATTATGGCGGTGCAGGAAAATGCAACACAATTAATGCGT
AGAGCGGCACAGGATTTCAAATTCATCACACATGCTGGATGGAGGCTATATCCAAGATTGTTGCGAC
AACGGTTCGCGATCGAGGACGCTACGGAGGGGGTGATTCATCATGTGATGCTAGGCCATTTAAGAT
ATTATGATGAAGATACAAGTATCGTGAAGTATCGCTTCCTTAACGATGGATCTTTAGATTGGAGGACT
TGGACAATTCCTTTACATCTGATGCGGACAGCAAGGTTGGGACATCTGCAACCGGAATCAATTTTAG
TCTTTATGCATAAAAGCCTACATGTCAGGTATGCTTTATGGTTGACCTCGCTCTGCTTGACACAATCC
CGGTGGTTGATTCAAAAGTTGCCTGAACTAACAGGAGGCACAGATGTACTTTATACACGTGCGTATG
TACATGCGGACAATCACAAAGTGCCAAATGTCAGAGATTTGATGATGAATGAAGTCTTCAGGAAGAT
CGATGATCATTGGGTGATTCAGAAGTGTCATACAACGAAGGAAGCGATTACTGTAACTGCAATTCAG
ATTCAGAGGTCGATCAGAGGTGATGGGCAGTGGGATACTCCGATGTTTCACCAATCAATGGCTCTG
TTAACACGATTGATTGTTTATTGGTTAACGGATGTGACTGAGAGAAGTGCTATCTTTCGGCTGACTTG
TTTCGCAATCTTCGGATGTAAGCCAACGGCTCGAGGTAGATATATTGATTGGGATGATCTTGGAACA
TTCATGAAGAATGTCTTGGATGGAAGAGATTTGACTGTTTTGGAAGATGAGACATGTTTTATTTCGAT
GATGAGGATGGCGATGTTGCATGTGCAGAGATCCAAGGTAGTGTGCGCAACTGTGTTGGAGGCGC
CATTAGAAATACAACAGGTTGGCCAGATCGTTGAAGTACCCTTTGATTTTATGCA**TAA**ttagattaaatttaaa
agtttgtacccgggaagtaggttaagatcatatcccctggttcacaa[redacted]

Figure 2.5: The complete nucleotide sequence of the NS1-encoding segment 5 cDNA of AHSV-6. The conserved 5' and 3' hexanucleotide sequences are highlighted in dark grey and the inverted heptanucleotide repeats in light grey. The translation initiation and termination codons are indicated in bold, while the ORF is indicated in capital letters. The ORF begins at position 36 to 38 and is terminated by the TAA codon at positions 1680 to 1682.

TABLE 2.1: *Comparative analysis of orbiviral NS1 gene nucleotide sequences*

Orbivirus	Length (bp)	Base composition				Non-coding region (bp)		Coding region (bp)
		%A	%C	%G	%T	5'	3'	
AHSV-6	1748	30.0	16.50	25.30	28.30	36	66	1644
AHSV-9	1751	29.98	16.45	25.30	28.27	36	69	1644
BTV-10	1769	31.0	17.7	23.7	27.7	34	79	1656
EHDV-2	1806	34.1	15.2	24.7	26.0	32	118	1656

TABLE 2.2: *The degree of nucleotide conservation of the NS1 gene of different AHSV serotypes and other orbiviruses. The similarities between AHSV-6 and the latter viruses are expressed as percentages of nucleotides identical in type and position.*

COMPARISON	AHSV-4	AHSV-9	BTV-10	BTV-13	EHDV-2
AHSV-6	97%	93%	44%	48%	42%

The nucleotide sequence of AHSV-6 NS1 gene was subsequently compared to the cognate genes of other orbiviruses. In a comparison of the AHSV-6 NS1 gene to that of BTV-10/13 (Lee & Roy, 1987) and EHDV-2 (Nel *et al.*, 1990), homologies of 44-48% and 42% were respectively observed The results are summarised in *Table 2.2*. A comparison of the 5' and 3' non-coding regions of the different NS1 genes revealed that the 35 nucleotide 5' non-coding region of the AHSV-6 NS1 gene is 1 and 3 nucleotides longer than that of BTV-10 and EHDV-2 and displayed a nucleotide homology of 71% and 69%, respectively. However, the 3' non-coding region of 70 nucleotides is 9 bp and 48 bp shorter than that of the cognate BTV-10 and EHDV-2 genes and displayed a nucleotide homology of 44% and 36%, respectively. Alignment of the AHSV-6, BTV-10 and EHDV-2 NS1 gene coding regions indicated a nucleotide homology of 43% and 41%, respectively.

2.3.3.2. Amino acid sequence of the AHSV-6 NS1 protein and comparison to the gene products of other orbiviruses

The amino acid sequence of AHSV-6 NS1 was deduced from the nucleotide sequence of the NS1 gene, using the ANTHEPROT computer program (Deléage *et al.*, 1988; Deléage *et al.*, 1989). The ORF of the NS1 gene is capable of encoding a polypeptide of 548 amino acids with a calculated molecular weight of 63 478 Da and a net charge of +5 at a neutral pH (*table 2.3*).

On protein level, 95%, 92% and 96% of the amino acids were identical in type and position in the comparison between AHSV serotypes 4 and 6, 4 and 9, 6 and 9 respectively (*Figure 2.6*). When amino acids of similar character were taken into consideration the homology increased to 96%, 94% and 98% in the alignments between 4 and 9, 4 and 6, 6 and 9 respectively. The N- and C-terminal regions of the cognate proteins shared the greatest levels of homology. Alignment comparisons (*Figure 2.7*) of the NS1 amino acid sequences between AHSV-6 and BTV-10/13/17, and AHSV-6 and EHDV-1/2 revealed an overall homology of 19% and 25% respectively, when only identical amino acids were taken into account. However, when both identical and similar amino acids were considered, the homology increased to 34% and 44%, respectively. The percentage homology found in each case is summarised in *Table 2.4*. In a three way best fit alignment, the aligned NS1 sequences could be divided into alternating regions of higher and lower similarity, as shown in *Figure 2.8*, and the N-terminal ends (aa 1-180) of the NS1 proteins were found to be generally more conserved than the C-terminal ends. The central region (aa 180-400) was the least conserved. Highly conserved regions of about 10 to 20 amino acids which contained a high percentage (> 70%) of identical amino acids could be identified in the three way comparison (*Figure 2.8*).

The amino acid composition of the AHSV-6 NS1 protein, together with that of the NS1 proteins of BTV and EHDV-2, is summarised in *Table 2.3*. AHSV NS1 contains 14 cysteine residues, while the BTV and EHDV counterpart contain 16 and 17 cysteine residues, respectively. The 14 cysteine residues were found to be conserved among AHSV-4, 6 and 9 and only 7 of these were conserved between AHSV-6 and BTV-10 with two more cysteine residues conserved in the immediate region. Furthermore, the three NS1 proteins contain similar amounts of tryptophan, tyrosine, serine and threonine residues. A characteristic feature of AHSV-6 NS1 is the abundance of hydrophobic residues and the low number of charged amino acids. The NS1 protein of AHSV-6, especially the C-terminal 400 amino acids, is highly hydrophobic, with a hydrophobic amino acid content of more than 43.6% and only 26.1% charged amino acids. The hydropathic plots of the three AHSV serotypes are nearly identical. The predicted hydrophilicity profile (Kyte & Doolittle, 1982) of AHSV NS1 (*Figure 2.9*) indicated that the 150 amino acids at

TABLE 2.3: *Comparison of the amino acid composition, net charge and estimated size of the NS1 proteins of AHSV-6, BTV-10 and EHDV-2. The deduced protein sequences were analysed using the ATHEPROT computer package.*

Amino acid residues	AHSV-6 number	BTV-10 number	EHDV-2 number
Alanine (A)	36	41	36
Arginine (R)	44	43	42
Asparagine (N)	20	20	24
Aspartic acid (D)	37	32	28
Cysteine (C)	15	16	17
Glutamine (Q)	27	26	28
Glutamic acid (E)	29	39	38
Glycine (G)	29	32	32
Histidine (H)	18	14	13
Isoleucine (I)	34	39	38
Leucine (L)	55	42	37
Lysine (K)	18	23	21
Methionine (M)	21	23	32
Phenylalanine (F)	23	26	30
Proline (P)	17	20	22
Serine (S)	21	25	17
Threonine (T)	34	23	27
Tryptophane (W)	11	13	12
Tyrosine (Y)	20	28	25
Valine (V)	39	27	32
Acidic (D+E)	66 (12%)	71 (13%)	66 (12%)
Basic (R+K)	62 (11%)	66 (12%)	63 (11%)
Aromatic (F+W+Y)	54 (10%)	67 (12%)	67 (12%)
Hydrophobic (Aromatic+I+L+M+V)	203 (37%)	198 (36%)	206 (37%)
Total amino acids	548	552	551
Net charge (pH 7.0)	+5	+7	+5
Size (Daltons)	63 478	64 446	64 580

TABLE 2.4: *Amino acid similarity comparisons among different AHSV serotypes and other orbiviruses. The overall similarities between AHSV-6 and the other viruses observed, are expressed as percentages when only identical amino acids are taken into account and also when both identical and similar amino acids are considered (values in brackets).*

COMPARISONS	AHSV-4	AHSV-9	BTV-10/13/17	EHDV-2
AHSV-6	95% (96%)	96% (98%)	19-28% (34-46%)	25% (44%)

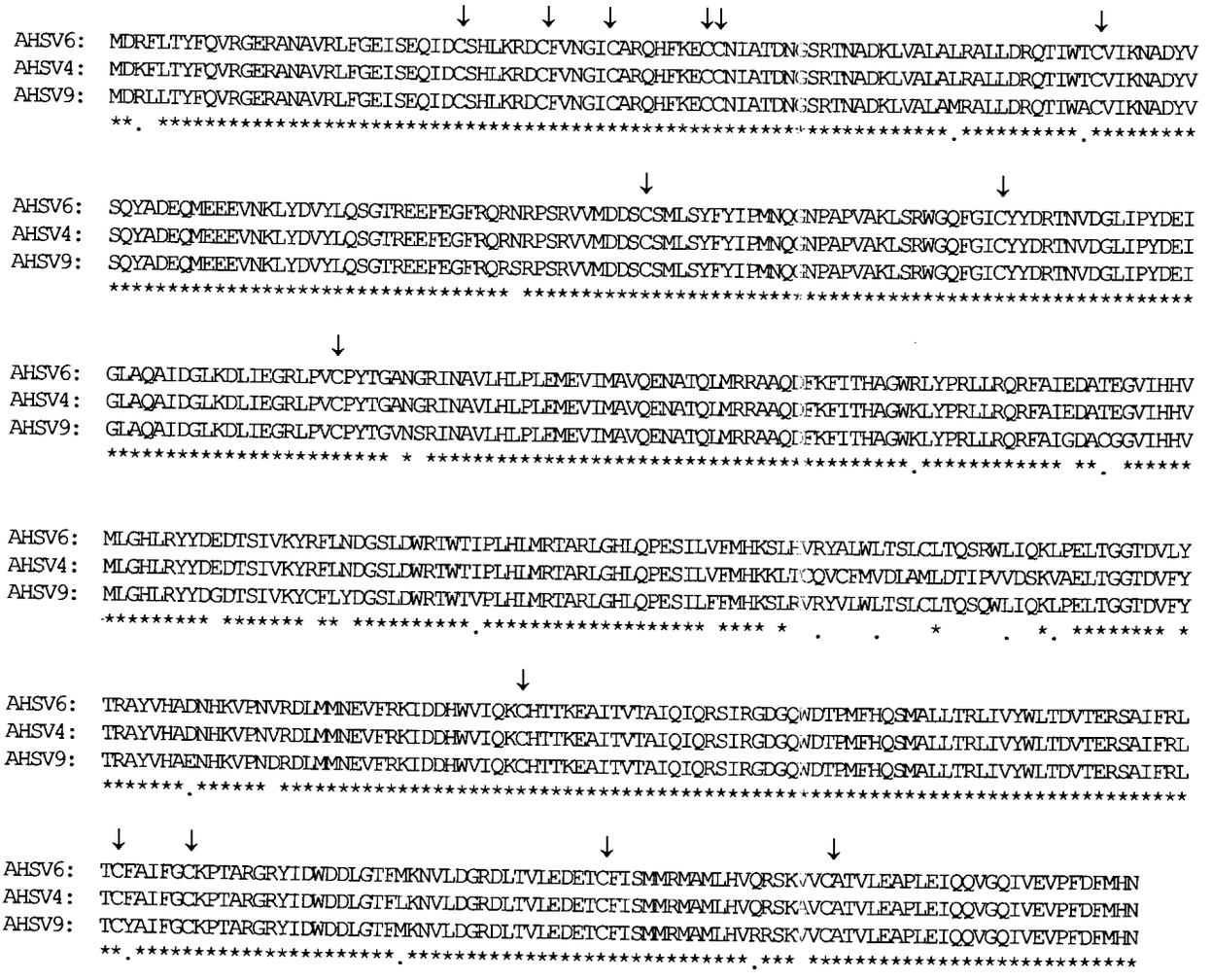

Figure 2.6: Alignment of the predicted amino acid sequences of the NS1 protein of AHSV serotypes 6, 4 and 9. Identical amino acids are indicated by asterisks (*) and similar amino acids by dots (.). In this alignment the amino acid homology is 95% and 96% and the amino acid similarity is 96% and 98% between serotypes 6 and 4 and 6 and 9, respectively. The position of 14 cysteine residues out of a total of 16 are conserved among AHSV-6, 4 and 9 (indicated by arrows).

Figure 2.7: Alignment of the predicted amino acid sequences of the NS1 protein of AHSV-6, -9, BTV-10, -13, -17 and EHDV-1 and -2. Identical amino acids are highlighted in blue and similar amino acids in purple. Six cysteine residues are conserved among the three orbiviruses (arrows). The underlined areas represent highly conserved regions containing more than 70% similar amino acids.

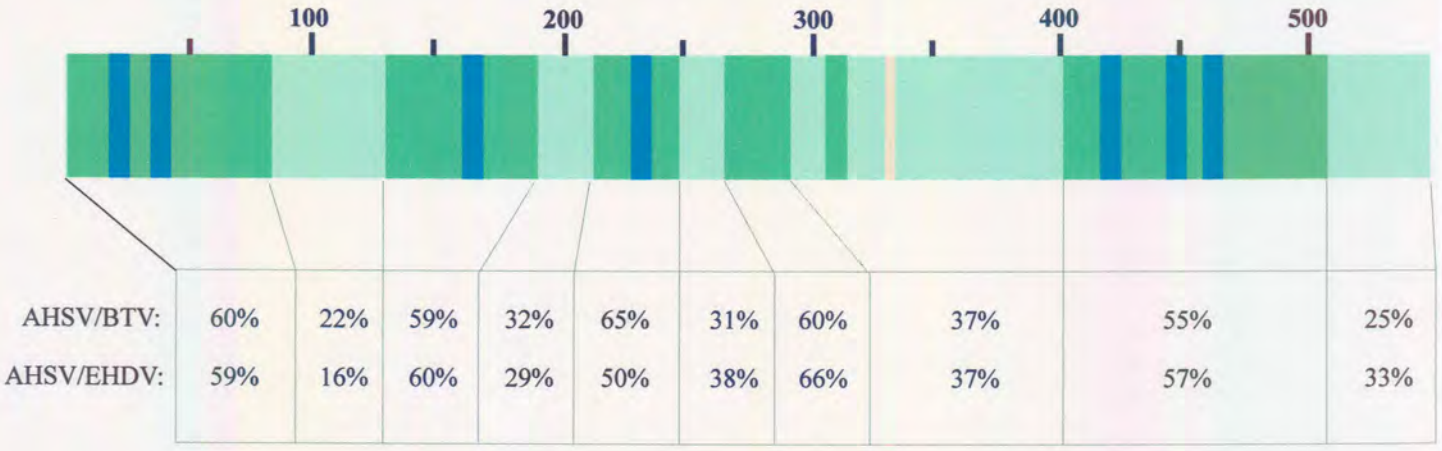

Figure 2.8: Percentage amino acid similarity in different NS1 proteins. Green represent region of >50% amino acid similarity in any two way comparison between AHSV-6, BTV-10 and EHDV-2. The dark blue areas represent regions of >70% similar amino acids in a three way comparison. The rest is regions with low similarity.

the N-terminal of the protein displayed largely hydrophilic regions with two relative small hydrophobic domains. This was followed by a large predominantly, hydrophobic domain stretching from amino acids 150 to 350. The C-terminal region was also characterised by alternating hydrophobic and hydrophilic regions, containing two relative large hydrophobic domains. The hydrophilicity profiles of the NS1 proteins of BTV-10 and EHDV-2 indicated a very high level of similarity to that of AHSV-6 NS1, particularly so in the hydrophobic regions. The hydrophobic domains were generally situated in the areas of highest amino acid similarity and their location is almost exactly conserved on the three different proteins (*Figure 2.10*).

N-glycosylation motifs (Asn-X-Ser/Thr, with X any amino acid residue) as well as different kinase phosphorylation sites were found when the deduced protein sequences of AHSV-6, BTV-10 and EHDV-2 was analysed against the Prosite database (Bairoch *et al.*, 1995). The location of these sites in the NS1 proteins of the three different orbiviruses does not correlate at all. The significance of the sites is unknown. Compared to protein sequences in the SwissProt database it showed no significant homology to proteins other than NS1 of other orbiviruses.

Secondary structure prediction (*Figure 2.10*), using four different methods in ANTHEPROT, of the NS1 proteins of AHSV-6, BTV-10 and EHDV-2 indicated a number of corresponding, alternating α-helixes. Five α-helixes were identified in the N-terminal 150 amino acids, while the C-terminal 150 amino acids contain 7 helixes. The central part of the NS1 protein contains another six α-helixes. β-strands and β-turns separate these helixes from each other. The hydrophilicity profile (Hopp & Woods, 1981) in combination with the antigenicity prediction (Welling *et al.*, 1989) indicated a hydrophilic region with strong antigenic properties in the C-terminal from amino acid 470 to 500 (*Figure 2.11*). The N-terminal also showed one strong antigenic site, which stretches from amino acid 55 to 77, within a hydrophobic region.

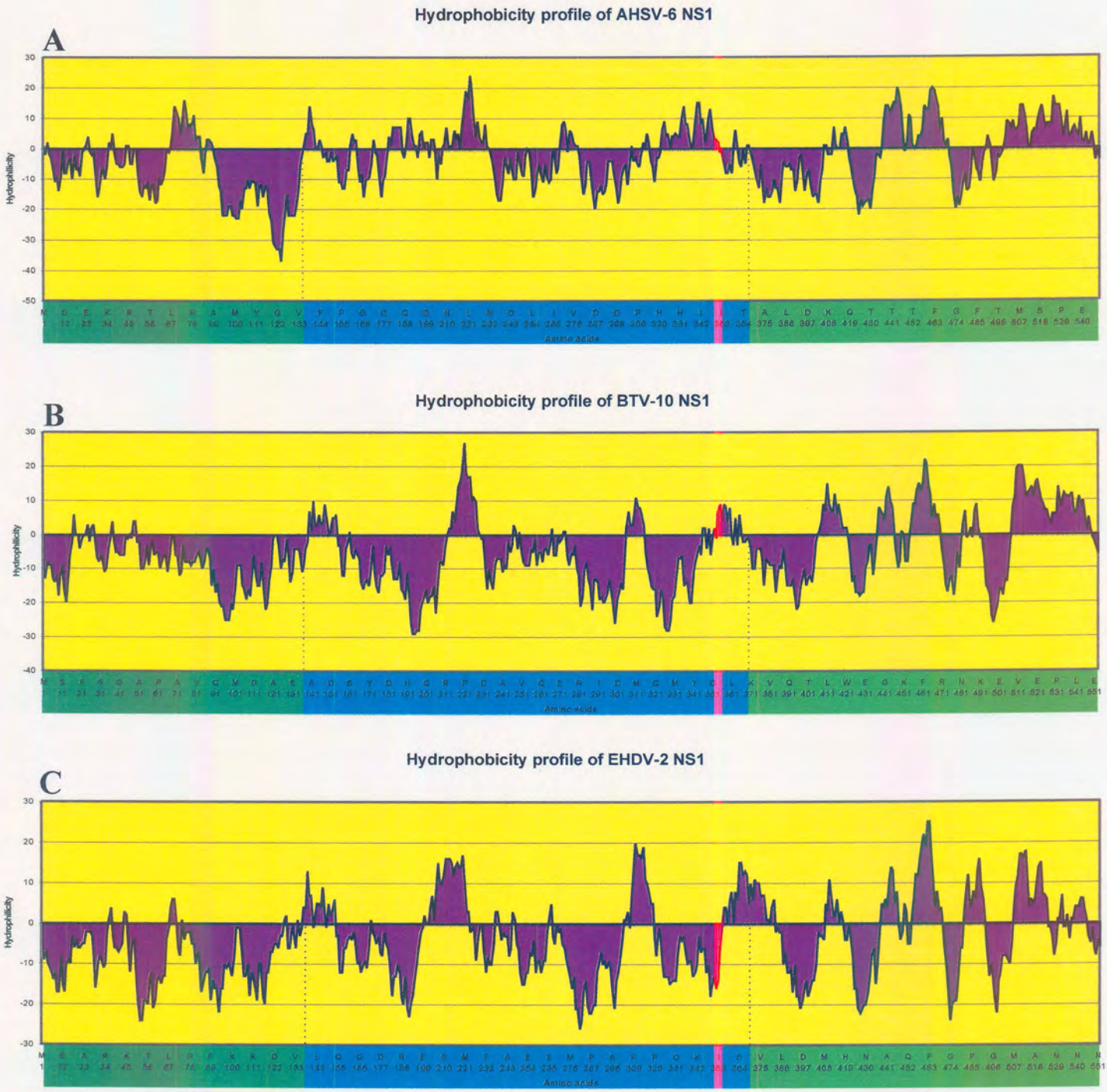

Figure 2.9: Comparisons of the hydropathicity profiles (Kyte & Doolittle, 1982) of NS1 of AHSV-6 (A), BTV-10 (B) and EHDV-2 (C), showing regions with a nett hydrophobicity (positive values) and a nett hydrophilicity (negative values) using a window size of 11. The central 250 amino acid region of the NS1 protein is highlighted in dark blue, while the N- and C-terminal regions is indicated in green.

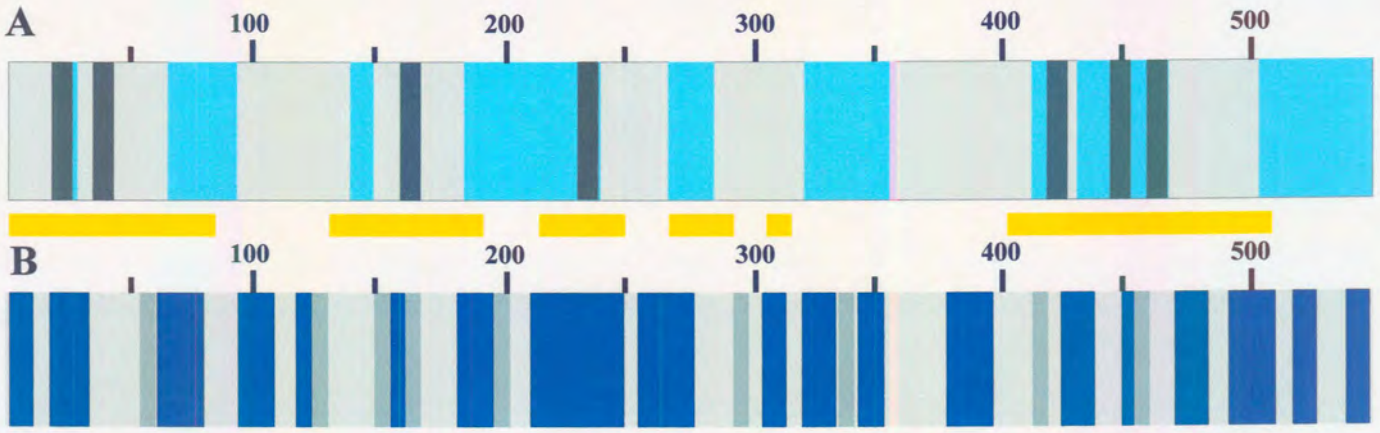

Figure 2.10: (A) Comparisons of the location of hydrophobic regions of NS1 of AHSV-6 and BTV-10. The black areas represent regions of >70% similarity in a three way comparison, while the blue areas represent conserved hydrophobic domains between AHSV and BTV. (B) Schematic representation of the secondary structure prediction of the NS1 protein of the three orbiviruses (AHSV, BTV and EHDV). The position of potentially conserved a-helixes (dark blue) B-sheet (light grey) and B-turns (dark grey) among these viruses is shown relative to conserved regions (>50%; yellow boxes) as well as conserved hydrophobic regions (blue in A).

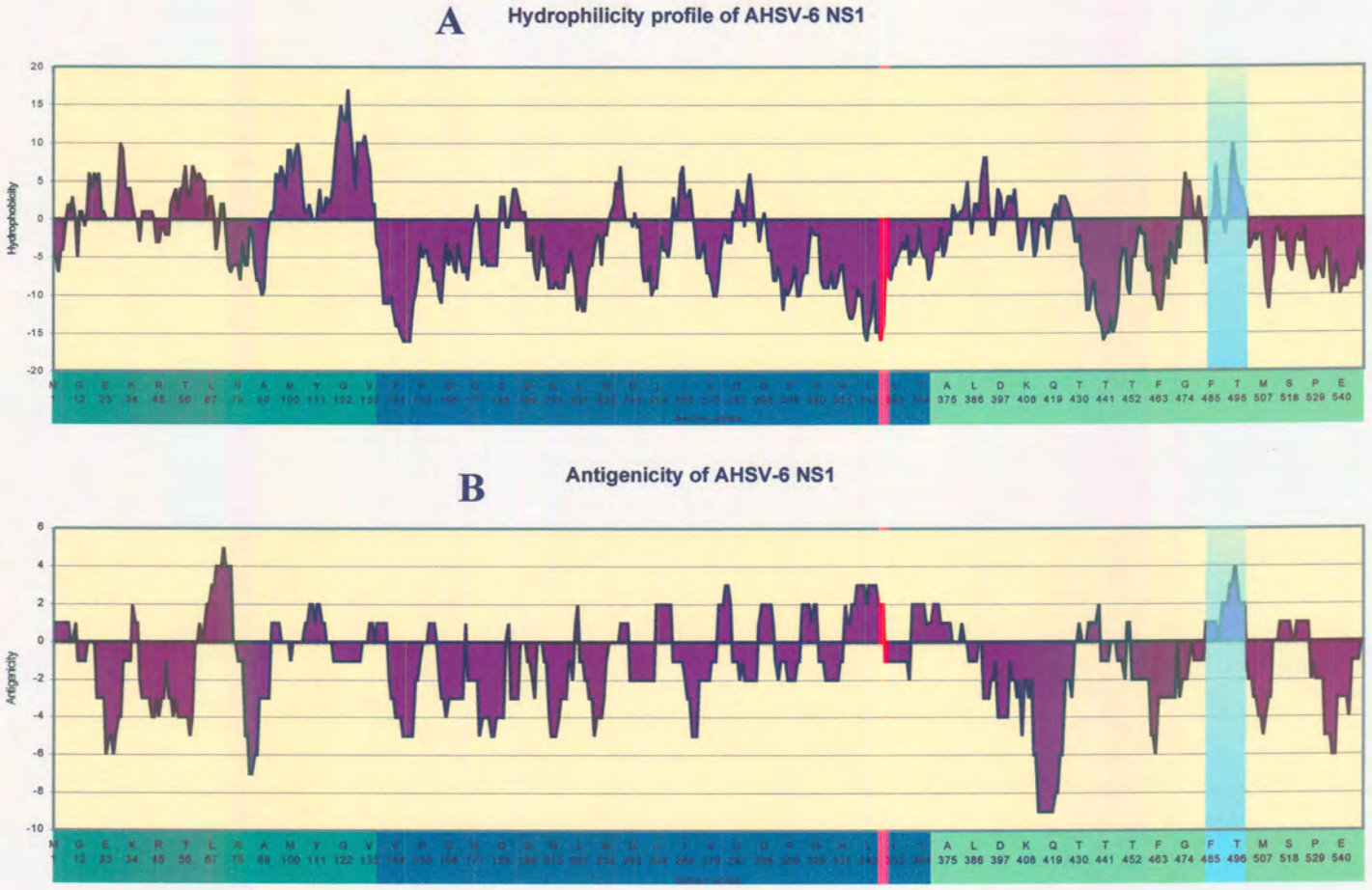

Figure 2.11: Comparisons of the hydrophilicity profile (A) (Hopp & Woods, 1982) and antigenicity profile (B)(Welling *et al.*, 1988) of AHSV-6 NS1. Areas with positive values have a nett hydrophilicity or antigenicity, while areas with negative values have a nett hydrophobicity or absence of antigenicity.

2.3.4. Modification and *In vitro* expression of the NS1 gene of AHSV-6

2.3.4.1. Modification of the NS1 gene for expression

In order to express the cloned cDNA copy of the NS1 gene, it was necessary to remove the poly-dG/dC tails flanking the 5' and 3' termini of the NS1 cDNA clone, which were present as a result of the original cloning strategy. The modification was carried out by means of a PCR method in which the oligonucleotide primers were designed to eliminate most of the 5' and 3' non-coding regions, except for the Kozak sequence flanking the AUG codon (Kozak, 1987). The primers, simultaneously incorporate flanking *Bam*H1 restriction sites in the PCR product in order to facilitate cloning into appropriate vectors (Nel & Huismans, 1991).

A PCR reaction was carried out as outlined in section 2.2.10 and the NS1 gene was successfully amplified as a discrete 1.65 kb band (*Figure 2.12A*), which corresponds to the coding sequence of the gene. The amplified product now contains the complete ORF with terminal restriction sites and is free of dC/dG homopolymer tails. Since the NS1 gene has unique *Hind*III and *Xho*I sites, 500 bp and 1400 bp from the 5' terminal end, the identity of the PCR product was confirmed by restriction with *Hind*III (*Figure 2.12A*). The PCR product was cloned into the pBS expression vector and a recombinant plasmid containing the PCR product under control of the T7 promotor was selected by restriction enzyme mapping with *Hind*III which cuts the vector once and also cuts asymmetrically in the NS1 gene. The desired recombinants yielded DNA fragments of 1.2 kb and 3.7 kb in length after digestion with *Hind*III and fragments of 350 bp and 4.6 kb after *Xho*I digestion (*Figure 2.12B, Figure 2.2*). Limited sequencing of the termini confirmed the full-length status of the PCR clone. Since errors could have been incorporated by *Taq* polymerase during the PCR, a chimeric NS1 gene, in which most of the central region of the PCR copy has been replaced by the original cDNA copy, was constructed in pBS as outlined in *Figure 2.2B*, instead of the conventional sequence verification. An approximately 1 kb region between position 503 and 1588 of the PCR copy (pBS-S5PCR) was excised by partial digestion with *HindIII* and complete digestion with *StyI* (*Figure 2.13A*) and replaced with the corresponding region of the original cDNA copy (pBR-S5.2)(*Figure 2.13B*). The 500 nucleotides at the 5' end and the 90 nucleotides at the 3' end of the original PCR copy was verified by sequencing and no difference between the PCR amplified ends and the original cDNA copy of the NS1 gene was observed. Recombinant pBS (*Figure 2.13C*) containing the complete chimeric gene was designated pBS-S5Hyb.

2.3.4.2. *In vitro* expression of the NS1 gene

The NS1 chimeric gene was expressed *in vitro* from the linearised pBS-S5Hyb template. *In vitro* transcription of the NS1 chimeric gene by T7 polymerase resulted in the synthesis of a (+)-strand RNA which was translated *in vitro* in a nuclease-treated rabbit reticulocyte lysate system. The mRNA directed the synthesis of a single 63 kDa protein, which corresponded to the NS1 protein, synthesised in AHSV-3-infected CER cells (*Figure 2.14*). The NS1 protein was expressed in large amounts *in vitro* which indicated that deletion of the 5' non-coding region of the NS1 gene excluding the Kozak sequence, did not significantly alter the expression of the gene.

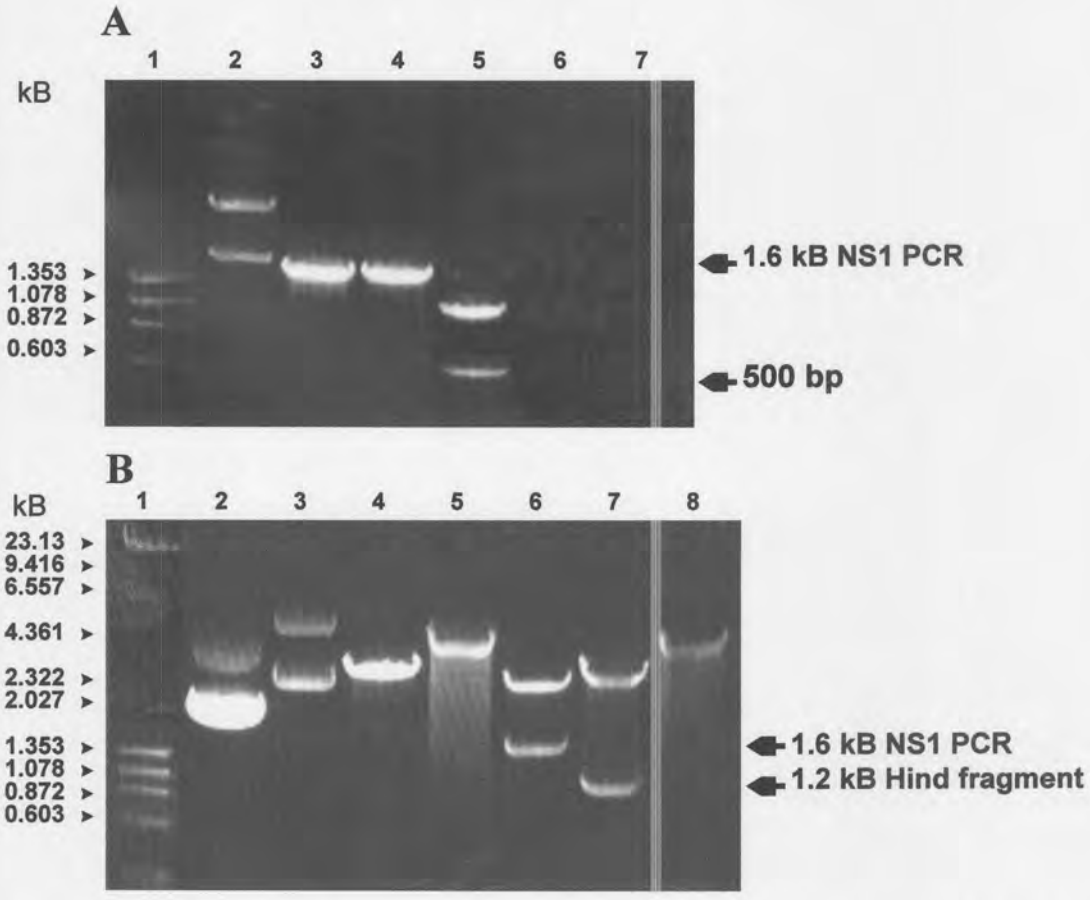

Figure 2.12: (A) Agarose gel analysis of PCR amplified fragments of AHSV-6 NS1 specific cDNA. Lane 1 represents a DNA molecular weight marker, with fragment sizes indicated in kb to the left. Lane 2 is *Pst* I digested p5.2cDNA. Lanes 3 and 4 represent the PCR amplified product of the NS1 gene. The 1.65 kB PCR fragments containing only the ORF of the NS1 gene are indicated. Lane 5 shows *Hind* III (cuts at position 502) digestion of the PCR amplified fragment, for verification. Lanes 6 and 7 are negative controls for the PCR reaction, containing no template or no primer, respectively. (B) Agarose gel analysis of the recombinant plasmid pBS-S5.2PCR (lane 3, uncut), constructed by cloning the PCR-tailored NS1 gene into the *Bam* H1 site of pBS (lane 2, uncut). pBS-S5.2PCR was linearised with *Xba* I (lane 5) or restricted with *Bam* H1 (lane 6), *Hind* III (lane 7) and *Xho* I (lane 8). See figure 2.2 for restriction enzyme map of the NS1 gene. Uncut pBS (lane 2) and linearised pBS (lane 4) were included as controls. The sizes of the DNA molecular weight markers (lane 1) are indicated to the left of the figure.

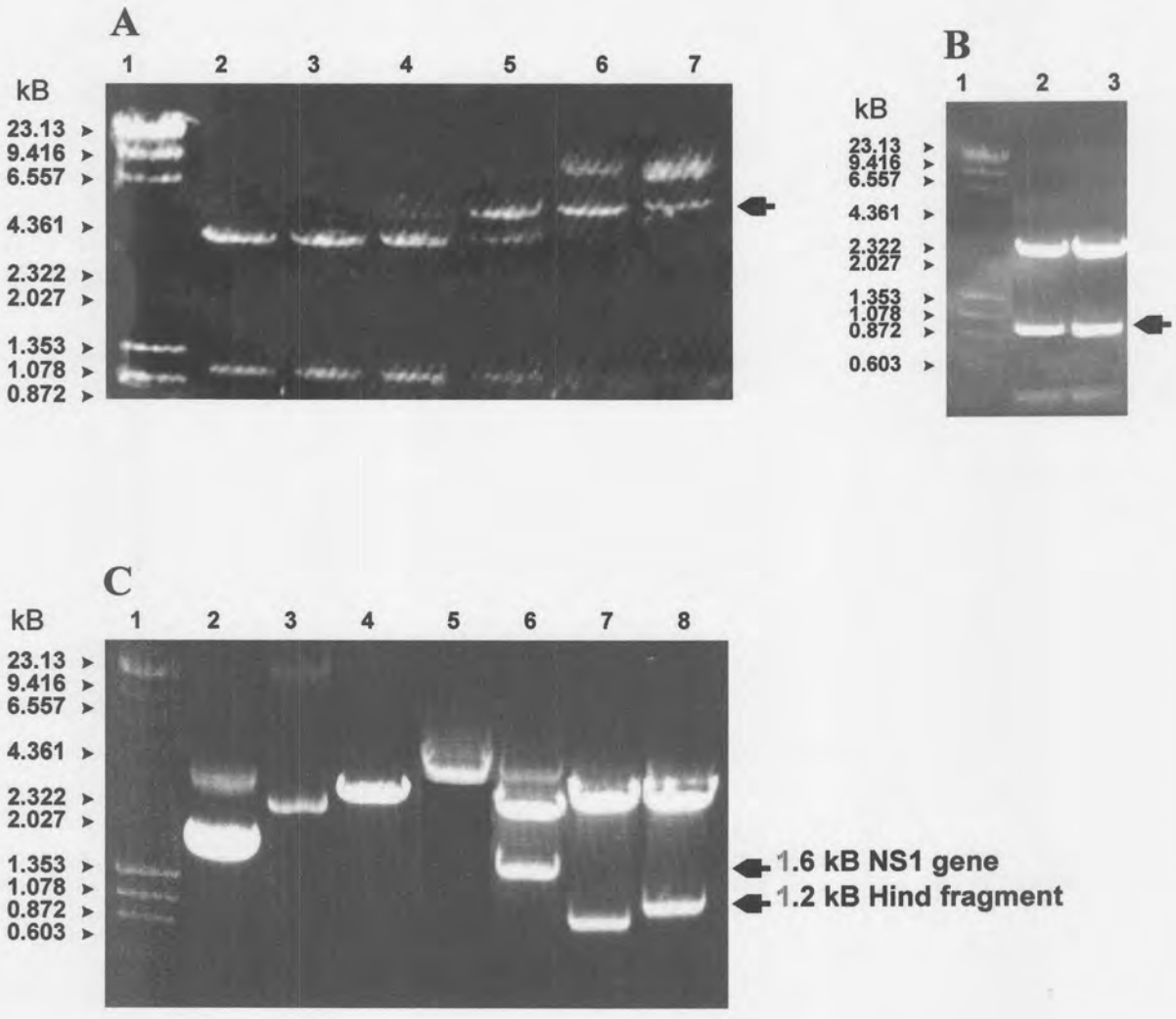

Figure 2.13: (A) An Agarose gel analysis of a partial *Hind* III digestion of the plasmid pBS-5.2PCR, through serial dilution. The sizes of fragments generated are 1.0 kb, 3.7 kb and 4.7 kb. The 4.7 kb fragment was produced after single digestion with *Hind* III and represented linear pBS-S5.2PCR(indicated by an arrow). (B) Complete *Hind* III and *Sty* I digestions of pUC-5.2cDNA (lanes 2 and 3). The 1.1 kb *Hind-Sty* fragment of the NS1 gene is indicated by an arrow. (C) Agarose gel analysis of the recombinant plasmid pBS-S5.2Hybr (lane 3, uncut), constructed by cloning 1.1 kb *Hind-Sty* cDNA derived fragment into the corresponding sites of pBS-S5.2PCR. pBS-S5.2Hybr was linearised with *Xba* I (lane 5) or restricted with *Bam* H1 (lane 6), *Hind* III (lane 7) and simultaneously with *Xho* I/*Sal* I (lane 8). See figure 2.2 for RE map of NS1 gene. The sizes of the DNA molecular weight markers (lane 1) are indicated to the left of the figure. Lanes 2 and 4 represent uncut and linearised pBS as controls.

The *in vitro* synthesised NS1 polypeptide was concentrated by centrifugation through a 40% sucrose cushion. Electron microscopic analysis of negatively stained samples revealed the presence of short tubular structures (result not shown) with a diameter of approximately 22 nm, which is similar to that of authentic AHSV tubules (Huismans & Els, 1979). The structure of the *in vitro* synthesised tubules appears to be less homogenous than that of authentic AHSV NS1 tubules described by Huismans and Els (1979). After verifying expression, the recombinant NS1 protein was further characterised by *in vivo* synthesis in insect cells, using a NS1 recombinant baculovirus.

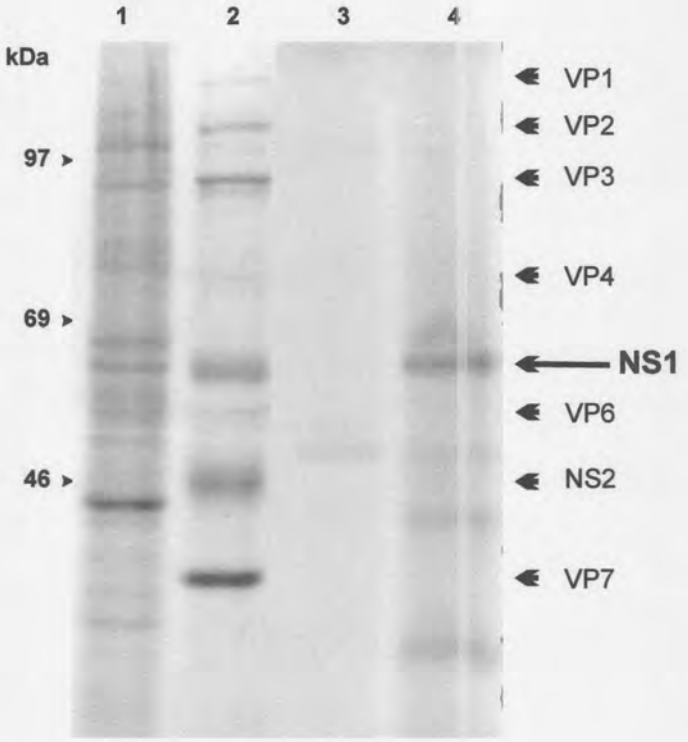

Figure 2.14: Autoradiograph of the ^{35}S-methionine labelled *in vitro* translation products directed by mRNA synthesised from AHSV-6 NS1 chimeric gene. Uninfected CER cells (lane 1) and CER cells infected with AHSV-3 (lane 2) were pulse labelled for 3 h with ^{35}S-methionine 16 h post-infection. *In vitro* translation of mRNA, synthesized from the NS1 gene directed the synthesis of a 63 kDa protein (lane 4) that corresponded in size to NS1 in AHSV-3-infected CER cells. Lane 3 represents rabbit reticulocyte translation products in the absence of any input mRNA.

2.3.5. Expression of the NS1 gene of AHSV-6 in insect cells by means of a recombinant baculovirus

2.3.5.1. Construction of a recombinant baculovirus

The BAC-TO-BAC™ baculovirus expression system, developed by Luckow *et al.* (1993), was used to express NS1 in insect cells. A recombinant baculovirus, containing the NS1 chimeric gene under control of the polyhedrin promoter, was constructed as outlined in *Figure 2.2C*. The NS1-specific insert was recovered from pBS-S5Hyb and cloned into the *Bam*H1 site, downstream of the polyhedrin promoter of the transfer vector, pFastbacI. A recombinant plasmid (pFB-S5Hyb), containing the NS1 gene in the correct transcriptional orientation, was identified by restriction mapping with *Hind*III and *Xho*I/*Xba*I. A plasmid yielding two *Hind*III fragments of approximately 1.2 kb and 5,4 kb and two *Xho*I/*Xba*I fragments of approximately 350 bp and 6.3 kb, as predicted for the NS1 gene to be in the correct orientation, was selected (*Figure 2.15*). A recombinant baculovirus shuttle vector (bacmid DNA) was then constructed by site-specific transposition of the cloned foreign gene into the baculoviral genome with the aid of the helper plasmid, which provides the transposition functions in *trans*. High molecular weight composite bacmid DNA was screened by dot-blot hybridisation and PCR amplification (*Figure 2.16*). Composite bacmid DNA, which yielded a 1.65 kb fragment with PCR and hybridised with segment 5-specific probe was transfected into Sf9 cells using a cationic lipid reagent (section 2.2.11.2). The supernatant containing the recombinant baculoviruses (Bac-AH6NS1) was harvested from transfected cells after 3-4 days. Progeny viruses were obtained by plaque-assay and used for the propagation of recombinant baculovirus stocks.

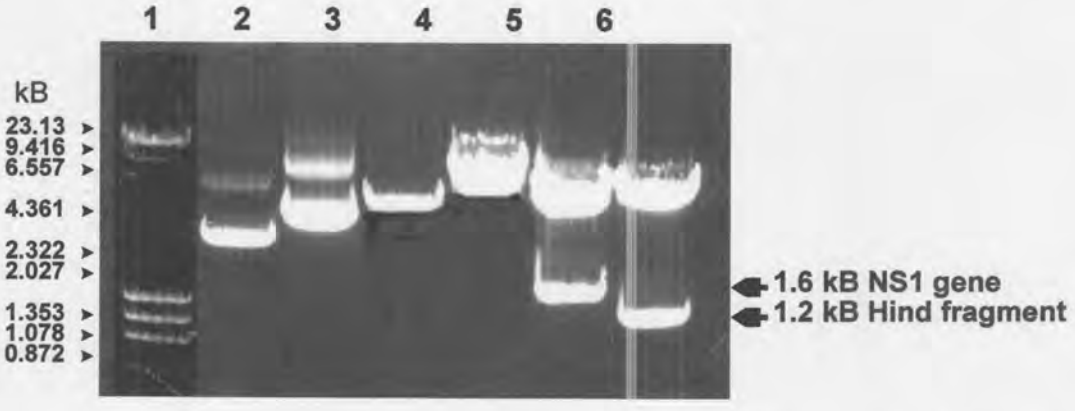

Figure 2.15: Agarose gel electrophoretic analysis of the recombinant plasmid pFB-S5.2Hybr, constructed by cloning the PCR/cDNA chimeric NS1 gene into the *Bam* H1 site of pFastbacI. Uncut pFB-S5.2Hybr (lane 3) was compared to uncut pFastbacI (lane 2) and was also restricted with *Xho I* (lane 5), *Bam H1* (lane 6) and *Hind III* (lane 7). Linearised pFastbacI (lane 4) was included as a control. See figure 2.2 for R.E. map of NS1 gene. The sizes of MWII andϕX174 DNA are indicated to the left (lane 1) of the figure.

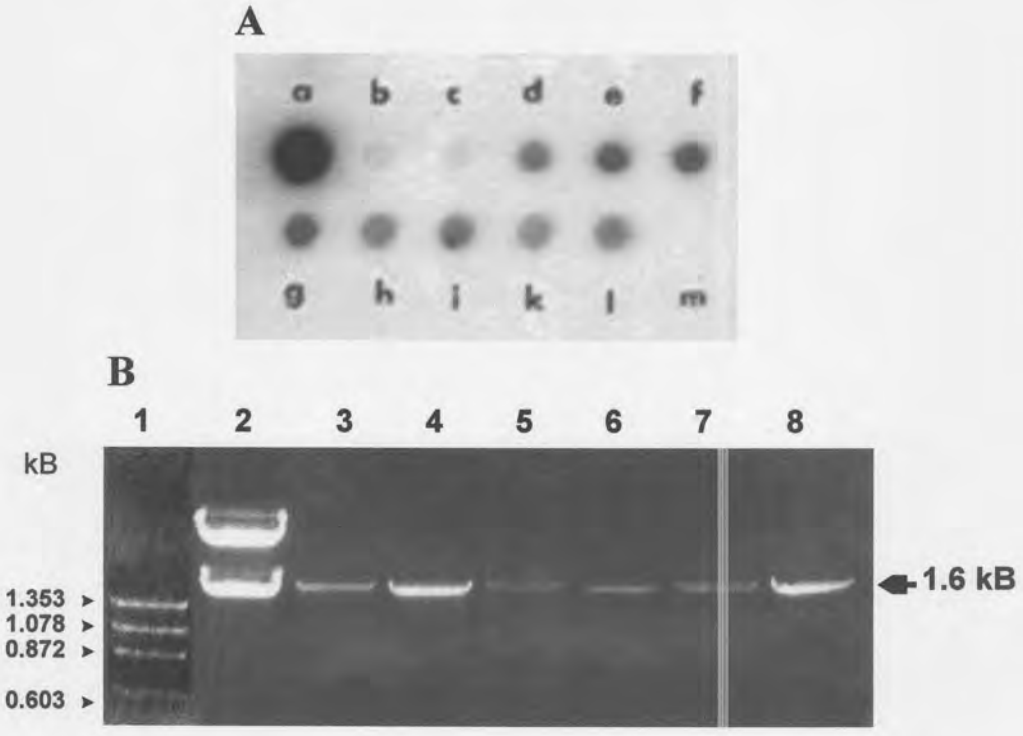

Figure 2.16: (A) An autoradiograph representing dot-blot hybridisation of a ^{32}P-labelled NS1-specific probe (pBR-S5.2) to recombinant bacmid DNA. The probe hybridised specifically to the NS1 gene. A positive control was pFB-S5.2Hybr (a) and DNA from blue bacmid colonies (b and c), and wild type pFastbac (m) served as negative controls. Dots d - l represent recombinant bacmid DNA which were selected for PCR amplification. (B) Agarose gel analysis of PCR amplified fragments from composite bacmids d - i (lanes 3 - 8). Lane 1 represent Hae III-digested ϕX174 DNA and lane 2 pFB-S5.2Hybr digested with Bam H1.

2.3.5.2. Expression and purification of AHSV-6 NS1 protein

Protein extracts were prepared from insect cells infected with the recombinant baculovirus, Bac-AH6NS1 and analysed by SDS-PAGE (*Figure 2.17*). The results revealed that the recombinant virus synthesised large amounts of a unique protein with a molecular size of 63 kDa, which is in agreement with the estimated size of the AHSV-6 NS1 protein. This protein was absent in mock- or wild type baculovirus-infected cells. To further confirm the identity of the 63 kDa protein, proteins synthesised in Bac-AH6NS1 infected Sf9 cells were pulse labelled with [^{35}S]methionine between 36 and 40 h p.i. and the labelled proteins were analysed by SDS-PAGE. Radio-labelled proteins from AHSV-3-infected CER cells were included for comparison. The unique protein expressed by BV-AHSV6-S5 was exactly the same size as the NS1 protein of AHSV-3 (*Figure 2.18A*). The yield of expressed NS1 in Bac-AH6NS1-infected cells was estimated to be approximately 1 mg/10^6 cells. It was not possible to confirm the viral origin of the putative NS1 by immuno-precipitation using rabbit anti-AHSV-6 antisera. The results were inconclusive since the NS1 protein was in a particulate form and precipitated under the same conditions as NS1-antibody complexes (results not shown). Electron microscopy analysis was used for confirmation (section 2.3.6).

The NS1 protein in lysates of cells infected with the recombinant baculovirus was subjected to sucrose gradient sedimentation analysis according to the method described by Huismans and Els (1979). Samples of each fraction from the discontinuous gradient were analysed by SDS-PAGE (*Figure 2.18B*). The results indicated that the largest amount of the 63 kDa protein was recovered from those sucrose gradient fractions in the region of 200-400 S, which suggests that the expressed protein is present in a particulate or polymerised form in the infected cells. A similar heterogeneous 400S complex of NS1 protein has been identified in AHSV-infected mammalian cells (Huismans & Els, 1979). The heterogenicity of the S values on sucrose gradients could be due to breakage during the purification process.

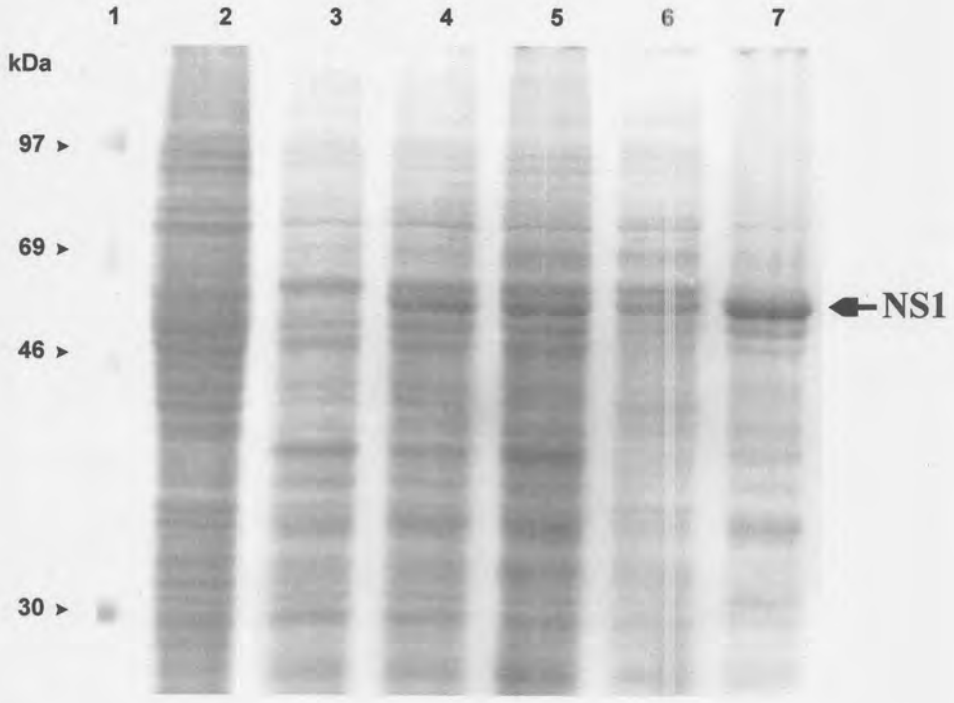

Figure 2.17: SDS-PAGE analysis of the expression of the NS1 protein in insect cells infected with a recombinant baculovirus containing the NS1 gene. *S. frugiperda* cells were mock-infected (lane 2), or infected with either the wild-type baculovirus (lane 3) or the recombinant baculovirus, Bac-AH6NS1 clones 3, 4 and 7 (lanes 4-6). Cells were harvested at 72 h post-infection and disrupted. Lane 7 represent partially purified NS1, by means of differential low speed centrifugation of cytoplasmic extracts of infected cells. Proteins were visualised after staining with Coomassie blue. The position of NS1 and molecular weight markers are indicated.

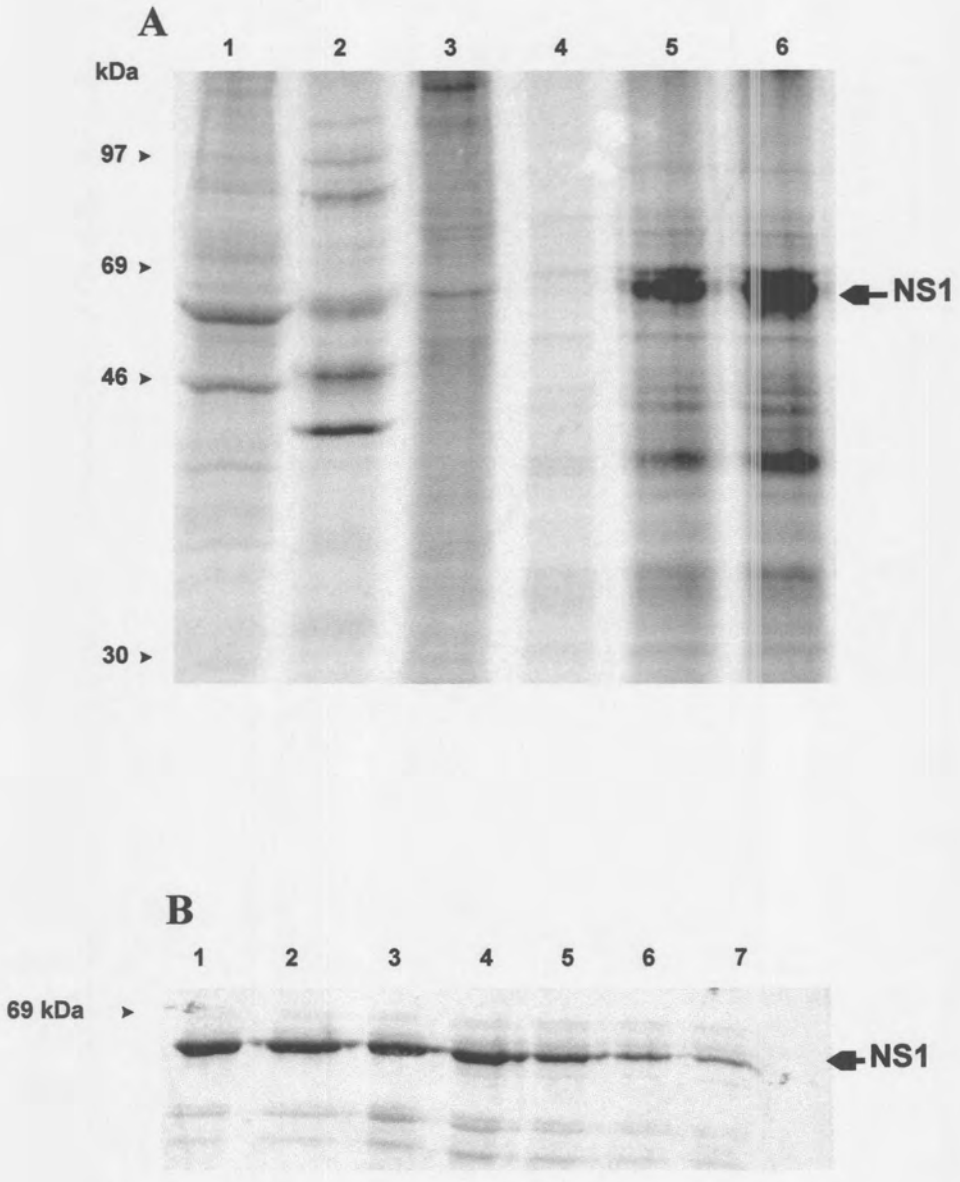

Figure 2.18: Autoradiograph of SDS-PAGE separated cell lysates of insect cells infected with recombinant and wild-type baculoviruses. Lanes 1 and 2 represent uninfected CER cells and CER cells infected with AHSV-3, pulse labelled for 3 h with ^{35}S-methionine, 16 h post-infection. Mock-infected (lane 3), wild-type infected (lane 4) and Bac-AH6NS1-infected (lanes 5 and 6) insect cells were pulse labelled 36 and 48 h post-infection. (B) Multimeric NS1 protein complexes were recovered by centrifugation through a 40% sucrose cushion and further purified by sedimentation on a 20-50% sucrose gradient. Fractions 4 to 10 (lanes 1-7) of 20 fractions, contained the NS1 protein complexes.

2.3.6. Electron microscopy of the NS1 protein complex

The 200-400 S NS1 complex was concentrated from sucrose gradient fractions by centrifugation for 2 h at 40 000 rpm. The pellet was resuspended in STE buffer and analysed by electron microscopy after negative staining. The results (*Figure 2.19A*) indicated that the material consisted almost exclusively of tubules of an average diameter of 23 ±2 nm and various lengths of up to 4 μm. The variation in length of the NS1 tubules may reflect the normal variation in tubule length or could be due to breakage during the purification process. The fine structure of the AHSV tubules was very different in appearance to those of BTV and EHDV tubules. AHSV tubules had an internal structure with a fine reticular "cross-weave" appearance. The central region of the tubules was characterised by alternating stretches of electron dense and less dense areas. The edges of the tubules were smooth and sharply defined with no visible pattern of subunits. There was no evidence of the ladder-like or segmented appearance found in the much wider BTV (68 nm) and EHDV (52 nm) tubules. In addition to the tubules flat, hollow, circular structures were also observed. The diameter of these structures corresponded to that of the AHSV tubules while their lumen had a diameter of approximately 7 nm. These structures probably represent cross-sections through tubules.

A small percentage of baculovirus-specific tubules (result not shown) were also observed. These tubules could be distinguished from the AHSV-specified tubules by the fact that they have a diameter of 40 nm and also by differences in fine structure. The identity of the AHSV tubules was verified by means of antibody decorating, using AHSV-6 antiserum (described in section 2.2.15). This involves binding of AHSV-6 antiserum to tubules, immobilised on grids. Different dilutions of the antiserum were used and decorating was clearly observed with a dilution of up to 1/2000. The NS1 tubules (*Figure 2.19B & C*) were distinguished from the wild-type baculovirus tubules in that they appeared darkly shadowed as a result of the antiserum decoration.

The sucrose gradient purified tubules were also investigated at high resolution with In-lens FESEM to gain more insight on the surface structure of the tubules. The tubules were present as a network and could be distinguished from baculovirus tubules according to their diameter. These tubules have a smooth surface structure with no indentations and projections (*Figure 19D & E*). This is in agreement with the absence of a ladder-like appearance in transmission electron micrographs.

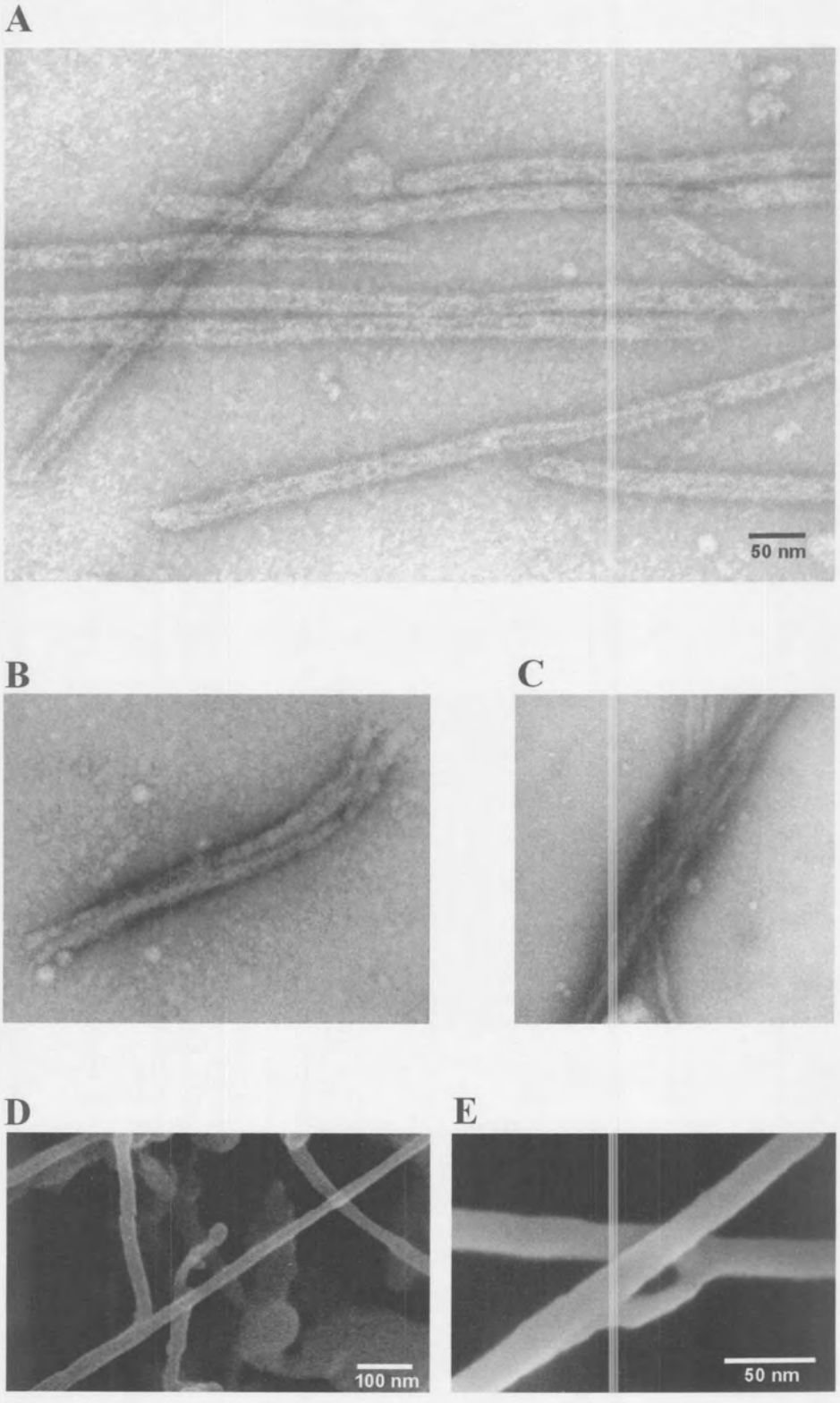

Figure 2.19: Negative contrast electron micrographs. The recombinant baculovirus-expressed NS1 tubules were purified by sucrose gradient centrifugation and stained with 2% uranyl acetate (A). The identity of the purified NS1 tubules were verified by decoration with anti-AHSV-6 antisera at 1:1000 (B) or 1:500 (C) dilutions before staining with uranyl acetate. The NS1 tubules could be distinguished from baculoviral tubule contaminants (not shown). Bar markers represents 50 nm. (D & E) In-lense SE micrographs of the surface of NS1 tubules. Bar markers represent 50 nm.

2.3.7. Electron microscopy of thin sections of recombinant baculovirus-infected cells

Recombinant baculovirus-infected Sf9 cells were fixed by glutaraldehyde treatment and thin sections prepared and processed for electron microscopy. The results are shown in *Figure 2.20*. Large amounts of tubules of various lengths and in different three-dimensional arrangements were observed in the recombinant virus-infected cells. These structures were absent in mock-infected (*Figure 2.20A*) and wild-type infected control cells. In recombinant virus-infected cells the tubules occurred mostly in the cytoplasm, but they have also occasionally been observed in the nucleus. Whether the tubules occurred in the nuclei because the nuclear membrane had been disrupted in the terminal stage of infection, is not known. In a few cases the tubules seemed to be associated with and aligned along unidentified fibrous material (*Figure 2.20B*). In most of the cell thin sections, the NS1 complexes could be seen as twisted and layered stacks and bundles, angular to each other with various configurations (*Figure 2.20C*). Both the structure and arrangement of the tubules were comparable to those of the tubular structures reported in AHSV-infected BHK cells (Huismans & Els, 1979). The number of tubules in the cytoplasm generally appeared to correlate directly with the number of viruses and virus-inclusion bodies in the enlarged nucleus of the recombinant virus-infected cells.

2.3.8. The effect of biophysical conditions on the morphology of AHSV NS1 tubules

The effects of different biophysical conditions on the morphology of the tubules were investigated and are summarised in *Table 2.5*. Aliquots of gradient purified tubules were resuspended in various test solutions and both the particulate and supernatant fractions analysed for the presence of NS1 protein. The fractions were also investigated by TEM. Tubule morphology was found to be affected by the ionic strength of the buffer solution in which it was resuspended. The tubules were found to be unstable at a $CaCl_2$ concentration of 0.2 M and higher, since NS1 was present in the pellet following low speed centrifugation. No tubules were observed under these conditions and only an amorphous mass of proteins was visible. In the presence of 1 M NaCl, most of the NS1 was retained in the supernatant. Although tubules could be observed, they appeared to be much shorter than normal (*Figure 2.21A*) and a large increase in the number of circular forms were observed. When treated with buffers of between 6.5 and 7.5, the tubule morphology was unaffected.

Treatment with buffers of between pH 8.0 and 8.5, resulted in severely affected tubule morphology (*Figure 2.21B*). The tubules were not only reduced in length but the fine structure was totally abolished and the NS1 protein became aggregated. Between pH 5.0 and 5.5 the tubules were generally of shorter length and the surface of the tubules appeared more uneven (*Figure 2.21C*). At pH 5.0 or less, the tubules appeared to be denatured and NS1 aggregated in an amorphous protein mass. At temperatures above 50°C, the NS1 was found in the pellet and the tubules were dissociated.

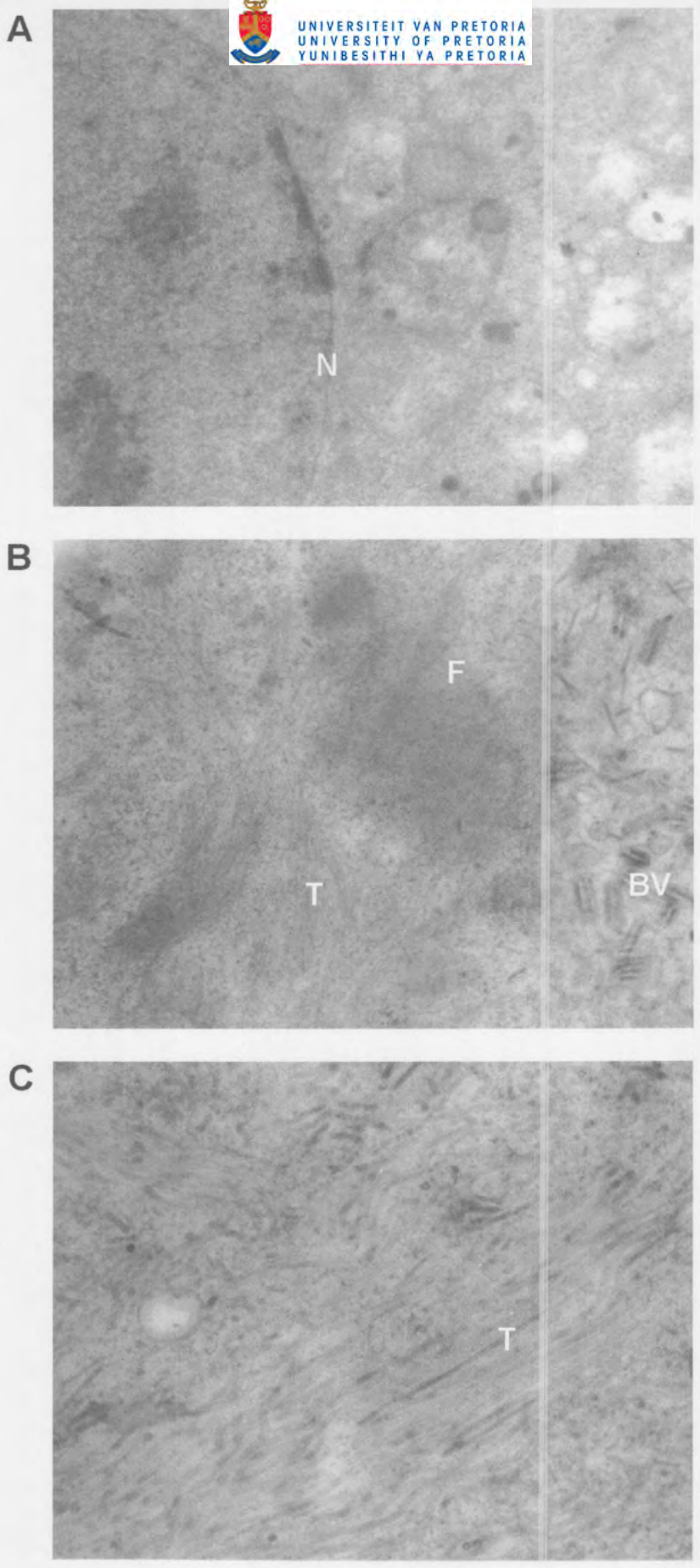

Figure 2.20: Negative contrast electron micrographs of thin sections of insect cells infected with the recombinant baculovirus Bac-AH6NS1. (A) represents an uninfected cells while (B) and (C) show bundles of NS1 tubules in the cytoplasm of infected cells. T, tubules; BV, baculovirus particles; F, fibrous material; N, nuclear membrane.

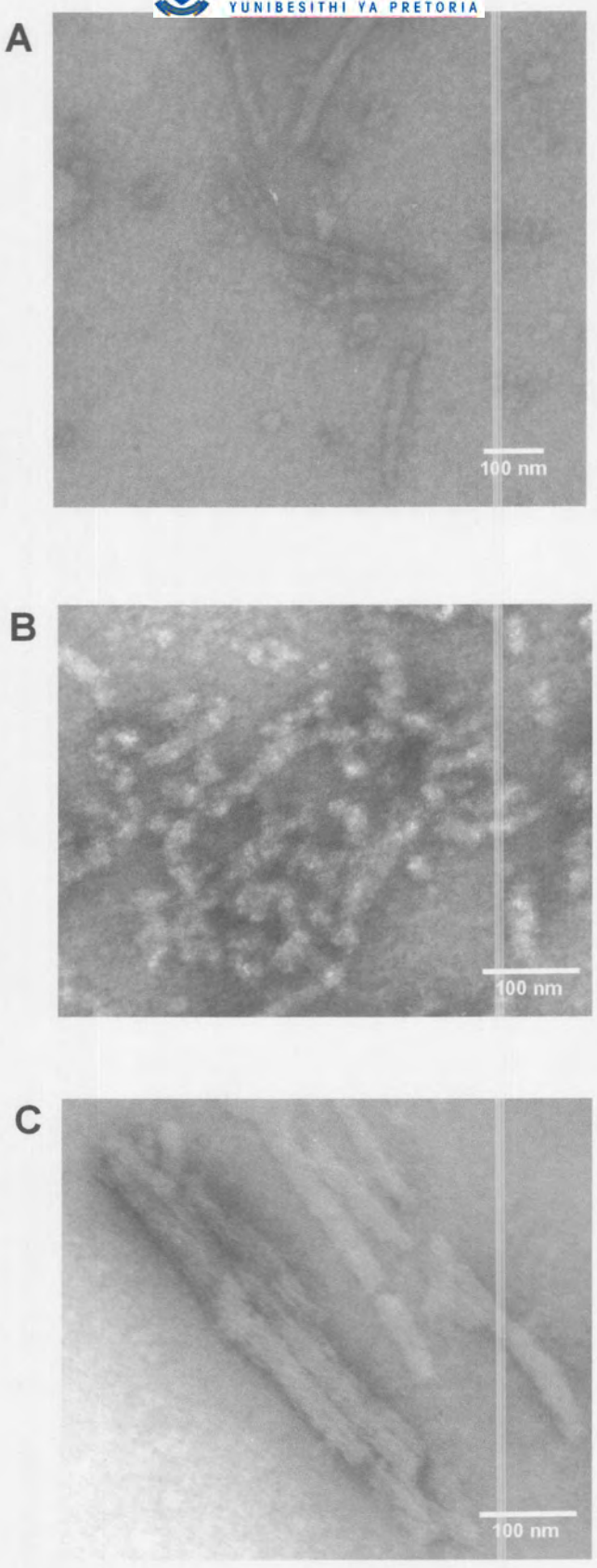

Figure 2.21: Electron micrographs of negatively stained tubules , treated with 1 M NaCl (A), buffer of pH > 8.0 (B) and buffer with pH 5.0 - 5.5 (C). Bar markers represents 100 nm.

TABLE 2.5: *Effects of different treatments on AHSV tubule morphology*

Treatment	Effect on morphology
pH	
<5.0	Tubules denatured; aggregated protein
6.0-8.0	Shortened tubules; filamentous strands
>8.0	Tubules denatured; aggregated fragments
Ionic strength	
0.2 M $CaCl_2/MgCl_2$	Tubules denatured; aggregated protein
<1 M NaCl/KCl	Shortened tubules; circular formation
>1 M NaCl/KCl	Tubules denatured; aggregated protein
Detergents	
Anionic	Tubules denatured; filamentous strands
Cationic	Tubules denatured; aggregated protein
Non-ionic (Tween 20/Triton X-100)	Tubules denatured; aggregated protein
Chelating agents	
1-3 mM EDTA	Fragmented short tubules
4-5 mM EDTA	Circular formation; no tubules visible
Reducing agents	
100 mM DTT	Shortened tubules
5% (v/v) Mercaptoethanol	Shortened tubules
Denaturing conditions	
M Urea	Tubules denatured; aggregated protein
SDS treatment	Tubules denatured; aggregated protein
Temperature	
4°C	Normal tubules
30-45°C	Normal tubules
45-60°C	Shorter tubules with end filaments
60-70°C	Filamentous network

2.4. DISCUSSION

The first part of this investigation was focused on the cloning and characterisation, through nucleotide sequencing, of the dsRNA segment that encodes the non-structural protein NS1 of AHSV-6. This information not only provides insight into the properties of the gene and deduced NS1 protein but more important assists in identifying regions for the insertion of foreign epitopes and the understanding of tertiary structure of the protein. The AHSV-6 NS1 protein was also expressed *in vitro* and in a baculovirus-based eukaryotic expression system.

The relationship among three different AHSV serotypes was investigated by comparing the determined AHSV-6 segment 5 nucleotide sequence and deduced amino acid sequences to that of the cognate genes of AHSV-4 (Mizukoshi *et al.*, 1992) and 9 (Nel, unpublished data). The NS1 gene of AHSV-6 was found to be 1748 nucleotides in length and differed only in three nucleotides in the 3' non-coding region from the NS1 gene of serotype 4. The longest open reading frame observed, contained 548 codons flanked by 5' and 3' non-coding regions of 35

and 70 nucleotides respectively. The presumed translation initiation codon conformed fully to the eukaryotic consensus sequence ($CX^{A}/_{G}XCAUGG$) proposed by Kozak (1987). The 5' and 3' termini of AHSV-6 NS1 were found to contain the characteristic conserved $GTT^{A}/_{T}AA$ and $AC^{A}/_{T}TAC$ terminal hexanucleotide sequences of AHSV RNA fragments proposed by Van Staden *et al.* (1991). These terminal sequences are a characteristic feature not only to AHSV, but to all orbivirus RNA segments investigated thus far (Rao *et al.*, 1983; Mertens & Sanger, 1985; Wilson *et al.*, 1990) although the sequence and which bases are conserved can vary between different *Orbivirus* species. A near identical inverted repeat sequence of 11 bp with a homology of more than 87% was identified in the 5' and 3' non-coding regions of AHSV NS1 gene. Short inverted repeat sequences adjacent to the 5' and 3' termini have been identified for all orbivirus dsRNA segments (Roy, 1989; Nel *et al.*, 1990; Anzola *et al.*, 1987; Steockle *et al.*, 1987; Moss *et al.*, 1992 a, b). It has been reported that the NS1 gene of EHDV contain a second inverted repeat sequence of 19 nucleotides in the 3' non-coding region in addition to the above described inverted repeats (Nel *et al.*, 1990). However, similar to the BTV NS1 gene no inverted repeat sequence was present in the 3' non-coding region of the NS1 gene of either AHSV-6 or 9. A comparison of the three cognate AHSV NS1 genes revealed a close relationship between AHSV-4 and 6 (97%) and somewhat less conservation between AHSV-6 and 9 (93%). The 5' non-coding region was found to be highly conserved among the three different serotypes, while less homology was observed in the 3' non-coding region. A comparison with the cognate NS1 gene (segment 5; 1769 bp long) of BTV-10/13/17 (Lee & Roy, 1987; Wang *et al.*, 1988) revealed 44% nucleotide similarity, which is in agreement with the results reported for AHSV-4 (Mizukoshi et al., 1992). The major difference in the length of the AHSV and BTV NS1 genes is due to the additional 7 nucleotides in the non-coding 3' region of the BTV NS1 gene, whereas the length of the coding regions differs by only 12 nucleotides (or 4 codons). The 3' non-coding region of EHDV-2 (Nel *et al.*, 1990) is 46 nucleotides longer than that of AHSV-6 and 9. The 3' terminal of the NS1 genes of all three viruses, although of different lengths, share the feature of being rich in thymidine residues. The nucleotide homology of the coding regions among AHSV, BTV and EHDV was found to be 47%, 46% and 62% respectively. The 5' non-coding region is even more highly conserved. Conserved nucleotide sequence at the 5' non-coding region appear to be a general feature of cognate orbivirus genome segments (Nel *et al.*, 1990).

According to Nel *et al.* (1990), the high level of conservation of the 5' leader sequences could be a reflection of the importance of these regions in controlling the relative rate at which the genome segments are transcribed or the mRNA species are translated. It has been shown in the case of reovirus that the relative rate of mRNA translation is determined by the 5' leader sequence. A characteristic feature of the NS1 encoding genome segments of orbiviruses is the

observation that these genome segments are much more frequently transcribed than the other segments (Huismans & Verwoerd, 1973; Huismans *et al.*, 1979).

The NS1 gene of AHSV-6 specifies a protein of 548 amino acids in length with an estimated molecular mass of 63 478 Da and a net charge of +5 at neutral pH. This is in agreement with the NS1 protein of AHSV-4 (M_r = 63 122; Mizukoshi *et al.*, 1992) and 9 (M_r = 63 378), but is four amino acids shorter than the BTV and EHDV equivalent. AHSV-6, BTV-10 (13 and 17) and EHDV-2 proteins all comprise a similar number of amino acids. The AHSV-6 gene product is 548 amino acids in length, with BTV and EHDV-2 both consisting of 552 amino acids. The proteins have similar sizes, with M_r of 63 478, 64 445 and 64 559 for AHSV-6, BTV and EHDV, respectively. Like the NS1 protein of BTV (Lee and Roy, 1987; Wang *et al.*, 1989), AHSV-6 NS1 has a low content of charged amino acids, as well as threonine and serine residues, but is particularly rich in cysteine residues. Monastyskaya *et al.* (1994) indicated that at least some of the conserved cysteines are essential for tubule formation. Point mutations of cysteine residues 337 and/or 340 resulted in the failure to form tubules. These cysteines probably play a role in the formation of the correct 3-D conformation of NS1 because it was indicated that inter-chain disulphide bonds are not involved in maintaining the tubule structure (Marshall *et al.*, 1990). These two cysteines are located in a hydrophilic region of the protein, unlike many other conserved cysteine residues (Monastyrskaya *et al.*, 1994).

A number of highly conserved regions (10-20 amino acids), containing approximately 70% identical amino acids, were identified in a comparison of the NS1 proteins of AHSV, BTV and EHDV (*Figure* 2). These conserved regions can further be reduced to a number of highly conserved amino acids which account for 9% of the total number of amino acids in a comparison of NS1 of AHSV, BTV, EHDV and BRDV (Moss & Nuttal, 1995). The AHSV-6 NS1 protein is, similar to AHSV-4 (Mizukoshi *et al.*, 1992), BTV (Lee and Roy, 1987) and EHDV NS1 (Nel *et al.*, 1990), predominantly hydrophobic with the hydrophobic residues accounting for as much as 43.6% of the total amino acids in NS1. This is significantly more than the 36-37% hydrophobic residues found in BTV and EHDV NS1 proteins. The hydropathic profile of AHSV-6 NS1 protein shows some similarity with that of BTV and EHDV NS1, and revealed that with some exceptions in the hydrophilic regions, the NS1 protein from the three different viruses had almost identical distributions of hydrophobic and hydrophilic domains. The hydrophobic domains of AHSV, BTV and EHDV are located in areas of highest amino acid similarity and their location is almost exactly conserved in the NS1 proteins of the three orbiviruses. These hydrophobic stretches are also conserved in BRDV NS1 (Moss & Nuttal, 1994) and may play an important role in tubule formation. It is interesting to note that although the location of these

hydrophobic domains is highly conserved, the diameter of the tubules into which they respectively polymerise can differ significantly.

Monastyrskaya *et al.* (1995) reported that deletion mutants of BTV-10 NS1 of up to 10 amino acids in the amino terminus or 20 to 43 amino acids from the carboxy terminus, failed to form tubules. This indicates that regions of both the N- and C-termini are important for tubule formation. Removal of five C-terminal amino acids or addition of 16 amino acids did not impair the ability of the derived NS1 to form tubules. This is in agreement with the finding that the N- and C-termini of the NS1 protein are the most conserved among AHSV, BTV and EHDV. Mikhailov *et al.* (1996) demonstrated that peptides of up to 109 amino acids, inserted at the C-terminus of BTV-10 NS1, allowed the formation of tubular structures. When insect cells were co-infected with three recombinant baculoviruses expressing chimeric NS1 proteins with different epitopes, they simultaneously assembled into the same tubule. These chimeric tubules, carrying foreign antigenic peptides, were highly immunogenic, even in the absence of adjuvants. Using the antigenic profile (Welling *et al.*, 1989) in combination with the hydrophilicity profile (Kyte & Doolittle, 1982) of the deduced amino acid sequences of the different AHSV NS1 proteins, a strong antigenic site was identified in the C-terminal 100 amino acids of the NS1 protein. This site corresponds to an antigenic epitope that was identified on BTV NS1 at position 474 to 502 (Du Plessis *et al.*, 1995).

As part of an investigation into studying the polymerisation of NS1 into tubules, the NS1 protein of AHSV-6 were expressed *in vitro* as well as in insect cells, using an improved baculovirus expression system. The level of NS1 expression *in vitro* was relative high, which is in agreement with the level at which NS1 is expressed in AHSV-infected cells (Huismans & Verwoerd, 1973; Venter, 1991). We have obtained evidence that the *in vitro* synthesised NS1 protein of AHSV forms small tubular structures, similar to those in recombinant baculovirus-infected cells. Although the structure of the *in vitro* synthesised tubules appears to be less homogenous than that of authentic or cell culture-produced AHSV NS1 tubules, it could be ascribed to pH or other physical conditions. This indicates that the ability of NS1 to form tubules of specific structure and diameter is primarily a function of the structural units as determined by the specific amino acid sequence. Nel *et al.* (1992) also reported the synthesis of tubules after *in vitro* translation of EHDV NS1. The NS1 protein of EHDV is predominantly present in a particulate form even when small amounts are synthesised, which indicates that the condensation of the NS1 into tubules occurs very rapidly (Nel & Huismans, 1991). This indicated that the ability to form tubules is self-primed and as such a function of the amino acid sequence of the NS1 protein.

To resolve the structure of AHSV-specified tubules, NS1 was expressed to a high level in insect cells by means of a recombinant baculovirus. The *in vivo* synthesised NS1 protein was present in a particulate or polymerised form that could be isolated on sucrose gradients as a tubular complex with a sedimentation value which was in agreement with that of authentic NS1 tubules from AHSV-infected CER cells (Huismans & Els, 1979). Electron microscopic analysis of the NS1 protein complexes indicated that they contained the characteristic AHSV tubules, with a similar morphology as described for authentic tubules isolated from AHSV-3 infected cells (Huismans & Els, 1979). This structure differed in many respects from those described for other orbiviruses such as BTV, EHDV (Huismans & Els, 1979; Urakawa & Roy, 1989; Nel & Huismans, 1991) and BRDV (Moss & Nuttal, 1994). The AHSV tubules were found to be 23 ±2 nm in diameter as compared to the 68 nm diameter of BTV NS1 tubules (Marshall *et al.*, 1990). They varied in length, but tubules of up to 4 μm were found. When the fine structure of these tubules was studied it became clear that there was no detectable ladder-like surface structure with linear periodicity as had been observed in the case of BTV, EHDV and BRDV (Urakawa & Roy, 1989; Nel & Huismans, 1991; Moss & Nuttal, 1995). No specific subunits were observed as in BTV and EHDV. Circular, flat, hollow structures were often seen which could represent cross-sections of tubules or very short subsections of larger tubules. Such circular forms have been reported to be an intermediate between BTV NS1 monomers and tubules and were shown to be able to recondense into tubules under appropriate conditions (Marshall *et al.*, 1990). The diameter of these circular structures was measured and corresponded to that of the tubules. The lumens of these circular forms were measured to be approximately 7 nm. Nel & Huismans (1991) described the difference in appearance of EHDV tubules stained with phosphotungstic acid (PTA) and uranyl acetate (UA). AHSV NS1 tubules were extremely unstable in the presence of PTA and no tubules were visible after staining with PTA, even at physiological pH and salt conditions. In-lens FESEM revealed a network of tubules. The surface structure of the NS1 tubules forms a continuity and no segments are visible.

Electron micrographs of thin sections of cells infected with the baculovirus NS1 recombinant indicated that the tubules occurred in the cytoplasm as bundles with random orientation. Urakawa & Roy (1988) have reported a close association of bundles of fibrous material with the tubules that are formed in *S. frugiperda* cells infected with a recombinant baculovirus that express the NS1 gene of BTV-10. In the case of BTV-infected cells, it has been shown that some but not all of the BTV tubules, together with a proportion of virus inclusion bodies and virus-like particles are cytoskeleton-associated (Eaton *et al.*, 1987; Eaton *et al.*, 1988; Hyatt & Eaton, 1988; Eaton *et al.*, 1990). It has also been suggested that NS1-rich fibrillar material condenses to form tubules after NS1 has been utilised in the process of virus morphogenesis (Eaton *et al.*, 1988). If soluble NS1 plays a role in viral morphogenesis, the condensation of

NS1 into tubules may only occur after a critical concentration of soluble NS1 has been reached. On the other hand it is possible that NS1 monomers are very rapidly added to the growing tubule filaments, after synthesis. In order to investigate the polymerisation of NS1 into virus-specific tubules, Nel & Huismans (1991) compared the ratio of particulate and soluble NS1 at different levels of expression. It was found that, even when a very small amount of NS1 was synthesised, almost all the NS1 was present in the particulate form.

Three dimensional studies of BTV NS1 tubules indicated that each tubule is composed of a coiled ribbon of NS1 dimers with 22 dimers per helix turn (Hewat *et al.*, 1992), while EHDV tubules contains only approximately 16 subunits per turn (Nel & Huismans, 1991). Although no clearly defined subunits in the AHSV tubules were identified, it could be illustrated that the AHSV NS1 tubules were more easily disrupted at a high ionic strength and at different pH conditions than BTV tubules. Marshall *et al.* (1990) reported that BTV tubules are reduced in length in a 0.5 M $CaCl_2$ solution while the AHSV tubules were completely denatured at 0.2 M $CaCl_2$. AHSV tubules were furthermore significantly reduced in length in 1 M NaCl. As in the case of BTV tubules (Marshall *et al.*, 1990), AHSV tubules were relatively resistant to low pH, but at an alkaline pH of 8.5 they were more susceptible to degradation than BTV tubules. The biophysical properties of AHSV NS1 versus BTV NS1 are summarised in *Table 2.6*. These results would suggest that AHSV tubules are more fragile than BTV tubules.

TABLE 2.6: *Biophysical properties of AHSV NS1 versus BTV NS1*

Property	AHSV tubules	BTV tubules
Acid sensitivity	Relative stable	Even more stable
Alkaline sensitivity	Extremely sensitive	Relative stable
Low ionic strength	Extremely sensitive	Relative stable
High ionic strength	Stable	Stable
Low temperature	Stable	Stable
High temperature	Sensitive	Sensitive
Ionic detergents	Extremely sensitive	Sensitive
Non-ionic detergent	Extremely sensitive	Stable
Chelating agents	Sensitive	Sensitive

There is as yet no evidence for a specific function of NS1 tubules in virus replication, although they may play a role in transport of mature virus particles from the virus inclusion bodies to the cell membrane where NS3 is involved in virus release. Although the amino acid sequence of NS1 and the structure and biophysical character of the tubules differ significantly among AHSV, BTV, EHDV and BRDV, their function may be conserved. Their synthesis is, however, a

characteristic feature of all orbiviruses investigated thus far. Marshall *et al.* (1990) has reported some similarities in the quaternary structure of BTV tubules and tubulin. Many different viruses such as rotaviruses (Kimura & Murakami, 1977), SV40 (Murphy *et al.*, 1986), reovirus (Dales *et al.*, 1963), Sendai virus (Moyer *et al.*, 1986) and others have been reported to be associated with or dependent on microtubules or microtubule-associated proteins (Hill & Summers, 1990) at some stage in their life cycle. Some evidence has accumulated that the formation of orbivirus tubules is an important event, which starts early in the infection cycle. In BTV-infected cells the NS1 mRNA is synthesised in a large excess in the very early period of the infection cycle (Huismans & Verwoerd, 1973; Huismans *et al.*, 1979). It has also been shown that tubules appear as early as 2 to 4 hours p.i. (Huismans & Els, 1979), are present in large numbers at 6 h p.i. (Eaton *et al.*, 1990) and that NS1 is synthesised in a significant excess when compared to the other viral proteins (Huismans, 1979). These results all indicate that NS1 is required in large amounts soon after infection.

Two unique antigenic regions of BTV NS1 were previously identified, one of which is located in the C-terminal hydrophilic region stretching from amino acids 470 to 500 (Du Plessis *et al.*, 1995). This region seems suitable for the insertion of epitopes in the construction of chimeric AHSV NS1 tubules. It is not known if the insertion of a foreign epitope in AHSV NS1 would influence the ability of AHSV NS1 to form tubular structures. It was shown in the literature that chimeric BTV NS1 tubules are highly immunogenic (Mikhailov *et al.*, 1996). NS1 tubules have many advantages over CLPs as epitope carriers. They are composed of a single protein, in contrast to CLPs, which consist of VP3 and VP7. Further, the expression level of the recombinant NS1 is generally extremely high (ca. 25% of the proteins synthesised in infected Sf cells)(Urakawa & Roy, 1988). Tubules are also easy to purify, and so they could provide an efficient and inexpensive system for the presentation of single or multiple foreign epitopes. It is furthermore likely that the use of multiple baculovirus gene expression vectors would increase the efficacy of formation of multiple epitope tubules, although this is yet to be investigated.

CHAPTER 3

ASSEMBLY OF EMPTY CORE-LIKE PARTICLES AND DOUBLE-SHELLED, VIRUS-LIKE PARTICLES OF AFRICAN HORSESICKNESS VIRUS BY CO-EXPRESSION OF FOUR MAJOR STRUCTURAL PROTEINS

3.1. INTRODUCTION

In order to increase our understanding of the assembly of the capsid proteins of AHSV, for the development of subunit vaccines and to study viral morphogenesis, it is necessary to investigate the interaction of the four major structural proteins of AHSV in the absence of other AHSV proteins and the viral genome. To investigate particle formation it was necessary to synthesise the proteins of interest in significant quantities using an appropriate expression system, in a near to native conformation.

The formation of complex structures such as viruses often requires the synthesis and interaction of several gene products. For example, seven structural proteins in different molar proportions are needed for the assembly of mature African horsesickness virus particles. Viral structures which contain multiple proteins encoded by separate genes or mRNA species and involving non-equimolar ratios of proteins present a more difficult and challenging objective to the study of viral morphogenesis. The AHSV and BTV cores present a puzzle of how a large complex, containing mismatched symmetry, can assemble (Roy, 1992; Roy, 1996; Roy *et al.*, 1997). Viruses of the family Reoviridae have received considerable attention from structural biologists. The structure of at least one member of each of the four major genera, Rotavirus, Orthoreovirus, Orbivirus, and Aquareovirus, has been determined using cryo-electron microscopy. Most of the structure-related research and the assembly of orbivirus particles have been carried out with BTV. The atomic structure of the core of BTV has recently been resolved by X-ray crystallography (Grimes *et al.*, 1998).

The assembly of the two major core proteins of BTV, VP3 and VP7, was demonstrated by simultaneous expression of the two proteins, using a dual gene recombinant baculovirus consisting of duplicated polyhedrin promoters of *Autographa californica* nuclear polyhedrosis virus. Recombinant baculoviruses synthesising both proteins produced core-like particles distributed throughout the infected insect cells. The BTV CLPs appeared to be similar in size and appearance to cores prepared from BTV. In the case of BTV, baculovirus multigene vectors have been developed to co-synthesise up to five BTV proteins in the same cell (Balyaev & Roy, 1993; Balyaev *et al.*, 1995).

For optimum synthesis of BT VLPs a quadruple gene expression vector, which utilises the polyhedrin and p10 promoters of AcNPV, has been used to synthesise the BTV VP2, VP3, VP5 and VP7 proteins. The expressed proteins assembled into virtually homogenous double capsid particles (French *et al.*, 1990).

In comparison to BTV, very little is known about the assembly of the structural proteins of AHSV and most of the focus has been on protective antigens and the development of subunit vaccines (Martinez-Torrecuadrada *et al.*, 1996). Until very recently a number of the genes that encode the capsid proteins had either not yet been cloned or had not been expressed. No work on the assembly of AHS VLPs has been published. One of the aims in AHSV research has been to clone, characterise and express all the genes that encode AHSV structural proteins, in order to identify potentially important differences between BTV and AHSV capsid proteins. Furthermore, to reveal common structural elements in cognate proteins of related orbiviruses, that can provide us with a better understanding of how the structure of individual proteins relates to their function. All ten different genome segments of AHSV, including VP1, VP3, VP4, VP5 and VP6 have now been cloned, sequenced and successfully expressed using recombinant baculoviruses. Subsequent structural and functional analysis of these recombinant proteins have provided information concerning the assembly, coding properties and replication of AHSV. The natural progression of future studies will be the examination of multiprotein structures such as the core-like and virus-like particles.

The assembly of virus-like particles by the co-expression of the four major structural proteins of AHSV presents several research opportunities. For example, the stages of viral assembly, the contribution of individual components to the assembly process and the nature of viral protein interactions can be investigated. An increased understanding in viral morphogenesis may aid in the development of antiviral agents, which specifically interfere with the assembly process. In addition, it is anticipated that the availability of large quantities of intact VLPs due to the authenticity in their biological and immunological properties could prove useful as viral vaccines, as they lack any genetic material and cannot replicate. The use of baculovirus-expressed subviral particles as vaccines against AHSV has potential advantages over attenuated viral vaccines since they are non-infectious in the target host.

Virus assembly within infected cells involves a precise sequence of macromolecular interactions. To unravel the individual steps involved in the assembly of the complete virion of AHSV, Maree *et al.* (1998) engineered the first of a series recombinant baculoviruses to make multicomponent structures resembling AHSV structure (CLPs). AHSV VP3 and VP7 were simultaneously expressed using two recombinant baculoviruses expressing each gene respectively. As in the case of BTV, the assembly of AHSV VP3 and VP7 into CLPs was self-primed and their structure resembled empty authentic

AHSV cores. The fine structure of the AHSV CLPs remains to be investigated and in order to accomplish this aim it is necessary to co-express large amounts of AHSV VP3 and VP7, using a dual vector. In the long term we hope to make the correlation between structural and functional differences of the individual viral proteins of AHSV and BTV. From a vaccine development point of view, CLPs may prove to be of great practical value. Firstly, the CLPs may provide the necessary scaffold for the correct conformational presentation of the relevant neutralising epitopes of VP2. Therefore, the co-expression of the CLPs with the outer capsid polypeptides of AHSV and their possible self-primed assembly into VLPs may prove to be important in eliciting a neutralising immune response in horses against AHSV. BTV VLPs were found to be highly immunogenic, even at low doses, compared to VP2 alone or mixtures of VP2 and VP5. Secondly, CLPs can be developed as an antigen delivery system expressing/carrying foreign epitopes on the surface of the CLPs. Chimeric BTV CLPs containing foreign epitopes of up to 39 amino acids were able to elicit humoral or T helper cell responses, depending on the epitope. In order to accomplish the aims of using the AHSV CLPs as antigen delivery systems, there is a requirement for a dual recombinant vector expressing large amounts of both major core proteins simultaneously and in the correct molar ratio.

Therefore, the objectives for this part of the investigation were, firstly to investigate the structure and assembly of AHSV major core proteins, VP3 and VP7, by co-expression of the two proteins in insect cells, and secondly to determine whether the outer capsid proteins of AHSV will spontaneously assemble on the CLPs to form VLPs.

3.2. MATERIALS AND METHODS

3.2.1. Materials

The baculovirus transfer vector, pFastbacDual, was obtained from Life Technologies. The late Prof. D. Botes of the Department of Biochemistry, University of Cape Town synthesised the oligonucleotide primers used in this section. The Klenow DNA polymerase enzyme, rapid DNA ligation kit and plasmid or PCR high pure purification kits were supplied by Boehringer Mannheim. Qiagen supplied the Qiagen^{R} plasmid mini-kit, while the Nucleobond^{R} and Wizard^{TM} columns were obtained from Macherey-Nagel and Promega, respectively. Life Technologies also supplied *E. coli* DH5α cells. AmpliTaq^{R} DNA polymerase FS, was supplied in the ABI PRISM^{TM} Big Dye Terminator Cycle Sequencing Ready Reaction kit (Perkin Elmer).

3.2.2. DNA manipulations and construction of dual transfer vectors

3.2.2.1. Insertion of AHSV-9 VP3 and VP7 genes into pFastbacDual

cDNA copies representing the complete coding sequences of the AHSV-9 segment 3 (S3) and segment 7 (S7) were cloned and manipulated for expression in the baculovirus system by Mr. S Durbach and Mrs. S Maree respectively in the laboratory of Prof. H. Huismans (Maree *et al.*, 1998). S. Durbach expressed the VP3 gene in

E.coli. The VP7 gene and a PCR-cDNA hybrid VP3 gene was constructed and expressed by S. Maree.

The PCR-tailored VP7 gene (Maree *et al.*, 1998) was excised from pBR-S7PCR by *Bgl*II digestion and cloned into the dephosphorylated, isocaudameric *Bam*H1 site of the dual baculovirus transfer vector, pFastbac-dual, using standard cloning procedures as described in Materials and Methods in chapter 2. *E.coli* XL1-Blue cells were used in the transformation and propagation of plasmids. Ampicillin and gentamycin resistant transformants were selected. The derived recombinant plasmids, which appeared larger than wild type pFastbac-Dual on a 1% agarose gel, were further characterised by restriction enzyme mapping. The plasmids were digested with *Sac*I to identify VP7 gene inserts and simultaneously digested with *Bam*H1 and *Hind*III to determine the orientation. A representative recombinant, containing the VP7 gene in the correct orientation for transcription of sense-RNA to be directed by the polyhedrin promoter, was selected (pFBd-S7.9).

The full length AHSV-9 PCR-cDNA VP3 hybrid gene (Maree *et al.*, 1998) suitable for cloning in the baculovirus transfer vector, was subsequently excised from the parent vector, pBR-S3Hyb, by *Bgl*II restriction. Following denaturing of the enzyme by heating at 65°C, nucleotides were added to the overhang termini by use of the Klenow DNA polymerase enzyme (Boehringer Mannheim). Typically 2 U of enzyme was incubated for 30 min in a total volume of 20 µl incubation buffer (50 mM Tris-HCL, 10 mM $MgCl_2$, 1 mM dithioerythritol pH 7.5) containing 0.5-1.0 µg digested DNA and 50 µM of each dNTP. The enzyme was denatured by heating at 65 °C for 5 min and removed by Geneclean™ purification of the fragments following electrophoresis. Alternatively the Klenow enzyme was removed by purification through PCR high pure purification kit (Boehringer Mannheim). The VP3 hybrid gene was blunt end ligated into the dephosphorylated *Sma*I site of pFBd-S7.9. Ligation was performed at 22°C overnight as described in section 2.2.8.3 using an insert:vector ratio of higher than 10:1. Transformation was performed using competent *E. coli* XL1-Blue cells according to the $CaCl_2$/heat shock method (section 2.2.4.1). Ampicillin and gentamycin resistant transformants were selected and a clone containing the VP3 hybrid gene under control of the p10 promoter (pFBd-S3.9-S7.9), was selected by restriction enzyme mapping with *Hind*III and/or *Eco*R1. The full-length status and orientation of the two genes in the pFastbac-Dual plasmid were verified by means of PCR, using VP3 and VP7 specific end primers (table 3.1), and automated cycle sequencing (section 4.2.5) with Ppolh and Pp10 specific primers. The PCR protocol followed was denaturation at 94°C for 3 min followed by 30 cycles of 1 min denaturation at 94°C, annealing for 45 sec at 55°C and elongation for 2 min (3 min for VP3 gene) at 72°C, for both amplification of VP3 and VP7 genes.

3.2.2.2. Insertion of AHSV-9 or AHSV-3 VP2 genes with AHSV-9 VP3 into the dual transfer vector

The recombinant pBS plasmids, pBS-AHSV3.2 and pBS-AHSV9.2, containing full length copies of AHSV-3 and AHSV-9 segment 2 genes respectively, cloned *Bam*H1/*Bgl*II in the T7 orientation were provided by Mr. Frank Vreede and Mr. Grant Napier (Department of Genetics, University of Pretoria). Both genes were proven to be full-length. Restriction enzyme mapping of the segment 2 gene of the two serotypes was performed to verify the orientation. The pBS-AHSV9.2 plasmid was digested with *Hind*III, and pBS-AHSV3.2 with *Xba*I, both enzymes cut asymmetrically once in the gene and once in the vector.

The first step in the construction of a dual vector containing both the VP3 and AHSV-9 or 3 VP2 genes was to clone the AHSV VP3 gene into the pFastbac-Dual vector using the cloning strategy as described in the previous section. A representative recombinant, which contained the gene of interest in the correct orientation for transcription of the sense RNA to be directed by the p10 promoter, was selected and designated pFBd-S3.9. Full-length AHSV-9 VP2 was recovered from pBS-AHSV9.2 by a triple digestion with *Sal*I, *Xba*I and *Sca*I in the

same incubation buffer and purified with the Geneclean™ kit. AHSV-3 VP2 (Vreede & Huismans, 1994) was cut out with *Sma*I, *Sal*I and *Sca*I digestions in the recommended salt buffers for the enzymes and gel purified. Plasmid pFBd-S3.9 was linearised by double digestion with *Sal*I and *Xba*I for cloning of AHSV-9 VP2 under control of the polyhedrin promoter. Alternatively, pFBD-S3 was digested with *Xba*I followed by Klenow repair of the sticky ends, chloroform extraction (2.2.5.1) and *Sal*I digestion for cloning of AHSV-3 VP2. The linearised plasmids were ligated to the full-length *Sal*I/*Xba*I restricted AHSV-9 segment 2 or *Sal*I/*Sma*I AHSV-3 segment 2 DNA, respectively. Ligation was performed using rapid DNA ligation kit (Boehringer Mannheim) which utilises T4 DNA ligase (2.2.8.3) together with ligase buffer and 1x DNA dilution buffer.

The ligation mixtures were used to transform *E. coli* DH5α cells, which were made competent by a modification/extension of the $CaCl_2$-based procedure (section 2.2.3.1.) as described by Hanahan *et al.* (1983 & 1991). An overnight culture of DH5α cells were grown in LB medium at 30°C until the OD_{550} reaches 0.4. The cells were collected and dispersed in $^1/_3$ volume CCMB80 transformation buffer (80 mM $CaCl_2$, 20 mM $MnCl_2$, 10 mM $MgCl_2$, 10 mM K.acetate). The cells were pelleted, supernatant decant and resuspended in a 1/12 of original volume CCMB80. After transformation with the ligation mix the culture was grown for 4 h in LB or SOC medium before plating out on LB-agar plates containing amp, tet and gent. Colonies with amp^R and $gent^R$ phenotype were isolated and characterised by restriction analysis. Recombinant plasmids with the correct transcriptional orientation of segment 2 relative to the polyhedrin promoter were selected and designated pFBd-S2.9-S3.9 and pFBD-S2.3-S3.9. The full-length status and orientation of segment 3 and segment 2 genes in the pFastbac-Dual plasmids were verified by means of PCR, using VP3 and VP2 specific end primers (table 3.1.), and automated cycle sequencing with Ppolh and Pp10 specific primers. The PCR protocol followed was 30 cycles of denaturation (96°C for 2 min), primer annealing (50°C for 45 sec) and elongation (29 cycles for 4 min and 1 cycle for 10 min at 72°C).

3.2.2.3. Cloning of AHSV VP5 and VP7 genes into the dual transfer vector

A recombinant pBS plasmid, pBS-AHSV9.6 containing the full length copy of AHSV-9 VP5 gene, cloned in the T7 orientation into the *Bam*H1 site of the vector, was obtained from Mrs. M du Plessis (Department of Microbiology, University of Pretoria) (Du Plessis & Nel, 1997). The AHSV-3 VP5 gene, previously cloned into pBS (pBS-AHSV3.6), was provided by Mr. Frank Vreede. The full-length status of the VP5 genes was verified with *Bam*H1 and *Hind*III or *Bgl*II digestions.

The AHSV-9/-3 VP5 genes was retrieved with *Bam*H1 digestion and purified using the Geneclean™ kit. The purified fragments were then ligated to dephosphorylated *Bam*H1-restricted pFastBAC-Dual, using the rapid DNA ligation kit according to the manufacturers' instructions. DH5α cells, made competent by the $CaCl_2$/$MnCl_2$ based method (3.2.1.2), were transformed and selected for amp and gent resistance. Possible recombinants which appears larger than pFastbac-Dual on a 1% agarose gel were characterised by restriction enzyme mapping with *Bam*H1, *Hind*III and *Bgl*II digestions. Representative recombinants (pFBd-S6.9 and pFBd-S6.3) containing the PCR-tailored serotype 9 and 3 VP5 genes in the correct orientation for transcription of the sense RNA from the polyhedrin promoter was selected.

The PCR-tailored AHSV-9 segment 7 DNA was recovered from pBS-S7 (T3 orientation) with simultaneous digestion with *Sma*I and *Xho*I in the recommended salt buffers and restriction conditions specified by the manufacturer. The plasmids pFBD-S6.9 and pFBd-S6.3 were also double digested with *Sma*I and *Xho*I and the effective digestion of both enzymes analysed by self-ligation of the linearised plasmid and transformation into

competent DH5α cells. The plasmid was only used for ligation if there was a significant reduction in the number of colonies compared to a positive control, where the same amount of *Sma*I cut plasmid was used. The purified *Sma*I/*Xho*I restricted VP7 fragment was ligated into the vector using rapid DNA ligation kit or an alternative protocol, using the condensing reagent PEG 8000 (15% of reaction volume) which suppresses intramolecular ligation and accelerate the rate of ligation of blunt-ended DNA described by Sambrook & Maniatis, 1988.

Transformation was performed using competent *E. coli* SURE cells. The cells were made competent using the TFB/FSB method (Hanahan *et al.*, 1983 & 1991). SURE cells grown at 30°C to mid log-phase were collected and made competent as described in the previous section using the TFB/FSB buffer (100 mM KCl, 42 mM $MnCl_2$, 10 mM $CaCl_2$, 3 mM $CoCl_3$ or $RuCl_2$ and 10 mM K.Acetate) or TSB/TSBG. After 4 h at 27-30°C incubation in LB medium containing tetracyclin, transformants were plated out on LB agar plates containing amp, tet and gent and incubated for at least 36 h at 27-30°C. Plasmids from a number of colonies were isolated, screened with dot blot hybridisation (2.2.5.2) and characterised by restriction analysis. Recombinant plasmids with the correct transcriptional orientation of the VP7 gene relative to the p10 promoter were selected by *Sac*I and *Bam*H1 restriction mapping and designated pFBd-S6.9-S7.9 and pFBd-S6.3-S7.9. The full-length status and orientation of the respective genes in the pFastbac-Dual plasmid were verified by means of PCR, using VP5 and VP7 specific end primers (Table 3.1.), and automated cycle sequencing with polh and p10 specific primers. The PCR protocol followed and automated cycle sequencing is described in sections 3.2.1.1 and 4.2.5, respectively.

Table 3.1. *Primers used for PCR identification of the different AHSV genes used in the construction of dual recombinant baculoviruses.*

Gene Target	End Specific	Oligonucleotide sequence	Denatu-ration	Annea-ling	Elonga-tion
AHSV-3 VP2	5' specific (PP1) 3' specific (PP2)	5'-CAC**AGATCT**GTTTAATTCACCATGGCTTCG-3' 5'-GAG**AGATCT**GTAAGTTGATTCACTTGGAGC-3'	96 °C 2 min	50 °C 45 s	72 °C 4 min
AHSV-9 VP2	5' specific (PP1) 3' specific (PP2)	5'-CAC**AGATCT**GTTTAATTCACCATGGCTTCG-3' 5'-GAG**AGATCT**GTAAGTTGATTCACTTGGAGC-3'	96 °C 2 min	50 °C 45 s	72 °C 4 min
AHSV-9 VP3	5' specific (SI5) 3' specific (SI3)	5'-GG**AGATCT**ATGCAAGGGAATGAAAGAATAC-3' 5'-GG**AGATCT**GGCTGCTAAA**T**CGTTGGTCG-3'	94 °C 1 min	55 °C 45 s	72 °C 3 min
AHSV-9 VP5	5' specific (PP7) 3' specific (PP8)	5'-CCA**GGATCC**GTTTATTTTTCCAGAGACC-3' 5'-CCA**GGATCC**GTATGTGTTTTTCCCCGC-3'	94 °C 1 min	53 °C 45 s	72 °C 2 min
AHSV-9 VP7	5' specific (SP2) 3' specific (SP3)	5'-CAC**AGATCT**TTCGGTTAGGATGGACGCG-3' 5'-CAC**AGATCT**GTAAGTGTATTCGGTATTGAC-3'	94 °C 1 min	55 °C 45 s	72 °C 2 min

* Unique restriction enzyme sites are shown in bold

3.2.3. Generation and selection of recombinant baculoviruses

Since the methods used here to generate dual recombinant baculoviruses differed in some aspects to the methods described in chapter 2 it is explained briefly.

3.2.3.1. Construction of composite bacmid DNA by transposition

Construction of recombinant baculovirus DNA was done by modification of the methods described in section

2.2.12. *E. coli* DH10BAC™ cells, containing the bacmid genome and helper plasmid were grown up in small overnight cultures at 27-30°C and made competent using the PEG/DMSO method (Chung & Miller, 1988). DH10BAC cells were grown to early log phase (OD_{550} = 0.5) in LB-broth supplemented with kanamycin and tetracyclin. Cells were pelleted and resuspended in $^1/_{10}$ volume of ice-cold LB-broth supplemented with 10% (w/v) PEG, 5% (v/v) DMSO, 10 mM $MgCl_2$ and 10 mM $MgSO_4$ (TSB medium). Cells were then kept on ice for 20 min. Aliquots of 200 µl of competent cells were placed in a test tube, approximately 0.5-1.0 µg of the recombinant donor plasmids (pFBd-S3.9-S7.9, pFBd-S2.9-S3.9, pFBd-S2.3-S3.9, pFBd-S6.9-S7.9 and pFBd-S6.3-S7.9) were added and incubated on ice for 30 min. To this was added 800 µl of TSBG medium (TSB-medium to which is added 20 mM glucose) and the mixture was incubated in a shake incubator at 27-30°C for 4 h to allow transposition and expression of plasmid-encoded antibiotic resistance genes to occur. Between 100 and 150 µl of transformed cells were then plated out onto LB-agar plates containing kanamycin, gentamycin, tetracyclin, X-gal and IPTG (section 2.2.12.2.) for selection. Plates were incubated inverted for 36 h to allow for expression of the blue/white phenotypes. If transposition of *Tn7* element into the bacmid occurs the *lacZ* gene is disrupted and recombinant colonies will be white versus non-recombinants, which are blue (2.2.12.2). White colonies were picked and streaked on identical plates to confirm their white phenotype.

3.2.3.2. Isolation and selection of composite bacmid DNA

The isolation of composite bacmid DNA was done following a protocol specifically developed for isolation of large plasmid DNA (> 100 kb) as was adapted for isolation of high molecular weight bacmid DNA (Amemiya *et al.*, 1994). Cell pellets from 1 ml suspension cultures were resuspended in 300 µl solution 1 (2.2.5), followed by the addition of 300 µl solution 2 (0.2 N NaOH, 1% SDS). Each tube was gently inverted and incubated at RT for 5 min. Following this, 300 µl of 3 M K.acetate pH 5.5 was added and the samples cooled on ice for 5-10 min. Each sample was centrifuged at maximum speed for 10 min and 800 µl absolute isopropanol was added to each supernatant. After 20 min at -20°C, DNA was pelleted and washed with 70% ethanol. Pellets were air dried and resuspended in 30 µl sterile ddH_2O and kept at 4°C. The solution was not to be vortexed or subjected to mechanical stress, as this may lead to shearing of the high MW bacmid DNA.

The potential recombinant bacmid DNA were selected further by means of PCR amplification. End specific primers or polh and p10 specific primers in combination with pUC/M13 amplification primers were used to amplify the different AHSV genes under the same conditions as described in section 3.2.2, using 5 µl of each recombinant bacmid DNA. As controls wild type bacmid DNA preparations and the recombinant pBS plasmids containing each gene of interest were also used as templates in separate reactions. In some cases dot blot hybridisation (section 2.2.6) was also used for selection of potential recombinant bacmid DNA. Approximately 200 ng of each potential recombinant bacmid DNA was denatured and dot spotted onto Hybond-N nylon membrane as described in section 2.2.6.2. The DNA was fixed with UV irradiation for 5 min and then hybridised using gene specific probes.

3.2.3.3. Transfection of Sf9 cells with bacmid DNA

Following isolation of the recombinant bacmid DNA, 0.9 x 10^6 cells were seeded in 35 mm six-well tissue culture plates (Nunclon™). Cells were allowed to attach for 1h at 27°C during which time transfection mixtures containing composite bacmid DNA were prepared as follows: 8 µl of recombinant bacmid DNA (1.5-2 µg) was diluted into 100 µl Grace's medium without serum or antibiotics, as this could inhibit uptake of exogenous DNA. A second solution containing 8 µl lipofectin™ or cellfectin™ reagent (Gibco BRL) or DOTAP (Boehringer Mannheim) in 100 µl Grace's medium without serum or antibiotics was also prepared, after which the two solutions were gently mixed and incubated at RT for 45 min. The cells were washed twice with 2 ml Grace's medium without serum or antibiotics. Then 800 µl of medium was added to the tubes, containing the DNA-lipid

complexes and the cells were overlaid with the lipid-DNA complexes. Cells were incubated for 6 h in a 27°C incubator to allow uptake of the recombinant bacmid DNA, after which time the transfection mixtures were removed and 2 ml Grace's medium containing serum and antibiotics was added. Cells were then incubated for a further 96 h, after which the viral supernatant was harvested. Preparation of high titre virus stocks was done as described in section 2.2.11.4 and the viruses designated DBac-S3.9-S7.9, DBac-S2.9-S3.9, DBac-S2.3-S3.9, DBac-S6.9-S7.9 and DBac-S6.3-S7.9.

3.2.3.4. *In vivo* mRNA hybridisation

Transcription of AHSV-9 genes in insect cells was tested using an *in situ* hybridisation method (Paeratakul *et al.*, 1988). Monolayers of Sf9 cells in 24 mm wells (3×10^5 cells/well) were either mock-infected or infected with the selected dual recombinant baculovirus (DBac-S2.9-S3.9, DBac-S2.3-S3.9, DBac-S6.9-S7.9 and DBac-S6.3-S7.9) at a MOI of 10 p.f.u./cell. The infected cells were harvested 48 h p.i., washed and kept in 300 µl PBS at -20°C. Approximately 1×10^5 cells were spotted onto Hybond C-extra nitrocellulose membranes (Amersham), prewetted in PBS, using a dot-blot microfiltration apparatus. Equal volumes of each sample were blotted in duplicate for detection of either the AHSV-9 VP3 or VP2 mRNA (infection with DBac-S2.9-S3.9) or the AHSV-9 VP7 or VP5 mRNA (infection with DBac-S6.9-S7.9). Cells were fixed onto the membranes at 4°C for 1 h in 1% gluteraldehyde, 3% NaCl, 10 mM NaH_2PO_4, 40 mM Na_2HPO_4 (pH 7.4) and rinsed three times with proteolitic buffer (50 mM EDTA, 0.1 M Tris-HCL, pH 8.0). Cells were digested in proteolitic buffer containing proteinase K (20 µg/ml) at 37°C for 30 min. Memebranes were air dried and immersed in prehybridisation buffer (50% formamide, 5 x SSPE, 0.1% milk powder) for 1 h followed by hybridisation with the AHSV-9 or -3 gene-specific radiolabelled probe. Radiolabelled probes were prepared as described in section 2.2.6.1. The probes were prepared from pBS-AHSV9.2, pBS-S3Hyb, pBS-AHSV9.6 and pBS-S7PCR recombinant plasmids.

3.2.4. Co-expression of AHSV capsid proteins in insect cells and purification of multimeric particles comprising different combinations of AHSV proteins

3.2.4.1. Analysis of polypeptides synthesised in infected insect cells

Monolayers of Sf9 cells were infected with the VP3/VP7, VP2/VP3 or VP5/VP7 dual recombinant baculoviruses at a MOI of 5 to 10 pfu/cell of each virus, as described in section 2.2.12. Sf9 cells were also mock infected or infected with the parent virus. Infected cells were harvested at 48 or 72 h p.i., pelleted, washed and resuspended in 1x PBS. Prior to electrophoretic analysis, protein samples were mixed with an equal volume 2x PSB (2.2.12). Proteins were resolved by 12% or 10% SDS-PAGE analysis (2.2.10.3). The time course for maximal protein expression was determined by repeating the infection and radiolabelling of the infected cells at time intervals 36 h, 42 h, 48 h and 54 h p.i., described in section 2.2.12.

3.2.4.2. Co-expression of different combinations of AHSV capsid proteins in insect cells and purification of expressed multimeric particles

S. frugiperda cells were infected at a multiplicity of 10-15 pfu with either the dual recombinant baculovirus or wild type virus or mock infected. Cells were harvested at 48-72 h post-infection, washed with 1 x PBS and lysed at 4°C in 50 mM Tris-HCL (pH 8.0), 150 mM NaCl, 0.5% Nonidet P-40 (TNN buffer) at a concentration of 2×10^7 cells/ml followed by mechanical shearing through a dounce apparatus. Nuclei were removed by low speed centrifugation at 1000 rpm for 5 min and washed twice in small volumes of TNN buffer. The cytoplasmic

fractions were pooled and subjected to differential centrifugation for 30 min at 5000 rpm in a J-21 Beckman centrifuge. The expressed particles were purified from the supernatant either by banding on a discontinuous sucrose gradient (40% and 68% (w/v) in 150 mM NaCl, 0.2 M Tris-HCl pH 8.0) after centrifugation at 35 000 rpm in a SW50.1 Beckman rotor (85 000 x g) for 3 h or on a self forming CsCl (35%) density gradients after centrifugation at 140 000 g for 18 h. Fractions forming at the 40% to 68% interface were collected (0.7-1.0 ml volume), diluted to 5 ml volume in 150 mM NaCl, 0.2 M Tris-HCl (pH 8.0) and pelleted at 85 000 g for 30 min. The particles were analysed by SDS-PAGE and examined by electron microscopy.

Sf9 cells were also co-infected with the AHSV-9 VP3/VP7 dual recombinant baculovirus and an AHSV-9 VP5 or VP2 single gene recombinant baculovirus at multiplicities of 5 pfu/cell. Similar co-infections were performed with the VP3/VP2 dual and VP7 single recombinant baculoviruses and VP5/VP7 dual and VP3 single recombinant baculoviruses. For the production of VLPs the co-infection were repeated using VP2.3/VP3 or VP2.9/VP3 in combination with VP5.9/VP7 dual gene recombinant baculoviruses or VP2.3/VP5.3 and VP3/VP7 recombinant baculoviruses at a MOI of not more than 10^5 pfu/cell. The assembled particles were recovered and purified through a 40 to 68% discontinuous sucrose gradients, centrifuging for 2 h at 4°C and 85 000 g or alternatively on an 10-40% (w/v) continuous sucrose gradient. The protein components of the fractions forming the 40% to 68% interface were collected, analysed by SDS-PAGE and examined by electron microscopy.

3.2.4.3. Stoichiometry of VP3 to VP7

Monolayers of Sf9 cells were infected with the dual-recombinant baculovirus at a multiplicity of 10 pfu per cell and incubated at 28°C for 2 h after which the inoculum was replaced with fresh Grace's medium to synchronise the infection. The infected cells were incubated for a further 24 to 36 h. Radiolabelling of the viral proteins was achieved as described in section 2.2.12. The cells were then harvested and washed in 1 x PBS and the expressed particles were purified on discontinuous sucrose gradients as already described. The particles were pelleted and mixed with protein dissociation buffer and the samples of various amounts were subjected to SDS-PAGE. After electrophoresis the gel was stained with Coomassie Blue, destained in 5% acetic acid and 5% methanol, dried and autoradiographed. The bands of VP3 and VP7 were excised from the dried gel and their activities (counts per minute) were determined after incubation in a liquid scintillation cocktail. The experiment was performed twice, and the results were pooled.

3.2.5. Electron microscopy of purified particles

Purified synthetic AHSV particles were adsorbed onto copper 400-mesh Formvar carbon-coated 400-mesh grids by floating the grids on droplets of the material for 2 min. After being washed twice with 150 mM NaCl, 0.2 M Tris-HCl (pH 8.0), the particles were negatively stained for 30 s on droplets of 2% (w/v) uranyl acetate. For immunodecorating studies, particles obtained from simultaneous expression of dual recombinant virus expressing CLPs and single recombinant virus expressing VP2 or VP5 were adsorbed to carbon-filmed grids and incubated in a 1:100 dilution of AHSV-3 VP5 or AHSV-9 VP2 monospecific antibodies for 30 min. The unbound antibody was washed briefly at the end of the interaction and the grid was then negatively stained as described. All grids were examined in a JEOL electron microscope at room temperature at 60 kV. Low dose micrographs were recorded at a 60 000x magnification. Controls included omission of the primary antibody as well as the dual virus alone.

3.3. RESULTS

3.3.1. Expression of the genes encoding the four major structural proteins of AHSV-9 in insect cells using dual recombinant baculovirus vectors

In order to produce CLPs, partial VLPs and VLPs, the different AHSV structural genes were cloned in different combination into the dual baculovirus donor vector (pFastbac-Dual). The dual constructs used to produce recombinant baculoviruses, that express the AHSV structural proteins, are summarised in table 3.2. The interaction of the structural proteins was investigated by means of co-infection experiments. The construction of the different dual vectors is described in this section.

Table 3.2: *Summary of the plasmid DNA constructs made for usage in the expression of the four major structural proteins of AHSV.*

pFastbac-dual construct	**Foreign genes and AHSV serotypes**	**Promoter**	Constructed by
pFBdS3.9-S7.9	AHSV-9 VP3 and AHSV-9 VP7	p10 polyhedrin	Francois Maree
pFBdS2.9-S3.9	AHSV-9 VP2 and AHSV-9 VP3	polyhedrin p10	Francois Maree
pFBdS2.3-S3.9	AHSV-3 VP2 and AHSV-3 VP3	polyhedrin p10	Francois Maree
pFBdS6.9-S7.9	AHSV-9 VP5 and AHSV-9 VP7	polyhedrin p10	Francois Maree
pFBdS6.3-S7.9	AHSV-3 VP5 and AHSV-9 VP7	p10 polyhedrin	Francois Maree
pFBdS2.3-S6.3	AHSV-3 VP2 and AHSV-3 VP5	polyhedrin p10	Renate Filter
pFBd-S6.9	AHSV-9 VP5	polyhedrin	Francois Maree
pFB-S2.9	AHSV-9 VP2	polyhedrin	Grant Napier

3.3.1.1. Construction of an AHSV-9 VP3 and VP7 dual-recombinant baculovirus transfer vector

The dual expression transfer vector, pFastbac-Dual, facilitates the introduction of two heterologous foreign genes, under control of the very late polyhedrin and p10 promoters, into a single recombinant virus. The strategy employed (*Figure 3.1A*) for the cloning of the full-length AHSV-9 VP3 and VP7 genes into pFastbac-Dual, was as follows. PCR tailored copies representing the complete coding sequences of the AHSV-9 segment 3 and segment 7 genes were used for co-expression in the BAC-TO-BAC baculovirus system. Both the VP3 and VP7 genes contain internal *Bam*H1 sites and the vector-specific *Bam*H1 site downstream of the polyhedrin promoter was therefore utilised in the first cloning step. A PCR-tailored copy of the VP7 gene was previously cloned by dG/dC-tailing into pBR322 by S. Maree and the recombinant plasmid pBR-S7PCR was utilised to obtain the full length VP7 gene of AHSV-9. The PCR-tailored VP7 gene was excised from pBRS7PCR by *Bgl*II digestion and cloned into the dephosphorylated *Bam*H1 site of the pFastbac-Dual vector under control of the polyhedrin promoter. The derived recombinant plasmids were characterised by restriction enzyme mapping with *Sac*I, which cleaves twice in the VP7 gene at position 250 and 1045, and simultaneous digestions *with Bam*H1 and *Hind*III, which respectively cleaves the DNA ca. 100 bp from the 5' end of the gene and in the multiple cloning site downstream of the polyhedrin promoter. A representative recombinant, yielding three fragments of 5.5 kb, 850 bp and 100 bp in the first digestion and two fragments of 5.3 kb and 1000 bp in the second digestion was selected. This clone contained the VP7 gene in the correct orientation for transcription of the sense-RNA to be directed by the polyhedrin promoter. The recombinant was designated pFBd-S7.9 and was used to insert the AHSV-9 VP3 gene.

A PCR tailored copy of the VP3 gene of AHSV-9, containing *Bgl*II restriction sites at the 5' and 3' termini, was cloned by homopolymer dG/dC tailing in pBR322 by Steven Durbach. A VP3 chimeric gene (pBR-S3Hyb) was constructed by Sonja Maree, in which the central 2.0 kb part of the PCR copy was replaced by the corresponding cDNA region. The VP3 chimeric gene was subsequently recovered from pBR-S3Hyb by *Bgl*II restriction and the ends filled up with Klenow. The VP3 chimeric gene was blunt end cloned into the dephosphorylated *Sma*I site of pFBd-S7.9 plasmid. Many of the derived plasmids were the same size, while some were smaller than pFBd-S7.9 when the ccc forms were compared, which implied that deletions had occurred. Many of the deletions involved the gent^R gene, which made the future selection on gentamycin essential. Plasmids which appeared larger than pFBd-S7.9 were further characterised by asymmetrical restriction with *Bam*H1, *Hind*III and/or *Eco*R1 in order to identify the full length VP3 and VP7 specific inserts as well as the correct transcriptional orientation of the VP3 hybrid gene. The VP3 gene specific *Hind*III site is located at ca. 2.3 kb and the *Eco*R1 site at ca. 300 bp from the 5' end and at vector-specific sites, downstream of the polyhedrin promoter (MCS). Plasmids yielding two fragments of ca. 4 kb and 5.1 kb with *Hind*III digestion and

two fragments of ca. 2 kb and 7.1 kb with *Eco*R1 digestion and three fragments of ca. 1.9 kb, 2.1 kb and 5.1 kb with simultaneous digestion with both enzymes were regarded as recombinant (*Figure 3.1B, C*). A representative clone containing the VP3 hybrid gene under control of the p10 promoter, was selected and designated pFBd-S3.9-S7.9. The yield of recombinants with VP3 in the correct transcriptional orientation was about 1-2% of all colonies screened, using the described strategy.

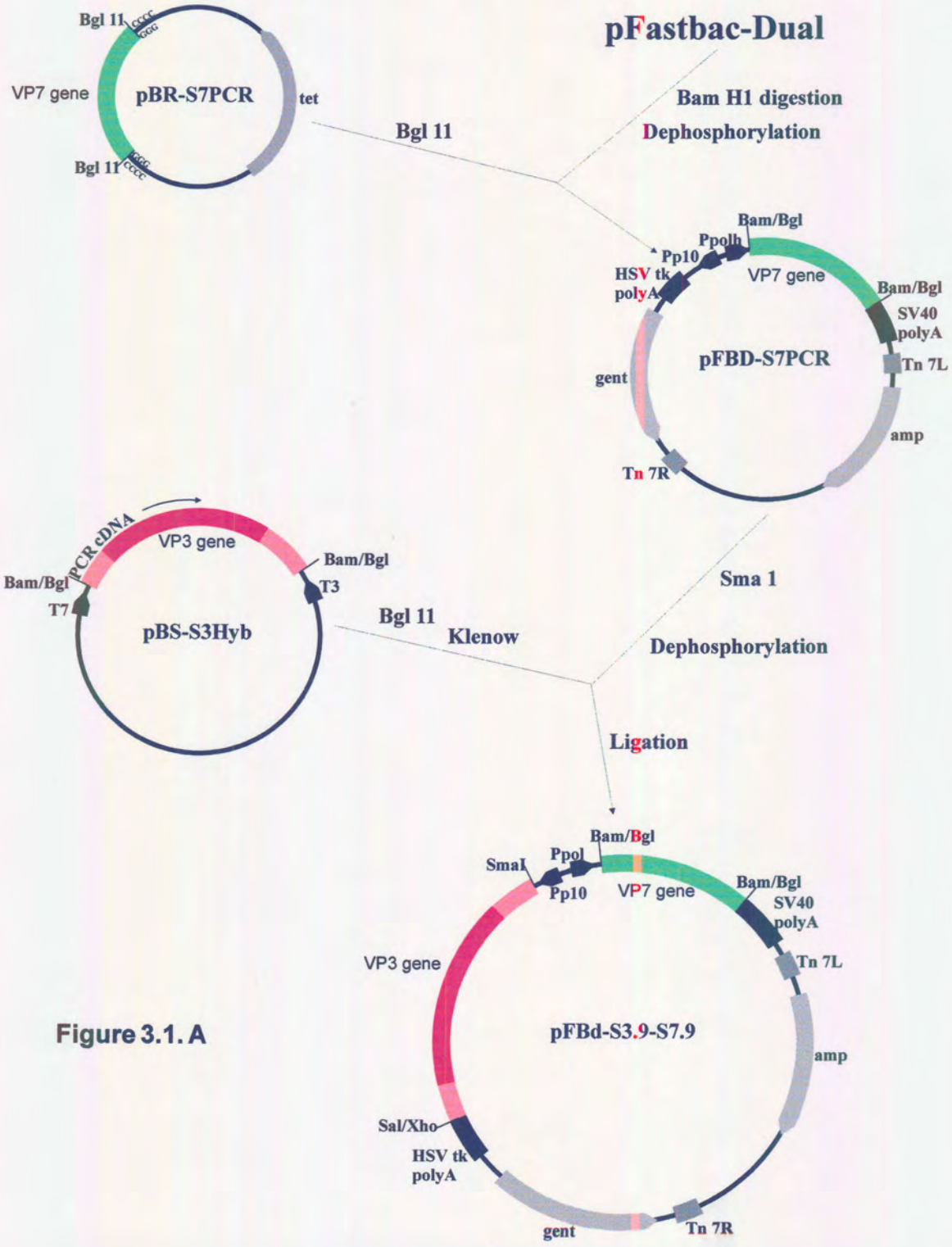

Figure 3.1. A

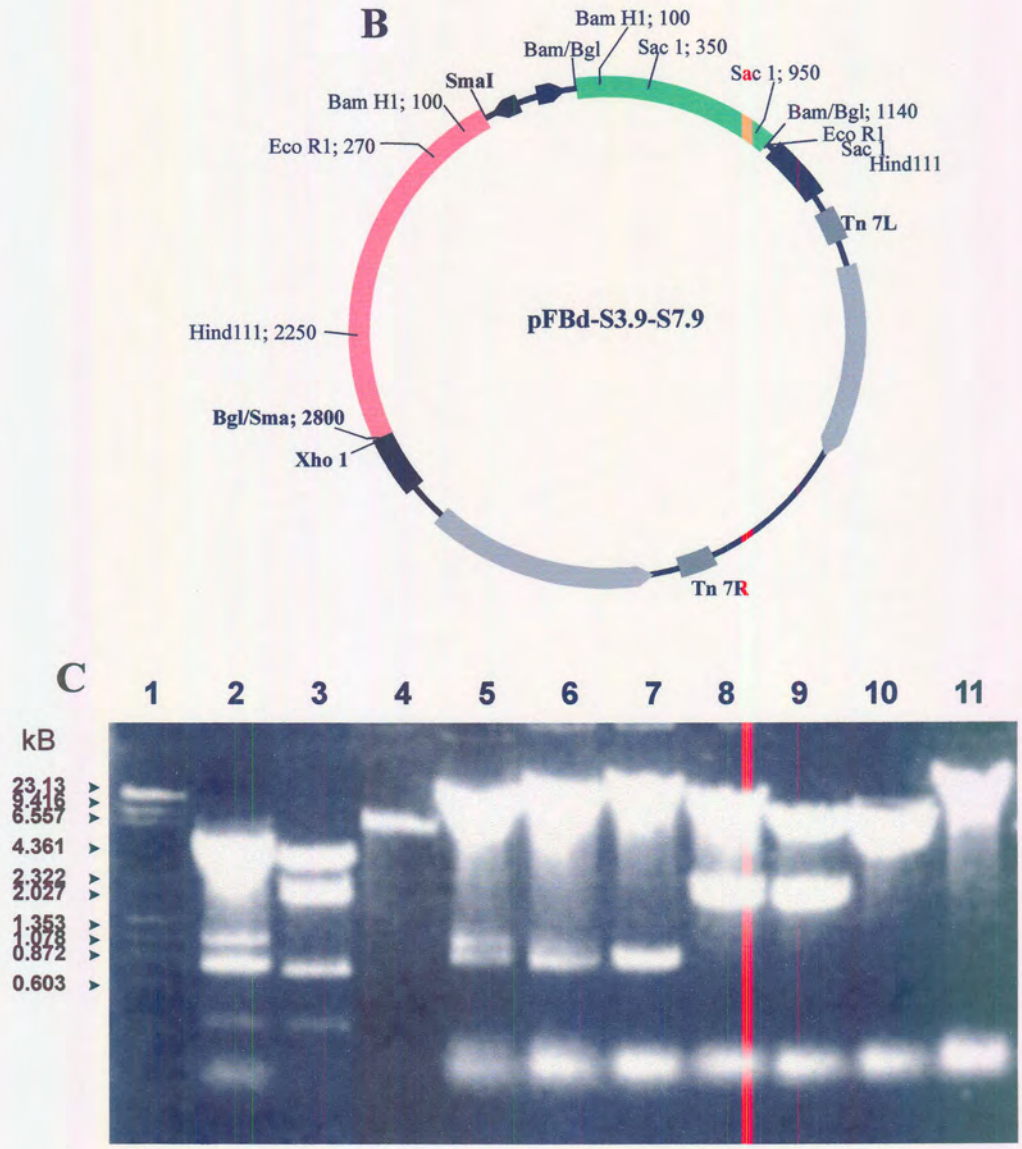

Figure 3.1: (A) A schematic diagram showing the strategy for cloning both AHSV-9 VP3 and VP7 genes into the dual expression transfer vector, pFastbac-Dual. The AHSV-9 VP3 and VP7 genes is shown in red and green, respectively. (B) A schematic representation of a partial restriction map of the dual recombinant plasmid, pFBd-S3.9-S7.9. (C) Agarose gel electrophoretic analysis of pFBd-S3.9-S7.9. The plasmids pBS-S7PCR (lane 2) and pBS-S3Hyb (lane 3) were digested with *Sac*I and *Hind*III/*Eco*R1, respectively. This, together with molecular weight markers MW11 and ϕx174 (lane 1) and linearised pFBd (lane 4), function as controls. Lane 5 represents pFBd-S7 digested with *Sac*I. Lanes 6-11 represent pFBd-S3.9-S7.9 digested with *Sac*I, *Bam*H1, *Eco*R1, *Hind*III/*Eco*R1, *Hind*III and *Sal*I, respectively. The sizes of the molecular weight markers are indicated to the left of the figure.

3.3.1.2. Construction of a dual-recombinant baculovirus transfer vector containing either AHSV-3 or AHSV-9 VP2 and AHSV-9 VP3 genes

The strategy employed for the cloning of both the full length VP2 gene of two AHSV serotypes and the VP3 gene into the dual transfer vector was as follows (*Figure 3.2*): In the first step the VP3 gene was cloned into the *Sma*I site of the pFBdual vector under control of the p10 promoter, essentially as described above. A representative recombinant, which contain the VP3 chimeric gene in the correct orientation for transcription of the sense RNA to be directed by the p10 promoter, was selected and designated pFBd-S3.9.

Secondly, the VP2 gene of both AHSV-3 and AHSV-9 were respectively cloned under control of the polyhedrin promoter, using two somewhat different strategies for each VP2 gene. Briefly, full length AHSV-9 segment 2 was recovered from pBS-AHSV9.2 (a PCR-cDNA chimeric copy of the AHSV-9 VP2 gene; cloned and constructed by Grant Napier) by triple digestion with *Sal*I, *Xba*I and *Sca*I. The strategy was aimed at separating the 3.2 kb VP2 gene from the pBS vector. *Sca*I cuts in the amp^R gene of pBS and digest the 3.2 kb vector into two shorter fragments of ca. 1.2 kb and 2.0 kb, which could be separated from the VP2 gene in a triple digestion. AHSV-9 VP2 was directionally cloned into the *Sal*I/*Xba*I sites of pFBd-S3.9. The identity and orientation of the AHSV-9 VP2 gene, with respect to the polyhedrin promoter, of recombinants was verified by restriction analysis with *Eco*R1 and/or *Hind*III (*Figure 3.3 A, B*). A plasmid yielding 750 bp, 2x 1.2 kb and 7.1 kb fragments with *Eco*R1 digestion and 2.4 kb, 3.7 kb and 5.1 kb fragments with *Hind*III digestions was selected and called pFBd-S2.9-S3.9.

The strategy for the cloning of AHSV-3 VP2 into pFBd-S3.9 differed as follows. A 3.2 kb fragment, representing the full length AHSV-3 VP2 gene was obtained by triple digestion of pBS-AHSV3.2 with *Sal*I, *Sma*I and *Sca*I. The VP2 gene was directionally cloned into pFBd-S3.9 and the correct orientation determined by restriction analysis with *Hind*III, *Eco*R1, *Xba*I and *Bam*H1. This was achieved on the basis of a AHSV-3 segment 2-specific *Xba*I site and *Bam*H1 site which cuts asymmetrically in the gene 2700 bp and 30 bp from the 5' terminus respectively and a vector-specific *Xba*I site downstream from the polyhedrin promoter or *Bam*H1 site 150 bp from the 5' terminus of the VP3 gene. Thus a plasmid yielding two XbaI fragments of approximately 9.8 kb and 500 bp and two *Bam*H1 fragments of 800 bp and 9.4 kb was selected and designated pFBd-S2.3-S3.9 (*Figure 3.4 A, B*).

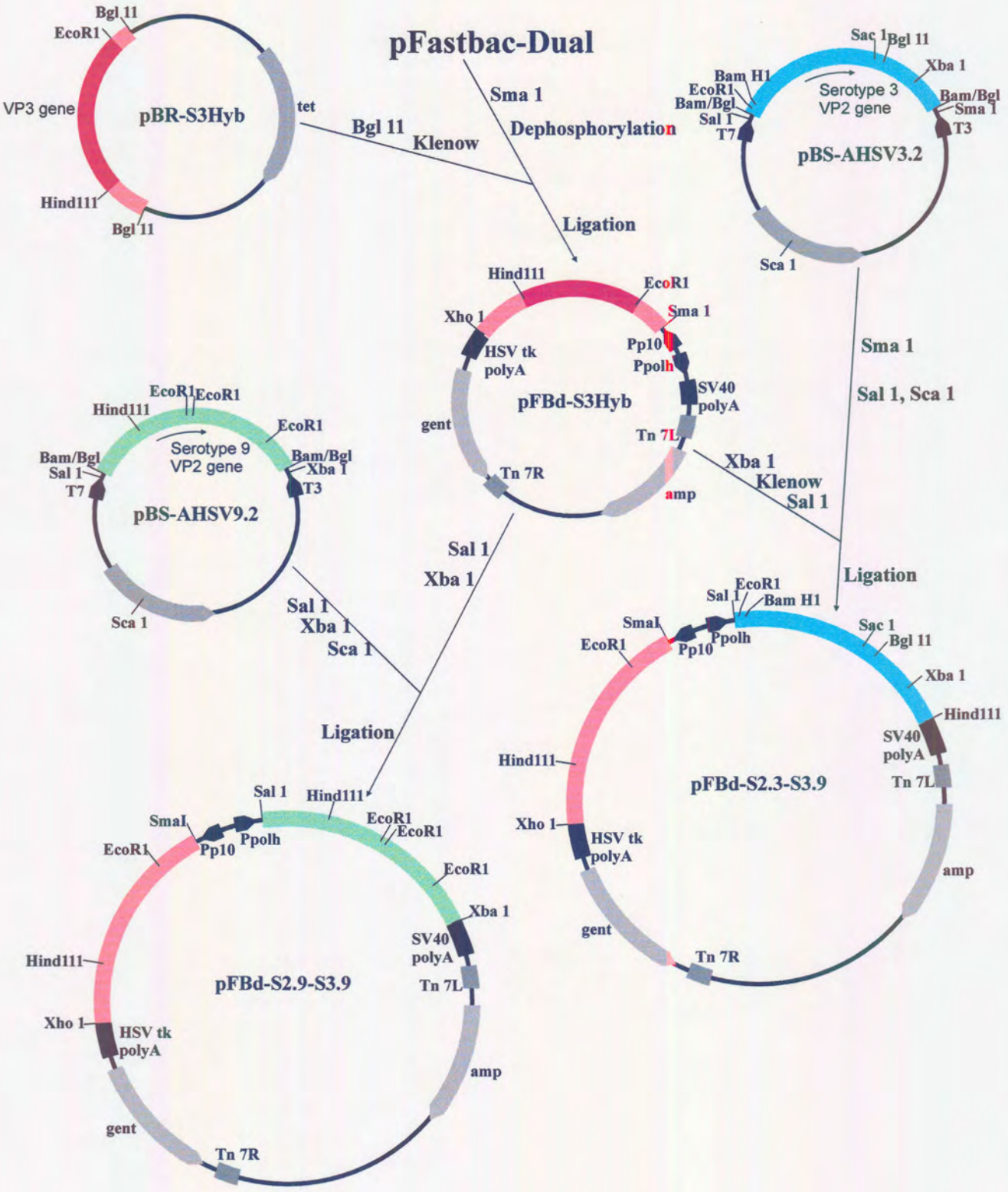

Figure 3.2: A schematic diagram of the strategy employed for the respective cloning of AHSV-3 and AHSV-9 VP2 genes in combination with AHSV-9 VP3 into the transfer vector pFastbac-Dual.

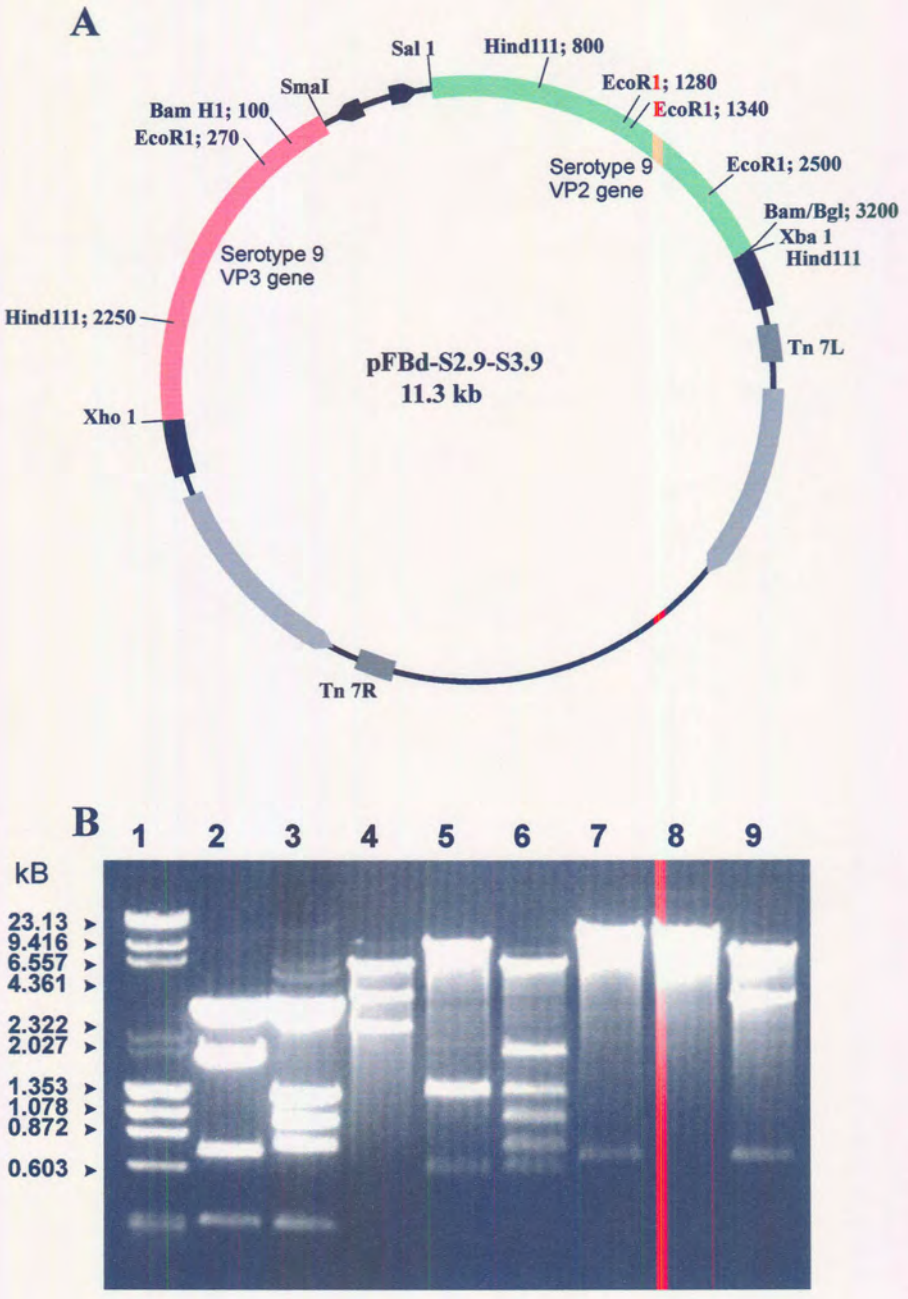

Figure 3.3: (A) A schematic representation of a partial restriction map of the plasmid pFBd-S2.9-S3.9, containing AHSV-9 VP2 and VP3 genes in the correct transcriptional orientation for expression by the polyhedrin and p10 promoters, respectively. The distance from the 5'end of the gene is indicated in bp next to each restriction enzyme site. (B) A restriction analysis of pFBd-S2.9-S3.9. The plasmids pBS-S3Hyb (lane 2) and pBS-AHSV9.2 (lane 3) digested with *Hind*III/*Eco*R1 were included as controls. Lanes 4-9 shows the fragments obtained after restriction with *Hind*III (4), *Eco*R1 (5), *Hind*III/*Eco*R1 (6), *Bam*H1 (7), *Xba*I (8) and *Bam*H1/*Xba*I (9), respectively. Lane 1 shows molecular weight markers with the sizes in kb indicated to the left of the figure.

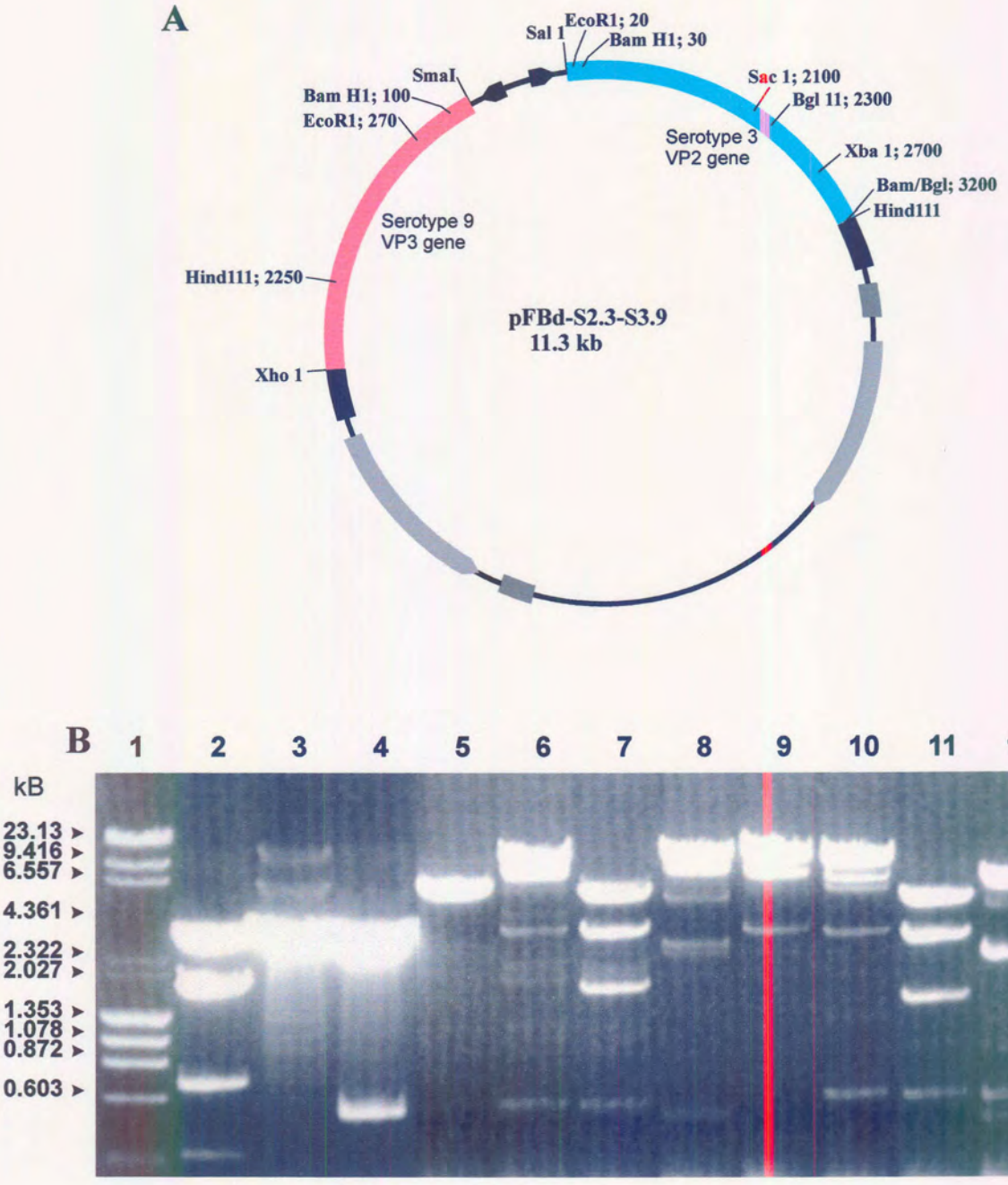

Figure 3.4: (A) A schematic representation of a partial restriction map of the plasmid pFBd-S2.3-S3.9, containing AHSV-3 VP2 and AHSV-9 VP3 genes in the correct transcriptional orientation for expression by the polyhedrin and p10 promoters, respectively. (B) A restriction analysis of pFBd-S2.3-S3.9. The plasmids pBS-S3Hyb (lane 2) digested with *Hind*III/*Eco*R1 and pBS-AHSV3.2 (lanes 3 and 4) digested with *Hind*III/*Eco*R1 and *Bam*H1/*Xba*I were included as controls. Lanes 5-12 shows the fragments obtained after restriction with *Hind*III (5), *Eco*R1 (6), *Hind*III/*Eco*R1 (7), *Xba*I (8), *Sal*I (9), *Bam*H1 (10), *Hind*III/*Bam*H1 (11) and *Bam*H1/*Xba*I (12), respectively. Lane 1 contains molecular weight markers and the sizes are indicated to the left of the figure.

3.3.1.3. Construction of recombinant baculovirus transfer plasmids containing both AHSV VP5 and VP7 genes

Different strategies were used for the construction of a dual transfer vector containing both the VP5 and VP7 genes of AHSV. Cloning of these two genes together in pFastbac-Dual was extremely inefficient and clones were exceptionally unstable. The only successful cloning strategy (*Figure 3.5 A*) that resulted in a recombinant, containing both AHSV-9 VP5 and VP7 genes, is described with specific reference to procedures that were found to be essential for the success of the cloning procedure.

In the first step AHSV-9 or AHSV-3 VP5 gene was cloned into pFastbac-Dual transfer vector. The VP7 gene contains an internal *Bam*H1 site and the vector-specific *Bam*H1 site, downstream of the polyhedrin promoter was therefore utilised in the first cloning step. The PCR-tailored DNA copies of AHSV-9 or -3 VP5 genes were recovered from pBS-AHSV9.6 and pBS-AHSV3.6 respectively and recloned into the dephosphorylated *Bam*H1 site of pFastbac-Dual. Recombinant plasmids, identified by *Bam*H1 digestion and yielded 1.5 kb fragments, were subjected to *Hind*III or *Bgl*II digestion in order to determine the orientation of the VP5 gene in pFastbac-Dual relative to the polyhedrin promoter. Restriction with *Hind*III cleaves the gene ca. 1000 bp from the 5' terminus and the plasmid within the multiple cloning site downstream of the polyhedrin promoter. *Bgl*II cuts in the gene, approximately 300 bp from the 5' end and twice in the vector at positions 2646 and 3116. A plasmid yielding two *Hind*III fragments of ca. 1000 bp and 5.7 kb and three *Bgl*II fragments of 2.4 kb, 2.7 kb and 470 bp was selected, pFBd-S6.9 (*Figure 3.5 C*). This cloning resulted in more than 55% recombinants of which approximately $^1/_3$ were in the desired orientation.

The PCR-tailored VP7 gene cloned in the T7 orientation of pBS (S. Maree) was excised from pBS-S7PCR by restriction with *Sma*I and *Sal*I, purified and cloned into the *Sma*I/*Xho*I site downstream of the p10 promoter of pFBd-S6.9 and pFBd-S6.3. (*Figure 3.5 B, C*). Dual recombinants were selected with *Sac*I, *Bam*H1, *Hind*III and *Eco*R1/*Xho*I digestions. Plasmids that yielded fragments of 850 bp and 7.0 kb (*Sac*I), 550 bp, 1.5 kb and 5.0 kb (*Bam*H1), 500 bp and 7.3 kb (*Hind*III) and 300 bp, 850 bp and 1.7 kb (*Eco*R1/*Xho*I) in the respective digestions were selected (pFBd-S6.9-S7.9 and pFBd-S6.3-S7.9). More than 50% of the derived plasmids were smaller than pFBd-S6.9 when ccc forms were compared, which implies that major deletions occurred. The emergence of this rearrangement or homologous recombination events could be reduced, using *E. coli* SURE cells with recombination deficient (*uvrC*$^-$, *umuC*$^-$ and *recB* and *recJ* mutations) and restriction negative (*mcrA*$^-$, *mcrCB*$^-$) phenotypes. The preparation of competent cells and transformation at < 30°C and selection of transformants on both ampicillin and gentamycin also played a role in reducing the number of deletions, since a great number of the recombinational events involved the gentamycin gene as

analysed by restriction enzyme mapping (results not shown). The presence of both AHSV-9 VP5 and VP7 genes were incompatible or homologous with sequences in the plasmid which cause the dual recombinant plasmid to be extremely unstable and deletions were detected with each generation of bacterial growth.

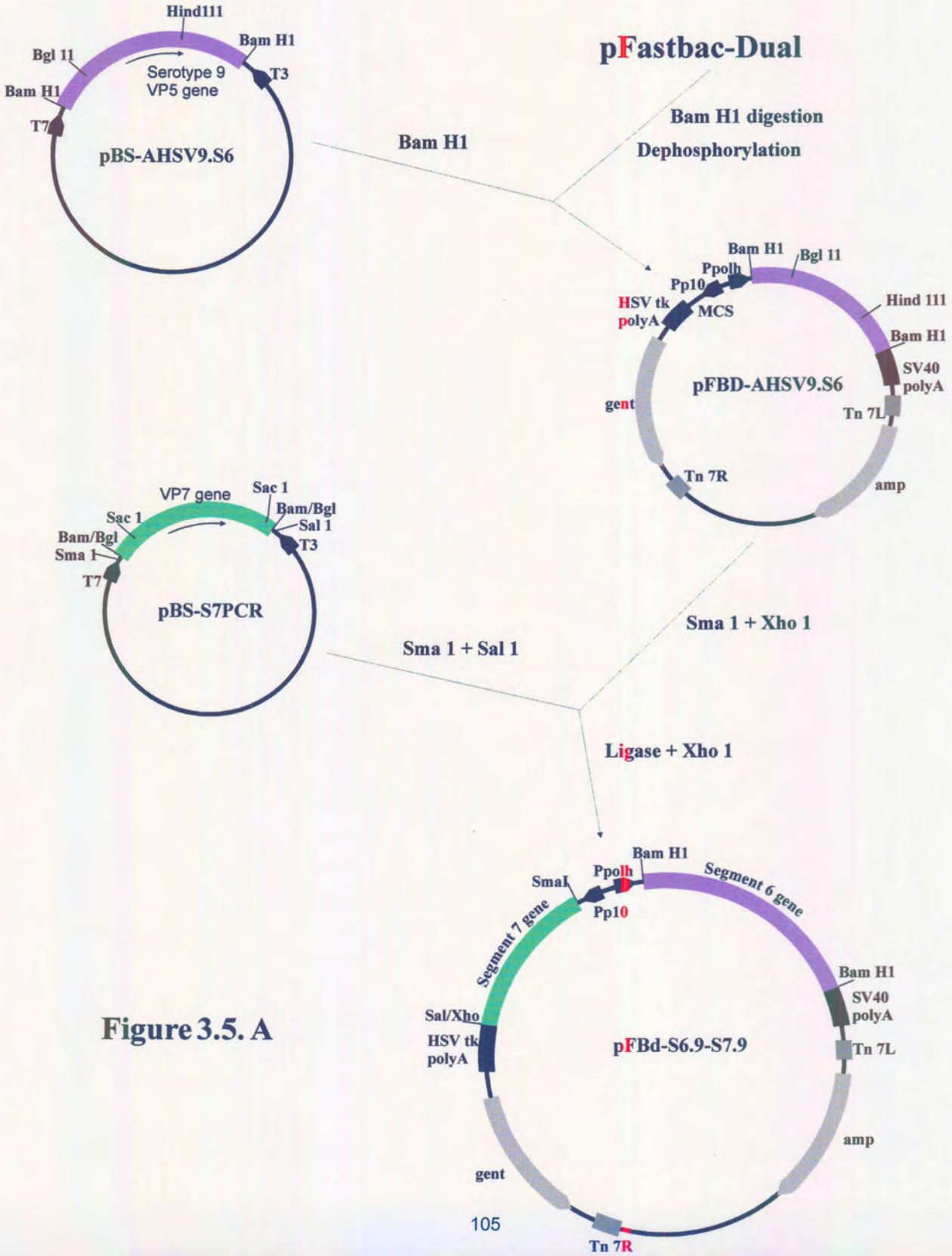

Figure 3.5. A

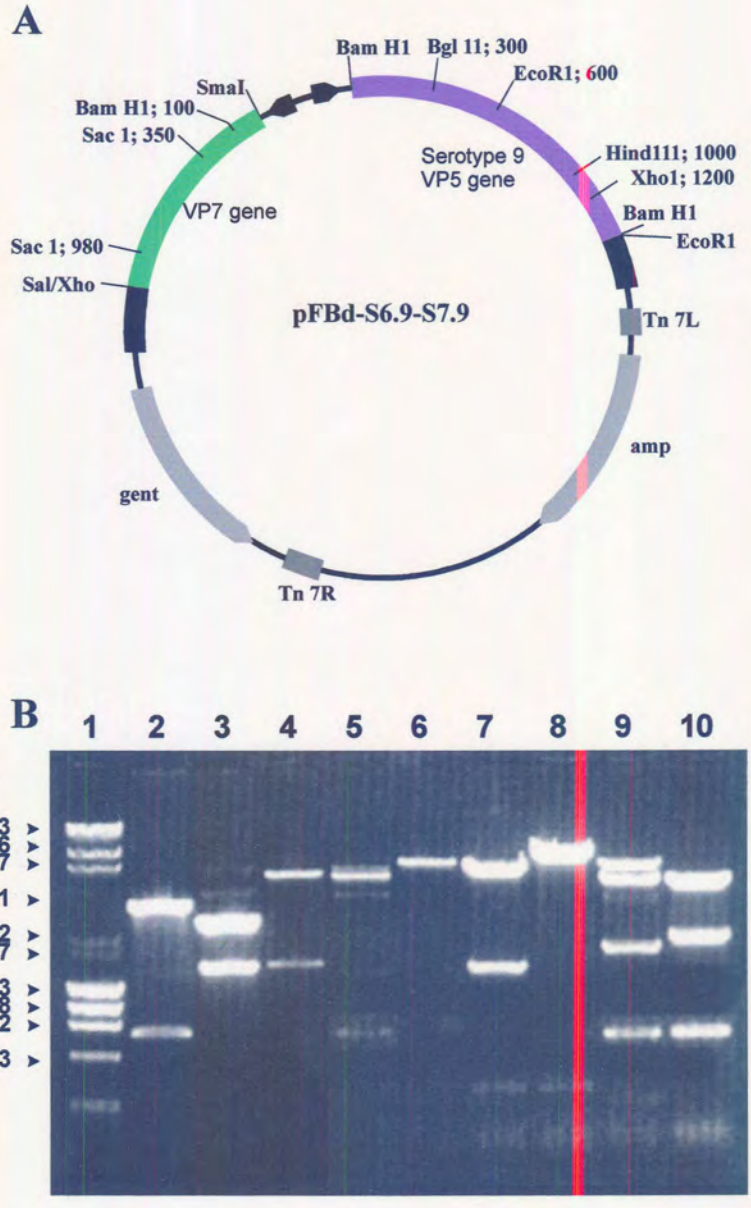

Figure 3.5: (A) A schematic diagram showing the cloning strategy for inserting both AHSV-9 VP5 and VP7 into the dual expression transfer vector, pFastbac-Dual. (B) A schematic representation of a partial restriction map of the recombinant dual transfer vector, pFBd-S6.9-S7.9, containing both genes in the correct transcriptional orientation for expression as non-fused proteins by the polyhedrin and p10 promoters, respectively. The distance in bp from the 5' end of each gene is shown next to the R.E site. (C) An agarose gel electrophoretic analysis of the dual recombinant plasmid, pFBd-S6.9-S7.9. The plasmid was restricted with *Bam*H1 (lane 7), *Hind*III (lane 8), *Eco*R1/*Xho*I (lane 9) and *Sac*I (lane 10) for identification and determining of orientation of the two genes. The pBS-S7PCR (lane 2) and pBS-AHSV9.6 (lane 3) plasmids, digested with *Sac*I and *Bam*H1, respectively, were included as controls together with the molecular weight markers MW11 and ϕx174 (lane 1). Lanes 5-6 represent pFBd-S6.9 digested with *Bam*H1, *Eco*R1/*Xho*I and *Hind*III.

3.3.1.4. Production of dual recombinant shuttle vectors (bacmids)

The next step in constructing dual recombinant baculoviruses expressing different combinations of the major structural proteins of AHSV-9 and AHSV-3 involves producing recombinant bacmids in *E. coli*. Plasmids pFBd-S3.9-S7.9, pFBd-S2.9-S3.9, pFBd-S2.3-S3.9, pFBd-S6.9-S7.9, pFBd-S6.3-S7.9 and pFBd-S6.9 (table 3.2) were transformed into competent *E.coli* DH10Bac cells containing the tetracyclin resistant helper plasmid, which supplies the Tn7 transposase functions and the bacmid DNA (kanamycin resistant). Putative infectious recombinant baculoviral DNA or composite bacmid DNA, containing two heterologous genes under control of the polyhedrin and p10 promoters respectively, was isolated. To confirm that each of the bacmids constructed, contained the respective genes of interest, selected regions of the bacmid DNA were amplified, using the AHSV gene specific primers (summarised in table 3.2) and the polyhedrin and p10 specific primers in combination with pUC/M13 amplification primers. The pUC/M13 primers are directed at sequences on either side of the mini-*att*Tn7 site, within the *lacZ*α-complementation region of the bacmid. The presence of amplified products of the correct size was determined by agarose gel electrophoresis (results not shown). PCR amplification of the respective composite bacmids containing the AHSV structural genes, produced PCR fragments, which corresponded to the VP2, VP3, VP5 and VP7 amplified gene products in the positive controls. These amplified products confirm that the bacmid DNA contained the complete genes of interest.

3.3.1.5. Construction of dual-recombinant baculoviruses

The final step to generate recombinant baculoviruses capable of replicating in insect cells and expressing the heterologous AHSV genes requires the composite bacmid DNA of the four different dual bacmids to be transfected into Sf9 insect cells using a cationic lipid reagent. Three different lipofection reagents were compared for their efficiency of transfection during the course of this investigation. Cellfectin was found to yield the best results (results not shown). Cells were harvested four days post-infection with transfection supernatants, and the proteins analysed by SDS-PAGE.

The transfected cell supernatants were subjected to plaque purification prior to the preparation of high tittered recombinant viral stocks. The viral stocks were titrated and used to re-infect cells at a known MOI of between 5-20 pfu/cell, as described in the following sections. Although it is not strictly necessary to include a plaque purification step, it was found that one round of plaque purification significantly enhanced the stability of protein expression. Viruses from different plaques had different levels of protein expression, varying from no expression to relative high levels of expression. This indicates that the transfection supernatant consist of a heterogeneous population of viruses, each showing different levels of expression. Plaque purification also decreased the amount of defective particles that compete with the complete virion for the cellular machinery and resulted in decreased protein expression from the recombinant viruses.

3.3.1.6. Detection of heterologous RNA synthesised in recombinant baculovirus-infected cells

To established whether active transcription of the foreign genes takes place, dual recombinant baculovirus infected cells were assayed for VP3 and VP2 or VP5 and VP7 mRNA production using an established *in situ* hybridisation procedure. Sf9 cells infected with DBac-S2.9-S3.9 and DBac-S6.9-S7.9 were harvested at 44 h p.i., the optimum time for high level synthesis of mRNA from the very late baculoviral promotors. Cells infected with the VP2/VP3 dual viruses were hybridised to the VP3.9- or VP2.9-specific radiolabelled probes, while those infected with the VP5/VP7 dual recombinants were hybridised to the VP7.9- or VP5.9-specific probes (*Figure 3.6*). Hybridisation of all the VP2/VP3 recombinant infected cell lysates with the VP3-specific probe yielded positive signals. VP2.9-specific probe only detected RNA from cells infected with AHSV-9 VP2/VP3 dual (DBac-S2.9-S3.9). RNA from insect cells infected with DBac-S6.9-S7.9 hybridised to both the VP7.9- and VP5.9-specific probes. These results indicated that active transcription of all the genes under control of either the p10 or polh promotors takes place.

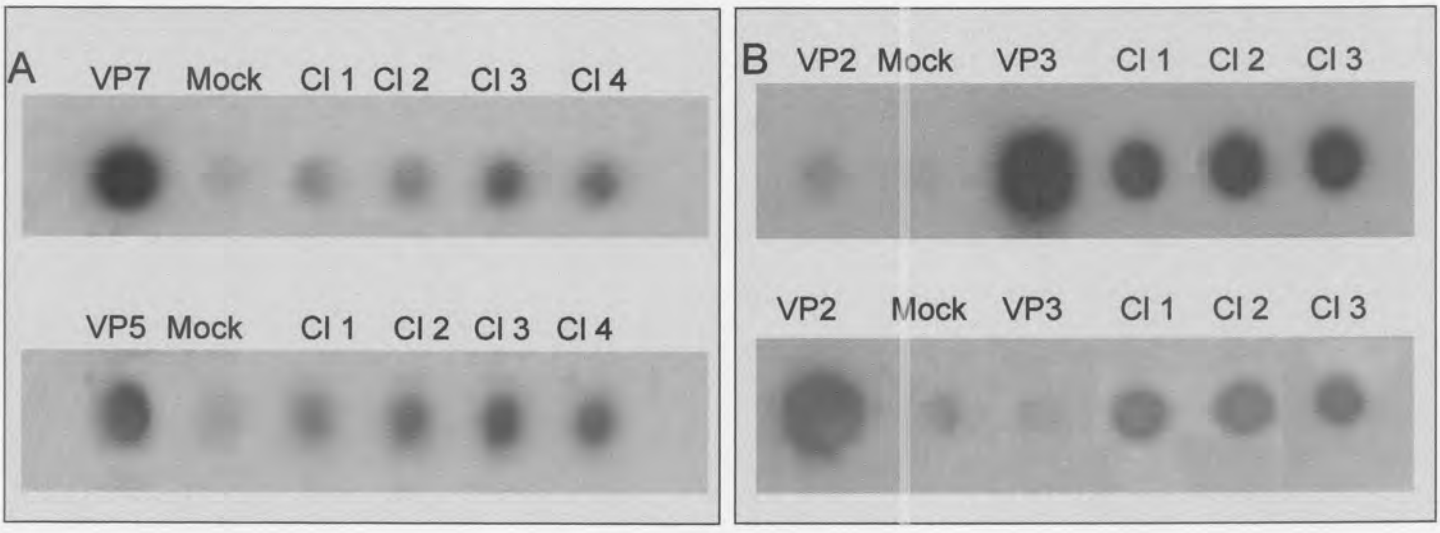

Figure 3.6: In situ Northern blot analysis of Sf 9 cells infected with dual recombinant baculoviruses. Infected cells were harvested 44 h p.i. (A) RNA from DBac-S5.9-S7.9 infected cells were hybridised to VP5(9) and VP7(9)-specific radiolabelled probes (synthesised from pBS-S7PCR and pBS-AHSV9.6 plasmids) and (B) DBac-S2.9-S3.9 infected cells were hybridised to VP2(9) and VP3(9) probes (derived from pBS-AHSV9.2 and pBS-S3Hyb plasmids). For comparison mock-infected cells (negative control) were included in the assay. Plasmid DNA containing the genes of interest served as positive controls.

3.3.2. Investigation of heterologous gene expression in Sf9 cells

In order to determine whether AHSV-9 VP3 and VP7 proteins were expressed from the dual baculovirus recombinant, *S. frugiperda* cells were infected with the VP3 and VP7 dual recombinant baculovirus (DBac-S3.9-S7.9). SDS-PAGE analysis of the infected cell polypeptides revealed that two unique protein bands which co-migrated with AHSV-9 VP3 (90 kDa) and VP7 (38 kDa) derived from recombinant baculoviruses which express VP3 or VP7 individually, were synthesised (*Figure 3.7 A*). No similar bands were observed in the wild-type or mock-infected Sf9 cells. The sizes of the expressed proteins agreed with those expected for VP3 and VP7 on basis of their amino acid compositions (i.e., 103 269 and 38 464 Dalton), respectively. Radioactive labelling of the infected cell polypeptides and comparison with authentic AHSV-infected polypeptides (*Figure 3.7 B*) provided confirmation that the expressed proteins represented authentic AHSV polypeptides and further confirmation was obtained from investigation of their ability to form CLPs. Western immunoblot analysis with antisera raised to AHSV-9 was not possible because the serum does not recognise the linear amino acid chains of VP3 and VP7.

The amount or yield of VP3 and VP7 protein produced by the recombinant baculoviruses was estimated and compared to previously reported levels of expression of these proteins in insect cells. In order to estimate the amount of VP3 and VP7 produced, lysates of recombinant virus infected cells (MOI = 10) at 72 h p.i., were subjected to SDS-PAGE along with various known amounts (0.25-1.0 mg) of Rainbow^{TM} marker (Amersham). Proteins were visualised by Coomassie blue staining. The yield of expressed AHSV-9 VP3 was estimated to be approximately 1-2 $\mu g/10^6$ cells while that of VP7 was in the order of 20-25 $\mu g/10^6$ cells (results not shown). The dual expression of VP3 and VP7 resulted in a yield lower than expression of the individual proteins (8-10 $\mu g/10^6$ for VP3 and 0.8-1.0 $mg/10^6$ for VP7). The level of expression of AHSV-9 VP3 was nevertheless higher than previously reported in the case of AcRP23-*lacZ* baculovirus expression (S. Durbach, 1998). The much higher level of VP7 (ca. 20-25 $mg/10^6$ cells) versus VP3 expression is in agreement with the *in vitro* results (Maree *et al.*, 1998). The ratio of VP3 versus VP7 expression was determined and it was found to be approximately 2:15, which is about the same molar ratio found for the BTV core (2:13). VP7 aggregated into large crystals in the cytoplasm identical to the crytalline structures described by Chuma *et al.* (1992) and Burroughs *et al.* (1994).

In order to determine if AHSV-3 VP2 and VP3, AHSV-9 VP2 and VP3 and AHSV-9 VP5 and VP7 were co-synthesised in recombinant virus-infected cells, monolayers of *S. frugiperda* cells were infected with the respective dual recombinant baculoviruses (DBac-S2.9-S3.9, DBac-S2.3-S3.9, DBac-S6.9-S7.9 and Dbac-S6.3-S7.9) and pulse labelled with ^{35}S-methionine from 32 to 36 h p.i. Mock and wild type baculovirus infected Sf9 cells and cells infected with recombinant baculoviruses expressing VP2, VP3, VP5 and VP7 individually were similarly prepared as controls. Following harvesting of the cells, the proteins in the cell lysates were resolved by SDS-PAGE and visualised by autoradiography. The results are shown in *Figure 3.8*. Discreet protein bands of approximately 116

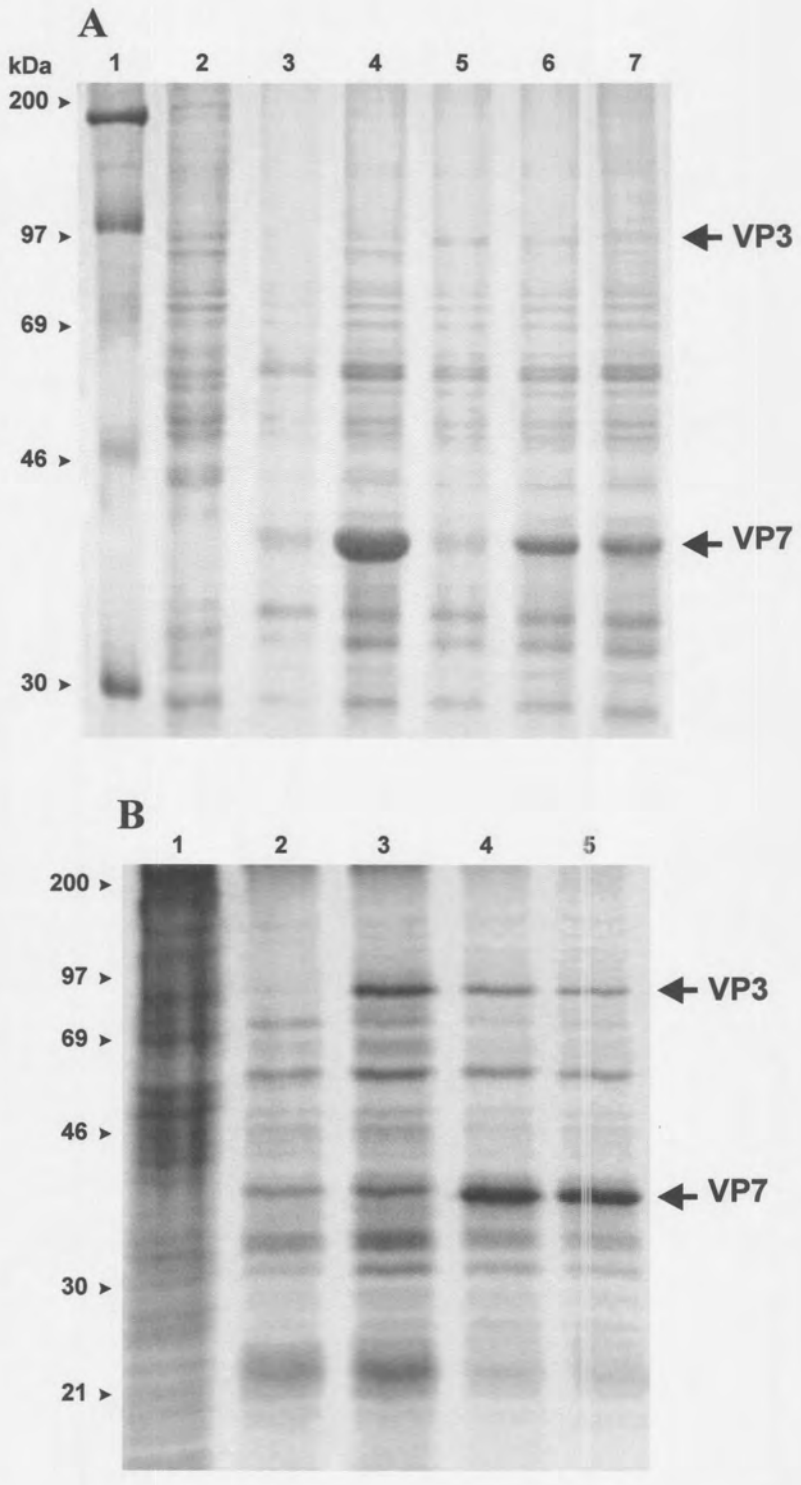

Figure 3.7: (A) SDS-PAGE analysis of cell lysates of insect cells infected with recombinant and wild-type baculoviruses. Lane 1, protein molecular weight marker; Lane 2, mock-infected Sf9 cells; Lane 3, wild type baculovirus; Lane 4, AHSV-9 VP7 recombinant baculovirus; Lane 5, AHSV-9 VP3 recombinant baculovirus; Lane 6 and 7, AHSV-9 VP3 and VP7 dual recombinant baculoviruses. Sizes of protein markers are indicated in kDa at the left of the figure. (B) Autoradiograph of ^{35}S-methionine labelled proteins separated by SDS-PAGE. Lane 1, mock-infected Sf9 cells; Lane 2, wild type baculovirus; Lane 3, AHSV-9 VP3 recombinant baculovirus; Lane 4 and 5, AHSV-9 VP3 and VP7 dual recombinant baculoviruses.

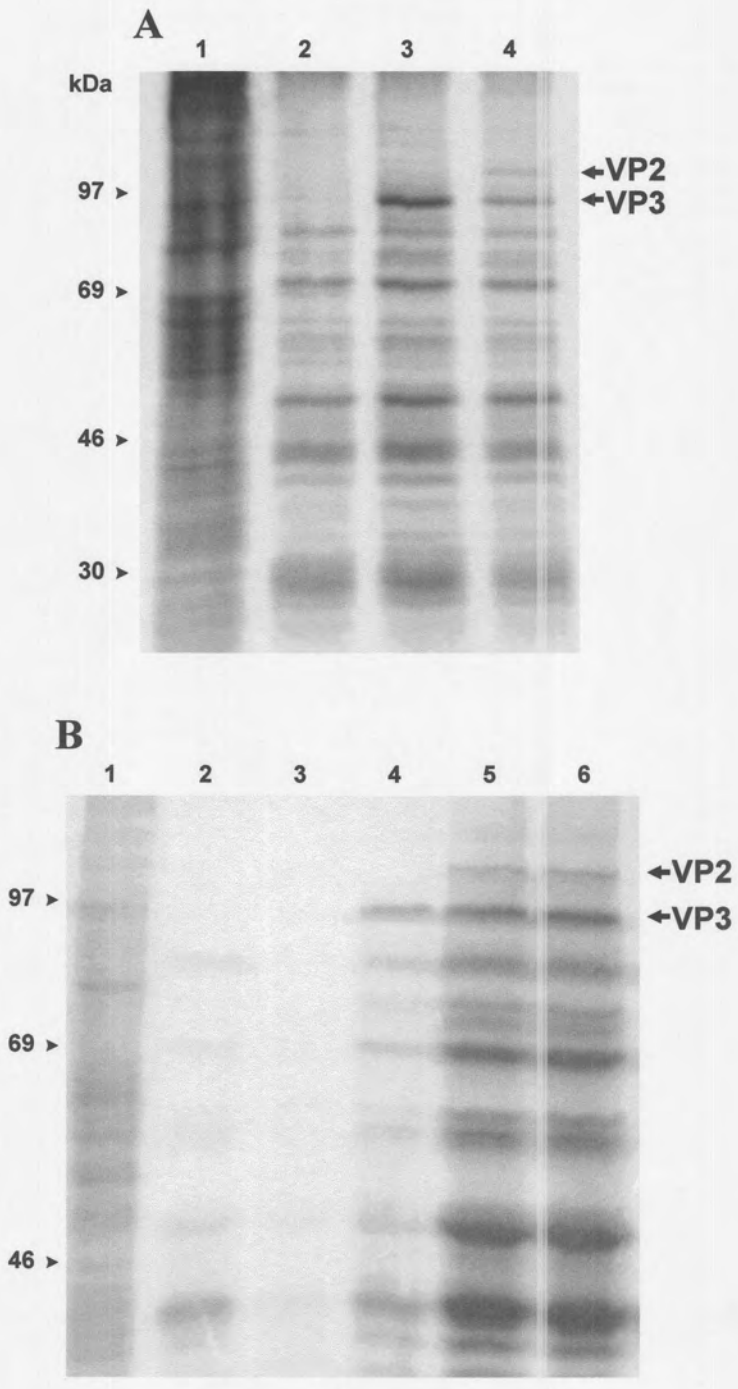

Figure 3.7: Autoradiograph of SDS-PAGE analysis of ^{35}S-methionine labelled proteins from cell lysates of insect cells infected with VP3/VP2 dual recombinant and wild-type baculoviruses. (A) Lane 1, mock-infected Sf9 cells; Lane 2, wild type baculovirus; Lane 3, AHSV-9 VP3 recombinant baculovirus; Lane 4, AHSV-9 VP2 and VP3 dual recombinant baculovirus. (B) Lane 1, mock-infected Sf9 cells; Lane 2, wild type baculovirus; Lane 3, AHSV-3 VP2 recombinant baculovirus; Lane 4, AHSV-9 VP3 recombinant baculovirus; Lane 5 and 6, AHSV-3 VP2 and VP3 dual recombinant baculoviruses.

kDa and 97 kDa that co-migrated with VP2 and VP3 in the positive controls, but were absent in mock and wild type infected cells, were present in both DBac-S2.9-S3.9 and DBac-S2.3-S3.9 infected cells. In DBac-S6.9-S7.9 and DBac-S6.3-S7.9 infected cells, two unique protein bands with approximate sizes of 64 and 38 kDa, respectively, were identified after separation on 10% SDS-PAGE and autoradiography, in the cell lysate (*Figure 3.9*). These proteins corresponded to VP5 and VP7 in the positive controls. The sizes of the expressed proteins agreed with those expected for VP2, VP3, VP5 and VP7 calculated from their amino acid compositions. Since the levels of expression were below that which could be determined with certainty by staining, confirmation that the expressed proteins represented authentic AHSV proteins was provided by immunoprecipitation with antisera raised to AHSV serotypes 9 and 3 (results not shown). The putative VP2 and VP3 proteins as well as VP5 were shown to react specifically with anti-AHSV serum, while no reaction was detected with mock-infected or wild-type infected cells. Immunoprecipitation of VP7 was non-specific since VP7 also precipitated in the control without serum as a result of the natural occurring large VP7 crystals.

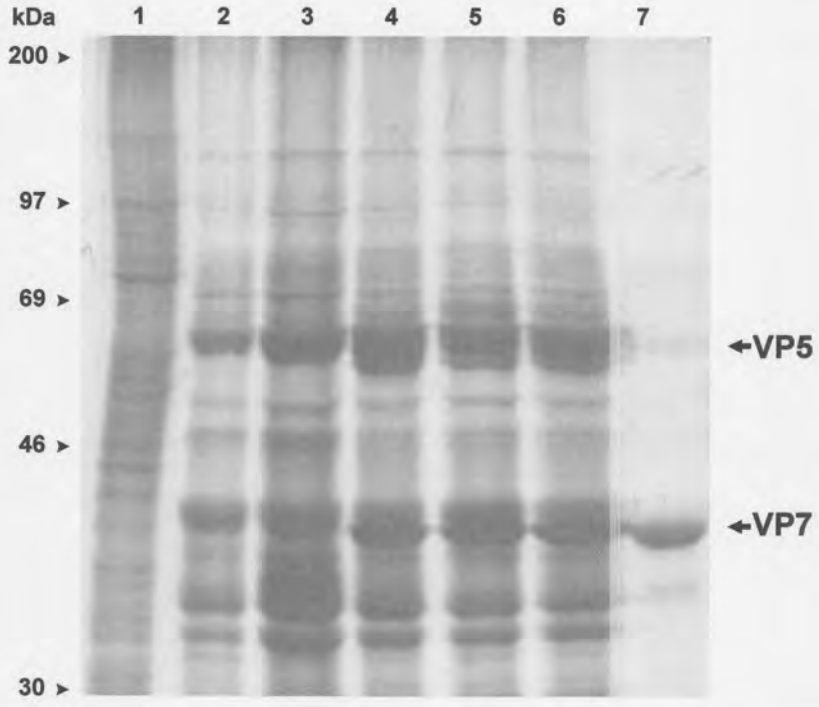

Figure 3.9: Autoradiograph of SDS-PAGE analysis of ^{35}S-methionine labelled proteins from cell lysates of insect cells infected with VP5/VP7 dual recombinant and wild-type baculoviruses. (A) Lane 1, mock-infected Sf9 cells; Lane 2, wild type baculovirus; Lane 3, AHSV-9 VP5 recombinant baculovirus; Lanes 4 and 5, AHSV-9 VP5 and VP7 dual recombinant baculoviruses; Lane 6, AHSV-3 VP5 and AHSV-9 VP7 dual; Lane 7, AHSV-9 VP7 recombinant baculovirus.

3.3.3. Co-expression, purification and electron microscopic evaluation of assembled particles

In order to produce CLPs, partial VLPs and VLPs, the different dual recombinant baculovirus constructs were used to infect or co-infect SF9 cells with the aim to express different combinations of the AHSV structural proteins. The co-infection experiments together with the various purification protocols followed, are summarised in table 3.3.

Table 3.3: *Summary of infections or co-infections performed with the various recombinant baculoviruses and particle purification methods (differential centrifugation, DC; discontinuous (DSG) and continuous (CSG) sucrose gradient; caesium chloride gradient, CsCl) used.*

Recombinant baculoviruses Dual (d) or single (s)	Foreign proteins (VP) AHSV serotypes	Possible assemblies	Purification methods
DBac-S3.9-S7.9	VP3/9 and VP7/9	CLPs	DSG, CSG, CsCl
DBac-S3.9-S7.9 DBac-S6.9 or 3	VP3/9 and VP7/9 VP5/9 or VP5/3	Partial VLPs (CLP + VP5)	DC, CSG
DBac-S3.9-S7.9 Bac-S2.9	VP3/9 and VP7/9 VP2/9	Partial VLPs (CLP + VP2)	DC, CSG
DBac-S2.9-S3.9 DBac-S6.9-S7.9	VP2/9 and VP3/9 VP5/9 and VP7/9	Homologous VLPs	DC, DSG
DBac-S2.3-S3.9 DBac-S6.3-S7.9	VP2/3 and VP3/9 VP5/3 and VP7/9	Heterologous VLPs	DC, DSG
DBac-S3.9-S7.9 DBac-S2.3-S6.3	VP3/9 and VP7/9 VP2/3 and VP5/3	Heterologous VLPs	DC, CSG, CsCl

3.3.3.1. Particles formed by assembly of VP3 and VP7 in insect cells

In order to determine whether expressed AHSV-9 VP3 and VP7 proteins could interact with each other and form complex structures, *S. frugiperda* cells were infected with the VP3 and VP7 dual recombinant baculovirus. Particles formed by the self-assembly of AHSV-9 VP3 and VP7 were purified on the basis of differences in their sedimentation rates (S) in a sucrose gradient. The particles were isolated by lysing infected Sf9 cells with a non-ionic detergent and purified on discontinuous sucrose gradients or self-forming CsCl gradients. After fractionation of the sucrose gradient and analysis by SDS-PAGE, the VP3 and VP7 complexes were identified in the region of

250 S, which is in agreement with previous results (Maree et al., 1998). In the CsCl, the particles banded at a density of 1.30 g/cm^3. Both the sedimentation coefficient and the density of the expressed particles was approximately half that of AHSV core particles derived from complete virions (Oellerman *et al.*, 1969; Huismans *et al.*, 1987; Burroughs *et al.*, 1994). This is expected since the particles do not contain any minor structural proteins or dsRNA. When examined by electron microscopy, the material was found to consists of core-like particles whose size and appearance were similar to those of authentic AHSV core particles prepared from AHSV-infected BHK cells (Burroughs *et al.*, 1994). The electron microscopic images of the empty synthetic particles revealed a dark central region with typical icosahedral symmetry (*Figure 3.10*). This was surrounded by a less electron dense layer with knobby morphological protrusions extending outwards. The particles appeared uniform in size and shape with an average diameter of 72 nm.

Capsomeres radiating 7.0 nm from the icosahedral subcore are clearly visible and appear as elongated tripods/prisms. The ring-like arrangement of the capsomeres (VP7 trimers) onto the VP3 subcore is also visible with five to six trimers in a circular arrangement. This indicated the pentameric arrangement of the capsomere on the surface of the CLPs. The distance between the trimers was approximately 7.0 nm and the trimers were arranged with its bottom domain onto the VP3 scaffold and its top domain facing outwards. Inside the CLP the VP3 layer appeared smooth and forms an icosahedral scaffold with six 5-fold axes visible. The VP3 and VP7 layer of the CLP is approximately 9.0 nm in diameter. The interaction of VP3 and VP7 were verified by antibody decoration, using monoclonal antisera raised against AHSV-3 VP7 (Van Wyngaard *et al.*, 1992). Electron micrographs revealed that each particle of interest was masked by a dark shadow resulting from the specific interaction of monoclonal VP7 antibodies with the VP7 outer shell (*Figure 3.10 B*). A few contaminating empty baculovirus capsids were present which were not captured by the VP7 monoclonal antibodies and therefore served as negative controls (results not shown).

The yield of CLPs produced was very low. Using 2 x 10^8 cells infected with plaque purified dual recombinant viruses at a MOI of 10-15 pfu/cell yielded only 1-2 μg of VP7 after purification on a sucrose gradient. This resulted in 1 to a maximum of 6 CLPs observed in a block on an electron microscope grid. Aggregations of CLPs and baculovirus proteins were also present. To increase the yield of CLPs the purification process was optimised, using the purification method described by Burroughs *et al.* (1994) with a few minor changes. Partial purification of CLPs from infected cell culture media was achieved using combinations or individual detergent treatments (0.05 - 0.5%Triton X-100, 0.1 - 0.5% Nonidet-P40 and 0.5 - 1.0% sodium N-lauroyl sarcosine (NLS)), with protease inhibitors and differential centrifugation using the procedure described in material and methods. This resulted in a reasonable detectable yield of VP3 and VP7 protein which were approximately 70% purified as analysed by SDS-PAGE. The presence of protease inhibitors made a significant

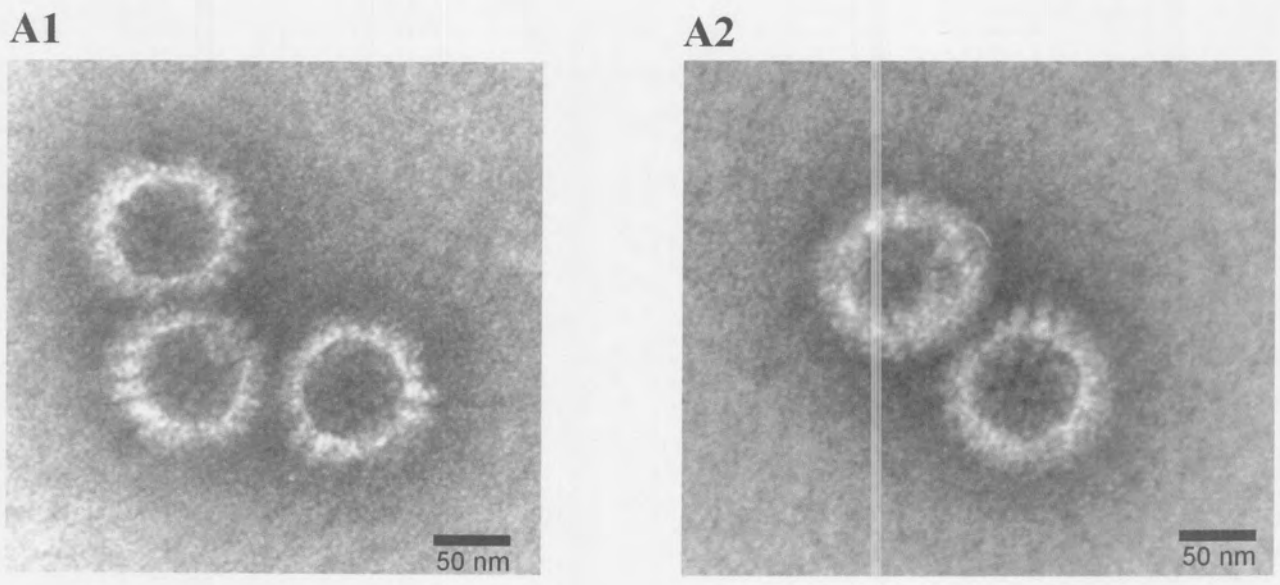

Figure 3.10: (A) Electron micrographs of empty AHSV CLPs synthesised in insect cells by a recombinant baculovirus expressing the two major AHSV core proteins VP3 and VP7. The expressed particles were purified on self-forming CsCl gradients and negatively stained with 2% aqueous uranyl acetate. (B) Negative contrast electron micrographs of the purified CLPs bound to VP7 monoclonal antibodies.

difference in the yield of CLPs recovered after purification. However, the CLPs were still contaminated with a large number of empty baculovirus capsids and baculovirus expressed tubules. Purification of this partial purified material by discontinuous sucrose gradient centrifugation still resulted in contaminating baculovirus structures, although free of cellular proteins and VP7 crystals. Maintenance of CLPs in 0.2% NLS or 0.2% Nonidet-P40 was essential to prevent irreversible aggregation. Although up to five or six CLPs could be found in an E.M field at 50 000 enlargement, this was not enough for high resolution structural studies using In-lense FESEM or for use in a subunit vaccine. Highly purified CLPs were obtained with CsCl centrifugation, although approximately 40% of the particles were lost during this procedure. The particles purified this way formed a sharp white band with a density of 1.30 g/ml.

The stability of the particles under different physicochemical conditions was also investigated. A purified preparation of CLPs were adsorbed onto E.M grids and treated with different solutions prior to negative staining. Treatment of the particle with a low salt buffer (< 50 mM NaCl) or high salt buffer (>1 M NaCl or $MgCl_2$) resulted in the loss of the capsomeres leaving a smooth inner subcore-like particle (SCLP). The CLPs appeared to be unstable at $MgCl_2$ concentrations higher than 1 M, which is in agreement with the results of Burroughs *et al.* (1994) and Mertens *et al.*, 1987 on the stability of AHSV and BTV cores, respectively. Like BTV and AHSV cores, the CLPs were stable in a wide range of pH conditions from about 6.0 to 9.0. A reducing agent (10 mM DTT) was used by Burroughs *et al.* (1994) for purification of complete AHSV virions. The stability of AHSV CLPs in the presence of DTT was also investigated, with no significant effect on the structure and was later incorporated during the purification process of VLPs.

3.3.3.2. Assembly of VP2 or VP5 proteins onto CLPs

To determine whether VP2 or VP5 can assemble onto cores in an *in vivo* system, the VP3/VP7 dual recombinant baculovirus and an AHSV-9 VP2 (Bac-AH9.2; constructed by G. Napier) or VP5 (pFBD-S5/9; section 3.3.1.3) single recombinant baculoviruses were employed to infect Sf9 cells, in order to co-express the three relevant genes in insect cells. The cells were co-infected with either Dual-S3.S7 and Bac-S6/(9 or 3) or Dual-S3.S7 and Bac-AH9.2 at strictly 5 pfu/cell of each recombinant virus. Protein complexes synthesised in infected cells were separated on the basis of differences in their sedimentation rates (S) in a sucrose gradient. The gradient was fractionated and the fractions analysed by SDS-PAGE. Three of the lower fractions contained very faint bands corresponding to the predicted sizes of VP3, VP5 and VP7 or VP2, VP3 and VP7 (result not shown). These fractions were pooled and the assembled particles recovered by high-speed centrifugation.

To analyse the morphology of these particles, both multimeric structures (one containing VP2, VP3 and VP7, the other VP5, VP3 and VP7) were examined by negative staining electron microscopy. In

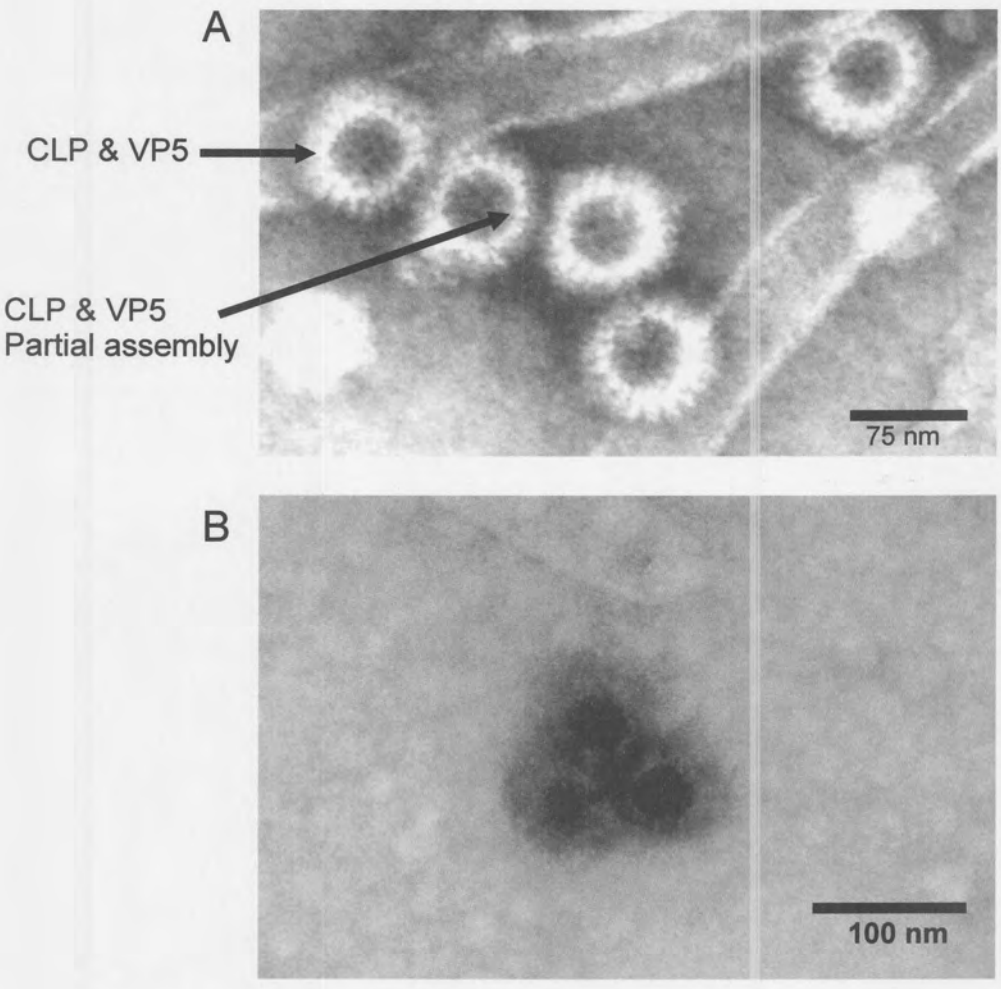

Figure 3.11 (A) Electron micrograph of partial VLPs synthesised in insect cells by co-infection of a dual VP3/VP7 recombinant baculovirus and a VP5 single recombinant baculovirus. Some partially assembled particles were also observed. The particles were purified on either a 30-68% discontinuous sucrose gradient or a 20-50% continuous sucrose gradient. (B) Negative contrast electron micrographs of the purified partial VLPs (CLPs & VP5) decorated with VP5 monospecific antisera and stained with uranyl acetate.

preparations from infections involving the VP3/VP7 dual recombinant vector, the only structures observed were CLPs. In contrast, the co-expression of VP3 and VP7 with either VP2 or VP5 proteins resulted in the formation of double-shelled particles (containing an additional protein layer) resembling authentic empty AHS virions (*Figure 3.11A & 3.12*). However, these double-shelled particles had a somewhat smaller diameter than reported for AHS virions, although larger than CLPs. These partial-VLPs with only one outer capsid protein (VP2 or VP5) had an approximate diameter of 76 to 78 nm, whereas the complete virion containing both outer capsid proteins measure approximately 82-84 nm. The electron microscopic images also indicated that the empty synthetic partial VLPs were characterised by a dark central region with typical icosahedral symmetry, identical to the empty CLPs. These empty partial VLPs were lacking the knobby protrusions characteristic of the surface of CLPs and cores, but were surrounded by a diffuse outer layer. The data were substantiated by a study using monospecific antibodies raised against VP5 or polyclonal serum against AHSV-9 (*Figure 3.11B & 3.12*). Conclusive results were obtained demonstrating that both VP2 and VP5 attach to the CLPs independently of each other.

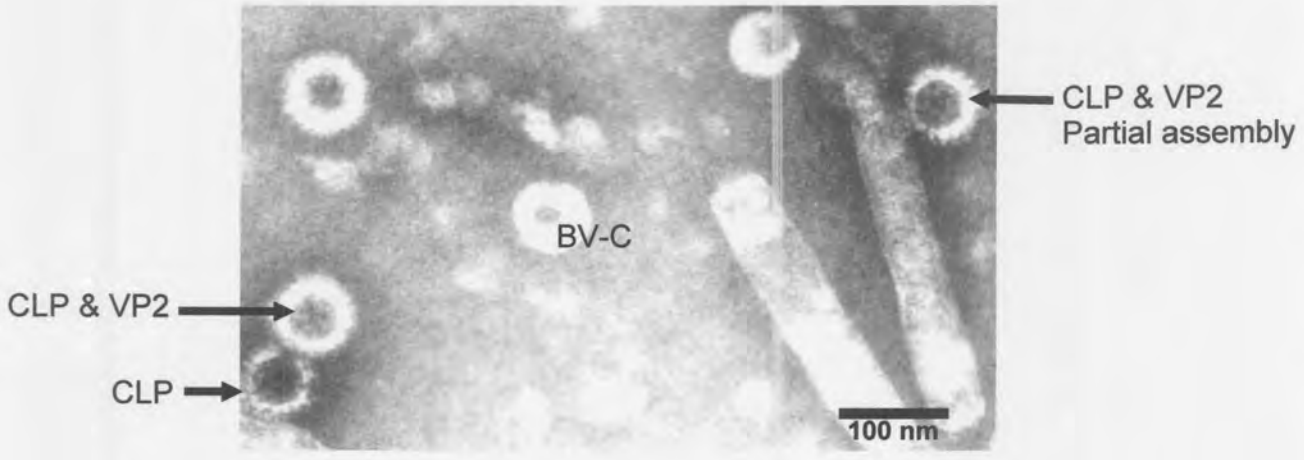

Figure 3.12: Electron micrograph of partial VLPs synthesised in insect cells by co-infection of a dual VP3/VP7 recombinant baculovirus and a VP2 single recombinant baculovirus. VP2 assembles spontaneously onto preformed CLPs in the absence of VP5. Partial assembled intermediates were also present in the sample (*right*). The particles were purified on either a 30-68% discontinuous sucrose gradient or a 20-50% continuous sucrose gradient.

3.3.3.3. Co-expression of four major structural proteins of AHSV in insect cells

To assess the interaction of the four major structural proteins of AHSV, insect cells were co-infected with both the VP2/VP3 and VP5/VP7 dual recombinant baculoviruses, in order to co-express VP2, VP3, VP5 and VP7. The cells were harvested at 48 h p.i. and lysed with a non-ionic detergent Nonidet-P40 under reducing conditions (DTT) in the presence of proteinase inhibitors, and the released particles were purified to homogeneity by centrifugation on discontinuous sucrose gradients. When examined by the electron microscope, some empty double-shelled particles were observed consisting of an electron dense core surrounded by a thick outer capsid. The yield of these particles was extremely low. SDS-PAGE analysis of fractions containing the particles failed to recognise the presence of the four major structural proteins. No more than 1 particle was visible in a number of fields under the electron microscope and most of these were partial CLPs. A few partial VLPs were observed, shown in *Figure 3.13*. Reasons for the low yield in VLP production is explained later.

The next step in the production of VLPs was to co-infect insect cells with the VP3/VP7 dual recombinant baculovirus and a VP2/VP5 (serotype 3) dual recombinant baculovirus. The latter was constructed by Renate Filter in the lab of H. Huismans. The expressed proteins made in infected cells assembled into double capsid particles the same as described above. Some simple CLPs were also observed in the preparation. Their diameters were estimated to be of the order of 72 nm and they exhibit similar morphology described in section 3.3.3. Most of all a range of intermediate structures

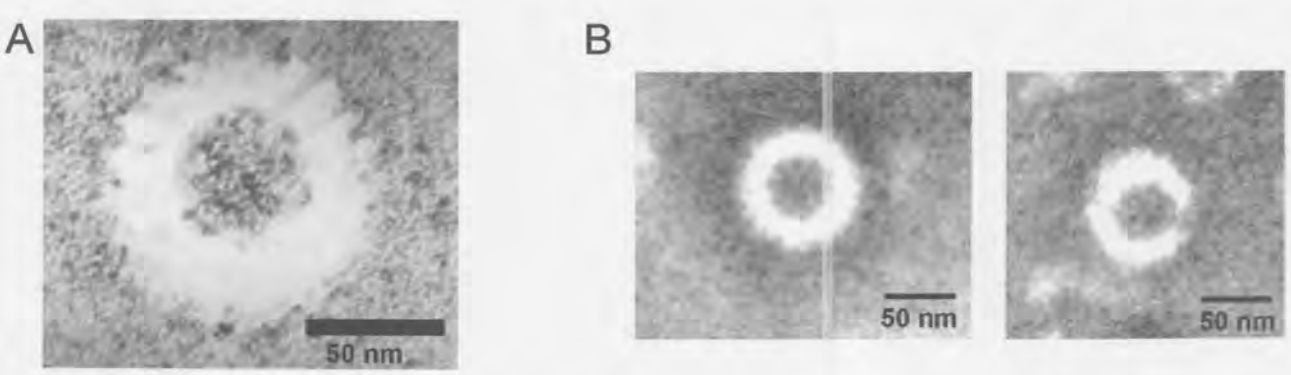

Figure 3.13: Electron micrograph of VLPs synthesised in insect cells. In (A) the particles were synthesised by co-infection of a VP2/VP3 and a VP5/VP7 dual recombinant baculoviruses. Self-assembly of all four major structural proteins of AHSV was observed. The yield of these VLPs was low and partial assembled intermediates were present in abundance. In (B) the empty AHSV double-shelled VLPs were synthesised by the co-infection of a VP2/VP5 and a VP3/VP7 dual recombinant baculoviruses. The particles were purified on either a 30-68% discontinuous sucrose gradient or a 20-50% continuous sucrose gradient.

were also observed, apparently with various amounts of the outer capsid proteins attached. These may reflect different stages in particle assembly. The centres of all types of particles (CLPs, VLPs, intermediate VLPs) exhibited an icosahedral configuration. The diameters of the largest particles were estimated to be in the order of 82 nm.

The yield of these VLPs was still extremely low which made the investigation of the fine structure difficult. Large distinctive crystals, which is formed by the accumulation of VP7 in the cytoplasm of infected cells, were observed. These crystals appeared similar to the crystalline structures found in AHSV-4 infected cells when observed under the light microscope (Chuma *et al.*, 1992; Burroughs *et al.*, 1994).

3.4. DISCUSSION

The primary objective of this study was to increase the understanding of the assembly of the four major structural proteins of AHSV by establishing whether the four proteins can interact spontaneously in the absence of other AHSV proteins and the viral genome. In order to study these aspects it was necessary to synthesise the proteins of interest in significant quantities using an appropriate expression system. Therefore, in this part of the investigation the aim was first of all to establish a useful model for studying protein-protein interaction in virus assembly and secondly to develop a system that could be used for the presentation of foreign antigenic determinants, including the VP2 protein of AHSV in its desired conformation. The first step towards the production of AHS VLPs was to produce CLPs to act as a scaffold for the assembly of the two outer capsid proteins.

Recently Maree *et al.*, (1998) were able to demonstrate the self assembly of AHSV-9 VP3 and VP7 by co-infection of insect cells with recombinant baculoviruses expressing each gene respectively. They laid the foundation for the assembly of AHS VLPs. However, the resulting CLPs were heterogeneous with respect to the amount of visible capsomeres, indicative of the formation of partially assembled particles. Partial assembly could be expected, because the strategy used relied upon co-infection of cells with individual VP3 and VP7 recombinant baculoviruses (Burroughs *et al.*, 1995). The multiplicity of infection of each recombinant virus varies from cell to cell which correlates with the level of protein expression (Maree *et al.*, 1999). A further disadvantage of co-infection is that the yield of CLP formation was extremely low. To overcome this variation in the ratio of VP3 to VP7 expression and the low yield of CLPs, an attempt was made to synthesise CLPs by simultaneous expression of the two major core proteins, VP3 and VP7, using a dual recombinant baculovirus. To express both proteins simultaneously in infected insect cells use was made of the Bac-to-Bac™ baculovirus expression system (Life Technologies).

The dual expression transfer vector, pFastbac-dual, utilises both the polyhedrin and p10 promoters for the expression of two heterologous foreign genes. The first strategical step involved the cloning of different combination of AHSV structural proteins, including proteins from different serotypes, in the dual transfer vector, each under control of its own promoter. The tailored DNA copies of AHSV segment 3 and 7 were cloned into pFastbac-dual under control of the p10 and polyhedrin promoters respectively. In an attempt to investigate the interaction of both outer capsid proteins with CLPs, two dual transfer vectors were constructed. In one dual vector either the AHSV-3 or 9 VP2 gene and the AHSV-9 VP3 gene were cloned under control of the polyhedrin and p10 promoter respectively, while the AHSV-3 or 9 VP5 gene and AHSV-9 VP7 gene were inserted in a second dual transfer plasmid. The use of different AHSV serotypes for the outer capsid proteins provide the means to investigate the formation of heterologous VLPs. This strategy, using a dual with VP2/VP3 and one with VP5/VP7 was followed for two reasons. First of all each of the major core proteins (VP3 and VP7) and outer capsid proteins (VP2 and VP5) will be directed from the same promoter, which means that each protein will be in the correct ratio for optimum particle formation. Secondly, when co-infected, cells infected with only one dual will form no particles and the only particles will be produced when both dual recombinants are present in the same cell. This will overcome the problem of intermediate structures formed by the co-infection of a VP3/VP7 dual and VP2/VP5 dual (French *et al.*, 1990). Dual recombinant composite bacmid DNA was constructed in *E. coli* cells by site-specific transposition of the genes and flanking regulatory sequences from the transfer vector into the bacmid genome with the aid of a helper plasmid. Recombinant baculoviruses were obtained by transfection of this composite bacmid DNA into *Spodoptera frugiperda* cells (Luckow *et al.*, 1993).

To investigate the assembly of AHSV VP3 and VP7, insect cells were infected with the VP3/VP7 dual recombinant baculovirus and VP3/VP7 complexes were purified from infected cells and analysed by electron microscopy. Expressed VP3 and VP7 were found to interact spontaneously to form core-like particles of the same size, appearance and stoichiometric arrangement of VP3 to VP7 as in authentic AHSV cores. This confirms the result from Maree et al. (1998). Uniform particles with a diameter of 72 nm, which structurally resembled cores prepared from AHSV-4 (Burroughs *et al.*, 1994) were visible with negative staining. The diameter is in agreement with that of BTV CLPs (Hewat et al., 1992) obtained from cryoelectron microscopic images. Native BTV cores are 69 nm in diameter (Prasad *et al.*, 1992), which is slightly smaller than that of BTV CLPs for an unknown reason. Only VP3 and VP7 were identified as the protein components of the expressed particles. Also the molar ratios of the two proteins were similar to those of VP3 and VP7 derived from infectious AHSV and also similar to the ratio found for BTV CLPs (Burroughs *et al.*, 1994). In contrast to virus-derived cores, the CLPs appeared empty, since it lacks nucleic acids and the minor structural proteins. This explains the lower density and sedimentation rate of the CLPs in comparison to complete virions

(Huismans *et al.*, 1987). The CLPs have a knobby surface structure, similar to cores derived from virus by removal of VP2 and VP5 (Burroughs *et al.*, 1994). This outer core layer is probably composed of VP7 trimers as for BTV (Grimes *et al.*, 1995). The VP7 capsomeres are easily removed from CLPs with a low salt buffer, resulting in a ring-like structure composed solely of VP3. Expression of VP3 in the absence of VP7, failed to identify any recognisable structure or SCLPs.

Assembly of these core-like particles from VP3 and VP7 demonstrated that these proteins provide the structural integrity of the core and that their formation in insect cells is not dependent on the presence of AHSV dsRNA or the minor core proteins. In addition, it can be concluded that the AHSV non-structural proteins are not required to either assist or direct the assembly of these empty particles. It should be noted that VP7 aggregates into large hexagonal crystals in infected cells, even when co-expressed with VP3, which could impede incorporation into particles. The functional significance of the VP7 crystals, if any, remains to be determined. It is postulated that these crystals represent a by-product, rather than an essential component of the AHSV replication process (Burroughs *et al.*, 1994).

Initial co-infection experiments with a dual vector containing BTV VP3 and VP7 and a recombinant vector with either BTV VP2 or VP5 failed to demonstrate the assembly of the individual capsid proteins onto the CLPs (French *et al.*, 1990). Liu *et al.* (1992) demonstrated *in vitro* the interaction of BTV VP2 and VP5 onto preformed CLPs. Whether the outer capsid proteins of AHSV or other orbiviruses can interact independently with the core was not previously known. Using the dual recombinant baculovirus expression vector containing AHSV VP3 and VP7 and a recombinant baculovirus containing either AHSV-3 VP5 or AHSV-9 VP2, a co-infection experiment was performed. The results demonstrated that the outer capsid proteins of AHSV, VP2 and VP5, do interact separately with CLPs *in vivo*. The VP2 and VP5 do interact only with the VP7 protein of the core. These data was confirmed by the co-expression of VP2 and VP3 or VP5 and VP3. Analysis of infected cell lysates with sucrose gradient centrifugation failed to obtain these proteins in the same fraction, which indicate that there was no association of VP2 or VP5 onto VP3 scaffolds in the absence of VP7. Further evidence that the multimeric structures represented empty CLPs with assembled VP2 or VP5 was provided by their ability to react with monospecific antisera. Liu *et al.* (1992) demonstrated that the level of interaction of VP2 to the CLP is much less when expressed in the absence of VP5. It is likely that during morphogenesis of the virus the proteins stabilise each other in the virion structure.

In a attempt to attach both outer capsid proteins to CLPs, experiments were performed involving co-infection of *S. frugiperda* cells with two dual recombinant baculoviruses, each containing two major structural proteins of AHSV. The one recombinant expressing VP2 and VP3 and another VP5 and

VP7, respectively were used to co-infect insect cells. This strategy of producing VLPs was used in order to eliminate the variable amount of CLPs and outer capsid proteins, which would lead to intermediate structures. This strategy resulted in a very poor yield of CLPs, possibly because the VP7 protein, in the presence of all four major structural proteins, still aggregates into crystals in infected cells. This could inhibit the incorporation into particles. It was also demonstrated by Maree *et al.* (1998) that variable amounts of VP7 incorporate during intracellular assembly as a direct result of the variation in the ratio of VP3 to VP7 expression in insect cells co-infected with VP3 and VP7 single recombinant baculoviruses. The absence of the full complement of the knobby protrusions or capsomeres on the CLPs surface may result in the failure of VP2 and VP5 to associate with the CLPs. To verify this statement it was also indicated, by the co-expression of VP2 and VP3 or VP3 and VP5, that VP5 and VP2 associate with VP7 trimers and not with the VP3 subcore. To overcome this problem, another co-infection experiment was performed, this time using the VP3/VP7 dual recombinant in combination with a VP2/VP5 dual recombinant.

Protein complexes comprising all four structural proteins corresponding to the estimated sizes of AHSV-9 VP2, VP3, VP5 and VP7 were isolated. Electron micrographic images of negatively stained complexes indicated that these particles largely resembled AHS virions. Unlike the native AHS virions, the empty double-shelled particles consisting of a core surrounded by a thick outer capsid. This outer capsid was visible as a diffuse layer in electron micrographs, similar to that of BT VLPs (French *et al.*, 1990; Hewat *et al.*, 1994), since these images show little surface detail. The diameter of the largest particles were estimated to be in the order of 81 to 84 nm, i.e., comparable to those of AHS virions (Oellerman *et al.*, 1969; Burroughs *et al.*, 1994) and BTV virions and VLPs (Huismans *et al.*, 1987; French *et al.*, 1990; Hewat *et al.*, 1994). A striking feature unique to the synthetic particles, is the empty centre, since it lacks the genome and minor core proteins. The VLPs appeared to vary with respect to the quantity of VP2 and VP5 on the outer layer, which confers in intermediate VLPs. This may be due to the variable amount of VP2 and VP5 incorporated during intracellular assembly as a direct result of the variation in the ratio of VP3 and VP7 expression to VP2 and VP5 expression in insect cells co-infected with the VP3/VP7 and VP2/VP5 recombinant baculoviruses. A similar range of particles were obtained with BTV when the production of VLPs relied on the co-infection of two dual expression vectors (French *et al.*, 1990; Hewat *et al.*, 1994) and only very few particles appeared complete.

Data obtained from Hewat *et al.* (1994) revealed that the outer capsid of BT VLPs exhibited a well-ordered morphology that contrasted strongly with that deduced by conventional staining methods. In the BT VLP it was observed that globular structures were located underneath sail-shaped surface structures. The globular proteins, presumed to be VP5, were located on the six-membered rings of the VP7 trimers of the BTV core and CLPs. The sail-shaped spikes were situated above the VP7

trimers and form 60 triskeleton-type motifs, which cover all but 20 of the VP7 trimers in the virion. It is likely that these spikes are the VP2 (Hewat *et al.*, 1992; Hewat *et al.*, 1994).

In this part of the investigation it was demonstrated that the co-expression of all four AHSV major structural proteins in insect cells, resulted in the intracellular formation of virus-like particles (VLPs) which structurally resembled AHS virions. These results confirm that all four major capsid proteins of AHSV are capable of self-assembly into the correct structure, as for the native virus capsid, when simultaneously expressed in cells. The low proportion of complete particles produced by the two recombinant baculoviruses is probably due to suboptimal expression ratios of the four proteins as well as the crystallisation of VP7. Given that (a) the AHSV CLPs assembled spontaneously by co-expression of VP3 and VP7, (b) coexpression of VP3, VP7 and VP5, or VP3, VP7 and VP2 gives rise to spherical intermediate particles which lose the VP2 or VP5 easily, leaving a CLP, and (c) co-expression of VP2, VP3, VP5 and VP7 resulted in the assembly of double-shelled VLPs, it appears that VP2 and VP5 interact separately of each other to VP7. According to Hewat *et al.* (1994) the presence of both outer capsid proteins are necessary for the incorporation of the VP7 trimers around the five-fold axis, while Liu *et al.* (1992) demonstrated that the two proteins stabilise each other in the complete virion.

The observation of the spontaneous formation of complete AHSV VLPs in the absence of the nonstructural proteins implies that the nonstructural proteins are not necessary for the formation of the viral capsid. However, they may be involved in the control of dsRNA packaging and/or prevention of RNA transcription during assembly, but more important they may be involved in optimising the assembly process for more efficient capsid formation.

CHAPTER 4

EFFECT OF SITE DIRECTED INSERTION MUTATION ON THE CRYSTAL FORMATION, SOLUBILITY AND CLP FORMATION OF AHSV-9 VP7

4.1. INTRODUCTION

AHSV VP7 is composed of 349 amino acids with a calculated M_r of 38 kDa and its sequence is highly hydrophobic (Roy *et al.*, 1991). Although the BTV VP7 also contains a high percentage of hydrophobic residues, BTV VP7 synthesised by recombinant baculoviruses is soluble in the trimeric form (Basak *et al.*, 1992). In contrast to BTV, AHSV VP7 aggregates in infected cells in large, flat hexagonal crystals with a maximum dimension of about 6 μm (Buroughs *et al.*, 1994; Chuma *et al.*, 1992). Such large structures represent a feature unique to AHSV among the orbiviruses investigated. The building block for the AHSV VP7 crystals is a trimeric molecule containing three VP7 subunits. The subunits interact with each other via hydrophobic contacts. Hydrophobic residues involved in these contacts probably contribute to the tendency of the protein to aggregate (Basak *et al.*, 1996). It has been reported that AHSV-4 VP7 also forms crystalline structures when expressed in insect cells (Roy *et al.*, 1991). The X-ray crystallographic structure of the top domain of AHSV VP7 has recently been resolved to a 2.3 Å resolution and was found to be very similar to that of the BTV VP7 trimers (described in chapter 1), as expected from the high degree of sequence similarity of the BTV and AHSV VP7 proteins (Basak *et al.*, 1996).

The AHSV VP7 crystals, purified from BHK cells infected with AHSV-9, were shown to be highly immunogenic, elicited a strong immune response and were effective as a subunit vaccine in a mouse model (Wade-Evans *et al.*, 1997; Wade-Evans *et al.*, 1998). Passive transfer of antibodies from immunised mice failed to protect syngeneic recipients from AHSV challenge, which indicates that an antibody response is unlikely to represent the primary mechanism involved in the protection induced by vaccination with VP7 crystals. It is therefore possible that immunisation with VP7 induces a protective T-cell response. Furthermore, the conformation and possibly the assembly of the VP7 into crystals appear to be important in the mechanism of protection against the heterologous serotype challenge. Based on these findings and reports that VP7 of BTV contains immunodominant, serotype cross-reactive T-cell epitopes (Angove *et al.*, 1998), it was decided to investigate the potential of baculovirus-expressed AHSV-9 VP7 as a particulate antigen delivery system for the presentation of foreign peptides. Expression of VP7 crystals as an antigen delivery

system in insect cells has several advantages. Baculovirus expression will provide an entirely satisfactory source of recombinant crystals for vaccine purposes. These particles present no risk of contamination with infectious virus and the disc-shaped crystals are easily purified in a one step ultracentrifugation process. The aim of this part of the investigation was to investigate the possibility of developing the major core structural protein, VP7, of AHSV as a particulate vaccine delivery system for presenting small peptides to the immune system.

VP7 protein is also the major constituent of the virus core and when co-expressed with VP3 assembles into CLPs (chapter 3). Alternative to the use of CLPs as scaffolds for the presentation of VP2 in its correct conformation, the CLPs also have the potential to be used as antigen delivery systems by the insertion of foreign immunogenic epitopes into VP7 under conditions that do not disrupt CLP assembly. The use of AHSV CLPs, to provide protection against AHSV has never been investigated, partly because of the low yield of CLPs produced (chapter 3). In the case of BTV, partial protection against BTV challenge was afforded by CLP vaccination (Roy *et al.*, 1994). Although extension mutants of BTV VP7, containing 48 amino acids of hepatitis B virus preS2 region at the N-terminus were able to form chimeric CLPs, these CLPs were quite unstable. These chimeric particles were indeed highly immunogenic, but the results indicated that the suitability of the N-terminus of BTV VP7 for the insertion of foreign epitopes, is relatively restricted (Le Blois & Roy, 1993; Belyaev and Roy, 1992). On the other hand in-frame addition of sequences at the C-terminus of BTV VP7 abolishes CLP formation, presumably due to lack of trimer-trimer interactions (Le Blois & Roy, 1993). Certain internal sites of BTV VP7, Ala145 and Gln238, have also been investigated as target sites for the insertion of foreign epitopes on the basis that both sites were located on exposed loops of VP7 and thus on the surface of the trimers and CLPs. Insertion of foreign epitopes into the BTV VP7 Gln238 site abrogated CLP formation. However, chimeric BTV CLPs were produced when sequences of variable lengths of up to 29 amino acids have been inserted into the Ala145 site. These CLPs were shown to elicit strong humoral immune responses against these epitopes.

The aims of this part of the investigation were first of all to identify regions in the VP7 top domain, which can be used as insertion sites for the display of epitopes or peptides. Secondly, to modify the AHSV-9 VP7 gene by means of site-specific insertion mutations, in order to create restriction enzyme sites to facilitate the insertion of foreign epitopes and to analyse the insertion mutants with respect to solubility, trimerisation and the ability to form hexagonal crystals as well as CLPs. Thirdly, to construct VP7/TrVP2 chimeras that express an immunogenic region of AHSV-9 VP2, on the surface of the VP7 protein.

4.2. MATERIALS AND METHODS

4.2.1. Materials

The oligonucleotide primers used in this section were obtained from Boehringer Mannheim. The pMOSBlue PCR cloning kit was supplied by Amesham and the TaKaRa Ex Taq™ polymerase Gibco BRL (Life technologies). Qiagen supplied the Qiagen® plasmid mini-kit tip 20, the high pure plasmid purification kit was obtained from Boehringer Mannheim, the Nucleobond® columns from Macherey-Nagel and Wizard™ columns from Promega. ABI PRISM™ Big Dye Terminator Cycle Sequencing Ready Reaction kit was purchased from Perkin Elmer Biosystems.

4.2.2. Site-directed insertion mutagenesis of VP7 and the construction of recombinant transfer vectors

To introduce an AHSV-9 VP2 epitope into the two identified hydrophilic domains of the AHSV-9 VP7 protein necessitated the insertion of unique restriction sites in both regions. Two VP7 insertion mutants with 18 additional nucleotides at positions 548 to 549 and 617 to 618 were constructed by a polymerase chain reaction method (PCR). The 18 additional nucleotides represents three unique restriction enzyme recognition sites that were inserted into the sequence that encode two conserved hydrophilic regions of the cloned and tailored DNA copy of the VP7 gene of AHSV-9. Each of the VP7 site-specific insertion mutants were constructed by making use of two different PCR approaches, which are outlined in *Figure 4.3* and *Figure 4.5*, respectively. In the more laborious method, the insertions were generated after ligation of selectively amplified fragments of the VP7 gene. Four primers and two separate PCR reactions were used for each insertion mutation. A set of external oligonucleotide primers specific for the 5' and 3' regions of the VP7 gene containing *Bgl*II sites at each terminal, was used to introduce *Bgl*II sites at both ends of the VP7 sequence. For each insertion mutation a set of two mutagenic primers were designed, which contained the specific restriction enzyme sites (*Hind*III, *Xba*I and *Xba*I, *Sal*I) to be inserted between nucleotide positions 548 and 549 and 617 and 618, respectively. The strategy of creating the insertion mutants involved amplifying the VP7 gene as two VP7-specific segments, which were then ligated to create a complete gene. The sequences of the mutagenic primers as well as 5'- and 3'-specific primers, both of which included *Bgl*II linker sequences are shown in Table 4.1. and the annealing temperatures of the respective primers are summarised in Table 4.2. The plasmid pBR-VP7PCR (obtained from S. Maree), containing the complete coding sequence of the AHSV-9 VP7 gene, was used as a template in the polymerase chain reaction.

Briefly, the two PCR reactions for each insertion mutation were performed using the cool start method. The separate reaction mixtures of 50 µl each, consisted of 5 µl 10 x TaKaRa Ex Taq™ polymerase buffer (20 mM $MgCl_2$, 500 mM KCl, 250 mM TAPS pH 9.3, 10 mM 2-mercaptoethanol), 8 µl of a 2.5 mM dNTP mixture, 0.5-5 ng of template plasmid (pBR-S7PCR), 100 pmol (950 ng) of each oligonucleotide primer and 2 U of TaKaRa Ex Taq™ polymerase (Life technologies). The PCR reactions were subjected to 30 cycles of amplification in an ABI termal cycler 9600 PCR machine. The thermal parameters used for the PCR were 2 min hold at 94°C, 30 sec at 94°C, 30 sec at 52°C, 1 min at 72°C for 5 cycles, 30 sec at 94°C, 30 sec at 58°C, 1 min at 72°C for 10 cycles, 30 sec at 94°C, 30 sec at 64°C, 1 min at 72°C for 15 cycles, and 10 min hold at 72°C (Table 4.2).

TABLE 4.1: *Sequences of PCR primers used for the construction of VP7 insertion mutants*

Mutation	Position, polarity and type of primer	Oligonucleotide sequence
ins177-178	548-549; -; insertion	5'-GC**TCTAGAAAGCTT**CCTTGGGGCTAGCAGCGC-3'
	548-549; +; insertion	5'-GC**TCTAGAGTCGAC**AGGGGGGACGCAGTCATG-3'
ins200-201	617-618; -; insertion	5'-GC**TCTAGAAAGCTT**GCACCTTGAGGATCAC-3'
	617-618; +; insertion	5'-GC**TCTAGAGTCGAC**TCACTTGAGAGCGCTCC-3'
External:	+; 5' end-specific	5'-CAC**AGATCT**TTCGGTTAGGATGGACGCG-3'
	-; 3' end-specific	5'-CAC**AGATCT**GTAAGTGTATTCGGTATTGAC-3'

* Unique restriction enzyme sites to be inserted are shown in bold

TABLE 4.2: *The annealing temperatures (T_m), including and excluding the extra bases, of the above primers are summarised.*

Primer	Number of nucleotides	T_m excluding	T_m including
mt177Rev (-)	32 bp (18 G+C)	62 °C	73 °C
mt177For (+)	32 bp (20 G+C)	60 °C	74 °C
mt200Rev (-)	31 bp (18 G+C)	54 °C	69 °C
mt200For (+)	31 bp (16 G+C)	54 °C	72 °C
VP7-5'For (+)	28 bp (15 G+C)	56 °C	61 °C
VP7-3'Rev (-)	30 bp (12 G+C)	55 °C	59 °C

Amplification was followed by cloning the amplicons into the PCR cloning vector, pMOSBlue (Amersham). Following electrophoresis of samples of each reaction mixture in a 1.0% agarose gel, the amplified PCR products were recovered from the respective reaction mixtures using Geneclean™ procedure (section 2.2.4.2) or alternatively extracted with chloroform/isoamylalcohol (section 2.2.4.1), to remove residual DNA polymerase. The PCR fragments were ligated in a 1:10 ratio to the T-vector using the reagents supplied by the manufacturer. The ligation mixtures were transformed into ultra-competent MOS*Blue* cells according to the manufacturer instructions. Recombinant plasmids were isolated from white recombinant colonies with amp^R and tet^R phenotype and identified by restriction enzyme mapping. Orientation of each fragment was determined using *Sac*I.

Full-length VP7 insertion mutants at positions 548-549 (amino acids 177-178; VP7mt177) and 617-618 (amino acids 200-201; VP7mt200) were reconstructed by a two step directional cloning procedure in

pFastbac1 so as to enable expression of the resultant product by means of the BAC-TO-BAC™ expression system. First the 5'-terminal domain of both VP7 mutants was recovered from pMB-177/5' and pMB-200/5' with *Bgl*II and *Xba*I and ligated into the *Bam*H1 and *Xba*I sites of pFastbac1 and recombinants selected by *Sac*I digestion. The 3'-terminus was cut from pMB-177/3' with *Xba*I and *Kpn*I and cloned into the pFB-177/5' containing the modified 5' region of VP7. The 3'-terminus of insertion mutant 200 was retrieved from pMB-200/3' with *Xba*I digestion and ligated into the dephosphorylated *Xba*I site of pFB-200/5' and recombinants with the correct orientation of the 3' fragment selected with *Sal*I and *Sac*I digestions. Recombinant pFastbac1 plasmids containing the two modified VP7 genes were selected with *Sac*I, *Hind*III, *Xba*I and *Sal*I digestions. The VP7 insertion mutant genes in pFastbac1 were designated pFB-VP7mt177 (containing insertion between amino acids 177 and 178) and pFB-VP7mt200 (containing insertion between amino acids 200 and 201). The insertion of the three restriction enzyme sites in both modified VP7 recombinant plasmids were verified by automated dye terminator cycle sequencing (section 4.2.4), before expression of the modified VP7 proteins.

In the second method, the VP7 insertion-specific mutants were constructed by a modification of the polymerase chain reaction method as described by Imai *et al.*, (1991). In this method two oligonucleotide primers, designed to amplify the target DNA in inverted tail-to-tail directions, were used to amplify the cloning vector together with the target VP7 sequence in one PCR reaction and thereby generating the desired insertions. The plasmid pBS-VP7PCR, containing the full-length tailored VP7 gene in the T7 orientation, was used as template and the set of two mutagenic primers containing the unique restriction enzyme sites, described above (table 4.1), were used for priming the reaction. Briefly, the PCR reaction mixtures consisted of 10 µl of 10 x Ex Taq™ buffer, 8 µl of a 2.5 mM dNTP mixture, 0.5-5 ng of template plasmid (pBS-S7PCR), 85 pmol of the sense and antisense primers and 2 U of TaKaRa Ex Taq™ polymerase (Life technologies). The thermal parameters used for the PCR were the same as described above except the elongation at 72 °C were extended to 4.5 min in each cycle. The amplicons were gel purified digested with *Xba*I, self-ligated and transformed into competent *E. coli* XI1Blue cells. The two resultant VP7-specific clones, designated pIM177 and pIM200, was characterised by *Sac*I, *Hind*III, *Xba*I and *Sal*I digestions and automated sequencing (section 4.2.4). The two modified VP7 genes were recovered by *Eco*R1 and *Kpn*I digestions and recloned into the *Eco*R1/*Kpn*I site of pFastbac1 which were designated pFB-InM177 and pFB-InM200, respectively. These recombinant transfer vectors were used to express the modified VP7 proteins in eukaryotic cells.

4.2.3. Insertion of AHSV-9 VP2 epitopes in the VP7-encoding DNA and construction of recombinant baculovirus transfer vectors

The introduction of an AHSV-9 VP2 epitope into the two identified hydrophilic domains of the AHSV-9 VP7 protein, were performed using the two modified VP7 genes containing the unique restriction sites. These modifications allows the insertion of sequences with complementary 5' and 3' overhangs into the target sites. Sequences representing AHSV-9 VP2 immunogenic epitopes can now be cloned directionally in the correct reading frame of the VP7 sequences encoding the hydrophilic regions. Seeing as the cloning strategy followed by Samantha Hopkins in producing the two chimeric VP7/TrVP2 proteins, using the two insertion mutants, has not been documented elsewhere, it is included in this section for reference purposes. The strategy followed for generating the chimeric proteins was as follows: the first step was to clone a 2.3 kb region of VP2, which contain the epitope of interest (amino acids 385 to 415 and nucleotides 1167 to 1257), into the *Hind*III site of VP7 mutant 200. The VP2 specific *Hind*III site at position 957 is in the correct reading

frame to the *Hind*III site inserted at position 548-549 of AHSV-9 VP7 gene.

The plasmid pBS-AHSV9.2 was digested with *Hind*III and the 2.3 kb DNA fragment representing the AHSV-9 VP2 was excised from the gel and purified by Geneclean™ extraction (section 2.2.4.2). The plasmid pFB-mt200 was linearised with *Hind*III and then ligated to the purified 2.3 kb *Hind*III-restricted AHSV-9 segment 2 specific DNA. Following transformation into competent *E. coli* XL1Blue cells, plasmids from a number of amp^+ and tet^+ colonies were isolated and characterised by restriction analysis. A recombinant plasmid with the correct orientation of the *Hind*III truncated segment 2, inserted into the *Hind*III site of pFB-VP7mt200, was selected. This intermediate mt200/VP2 chimera was completely restricted with *Xba*I and partially restricted with *Eco*R1 for 1h using 2-3 μg of DNA. The enzymes were heat-inactivated at 65 °C for 15 min and the ends filled up using Klenow DNA polymerase and 50 μM dNTPs (section 3.2.1.1). Filling up of the overhang termini was necessary to correct the reading frame as well as to enable the ligation of two incompatible ends. The restricted fragments were separated on a 0.7% agarose gel and the approximately 6.3 kb DNA band was excised from the gel and purified by Geneclean™ extraction. The DNA was self-ligated, transformed into XL1Blue cells and plated out as above. Plasmid DNA from a large number of colonies was isolated and the covalently closed circular form compared to that of pFB-VP7mt200 before further characterisation with restriction enzyme digestions. The VP7mt200 with VP2-specific insert (mt200/TrVP2) were sequenced to confirm the segment 2 status of the insert and the correct reading frame (section 4.2.4).

The second chimera was constructed by retrieving the segment 2 specific insert from pFB-200/VP2 by *Hind*III and *Sal*I digestion in the appropriate RE buffer. The 300 bp fragment was cloned directionally into the corresponding sites of pFB-mt177 to create pFB-mt177/TrVP2.

4.2.4. Construction of recombinant pFastbacDual transfer vectors containing AHSV-9 VP3 and recombinant VP7 genes

The recombinant dual transfer vector, pFBd-S3.9-S7.9, was utilised for the cloning of the recombinant VP7 genes with VP3. The plasmid pFBd-S3.9-S7.9 was partially digested with *Bam*H1 (section 2.2.10) and completely digested with *Pst*I. The recombinant and chimeric VP7 genes were obtained by simultaneous restriction with *Bam*H1 and *Pst*I in a suitable salt buffer of plasmids pFB-mt177, pFB-mt200, pFB177/TrVP2 and pFB200/TrVP2. Ligation, transformation and selection was performed as described in section 3.2.1.1. Recombinant pFastbacDual transfer vectors were used to construct dual recombinant baculoviruses.

4.2.5. Dye terminator cycle sequencing of the VP7 insertion mutants

All sequencing reactions were done by cycle sequencing using dye-labelled terminators. Amplification of template strands was done using AmpliTaq^R DNA polymerase FS, a mutant form of Taq DNA polymerase, which has essentially no 5'□3'exonuclease activity as well as drastically reduced discrimination against incorporation of dideoxynucleotides, leading to much lower concentrations of dye-labelled terminators having to be used. AmpliTaq^R DNA polymerase FS, was supplied in the ABI PRISM™ Big Dye Terminator Cycle Sequencing Ready Reaction kit (Perkin Elmer). Kits were stored at -20°C with the dye terminator solutions being shielded from light.

4.2.5.1. Template purification and quantitation

Recombinant pFastbac1 and pBS vectors containing the desired fragments were purified using one of the following plasmid purification kits to ensure optimal quality of DNA template for automated sequencing: the Qiagen^{R} plasmid mini-kit tip 20 (Qiagen), high pure plasmid purification kit (Boehringer Mannheim), Nucleobond (Macherey-Nagel) and Wizard columns (Promega). Manufacturers instructions were followed for all plasmid purifications. All these purification methods are based on a modified alkaline lysis procedure (section 2.2.4), followed by binding of the plasmid DNA either to an anion-exchange resin under appropriate low salt and pH conditions or to the surface of glass fibres or silica materials in the presence of a chaotropic salt. In both cases the binding process is specific for nucleic acids and the bound DNA is purified from salts, proteins and other cellular impurities, prior to elution.

The quality and quantity of the DNA templates were analysed using at least two of the following three methods. A 1% analytical agarose gel comparing a dilution series of the appropriate linearised plasmid DNA with a DNA standard size marker with known concentration. Secondly, the optical density of each sample was measured spectrophotometricly at 260 nm, 280 nm and 320 nm, using a Beckman DU® 64 spectrophotometer. The concentration of the DNA was calculated from the 260 nm reading, using the extinction coefficient for dsDNA as $1A_{260}$ = 50 μg/μl, while the 260 nm to 280 nm ratio gave an indication of the purity of the sample. The reading at 320 nm is an indication of the amount of salts present in the sample. The third method is based on the measurement of the change in fluorescence characteristics of Bizbenzimide (Hoechst 33258) in the presence of DNA, using the Hoefer DyNA Quant^{TM} 200 fluorometer. Measurements were done according to the manufacturer's instructions using 2 μl of the unknown DNA sample in 2 ml of assay solution (0.1 μg/ml Hoechst in 0.2 M NaCl, 10 mM Tris-HCL, 1 mM EDTA, pH 7.4). The final concentration was determined using the formula for a straight line (y = mx + b).

4.2.5.2. Cycle sequencing reactions

For PCR based cycle sequencing reaction, 3.2 pmole of the polyhedrin-specific primers or VP7-specific primers were used, together with 250 ng double-stranded template, 8 μl of the Terminator Ready Reaction mix and the reaction volume made up to 20 μl with ddH_2O. Half reactions with the same amount of template and primer were also successfully used. All thermal cycle reactions were done in an ABI termal cycler 9600 with heated lid, obviating the need for light mineral oil overlays. A rapid thermal ramp to 96°C was followed by incubation at 96°C for 10 sec, rapid cooling ramp to 50°C for annealing, rapid thermal ramp to 60°C and continued incubation at 60°C for 4 min to enable primer extension. This cycle was repeated 25 times, followed by rapid cooling to 4°C. Excess dye terminators were removed through simplified ethanol precipitation as follows: the 20 μl PCR reaction was added to 16 μl ddH_2O and 64 μl 98% ethanol in a clean tube, with the solution containing no salts. The DNA fragments were precipitated for 10 min at room temperature and centrifuged for 25 min in a microfuge. The pellet was rinsed with 70% ethanol, repelleted and air-dried.

4.2.5.3. ABI PRISM^{TM} Sequencing

All sequencing reactions were analysed using an ABI PRISM 377 sequencer. Dried samples were resuspended in 3.0 μl sequencing loading buffer (5:1 ratio of deionized formamide to 25 mM EDTA pH 8.0 containing 50 mg/ml dextran blue) prior to loading. The samples were denatured by heating to 95°C for 2 min. Samples were placed on ice and 1.5 μl were loaded on a 4% denaturing polyacrylamide gel and run for 7 h at

1.6 kV. Sequences were analysed using the ABI PRISM Sequencing Analysis™ program, as well as the ABI PRISM Navigator™ program and aligned using Clustal X (Thompson *et al.*, 1994). Translated sequences were submitted to the National Centre for Biotechnology Information (NCBI) using the BLAST network server and the SwissProt database (Altschul *et al.*, 1990). Hydropathy plots of VP7, mt177 and mt200 were prepared using the ANTHEPROT package (Geourjon *et al.*, 1991; Geourjon & Deleage, 1995) and the Hopp and Woods predictive method (Hopp & Woods, 1981 & 1983).

4.2.5.4. Structural modelling

A three-dimensional model of the insertion mutant proteins was constructed using the MODELLER 4 package and a Silicon Graphics Power Indigo Extreme workstation (Sali & Blundell, 1993). The X-ray crystallographic structure of AHSV-4 VP7, obtained from Brookhaven Protein Database, was used as an initial template for model building. The models were based on an optimal alignment of the insertion mutants to the VP7 template. The homology structure was calculated by the satisfaction of spatial restraints as described by empirical databases. Structures were visualised with Rasmol (Massachusetts University).

4.2.6. Production of recombinant single and dual baculoviruses

The construction and isolation of composite bacmid DNA was done as described in sections 3.2.2 and 3.2.3, using the recombinant transfer vectors pFB-mt177, pFB-mt200, pFB177/TrVP2, pFB200/TrVP2, pFBD-S3.177, pFBD-S3.200, pFBD-S3.177/TrVP2 and pFBD-S3.200/TrVP2. Transfection was performed as in section 3.2.4 using cellfectin, recombinant viruses were plaque purified and high titered stocks prepared. Recombinant baculoviruses were designated Bac7mt177, Bac7mt200, Bac177/VP2tr and Bac200/VP2tr and dual recombinant baculoviruses Dual-VP3.177, Dual-VP3.200.

4.2.7. Synthesis and purification of the VP7 and recombinant protein complexes

S. frugiperda cells in 75 cm^3 tissue culture flasks (1 x 10^7 cells/flask) were infected with the recombinant baculoviruses BacVP7, Bac7mt177, Bac7mt200, Bac177/VP2tr or Bac200/VP2tr at a MOI of 5-10 pfu/cell. The infected cells were harvested after an incubation period of 72 h at 28°C. Subcellular fractions were then prepared essentially according to the procedures described by Chuma *et al.* (1992), Burroughs *et al.* (1994) and Basak *et al.* (1996). The infected cells were concentrated by centrifugation at 2000 rpm for 5 min at 4°C and washed twice with 1 x PBS. The cell pellets were resuspended in TNN lysis buffer (10 mM Tris-HCl pH 8.0, 150 mM NaCl containing 0.25% Nonidet P-40) at 2 x 10^7 cells per ml and incubated on ice for 15-30 min. Following homogenisation of the cell suspension by 15 strokes with a dounce homogeniser, the nuclei were removed from the cell lysate by centrifugation at 1000 rpm (160 x g) for 10 min. In order to recover the maximum amount of crude protein, the process of cell lysis and extraction of cytoplasmic fraction was repeated three times. The supernatant was then loaded onto a 40% to 70% (w/v) discontinuous sucrose gradient in 0.2 M Tris-HCl (pH 7.5-8.0). The gradients were centrifuged at 20 000 rpm for 1 h at 4°C in a SW50.1 Beckman rotor. The particulate fraction (pellet) was resuspended in 1/10 of the original fraction volume in 10 mM Tris-HCl (pH 8.0) and re-centrifuged on a self-forming CsCl gradient (density 1.32 g/ml CsCl) for >16 h at 38 000 rpm in a Beckman SW50.1 rotor. The material formed a sharp white band and was

recovered and dialysed against Tris-HCl buffer or diluted (1:4) with 0.2 M Tris-HCl (pH 8.0) and re-centrifuged at 20 000 rpm for 1 h in a Beckman SW50.1 rotor. Alternatively, the cytoplasmic fraction was loaded onto a 40% to 70% (w/v) continuous sucrose gradient and centrifuged at 12 000 rpm (13 000g) for 1h at 4°C in a SW41 Beckman rotor. The gradients were fractionated from the bottom in 12x 1 ml fractions. The fractions containing the AHSV-9 VP7, VP7 insertion mutants and VP7/VP2 chimeric proteins were pooled, diluted 4x in 10 mM Tris-HCl (pH 8.0) and the proteins recovered by centrifugation at 20 000 rpm in a SW50.1 rotor. The purity of the protein was finally checked using SDS-PAGE analysis.

4.2.8. Solubility assays and purification of recombinant VP7 proteins

Infected Sf9 cells were harvested 72 h post-infection, washed in 1 x PBS, resuspended in cold TNN lysis buffer and homogenised at 4°C. Cell debris and nuclei were then pelleted by low speed centrifugation as described above. The nuclei were then washed at least three times with TNN lysis buffer and all the cytoplasmic fractions were pooled. The cytoplasmic extract was separated into a soluble fraction and a particulate fraction by centrifugation at 5 000 rpm for 30 min at 4 °C in a Beckman J21 supercentrifuge. The VP7 protein remaining in the soluble fractions was precipitated by adding the required amount of ice-cold, saturated ammonium sulphate (in 100 mM Tris-HCL, pH 7.5) to the soluble extract to provide a final concentration of 20% (v/v). The precipitated protein was pelleted by centrifugation and resuspended in TNN buffer at 1/10 of the original volume. The particulate fraction was resuspended in TNN buffer in 1/10 of the original fraction volume and banded on a 40% to 70% continuous sucrose gradient as described above. All fractions were analysed by SDS-PAGE.

4.2.9. Analysis by scanning electron microscopy

Samples of purified VP7 specific protein were fixed in phosphate buffered 2.5% formaldehyde/0.1% glutaraldehyde at room temperature for 30 min. The fixed particulate protein samples were filtered onto a 0.2 μm nylon filter, washed three times in 0.075 M NaH_2PO_4/Na_2HPO_4 and then dehydrated by successive treatment of 30%, 50%, 70%, 90% and 100% ethanol. The treatment with 100% ethanol was repeated three times after which the filters were air-dried, mounted onto a stub and spatter coated with gold-beladium, a few atoms thick followed by a layer carbon. The stub was viewed at 5.0 kV in a Jeol scanning electron microscope.

4.2.10. Purification and analysis of CLP formation

Sf9 cells were infected at a M.O.I. of 5-10 pfu per cell with dual recombinant baculoviruses expressing AHSV-9 VP3 and the VP7 insertion mutant proteins or VP7/VP2 chimeric proteins. Cells were harvested 48 h p.i., rinsed with 1x PBS and lysed at 4°C in TNN buffer. Particles were purified by sucrose gradient centrifugation as described in section 3.2.5.2. CLPs were analysed by SDS-PAGE and examined by electron microscopy after resuspension in 150 mM NaCl, 0.1 M Tris-HCL pH 8.0.

4.3. RESULTS

4.3.1. Molecular structure modelling of the VP7 protein

Hydropathic profile analysis of VP7 (*Figure 4.1*) indicates that the amino-terminal region of VP7 is considerably less hydrophobic than the carboxy terminus, while the central region of the VP7 amino acid sequence (residues 120 - 249), which represents the top domain of VP7, displayed alternating hydrophilic and hydrophobic stretches. Mapping the hydrophobicity plots to the solvent-accessible surface of AHSV VP7, has shown the presence of at least one large and three smaller hydrophilic regions, of four to eight amino acids, which are prominent in the middle domain of the VP7 amino acid sequence. The four linear hydrophilic domains most accessible to the aqueous environment of the VP7 protein are amino acids 141 to 146, 167 to 178, 196 to 201 and amino acids 237 to 242 (*Figure 4.1*). Secondary structure predictions of VP7 indicated that these hydrophilic domains are located in β-turns between the β-sheet structures, characteristic of the amino acid region 120 and 250. These domains could be suitable targets for the insertion of short, foreign, immunogenic peptides. A model of the three-dimensional structure of VP7 was obtained with the RASMOL computer program to identify amino acids located on the surface of the VP7 trimer (*Figure 4.2*). From the available crystallographic data, the four linear hydrophilic regions are located on the surface of the trimeric VP7 molecule when the hydrophobicity plots are compared to the surface structure of the VP7 trimers. Three of the four hydrophilic regions, which are optimally located and accessible on the surface of the top domain of AHSV VP7 trimeric molecule, are indicated (*Figure 4.2*). The first hydrophilic region is located between amino acids 141 to 146 (144 to 145 best possible position), the second between amino acids 163 to 180 (best location 177 to 178) and the third between 196 and 201 (best location between 200 to 201) and the last site at position 237 to 242. The last site is not very accessible on the surface. The two most promising sites were found to be 177 - 178 and 200 - 201. The arginine at position 178 forms part of a RGD motif, which is located on a highly flexible loop which stretches from amino acid 175 to 180 and represents an ideal site for the insertion of peptides, since it loops out and is exposed on the surface of VP7. These two sites were therefore targeted for modification to facilitate the insertion of antigenic determinants.

In order to enable the insertion of small peptides into these target sites, it was necessary to introduce unique restriction enzyme sites in the VP7 nucleotide sequence corresponding to the two hydrophilic regions. As a first step the sites were modified by the insertion of three restriction enzyme sites, *Hind*III, *Xba*I and *Sal*I that are absent in the VP7 gene of AHSV-9. *Hind*III, *Xba*I and *Sal*I, encode lys-leu (AAGCTT), ser-arg (TCTAGA) and val-asp (GTCGAC), respectively. The amino acids encoded by the 18 nucleotides are either hydrophilic (positive, e.g. K and R, or negatively, e.g. D, charge) or neutral (e.g. L, S and V), which it is assumed will have little or no influence on the structure of VP7. The effect of the six inserted amino acids on the solubility, trimer formation and the structure of the VP7 crystals were investigated.

Figure 4.1: Hydrophilicity (a) and antigenicity profiles (b) of AHSV-9 VP7 in comparison with the predicted solvent-accessiblity (c). Hydrophilicity and antigenicity was predicted according to Hopp & Woods (1981) and Welling *et al.* (1989), respectively. Areas with positive values have a nett hydrophilicity while areas with negative values have a nett hydrophobicity.

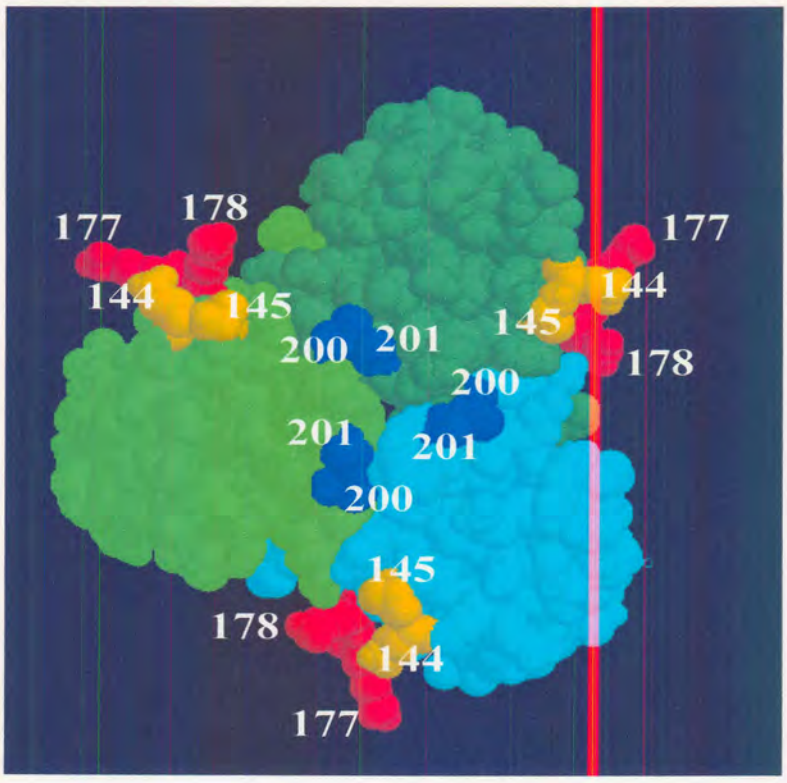

Figure 4.2: A schematic representation of the three-dimensional structure of AHSV VP7 trimer, looking vertically into the top of the trimer. The three VP7 monomers are highlighted in light blue, light green and dark green. The tripeptide RGD (residues 177-179) is highlighted in red. Two other hydrophilic regions, exposed to the surface of the trimer are amino acid residues 199 - 201 (dark blue) and 143 - 145 (orange). The red and dark blue sites were targeted for modifications and insertions.

4.3.2. Construction of recombinant baculovirus transfer vectors containing the mutagenised DNA copies of the VP7 gene

An insertion of the 6 amino acids encoded by the 18 nucleotides of the three unique restriction enzyme sites was introduced in the correct reading frame between nucleotides 548 to 549 (codons 177 to 178) and nucleotides 617 to 618 (codons 200 to 201), respectively, using two different PCR methods. In one of these methods (*Figure 4.3*) two synthetic oligonucleotide primers were designed in inverted tail-to-tail directions and used in combination with the 5' and 3' external VP7 specific primers (table 4.1). The two sets of mutagenic primers contained nucleotides at their 3' ends, which were identical or complementary to the coding sequence of the VP7 gene, which flanked the sequence where the insertion was to be introduced. In addition, the 14 nucleotide extended 5' ends of the primers specified two unique restriction enzyme sites, namely *Hind*III and *Xba*I for the reverse primers and *Sal*I and *Xba*I for the forward primers, along with two clamp bases. The choice of the three sites was motivated by the observation that the AHSV-9 VP7 gene does not contain these restriction enzyme sites. This allows for the rapid and cost-effective insertion of sequences encoding for foreign epitopes, as well as for easy screening of the resulting recombinant plasmids.

Amplification with the two sets of primers resulted in DNA fragments of expected sizes of 590 bp and 550 bp in the case of the mt177 mutagenic primers and 620 bp and 520 bp using the mt200

mutagenic primers (*Figure 4.4 A*). The sizes of the amplified PCR products were in agreement with the size predicted from the VP7 sequence. The PCR products were cloned into the pMosBlue T-vector. Restriction of recombinants with *Bgl*II and *Xba*I, which cut at opposite ends of the PCR products, excised fragments of the same size as the amplified fragments described above, and the orientation of the insert was determined by *Sac*I digestion followed by agarose gel electrophoresis of the restriction fragments (data not shown). The 177/5', 177/3' and 200/5' fragments were in the T7 orientation while 200/3' were in the SP6 orientation in the recombinant pMosBlue vectors. The full-length mutagenised VP7 genes were constructed in pFastbacI transfer vector by a two step cloning procedure. In the first step the 5' fragment of each VP7 insertion mutant (177/5' and 200/5') were recovered by *Bgl*II and *Xba*I digestion and cloned directionally into the *Bam*H1 and *Xba*I sites of the bacmid transfer vector, pFastbac1, to create the pFB-177/5' and pFB-200/5' intermediates (*Figure 4.3*). Recombinant plasmids were selected from which ca. 490 bp or 520 bp fragments were excised with *Bam*H1 and *Xba*I digestion, in the case of insertion mutant 177 and 200, respectively. In the second step the 3' end of the insertion mutant 177 was recovered by *Xba*I and *Kpn*I digestion, while the 3' end in the case of mutant 200 was recovered by only *Xba*I digestion because of difference in orientation. The 3' end of insertion mutant 177 was cloned by directional cloning into the *Xba*I and *Kpn*I site of the recombinant pFB-177/5' intermediate, which resulted in the loss of the largest part of the multiple cloning site of pFastbac1 except for the *Kpn*I and *Hind*III sites. Recombinant plasmids that displayed the full-length VP7 gene, containing the three restriction enzyme sites, were selected following restriction enzyme mapping with *Bam*H1, *Sal*I, *Sac*I and *Hind*III individually or in combinations. One such clone was selected, designated pFB-mt177 (*Figure 4.4 B*). Since the *Hind*III site present in the vector would complicate future cloning into the mutant 177 gene, the *Hind*III site in the vector was deleted by partial digestion with *Hind*III, filling up of the overhangs with Klenow, self-ligation and restriction enzyme mapping as described above. The 3' end of insertion mutant 200 was cloned into the dephosphorylated *Xba*I site of pFB-200/5' intermediate. Recombinant plasmids with the 3' end in the correct orientation were identified by restriction enzyme mapping with *Sac*I and *Sal*1-*Sma*I combination. A recombinant which yielded fragments of the expected sizes was selected and designated pFB-mt200 (*Figure 4.4 C*). The *Xba*I and *Hind*III sites, still present in the multiple cloning site of the vector, were deleted by means of partial digestions and self-ligation of the vector. In order to verify the integrity of the desired insertions the nucleotide sequence of both VP7 specific insertion mutants were analysed by automated dideoxynucleotide sequencing.

In the second method (*Figure 4.5*) the site-directed insertion mutagenesis was performed in a one step PCR process, in which the amplification was carried out using the two synthetic mutagenic primers which were designed in an inverted tail-to-tail direction (table 4.1). Using the cloned copy of the full-length VP7 gene in pBS322 (pBS-S7PCR) as template and the primers and PCR reaction conditions described in section 4.2.2, a major DNA band of approximately 4.3 kb was synthesised for each insertion mutant. The size of the amplified PCR product was in agreement with the size

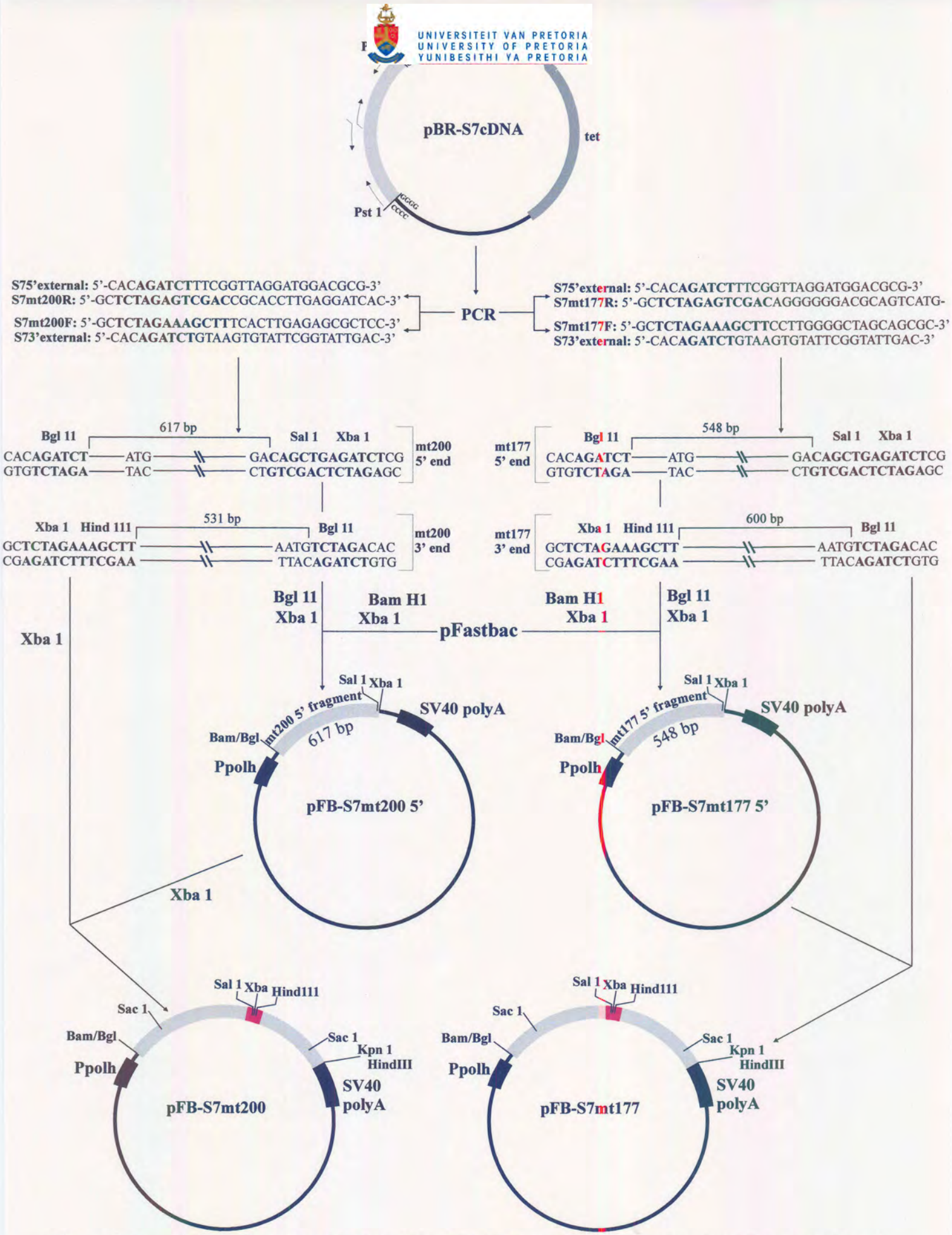

Figure 4.3 Schematic representation of the first PCR method used to construct the recombinant transfer vectors containing the mutagenised DNA copies of the VP7 gene. In this method two oligonucleotide primers were designed in inverted tail-to-tail directions and used in combination of the 5' and 3' external VP7 specific primers.

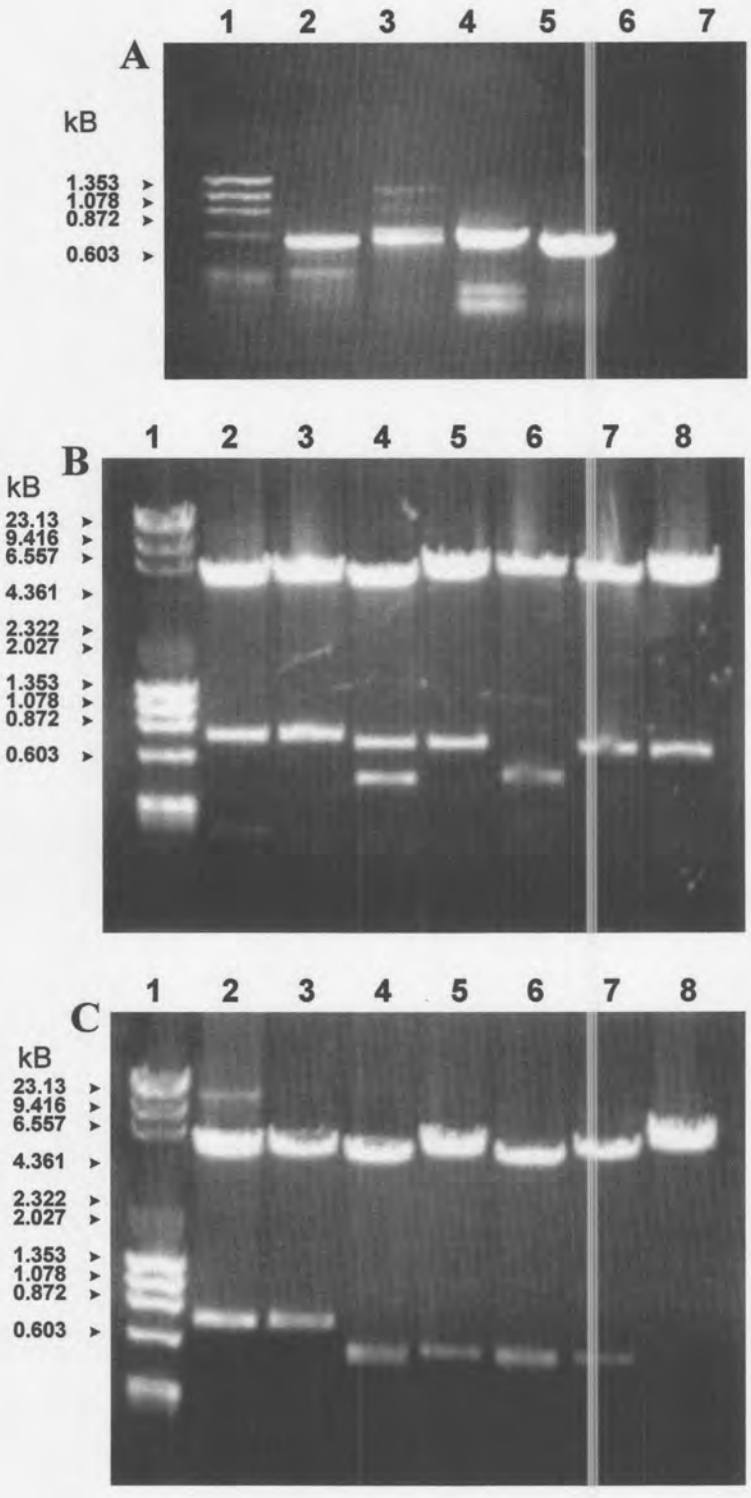

Figure 4.4: (A) Agarose gel electrophoretic analysis of the DNA products obtained by PCR amplification of the AHSV-9 VP7 gene (pBR-S7cDNA), using two inverted tail-to-tail mutagenic primers in combination with VP7 5' and 3' end specific primers. Lane 1 represents HaeIII digested ϕx174 DNA and the relevant sizes are indicated to the left of the figure. Lanes 2 and 3 shows the PCR amplified products of the 5' end and 3' end of VP7 using the primers for insertion mutant 177. Lanes 4 and 5 contain the products of the 5' and 3' ends of VP7 using insertion mutant 200 reverse and forward primers, respectively. Lanes 6 and 7 represents negative controls, containing primers but no template. (B and C) Agarose gel electrophoretic analysis of the recombinant pFastbac plasmids constructed by the cloning of the two PCR DNA fragments of each insertion mutant to generate two full length mutagenised VP7 genes. The derived recombinant plasmids pFB-mt177 (B) and pFB-mt200 (C) were restricted with *Sac*I (lane 3), *Hind*III/*Bam*H1 (lane 4), *Hind*III (lane 5), *Bam*H1/*Sal*I (lane 6), *Sal*I/*Kpn*I (lane 7) and *Xba*I (lane 8). Lane 1 include molecular weight markers MWII and ϕx174 DNA. *Sac*I digested pBS-S7PCR (lane 2) was included as an additional size marker.

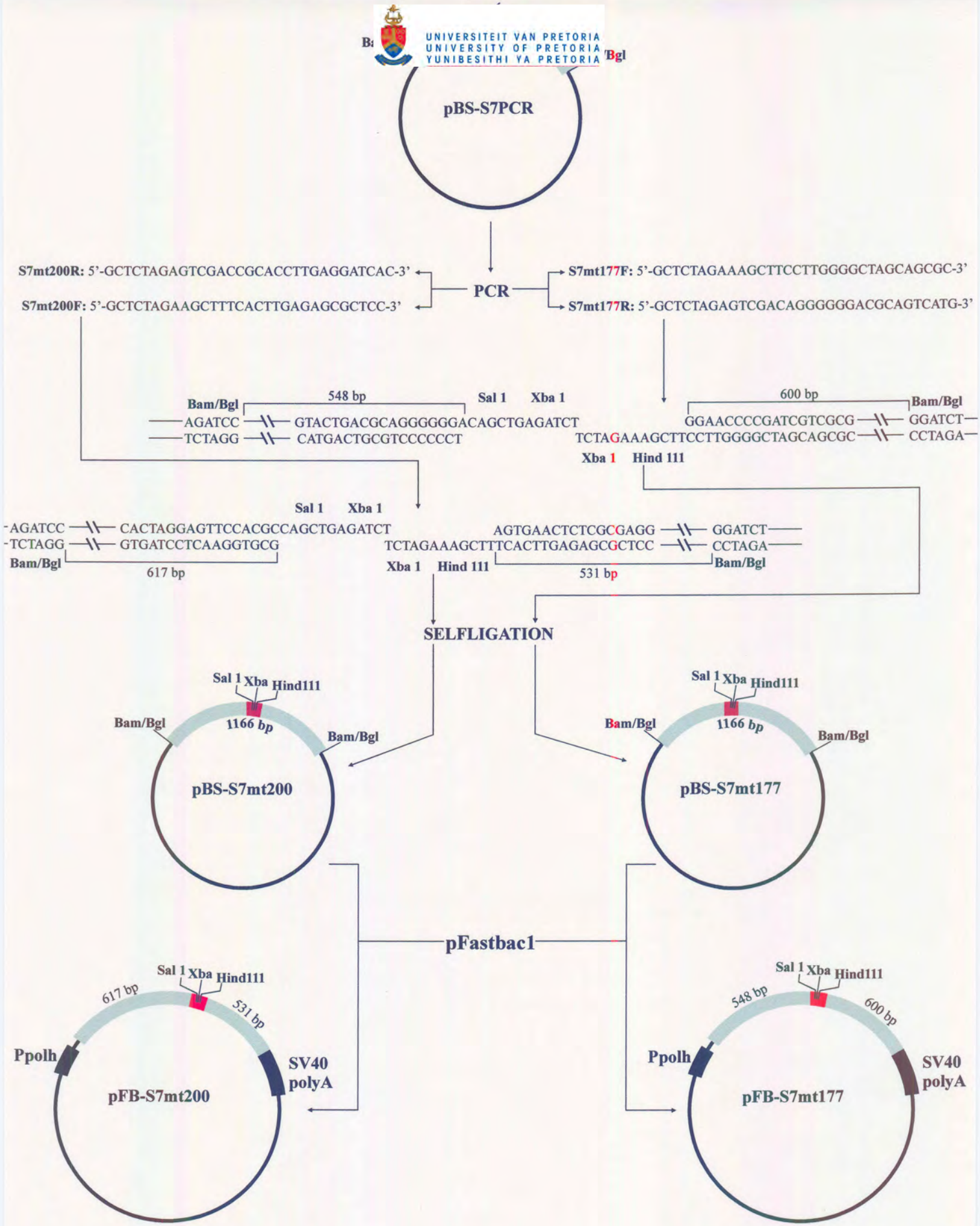

Figure 4.5 In the second method used for insertion mutagenesis the insertion was performed in a one step PCR process. The amplification was carried out using two primers designed in an inverted tail-to-tail direction, tagged at their 5' ends with the chosen R.E. sites.

predicted for the cloning vector (3.2 kb) together with the mutagenised VP7 gene (ca. 1.15 kb). The identity of the purified 4.3 kb PCR product was confirmed by restriction with *Sac*I, which is known to cut twice in VP7 at nucleotide position 200 and 1045. Three fragments of 350 bp, 500 bp and 3.4 kb for mt177 and 410 bp, 440 bp and 3.4 kb for mt200, characteristic of VP7, were generated for each insertion mutant PCR product. Since each of the mutagenic flanking primers contained *Xba*I linker sequences, the purified PCR products were digested with *Xba*I and subsequently self-ligated. Restriction of both insertion mutants (pMt177 and pMt200) with *Bam*H1 (ca. 100 bp from 5' end of VP7) and *Eco*R1 (only cut in MCS) excised a fragment approximately 100 bp smaller than that of the wild-type VP7 gene copy. Restriction with *Hind*III, and *Sal*I generated fragments of approximately 600 bp and 520 bp for mutants 177 and 200 respectively. These results indicate that insertion of the three unique restriction enzyme sites into the VP7 gene was successful at both domains selected. The integrity of the two insertion mutations was subsequently verified by automated dye terminator cycle sequencing.

The mutagenised VP7 genes were excised from pMt177 and pMt200 and directionally cloned into the *Eco*R1/*Kpn*I site of the pFastbac vector, which resulted in the removal of the largest part of the MCS of the vector. Recombinant plasmids from which ca. 850 bp fragments were excised by *Sac*I digestion, were selected for further restriction enzyme analysis. Clones that displayed the correct transcriptional orientation were selected following restriction enzyme mapping with *Hind*III, which recognises a site in the MCS of the vector and cuts asymmetrically in both insertion mutants 550 bp and 620 bp from the 5' end of InM177 and InM200, respectively. One representative clone was selected for each insertion mutant and designated pFB-Mt177 and pFB-Mt200.

4.3.3. Sequence verification and molecular modelling of the modified VP7 proteins

The sequences of the recombinant VP7 clones in pFastbac1 were confirmed by automated nucleotide sequencing. No nucleotide alterations other than the specified insertions were observed in the VP7 mutant genes, constructed using both strategies (*Figure 4.6*). Therefore, pFB-mt177 and pFB-mt200 were utilised in subsequent cloning procedures and for expression. Analysis of the electropherograms indicated that the 18 nucleotides, encoding the 6 amino acids K L S R V D were inserted. The correct reading frame of the insertional genes was verified by translation of the sequences and comparing them with the original VP7 amino acid sequence (*Figure 4.7*).

The hydropathic profiles of VP7mt177 and VP7mt200 deduced amino acid sequences were compared to that of AHSV-9 VP7. Although the profiles were identical in the unmodified regions of the three proteins as will be expected, the regions of the insertional mutants, which were targeted during mutagenesis, showed an increase in hydrophilicity (*Figure 4.8*), which also differed between the two insertion mutants. The insertion of the six amino acids between amino acids 177 and 178 of

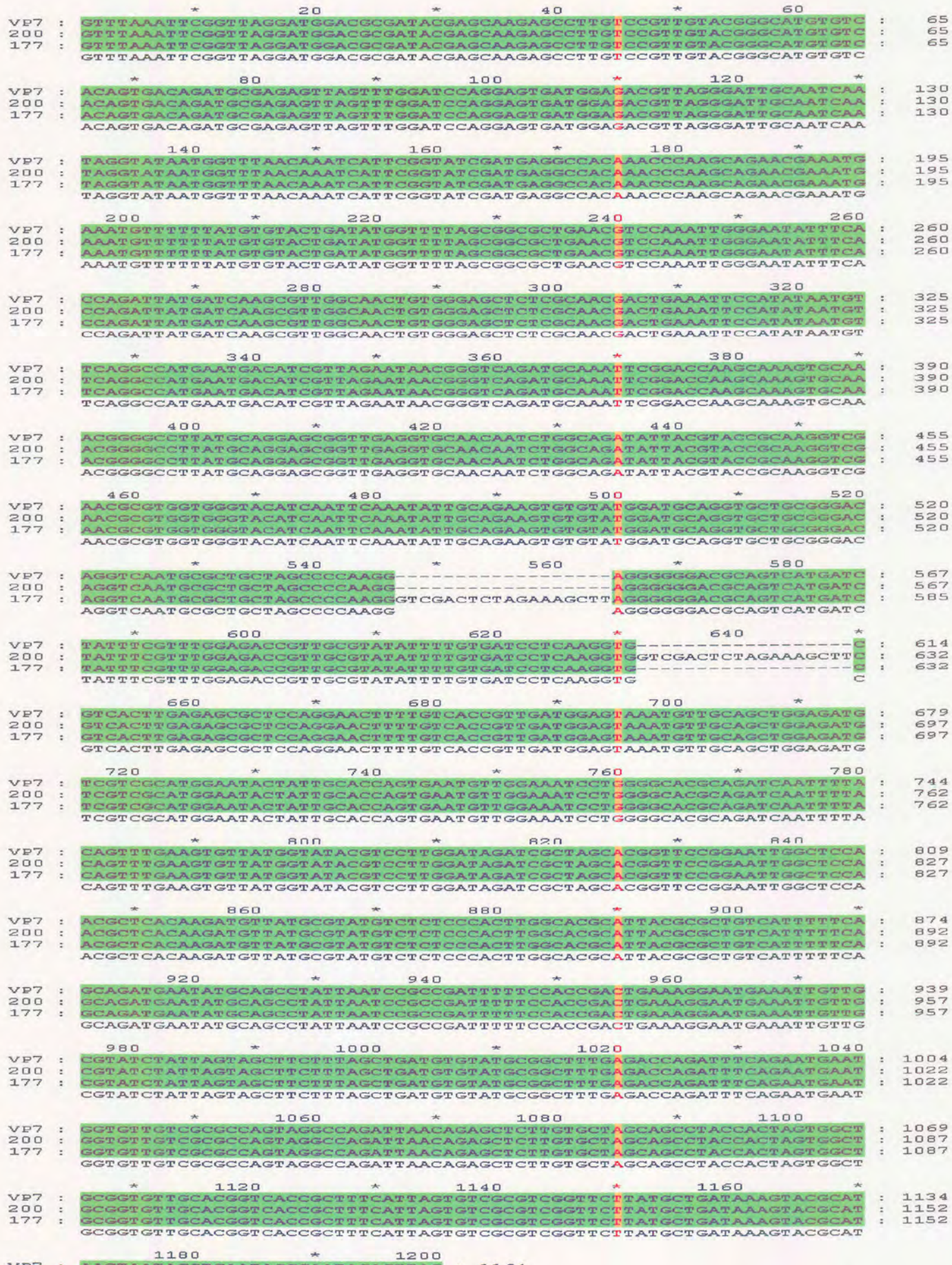
VP7 : GTTTAAATTCGGTTAGGATGGACGCGATACGAGCAAGAGCCTTGTCCGTTGTACGGGCATGTGTC : 65
200 : GTTTAAATTCGGTTAGGATGGACGCGATACGAGCAAGAGCCTTGTCCGTTGTACGGGCATGTGTC : 65
177 : GTTTAAATTCGGTTAGGATGGACGCGATACGAGCAAGAGCCTTGTCCGTTGTACGGGCATGTGTC : 65
VP7 : ACAGTGACAGATGCGAGAGTTAGTTTGGATCCAGGAGTGATGGAGACGTTAGGGATTGCAATCAA : 130
200 : ACAGTGACAGATGCGAGAGTTAGTTTGGATCCAGGAGTGATGGAGACGTTAGGGATTGCAATCAA : 130
177 : ACAGTGACAGATGCGAGAGTTAGTTTGGATCCAGGAGTGATGGAGACGTTAGGGATTGCAATCAA : 130
VP7 : TAGGTATAATGGTTTAACAAATCATTCGGTATCGATGAGGCCACAAACCCAAGCAGAACGAAATG : 195
200 : TAGGTATAATGGTTTAACAAATCATTCGGTATCGATGAGGCCACAAACCCAAGCAGAACGAAATG : 195
177 : TAGGTATAATGGTTTAACAAATCATTCGGTATCGATGAGGCCACAAACCCAAGCAGAACGAAATG : 195
VP7 : AAATGTTTTTTTATGTGTACTGATATGGTTTTAGCGGCGCTGAACGTCCAAATTGGGAATATTTCA : 260
200 : AAATGTTTTTTTATGTGTACTGATATGGTTTTAGCGGCGCTGAACGTCCAAATTGGGAATATTTCA : 260
177 : AAATGTTTTTTTATGTGTACTGATATGGTTTTAGCGGCGCTGAACGTCCAAATTGGGAATATTTCA : 260
VP7 : CCAGATTATGATCAAGCGTTGGCAACTGTGGGAGCTCTCGCAACGACTGAAATTCCATATAATGT : 325
200 : CCAGATTATGATCAAGCGTTGGCAACTGTGGGAGCTCTCGCAACGACTGAAATTCCATATAATGT : 325
177 : CCAGATTATGATCAAGCGTTGGCAACTGTGGGAGCTCTCGCAACGACTGAAATTCCATATAATGT : 325
VP7 : TCAGGCCATGAATGACATCGTTAGAATAACGGGTCAGATGCAAATTCGGACCAAGCAAAGTGCAA : 390
200 : TCAGGCCATGAATGACATCGTTAGAATAACGGGTCAGATGCAAATTCGGACCAAGCAAAGTGCAA : 390
177 : TCAGGCCATGAATGACATCGTTAGAATAACGGGTCAGATGCAAATTCGGACCAAGCAAAGTGCAA : 390
VP7 : ACGGGGCCTTATGCAGGAGCGGTTGAGGTGCAACAATCTGGCAGATATTACGTACCGCAAGGTCG : 455
200 : ACGGGGCCTTATGCAGGAGCGGTTGAGGTGCAACAATCTGGCAGATATTACGTACCGCAAGGTCG : 455
177 : ACGGGGCCTTATGCAGGAGCGGTTGAGGTGCAACAATCTGGCAGATATTACGTACCGCAAGGTCG : 455
VP7 : AACGCGTGGTGGGTACATCAATTCAAATATTGCAGAAGTGTGTATGGATGCAGGTGCTGCGGGAC : 520
200 : AACGCGTGGTGGGTACATCAATTCAAATATTGCAGAAGTGTGTATGGATGCAGGTGCTGCGGGAC : 520
177 : AACGCGTGGTGGGTACATCAATTCAAATATTGCAGAAGTGTGTATGGATGCAGGTGCTGCGGGAC : 520
VP7 : AGGTCAATGCGCTGCTAGCCCCAAGG----------AGGGGGGACGCAGTCATGATC : 567
200 : AGGTCAATGCGCTGCTAGCCCCAAGG----------AGGGGGGACGCAGTCATGATC : 567
177 : AGGTCAATGCGCTGCTAGCCCCAAGGGTCGACTCTAGAAAGCTTAGGGGGGGACGCAGTCATGATC : 585
VP7 : TATTTCGTTTGGAGACCGTTGCGTATATTTTGTGATCCTCAAGGTC----------C : 614
200 : TATTTCGTTTGGAGACCGTTGCGTATATTTTGTGATCCTCAAGGTGGTCGACTCTAGAAAGCTTC : 632
177 : TATTTCGTTTGGAGACCGTTGCGTATATTTTGTGATCCTCAAGGTG----------C : 632
VP7 : GTCACTTGAGAGCGCTCCAGGAACTTTTGTCACCGTTGATGGAGTAAATGTTGCAGCTGGAGATG : 679
200 : GTCACTTGAGAGCGCTCCAGGAACTTTTGTCACCGTTGATGGAGTAAATGTTGCAGCTGGAGATG : 697
177 : GTCACTTGAGAGCGCTCCAGGAACTTTTGTCACCGTTGATGGAGTAAATGTTGCAGCTGGAGATG : 697
VP7 : TCGTCGCATGGAATACTATTGCACCAGTGAATGTTGGAAATCCTGGGGCACGCAGATCAATTTTA : 744
200 : TCGTCGCATGGAATACTATTGCACCAGTGAATGTTGGAAATCCTGGGGCACGCAGATCAATTTTA : 762
177 : TCGTCGCATGGAATACTATTGCACCAGTGAATGTTGGAAATCCTGGGGCACGCAGATCAATTTTA : 762
VP7 : CAGTTTGAAGTGTTATGGTATACGTCCTTGGATAGATCGCTAGCACGGTTCCGGAATTGGCTCCA : 809
200 : CAGTTTGAAGTGTTATGGTATACGTCCTTGGATAGATCGCTAGCACGGTTCCGGAATTGGCTCCA : 827
177 : CAGTTTGAAGTGTTATGGTATACGTCCTTGGATAGATCGCTAGCACGGTTCCGGAATTGGCTCCA : 827
VP7 : ACGCTCACAAGATGTTATGCGTATGTCTCTCCCACTTGGCACGCATTACGCGCTGTCATTTTTCA : 874
200 : ACGCTCACAAGATGTTATGCGTATGTCTCTCCCACTTGGCACGCATTACGCGCTGTCATTTTTCA : 892
177 : ACGCTCACAAGATGTTATGCGTATGTCTCTCCCACTTGGCACGCATTACGCGCTGTCATTTTTCA : 892
VP7 : GCAGATGAATATGCAGCCTATTAATCCGCCGATTTTTCCACCGACTGAAAGGAATGAAATTGTTG : 939
200 : GCAGATGAATATGCAGCCTATTAATCCGCCGATTTTTCCACCGACTGAAAGGAATGAAATTGTTG : 957
177 : GCAGATGAATATGCAGCCTATTAATCCGCCGATTTTTCCACCGACTGAAAGGAATGAAATTGTTG : 957
VP7 : CGTATCTATTAGTAGCTTCTTTAGCTGATGTGTATGCGGCTTTGAGACCAGATTTCAGAATGAAT : 1004
200 : CGTATCTATTAGTAGCTTCTTTAGCTGATGTGTATGCGGCTTTGAGACCAGATTTCAGAATGAAT : 1022
177 : CGTATCTATTAGTAGCTTCTTTAGCTGATGTGTATGCGGCTTTGAGACCAGATTTCAGAATGAAT : 1022
VP7 : GGTGTTGTCGCGCCAGTAGGCCAGATTAACAGAGCTCTTGTGCTAGCAGCCTACCACTAGTGGCT : 1069
200 : GGTGTTGTCGCGCCAGTAGGCCAGATTAACAGAGCTCTTGTGCTAGCAGCCTACCACTAGTGGCT : 1087
177 : GGTGTTGTCGCGCCAGTAGGCCAGATTAACAGAGCTCTTGTGCTAGCAGCCTACCACTAGTGGCT : 1087
VP7 : GCGGTGTTGCACGGTCACCGCTTTCATTAGTGTCGCGTCGGTTCTTATGCTGATAAAGTACGCAT : 1134
200 : GCGGTGTTGCACGGTCACCGCTTTCATTAGTGTCGCGTCGGTTCTTATGCTGATAAAGTACGCAT : 1152
177 : GCGGTGTTGCACGGTCACCGCTTTCATTAGTGTCGCGTCGGTTCTTATGCTGATAAAGTACGCAT : 1152
VP7 : AAGTAATACGTCAATACCGAATACACTTAC : 1164
200 : AAGTAATACGTCAATACCGAATACACTTAC : 1182
177 : AAGTAATACGTCAATACCGAATACACTTAC : 1182

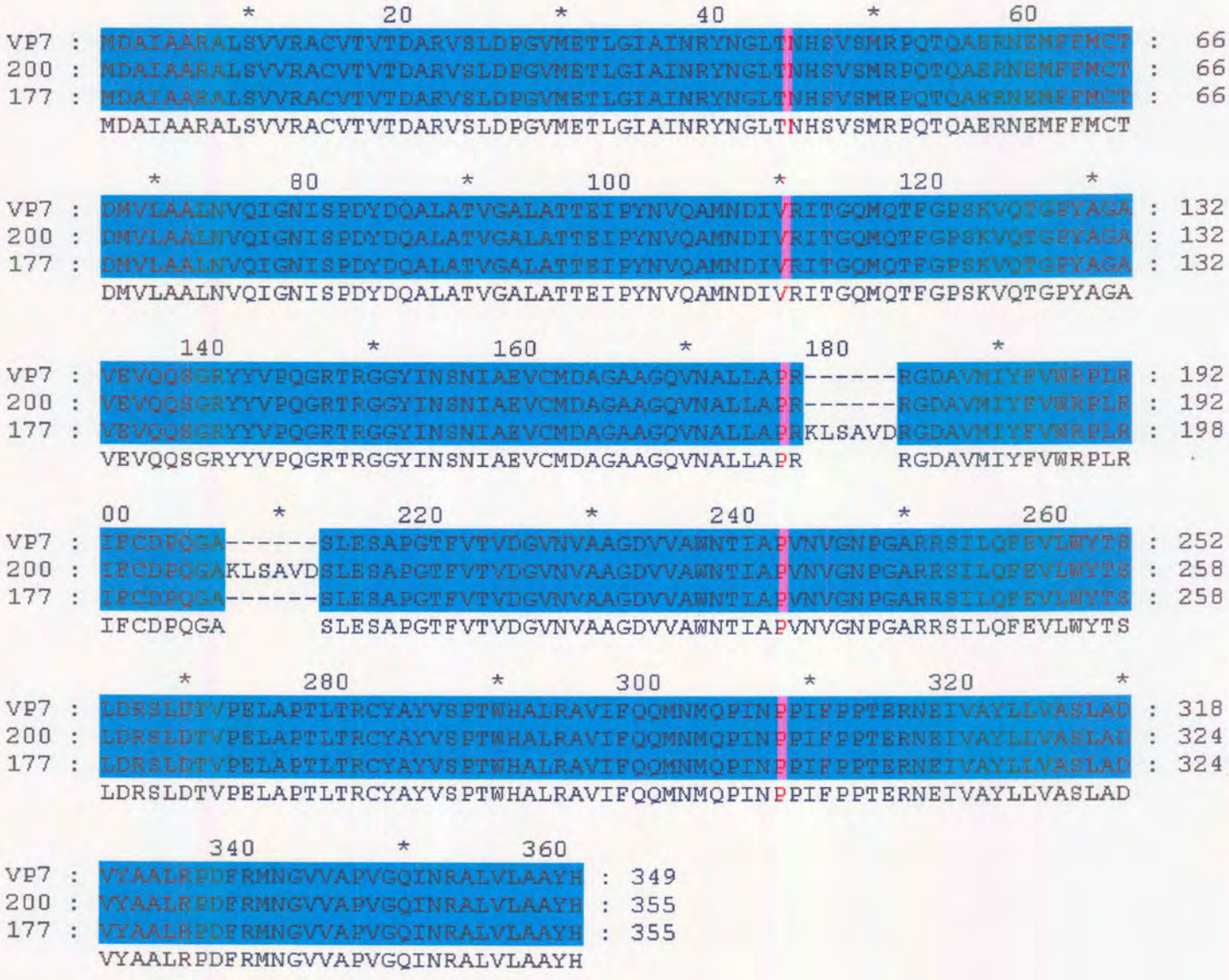

Figure 4.6: (Previous page) Alignment of the nucleotide sequences of the two insertion mutants mt177 and mt200 with the VP7 gene. No nucleotide alterations were found other than the 18 nucleotides inserted by means of PCR-directed site-directional insertional mutation.

Figure 4.7: Comparison of the deduced amino acid sequences of VP7 and insertion mutants 177 and 200. The extra six amino acids, as a result of the insertion of the three restriction enzyme sites, in the two chosen hydrophilic sites in the top domain of VP7 are visible. The rest of the amino acid sequences are identical.

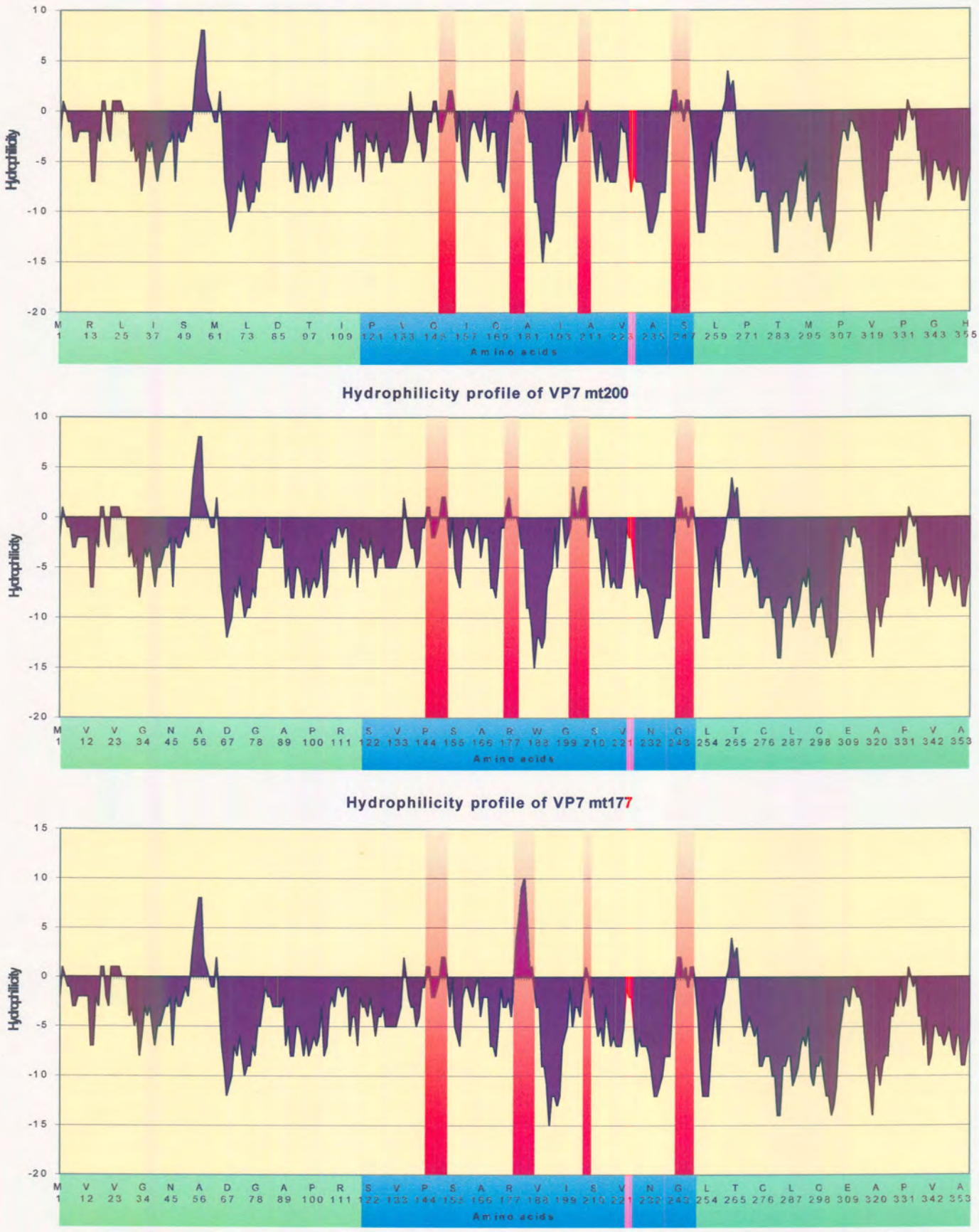

Figure 4.8: Comparison of the hydrophilicity profiles of AHSV-9 VP7 with that of the two insertion mutants mt177 and mt200. Hydrophilicity was predicted according to Hopp & Woods (1981) utilising the ATHEPROT computer program. Areas with positive values have a nett hydrophilicity while areas with negative values have a nett hydrophobicity.

VP7 resulted in a large increase in hydrophilicity of at least 5 times that of normal VP7 (from 2 to 10), in that area. The insertion of the same six amino acids between amino acid 200 and 201 resulted in a mild increase in hydrophilicity from 2 to 4.

A model of the three-dimensional structure of VP7mt177 and VP7mt200 was prepared using a homology-based method incorporating the satisfaction of spatial restraints. The MODELLER package generates a model of the new protein using a known three-dimensional structure together with a sequence alignment, in this case with AHSV-4 VP7 (*Figure 4.9*). The modelled structure of both VP7mt177 and VP7mt200 monomers shows a backbone conformation (green and red respectively) identical to VP7. The six extra amino acids in position 177-178 and 200-201 looped out of the VP7 backbone, facing the aqueous environment. This indicated that the extra amino acids would probably not influence the structure of the modified VP7 proteins, by preventing the hydrophobic associations necessary to form the VP7 3-D structure (represented in *Figure 4.9*).

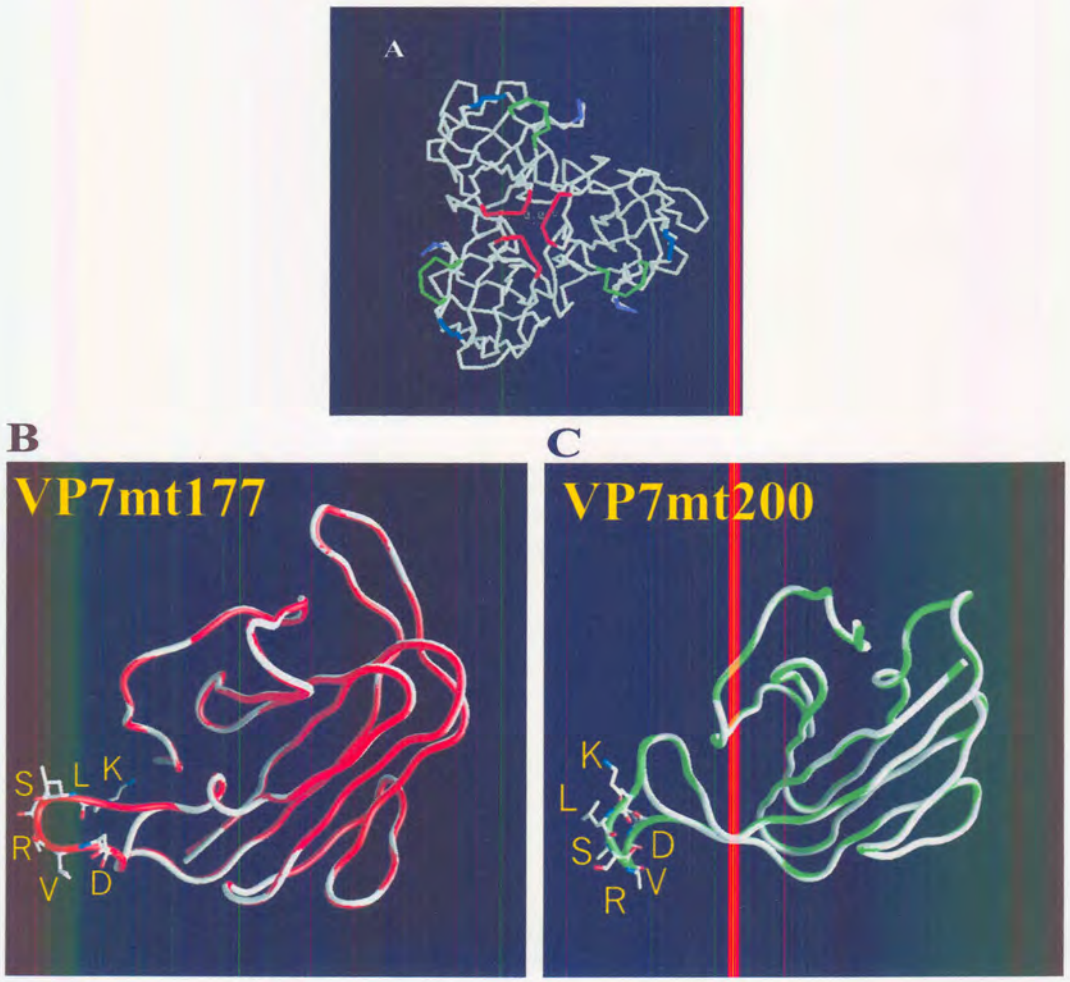

Figure 4.9: A schematic representation of the structure of the insertion mutants mt177 (B) and mt200 (C) monomers as predicted by the MODELLER package. The carbon-a traces of mt177(red) and mt200 (green) in comparison with VP7 (white) is shown. The side chains of the six inserted amino acids are indicated by fine lines and are shown to loop out of the surface of the two proteins. The assembly of the mutagenised VP7 monomers into trimers is shown in (A) with the 177 insertion indicated in green and the 200 insertion in red.

4.3.4. The construction of dual recombinant baculovirus transfer vectors containing AHSV-9 VP3 in combination with VP7mt177 and VP7mt200

The VP3-VP7 dual recombinant transfer vector constructed in chapter 3 (3.2.2.1), pFBd-S3.9-S7.9, was utilised for the cloning of the modified VP7 genes with VP3. The pFBd-S3.9-S7.9 vector was partially digested with *Bam*H1, to obtain restriction at the *Bam*H1 site located 100 bp from the 5' end of the VP7 gene, but not at the second *Bam*H1 site within the VP3 gene. After linearisation, the *Bam*H1 was removed by column purification and the plasmid was completely digested with *Pst*I, which cuts once in the vector downstream of the VP7 gene. The 8.1 kb fragment, containing the vector, the complete VP3 gene and 100 bp from the VP7 gene, was recovered through gel purification. The plasmids, pFB-mt177 and pFB-mt200 were completely digested with *Bam*H1 (cuts at ca.100 bp from 5' end) and *Pst*I (cuts in MCS) and the 1.0 kb and 1.9 kb fragments, respectively, recovered after gel purification. The recombinant VP7 *Bam*H1-*Pst*I fragments were directionally cloned into the corresponding sites of pFBd-S3.9-S7.9. Plasmids yielding 850 bp and 8.3 kb fragments after *Sac*I digestion contained the full-length VP7 insertion mutant genes (*Figure 4.10*). Recombinant plasmids were selected and called pFBd-S3.9-177 and pFBd-S3.9-200.

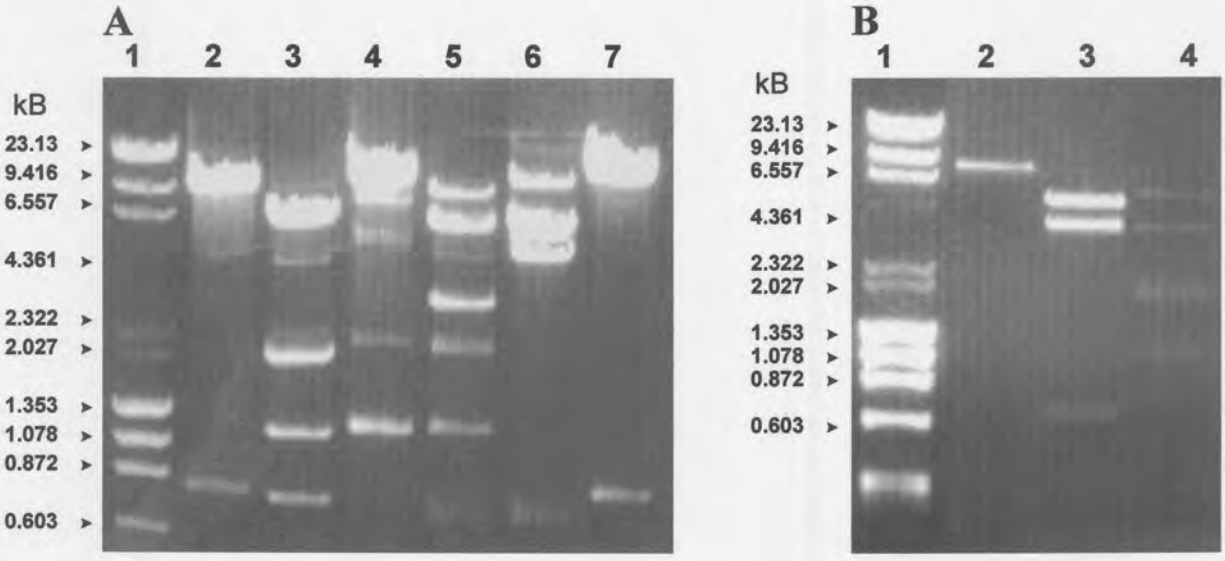

Figure 4.10: Agarose electrophoretic analysis of pFBd-S3.9-mt177 and pFBd-S3.9-mt200. (A) pFBd-S3.9-mt177, containing the AHSV-9 VP3 gene under control of the p10 promoter and VP7mt177 under control of the polyhedrin promoter, was digested with *Sac*I (lane 2), *Hind*III/*Eco*R1 (lane 3), *Eco*R1/*Sal*I (lane 4), *Eco*R1/*Xba*I (lane 5) and *Bam*H1 (lane 7). (B) pFBd-S3.9-mt200 was restricted with *Sac*I (lane 2), *Xba*I (lane 3) and *Hind*III/*Eco*R1 (lane 4).

4.3.5. Baculovirus expression of the VP7 insertion mutants

4.3.5.1. Construction and selection of recombinant baculoviruses

Infectious recombinant baculoviral DNA, containing either the mt177 or the mt200 insertion mutations under control of the polyhedrin promoter, was constructed. The recombinant transfer plasmids, pFBmt177 and pFBmt200, were transposed into the bacmid genome and each transposition was verified by means of PCR. The bacmid DNA was amplified using VP7 specific 5'-terminal primer and M13 reverse primer. The presence of amplified product of the correct size of 1.6 kb for the VP7 insertion mutants (mt177 and mt200) was determined by agarose gel electrophoresis (results not shown). The best efficiency of transfection was obtained when cellfectin was used. High titre recombinant virus stocks (10^8 - 10^9 pfu/ml) were prepared from plaque purified recombinant baculoviruses. Dual recombinant baculoviruses were generated in the same manner from the transfer plasmids pFBd-S3.9-177 and pFBd-S3.9-200.

4.3.5.2. Expression of the modified VP7 proteins in Sf9 cells

Monolayers of Sf9 cells were infected with Bac-mt177, Bac-mt200 and Bac-AH9VP7, which expresses the full-length VP7 gene (constructed by S. Maree). Proteins from infected cell lysates were resolved by SDS-PAGE (*Figure 4.11*). A unique protein band corresponding approximately to the expected size of 39 kDa was synthesised for each of the mutagenised VP7 proteins. The two insertion mutants of VP7 migrated slower through the gel compared to that of wild-type AHSV VP7. The sizes of these two proteins correspond to that of VP7 plus the six extra amino acids (± 1 kDa; total M_r = 39 kDa) and the size difference is visible on a 12% SDS-PAGE gel, which has a resolution of approximately 1 kDa. The insertion mutants of VP7 were synthesised approximately at the same level as wild-type VP7, which indicated that the insertion of extra amino acids did not significantly affect the expression levels (*Figure 4.11*). Maximum expression of VP7 and mt200 was obtained 4 days post-infection, while mt177 gave the highest levels at 3 days p.i. The levels of expression of AHSV-9 VP7, mt200 and mt177 were estimated to be approximately 1-2 mg/2 x 10^7 infected Sf9 cells. Further analysis of the putative VP7, mt177 and mt200 proteins was deemed unnecessary on the basis of the high level expression and visibility on Coomassie blue stained gels.

4.3.6. Solubility and sedimentation analysis of the VP7 insertion mutants

The baculovirus expressed VP7 spontaneously assembles into trimers, which interact to form hexagonal crystals, and as a result is highly insoluble. To determine whether the incorporation of six amino acids, in the top domain of VP7 will have an effect on the solubility of VP7 trimers, the different recombinant VP7 proteins were analysed using simple centrifugation, as well as sedimentation analysis. Cytoplasmic extracts containing the recombinant VP7 proteins were

prepared and separated into soluble and particulate fractions by means of low speed centrifugation (section 4.2.8) followed by SDS-PAGE analysis (*Figure 4.12*). Similar to wild-type VP7, the insertion mutant mt200 protein was predominantly found in a particulate form (>90%), although the amount of soluble mt200 is consistently more than VP7. In contrast to VP7 and mt200, insertion mutant mt177 was separated into approximately equal amounts of a particulate fraction and a soluble fraction. This result indicated that the insertion of six amino acids into the top domain of AHSV VP7 does increase the solubility of VP7 trimers. This is especially true when the incorporation occur in the RGD loop of AHSV VP7, which had a strong positive effect on the solubility of the protein, since approximately 50% of the protein was recovered from the soluble fraction followed low speed centrifugation.

To determine if the ratio of soluble VP7 trimers to particulate VP7 remains the same during the different stages of protein expression, the ratio was determined over a period of time starting at the earliest time of expression where the levels of expression are still low. Synchronised infected Sf9 cells were pulse labelled with ^{35}S-methionine from 18 h post-infection at 6 hourly intervals up to 40 h p.i. For each time interval the solubility of the proteins was analysed as described before. It was evident from this experiment (results not shown) that as soon as the VP7 and mt200 proteins are synthesised, they aggregate into large structures, which subsequently are recovered predominantly in the particulate form. The soluble form of mt200 was always more than that of VP7. For mt177, more protein was recovered from the soluble fraction early on in the infection. As the infection progressed and the expression levels of mt177 increased, more protein was visible in the particulate form. These results indicate that although mt177 is more soluble than either VP7 or mt200, it still aggregates into large particulate structures when synthesised at high levels.

The cytoplasmic extracts from cells infected with the modified VP7 recombinant baculoviruses were also fractionated on sucrose gradients and compared after SDS-PAGE analysis (*Figure 4.13*). Like wild-type VP7 the insertion mutant mt200, sedimented as a large homogeneous complex near the bottom of the gradient. The sedimentation value of VP7 and mt200 was estimated to be >900 S and almost all the protein was recovered from the bottom fractions of the gradient (fractions 1-5; *Figure 4.14*). This indicates that the VP7 and mt200 proteins are present as large structures in the infected cells. The mt177 protein on the other hand was present as a complex mostly found at the top of the gradient (fractions 9-11) with an S value of 75 (*Figure 4.13*). Only a small amount of mt177 protein (approximately 30%; *Figure 4.14*) was present in the bottom of the gradient (fractions 1-4) at the same position as VP7.

From these results there was no indication that the trimeric structures formed by VP7 were disrupted by the introduction of six amino acids. It appears that the VP7 protein still folds in the

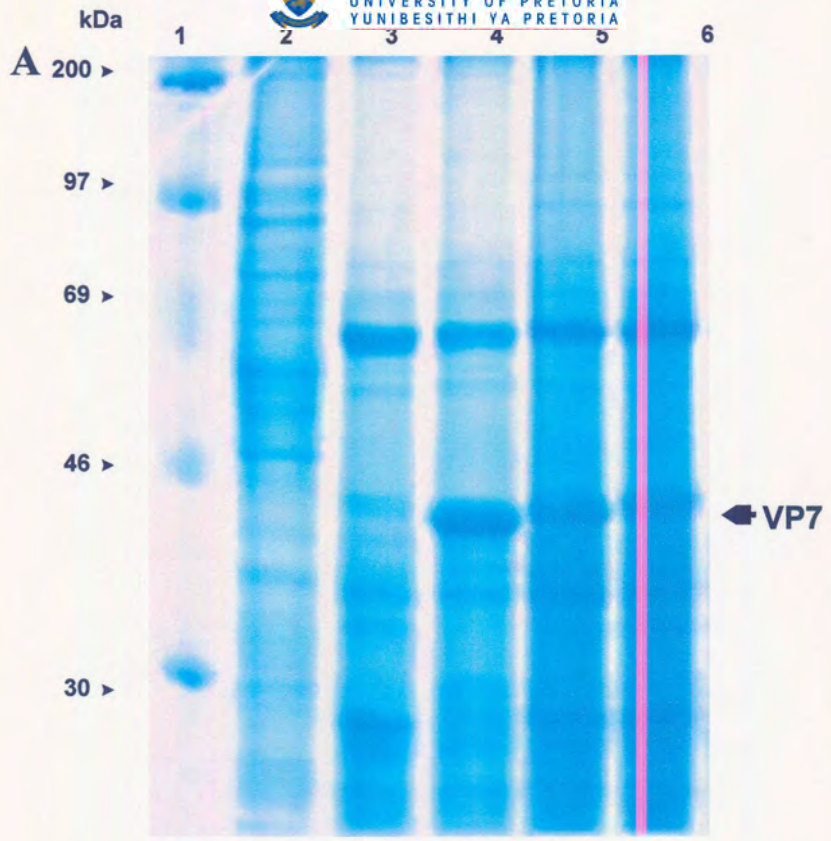

Figure 4.11: SDS-PAGE analysis of the recombinant VP7 protein expression in insect cells. Lane 1 contains rainbow molecular weight marker. Lanes 2 and 3 contain extracts of cells mock-infected or infected with wild-type baculovirus. Lane 4 contains extracts of cells infected with VP7 recombinant baculovirus. Lanes 5 and 6 contain cell lysates of cells infected with recombinant baculoviruses Bac-mt177 and Bac-mt200, respectively.

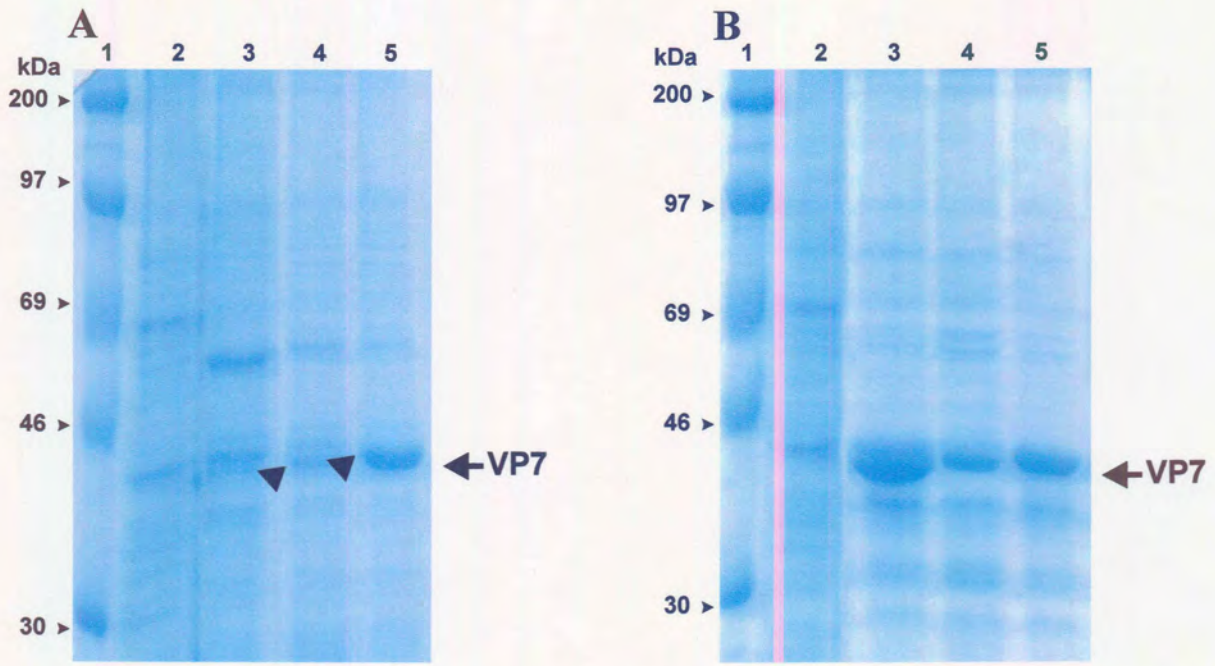

Figure 4.12: Differential centrifugation of the cytoplasmic extracts from Bac-AH9VP7, Bac-mt200 and Bac-mt177 infected cells. The cytoplasmic extracts were separated into a soluble (A) and particulate (B) fractions using low speed centrifugation at 5000 rpm for 30 min. For A and B: lane 2 represent cell lysate from wild-type infected Sf9 cells, lane 3 VP7 soluble/particulate fractions, lane 4 insertion mutant 200 soluble/particulate fraction and lane 5 insertion mutant 177 soluble/particulate fraction. Sizes of protein markers (lane 1) are indicated in kDa at the left of the figure.

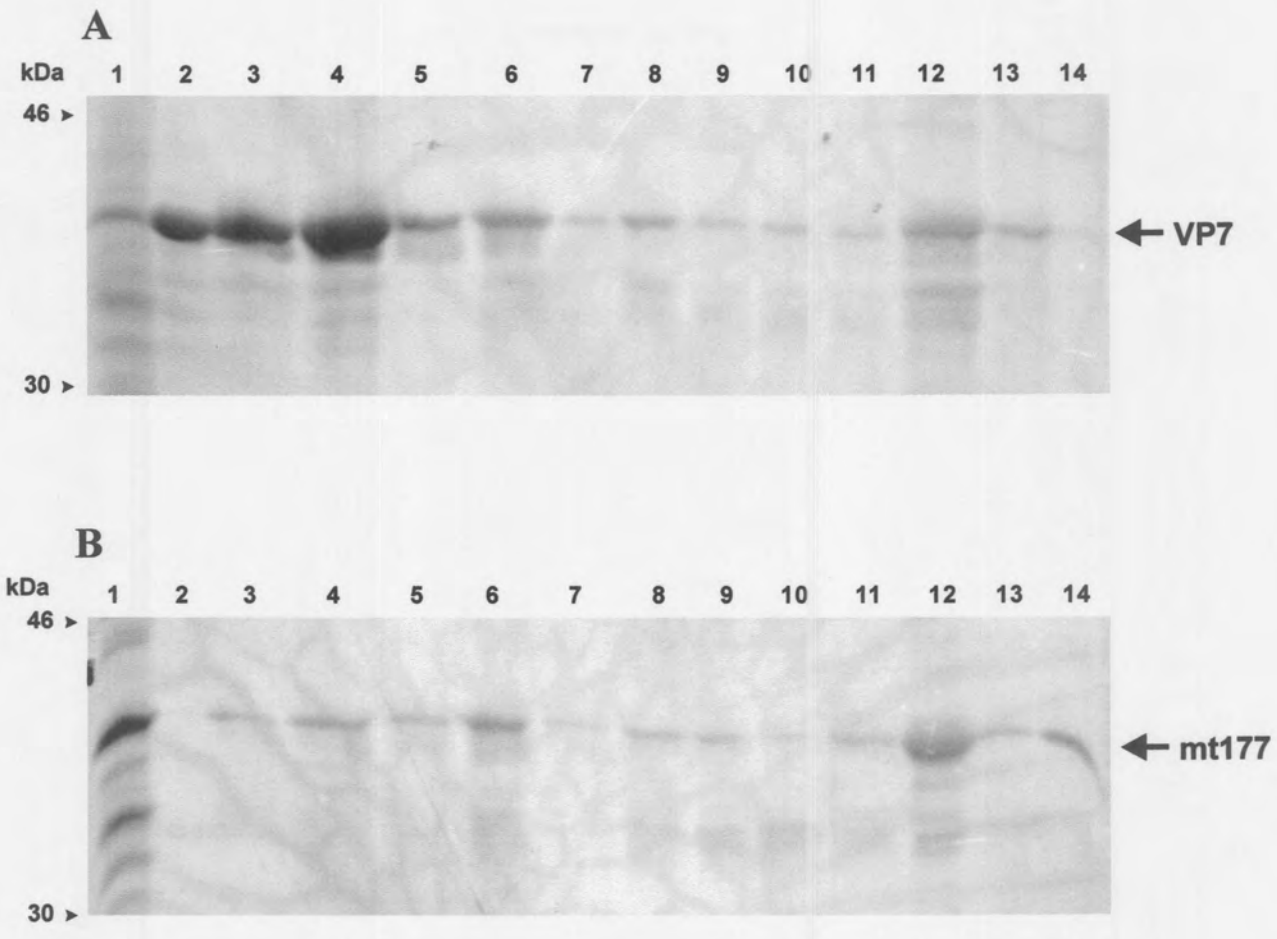

Figure 4.13: Sedimentation analysis of the cytoplasmic extracts from Bac-AH9VP7 (A) and Bac-mt177 (B) infected cells by sucrose density centrifugation. The cells were radioactively labelled 48 h p.i. Prior to sucrose gradient centrifugation the cytoplasmic extracts were separated in a soluble and particulate fractions by differential centrifugation. The particulate fractions were collected and used for the sedimentation analysis. A sample (1/100) of the soluble fractions were loaded in lane 1. Fractions were collected from the bottom (lane 2) to the top (lane 14) of each gradient and a 1/10 of each fraction analysed by autoradiography after resolution by SDS-PAGE.

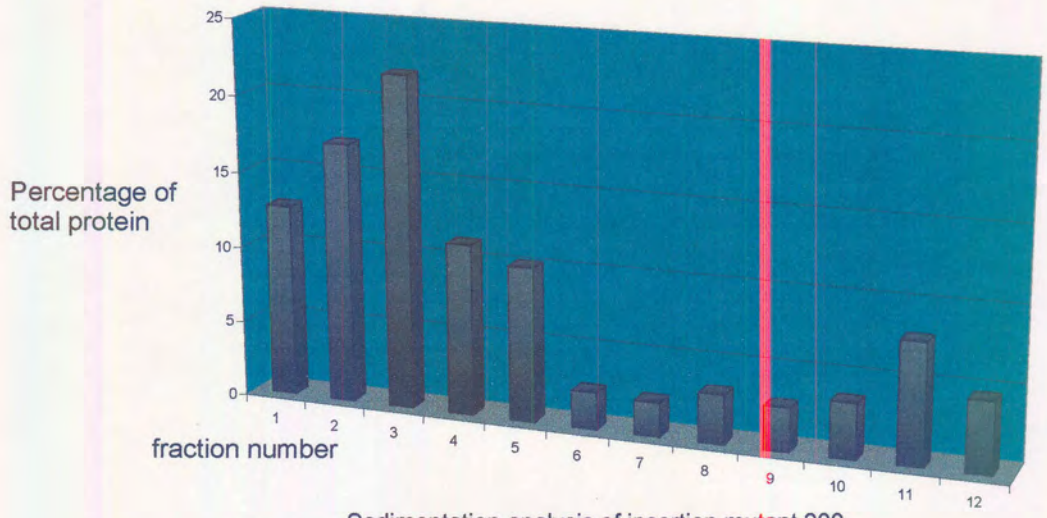

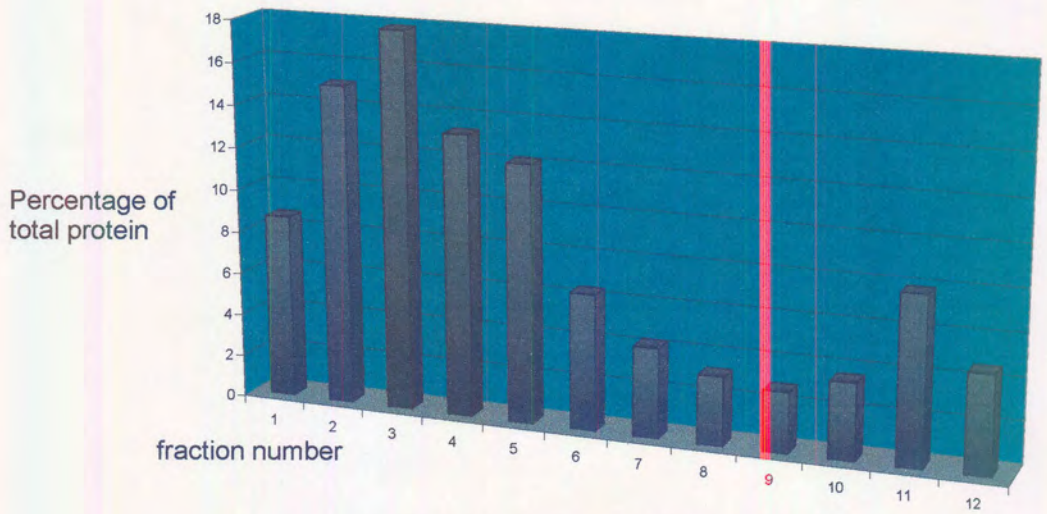

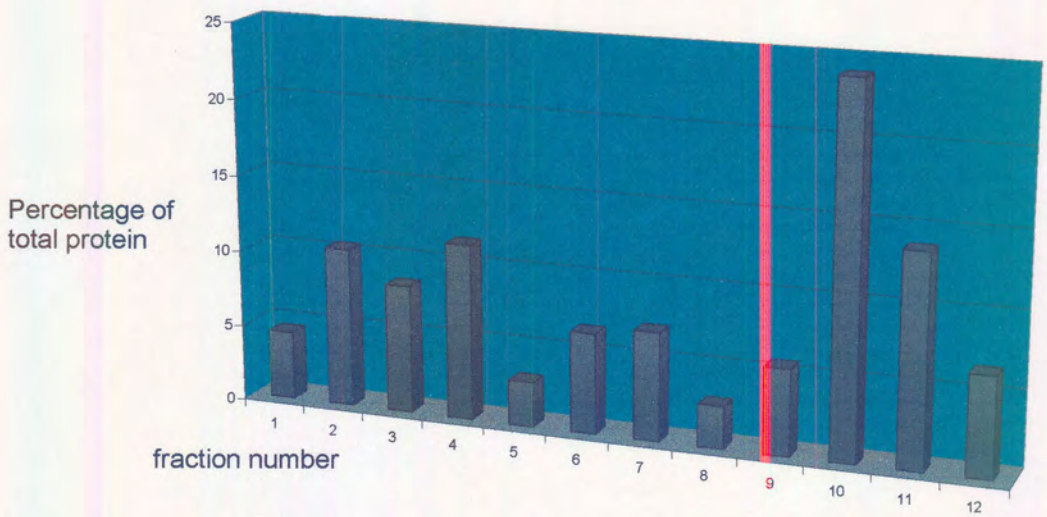

Figure 4.14: Sedimentation analysis of the cytoplasmic extracts from Bac-AH9VP7 and Bac-mt177 infected cells by sucrose density centrifugation. The cells were radioactively labelled 48 h p.i. Prior to sucrose gradient centrifugation the cytoplasmic extracts were separated in a soluble and particulate fractions by differential centrifugation. The particulate fractions were collected and used for the sedimentation analysis. A sample (1/100) of the soluble fractions were loaded in lane 1. Fractions were collected from the bottom (lane 2) to the top (lane 14) of each gradient and a 1/10 of each fraction analysed by autoradiography after resolution by SDS-PAGE. The fraction of the total amount of protein in each fraction is indicated as a percentage (y axis).

correct 3-D orientation and also forms its trimeric structure. Although the VP7 particulate structures are relatively stable under a wide variety of ionic strength and pH conditions, it was found that the crystal structure was partially disrupted with the use of high concentration of Nonidet-P40 (>0.5%) during cell lysis. This caused the VP7 structures to be present as a more heterogeneous complex on the sucrose gradient. On the other hand too little Nonidet-P40 (<0.1%) resulted in inefficient cell lysis. The optimum concentration of the non-ionic detergent was found to be approximately 0.25%, which resulted in minimum disturbance of the crystal structures.

4.3.7. Purification and electron microscopy analysis of modified VP7 complexes

The identity of the modified VP7 proteins was confirmed by their ability to form crystals or CLPs (next section). Crystal formation was analysed by means of light microscopy and scanning electron microscopy. Approximately 2 days following infection, the cellular cytopathic effects of a baculovirus infection became apparent. In addition, cells infected with Bac-mt200 exhibited distinct disc-shaped crystals as in cells infected with the recombinant baculovirus containing the unmodified VP7 gene. Cells infected with Bac-mt177 lacked any such crystals, although structures that appear more round were visible after 3 to 4 days p.i. (results not shown). Insect cells infected with other types of recombinant or wild type baculoviruses lacked any such structures. These structures exhibited variation in both size and number per cell, usually containing between one and three crystals. The ability of AHSV VP7 insertion mutants to form morphological structures was utilised to subsequently purify the proteins by one step linear sucrose gradient centrifugation. Sucrose gradient peak fractions, containing the protein of interest, were pooled and the protein recovered by high-speed centrifugation. The gradient purified VP7 proteins were then examined with SEM.

The results obtained in the sucrose gradient assay indicated that the baculovirus expressed modified VP7 proteins differ in their ability to form crystals. Hexagonal crystals, similar to that formed by wild-type AHSV VP7, were observed in the case of the insertion mutant mt200. A typical preparation of mt200 crystals examined at low magnification in a SEM revealed large numbers of intact and fragmented flat, hexagonal structures with a maximum diameter of 6 μm (*Figure 4.15*). When examined at higher magnification by TEM, it was found that these structures were composed of a highly ordered two-dimensional crystalline lattice. SEM analysis of purified mt177 protein from the bottom fractions of the gradient revealed the presence of a large number of rounded particulate structures. No recognisable hexagonal crystals were observed. These structures were essentially homogeneous with a diameter of up to 5 μm (*Figure 4.16*). Since the mt177 protein in the bottom fractions was more than 95% purified as determined by SDS-PAGE (*Figure 4.13*) it is assumed that these ball-like structures are composed of the mt177 protein. There was no indication of any recognisable structure in the top fractions of the mt177 gradient. The mt177 protein in these

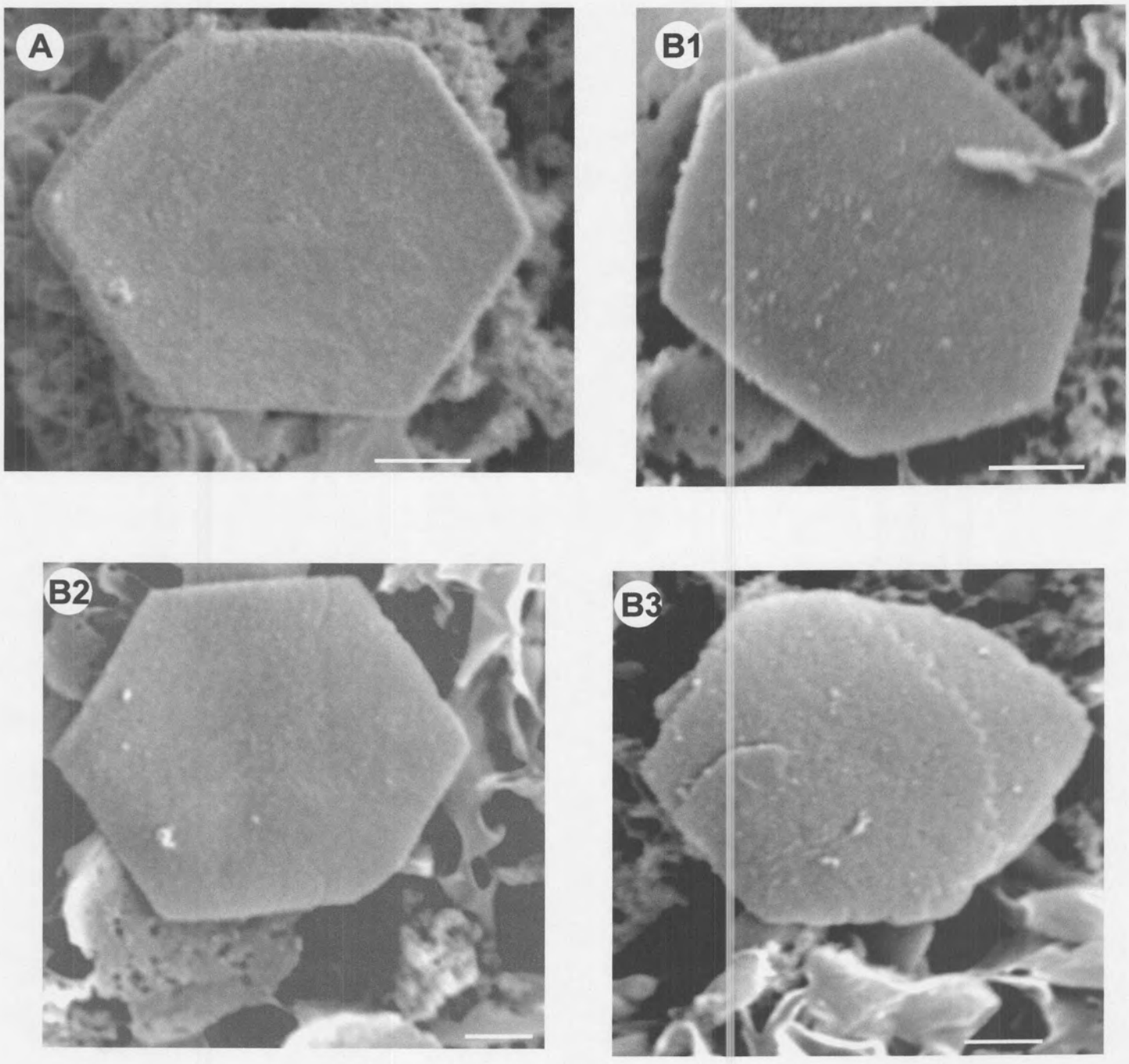

Figure 4.15: Scanning electron micrographs of sucrose gradient purified VP7 (A) and mt200 (B1-3) crystals, spatter coated with gold-beladium. Mt200, like VP7, aggregate into crystals with an intact haxagonal profile, with the same lattice detail as described by Buroughs *et al.* (1994). The bar markers represent 1 um.

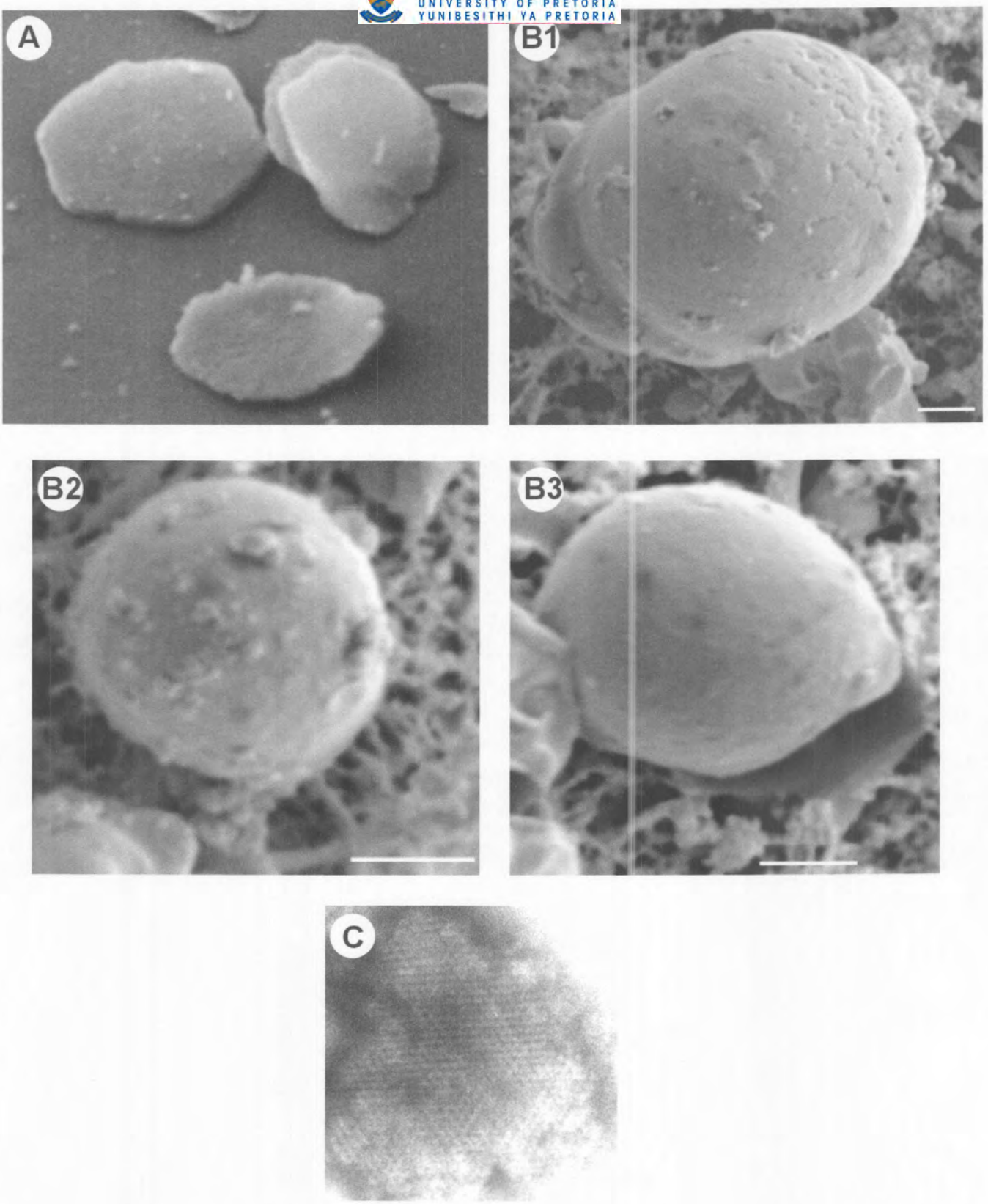

Figure 4.16: Scanning electron micrographs of purified VP7 crystals (A) and mt177 ball-like structures (B1-3). Mt177 did not show the same intact hexagonal outline as VP7. The bar markers represent 1 um.

fractions may represent soluble trimeric form of the insertion mutant mt177 protein. When examined with TEM the mt177 proteins also assemble into the highly ordered two-dimensional crystalline lattice seen with VP7 and mt200 (*Figure 4.16*).

4.3.8. CLP formation using VP7 insertion mutants

The integrity of the three-dimensional structure of the VP7 insertional mutants and chimeras was analysed according to their ability to form CLPs when co-expressed with VP3. Recombinant baculoviruses containing the VP3 gene and either the mt177 or mt200 gene, was constructed (Bac-VP3.9-mt177 and Bac-VP3.9-mt200). To verify expression, proteins from insect cells infected with Bac-VP3.9-mt177 and Bac-VP3.9-mt200 were analysed by SDS-PAGE. For comparison, cells were either mock infected or infected with the wild type virus or Bac-S3.9-S7.9. By comparison with mock infected or wild type baculovirus infected cell lysates, each of the dual recombinant baculovirus clones synthesised two unique protein bands which corresponded with VP3 and VP7 in Bac-S3.9-S7.9 infected cells (*Figure 4.17*). One band was approximately 90 kDa, the estimated size of AHSV-9 VP3, while the other displayed a somewhat slower mobility than VP7, at approximately 39 kDa. This was expected, since the two insertion mutants contained six extra amino acids with an estimated molecular mass of ±1 kDa as explained in section 4.3.5.2.

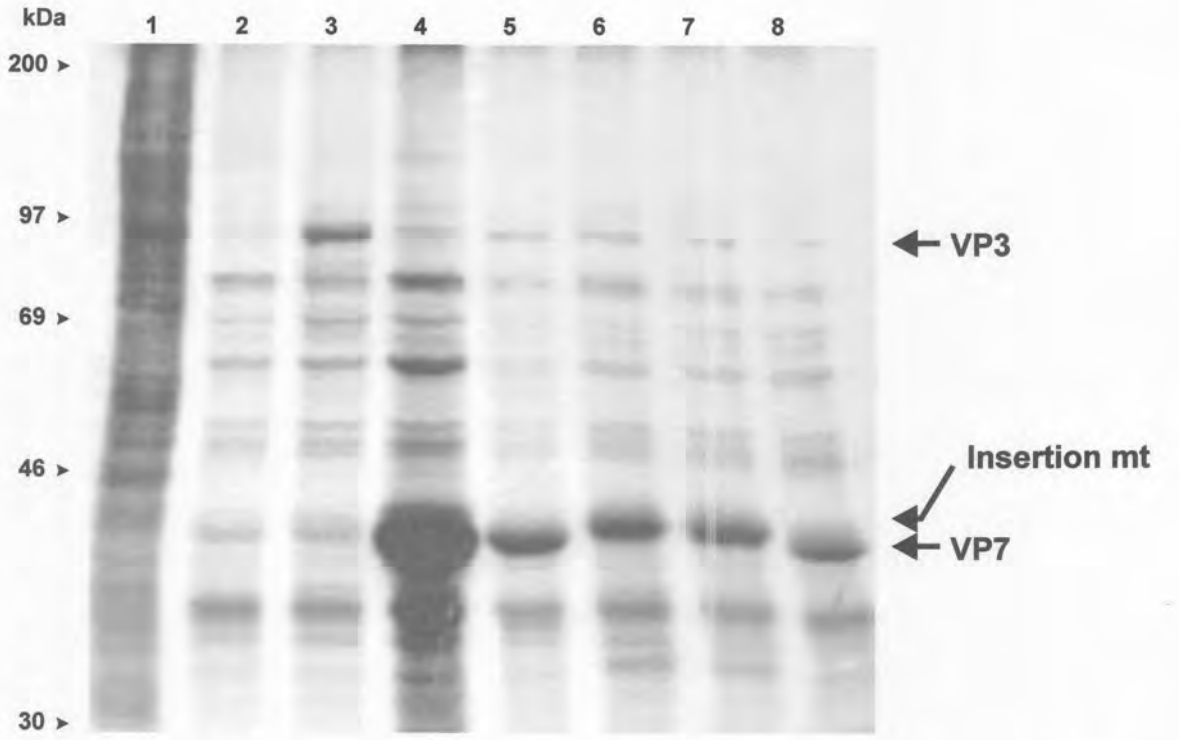

Figure 4.17: Autoradiograph of ^{35}S-methionine labelled proteins resolved by SDS-PAGE to evaluate co-expression of AHSV-9 VP3 and the VP7 insertion mutants in insect cells by dual recombinant baculoviruses. Sf9 cells were mock-infected (lane 1), infected with wild-type baculovirus (lane 2), Bac-VP3 (lane 3), Bac-VP7 (lane 4), DBac-S3.9-S7.9 (lane 5 and 8), Bac-S3.9-mt177 (lane 6) and Bac-S3.9-mt200 (lane 7). The positions of VP3, VP7 and mutagenised VP7 are indicated by arrows.

To investigate whether the two VP7 insertion mutants are capable of forming CLPs in the presence of AHSV-9 VP3, insect cells were infected with the dual recombinant baculoviruses and lysates of infected cells fractionated on sucrose or CsCl gradients. When the protein components of the gradient fractions were analysed by SDS-PAGE, both the VP3 and the insertion mutants of VP7 were identified. It was found that the insertion mutants of VP7 formed a complex with VP3, which sedimented with the same sedimentation rate as particles formed by unmodified VP7 and VP3. Particles were also recovered from CsCl gradient, indicating that the particles are as stable as CLPs derived from unmodified VP7 under high-salt conditions. The protein complexes were recovered from the gradients by high-speed centrifugation and analysed by electron microscopy after negative staining with uranyl acetate.

The yield of protein complexes recovered from the VP3 and VP7mt177 gradient was much higher than that generated by expression of VP3 with either an unmodified VP7 or with VP7mt200. Since both VP3 and VP7mt177 were present in the particulate fractions, it was the first indication that these proteins could assemble to form CLPs. The results suggest that the modification in the amino acid position 177 to 178 may have an influence in the solubility of the VP7 protein, but not on the 3-D structure or trimerisation of VP7. The increase in solubility may result in an increase in the number of VP7 trimers that are available for attachment to subcores, composed of VP3. As a result, conditions for the formation of CLPs were more favourable than with unmodified VP7, which by preference aggregate into crystals.

Electron micrographs of purified CLPs derived from co-expression of AHSV-9 VP3 and either of the two VP7 insertion mutants, revealed morphological structures similar to authentic AHSV cores and CLPs assembled from wild-type AHSV VP3 and VP7 proteins (*Figure 4.18*). Like unmodified CLPs, the 177CLPs and 200CLPs were empty, with the typical icosahedral symmetry. The knobby morphological protrusions, representing VP7 trimers, extended outwards. High salt, pH fluctuation between 6.0 and 8.5 and storage at 4°C of the CLPs composed of VP7mt177 or VP7mt200 and VP3 had no influence on the surface knob-like structures. This indicated that the modifications to VP7 did not influence the stability of CLPs. In addition, treatment of the VP7 insertion mutant CLPs with a low salt buffer led to the loss of the surface capsid structures and derivation of subcore-like particle similar to those found by Burroughs *et al.* (1994) and Oellerman (1969). The identity of the CLPs was verified by antibody decorating of the particles using monoclonal VP7 antibodies (Van Wyngaard *et al.*, 1992). Each particle was masked by a dark shadow resulting from the specific interaction of monoclonal VP7 antibodies with the VP7 outer shell, which confirmed the VP7 nature of the trimers.

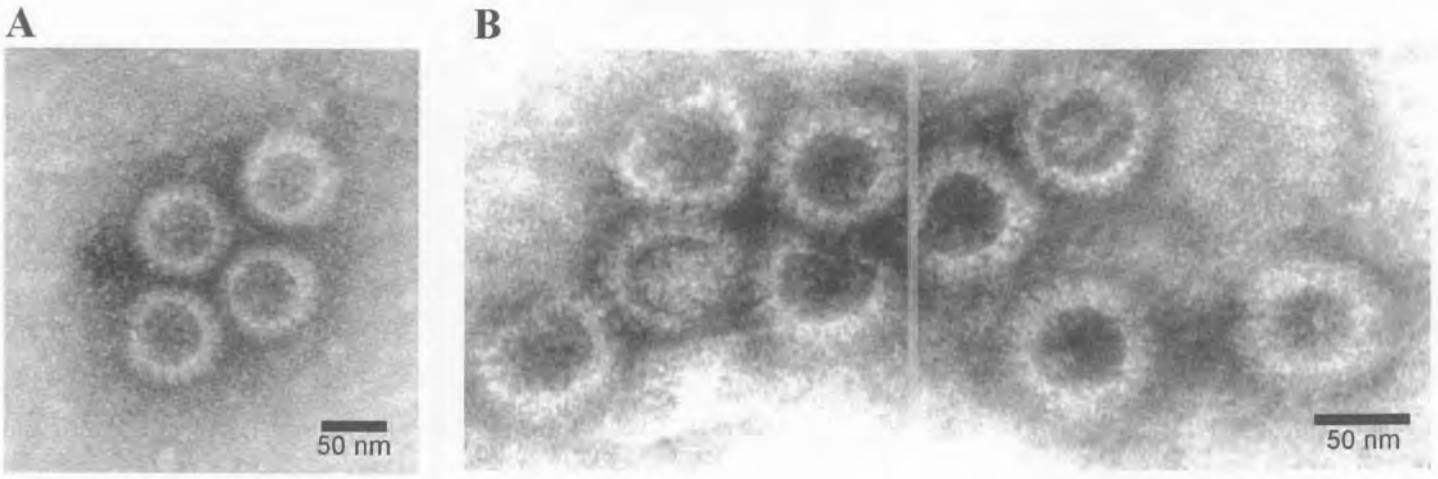

Figure 4.18: Electron microscopy of purified CLPs obtained from the co-expression of the two VP7 insertion mutants mt200 (A) and mt177 (B) with AHSV-9 VP3 in insect cells. The sucrose gradient purified particles were stained with 2% uranyl acetate.

4.3.9. Construction of recombinant baculovirus transfer vectors containing VP7/TrVP2 chimeric genes

In order to determine what the effect insertion of a foreign polypeptide will have on the solubility, and trimerisation of the VP7 protein, two VP7 chimeric genes were constructed which contained a fragment overlapping a previously identified immunogenic region of AHSV-9 VP2 (amino acid 385 - 415). A region of the VP2 gene from *HindIII* (position 957) to *EcoR1* (position 1260), was directionally cloned into the unique introduced restriction sites of mt177 and mt200. The unique restriction sites inserted into VP7 allows the insertion of the AHSV-9 VP2-specific DNA fragment by directional cloning in the correct reading frame of the VP7 sequence. Seeing as the cloning strategy, followed by Samantha Hopkins in producing the two chimeric VP7/TrVP2 proteins, has not been documented elsewhere, it is included in this section for reference purposes. The strategy for the construction of the chimeras is summarised in *Figure 4.19 A*.

A large AHSV-9 VP2 fragment which contained the nucleotide sequence that corresponds to amino acid region 313 to 415 (957 –1260 bp) of VP2 was recovered by *HindIII* digestion from pAHSV9.2 (3.2.2.2). The *Hind*III cuts asymmetrically in the VP2 gene ca. 957 bp from the 5' end and once in the vector downstream of the VP2 gene and excised a 2300 bp fragment that was cloned into the

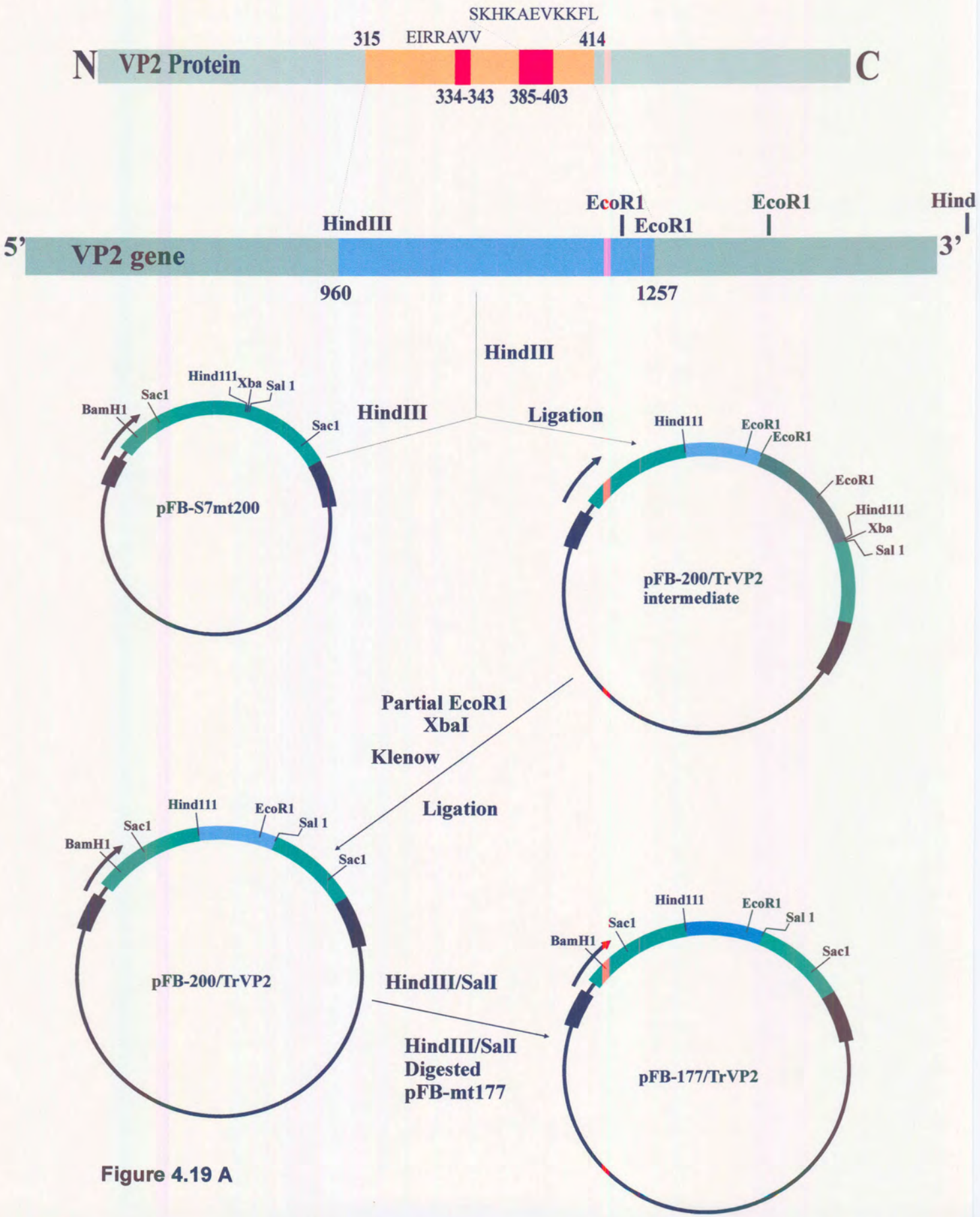
SKHKAEVKKFL
315
EIRRAVV
414
N
VP2 Protein
C
334-343
385-403
HindIII
EcoR1
EcoR1
EcoR1
Hind
5'
VP2 gene
3'
960
1257
HindIII
HindIII
Ligation
Hind111
Xba
Sal 1
Sac1
BamH1
pFB-S7mt200
Hind111
EcoR1
EcoR1
EcoR1
Hind111
Xba
Sal 1
pFB-200/TrVP2
intermediate
Partial EcoR1
XbaI
Klenow
Ligation
Hind111
EcoR1
Sal 1
Sac1
BamH1
Sac1
pFB-200/TrVP2
HindIII/SalI
HindIII/SalI
Digested
pFB-mt177
Hind111
EcoR1
Sal 1
Sac1
BamH1
Sac1
pFB-177/TrVP2

Figure 4.19 A

HindIII site of modified VP7 protein mt200. Recombinants in the correct orientation were selected with simultaneous *EcoR1* and *Sal1* digestions and yielded fragments of ca. 6.1 kb, 1.2 kb and 700 bp. The mt200/VP2-intermediate was partially restricted with *EcoR1*, which cut thrice in the VP2-specific fragment (at positions ca. 1180, 1260 and 2500) and completely digested with *Xba*I, in order to remove the 3' 2.0 kb region of the VP2 gene. A fragment of 6.6 kb was gel purified, the non-complementary overhangs were filled up by Klenow to restore the reading frame and self-ligated. Recombinant plasmids, which were linearised with *Eco*R1, which cuts once in the VP2-specific insert (ca. 1180 of VP2; the other VP2-specific *Eco*R1 sites and the one in the vector was removed; see *Figure 4.19 A* and section 4.3.2), were selected for further restriction enzyme analysis. Clones that contained the VP2 DNA sequence of interest were selected following simultaneous digestion with *Hind*III and *Sal*1 (*Figure 4.19 B*). A final construct containing the 303 bp *Hind*III-*Eco*R1 (957-1260) fragment of AHSV-9 VP2 was selected and named pFB-200/TrVP2. The reading frame was verified by automated sequencing using VP7 specific primers.

The VP2-specific domain was recovered from mt200/VP2 chimera (pFB-200/TrVP2) by *HindIII* and *Sal1* digestion and cloned directionally into the corresponding sites of the modified VP7 protein mt177, in order to construct the mt177/VP2 chimera. This cloning strategy positioned the VP2-specific insert in the correct reading frame of VP7mt177. Restriction of recombinant plasmids with

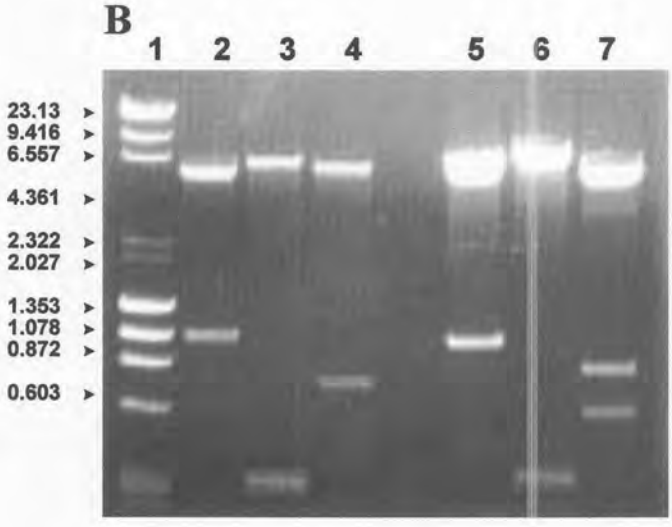

Figure 4.19: (A) A schematic diagram of the cloning strategy for the construction of two VP7/TrVP2 chimeric genes for expression in the Bac-to-Bac baculovirus system. (B) Agarose gel electrophoretic analysis of the two recombinant chimeric VP7 gene cloned into pFastbac transfer vector. The 177/TrVP2 chimera was digested with *Sac*I (lane 2), *Hind*III/*Sal*I (lane 3) and *Bam*H1/*Sal*I (lane 4) to identify the VP2 specific insert. The 200/TrVP2 chimera was restricted with the same enzymes in lanes 5 - 7 respectively. The sizes of the DNA molecular weight markers are indicated to the left of the figure.

*Sac*I indicated the presence of an insert of the expected size (303 bp) between the VP7-specific *Sac*I sites (ca. 200 and 1050). The correct translational orientation was verified by restriction enzyme mapping with *Bam*H1 and *Eco*R1, which recognises one site in the VP7-specific sequence, 100 bp from the 5' end and one site in the VP2-specific fragment, 750 bp from the 5' end of the chimeric gene, respectively. Recombinant chimeras that yielded fragments of sizes (ca. 650 bp) were selected and designated pFB-mt177/TrVP2 and the correct reading frame was confirmed by nucleotide sequencing.

Analysis of the resulting sequences of the two chimeric genes revealed that in each instance there is no divergence between the wild type and chimeric sequence of VP7 or between the inserted VP2 fragment and the original AHSV-9 VP2 sequence. The hydropathy plots of the deduced amino acid sequences of the two chimeras showing profiles similar to VP7 except for the region of the VP2 insertion. The profile in this region (indicated in blue), compare to the corresponding region in the VP2 protein. The hydropathic profiles of the two chimeras showed a profile of a combination between VP7 and VP2. The profiles of the 5' 177 or 200 amino acids and the 3' 171 or 148 amino acids of the 177/TrVP2 and 200/TrVP2 chimeras are identical to that of VP7. The inserted 101 VP2 specific amino acids showed the same profile as the corresponding region in the VP2 protein, which is characterised by four large hydrophilic peaks separated by two large and one small hydrophobic regions (*Figure 4.20*).

4.3.10. Expression of the two VP7/TrVP2 chimeric genes in insect cells

Composite bacmid DNA, containing mt177/Tr9.V2 or mt200/Tr9.V2 chimeric genes, was constructed as described before and used to transfect insect cells. Recombinant baculoviral stocks were prepared directly from the transfection supernatants and used to re-infect cells for protein expression. The VP7/VP2 chimeric proteins, expressed by the baculovirus recombinants, Bac-177/TrVP2 and Bac-200/TrVP2, were analysed by SDS-Page. The two VP7/TrVP2 chimeras with an estimated molecular weight of 52 kDa, as predicted for VP7 plus the 101 amino acids of the VP2-specific insert, separated accordingly on the SDS-PAGE gel. No similar bands were visible in the wild type or mock-infected Sf9 cells (*Figure 4.21*). The expression levels of the two VP7/VP2 chimeric proteins were lower than that of wild-type VP7. This could be due to the fact that Bac-177/TrVP2 and Bac-200/TrVP2 were not plaque purified as in the case of VP7, mt177 and mt200 recombinant baculoviruses. The lower expression results of the Bac-mt177 and Bac-mt200 before plaque purification confirmed this observation (result not shown). Increasing the expression levels of the chimeric proteins was deemed to be unnecessary. Maximum expression of the two chimeric proteins was obtained 4 days post-infection. The yields of expressed mt177/TrVP2 and mt200/TrVP2 were estimated to be roughly 100-150 μg/2 x 10^7 infected Sf9 cells. No crystals, or any other recognisable structure, were visible under the light microscope in insect cells infected with either of the two chimeric VP7/TrVP2 recombinant baculoviruses.

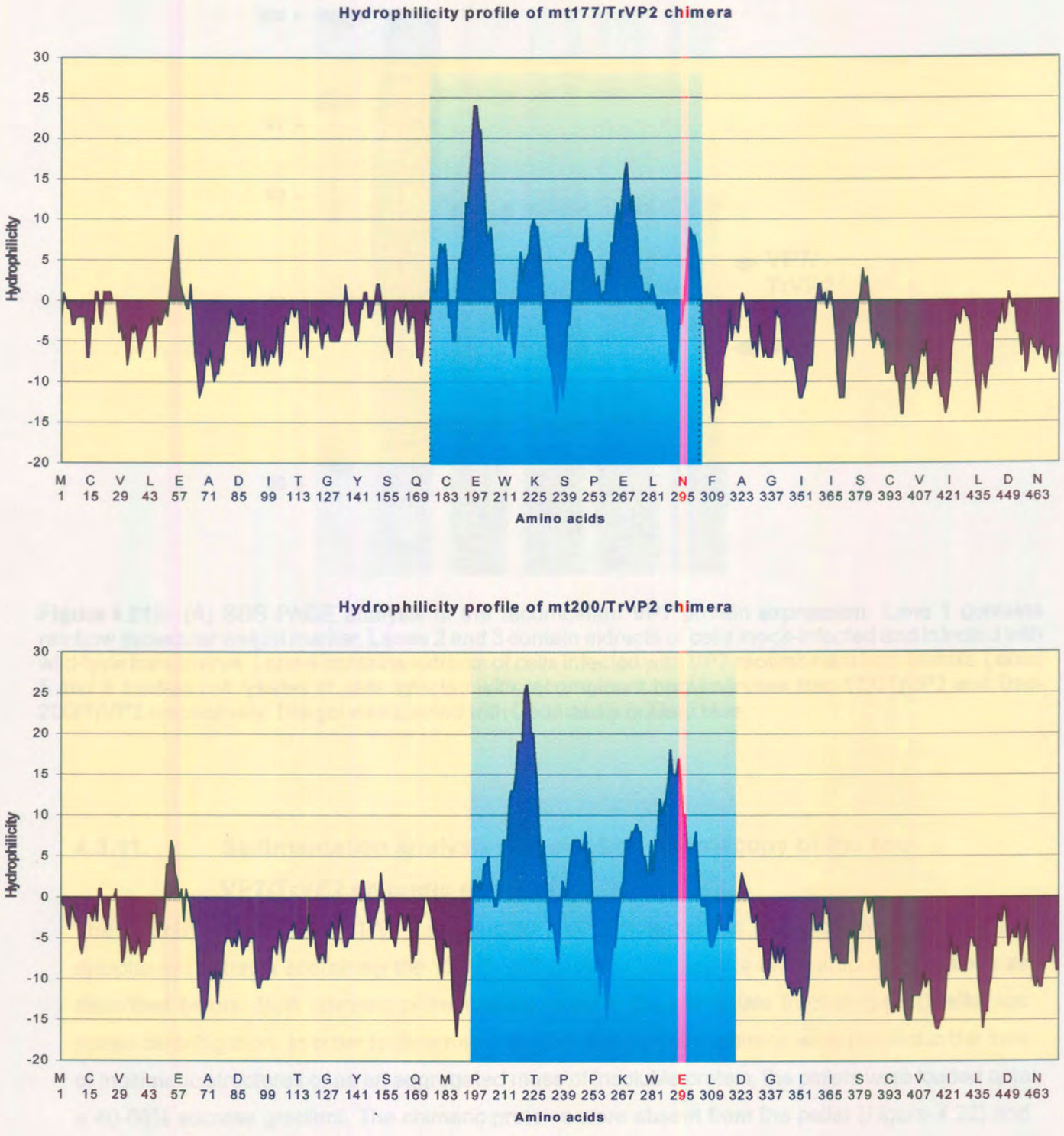

Figure 4.20: Comparison of the hydrophilicity profiles of the two chimeric proteins mt177/TrVP2 and mt200/TrVP2. Hydrophilicity was predicted according to Hopp & Woods (1981) utilising the ATHEPROT computer program. Areas with positive values have a nett hydrophilicity while areas with negative values have a nett hydrophobicity. The hydrophilicity profiles shows the insertion of the VP2 region stretching from amino acids 313 to 415, containing predominantly hydrophilic domains (indicated by blue bar at top of graph).

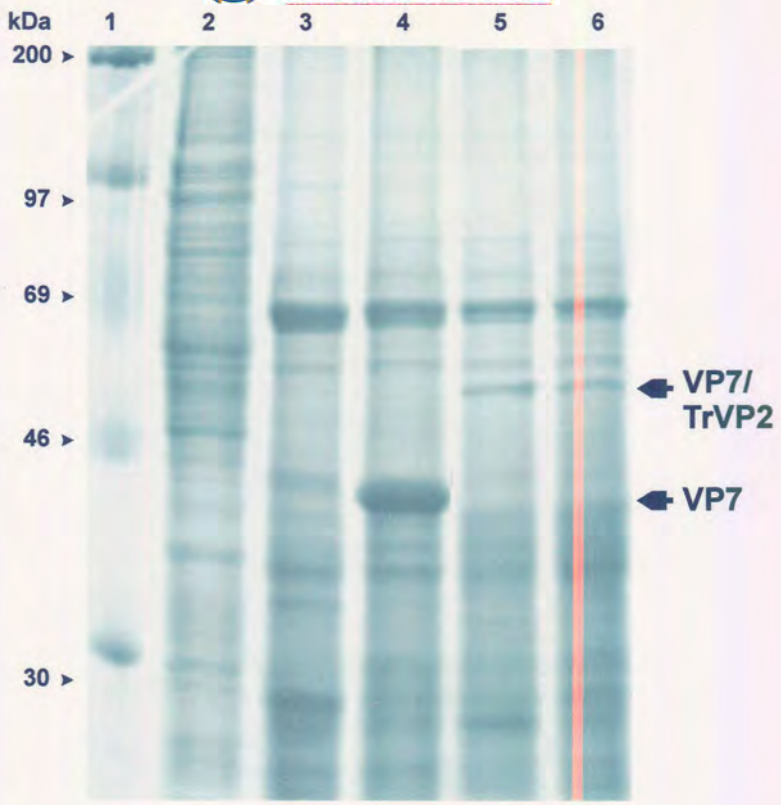

Figure 4.21: (A) SDS-PAGE analysis of the recombinant VP7 protein expression. Lane 1 contains rainbow molecular weight marker. Lanes 2 and 3 contain extracts of cells mock-infected and infected with wild-type baculovirus. Lane 4 contains extracts of cells infected with VP7 recombinant baculovirus. Lanes 5 and 6 contain cell lysates of cells infected with recombinant baculoviruses Bac-177/TrVP2 and Bac-200/TrVP2 respectively. The gel was stained with Coomassie brilliant blue.

4.3.11. Sedimentation analysis and electron microscopy of the two VP7/TrVP2 chimeric proteins

The solubility of the mt177/TrVP2 and mt200/TrVP2 proteins was analysed by separating the cytoplasmic extracts containing the VP7/TrVP2 proteins into soluble and particulate fractions as described before. Both chimeric proteins were found in the particulate fraction (pellet), after low speed centrifugation. In order to determine whether the chimeric proteins were present in the form of multimeric structures or as an aggregated mass of insoluble protein, the pellets were loaded onto a 40-68% sucrose gradient. The chimeric proteins were absent from the pellet (*Figure 4.22*) and therefore not an insoluble mass of protein. It was found that for both chimeric proteins the largest fraction was found as a heterogeneous complex in the gradient. The structures formed by the two chimeric proteins were much smaller than that of the normal VP7 protein (fractions 6-9) as determined by their lower S value. The results obtained in the sucrose gradient assay indicated that the baculovirus expressed chimeric VP7 proteins differ in their ability to form particulate structures. It was thought that these differences might be related to the ability or inability of the chimeras to form trimers or alternatively to increased solubility.

Peak fractions from the sucrose gradient containing either the mt177/TrVP2 or mt200/TrVP2 chimeric proteins were pooled and the recovered protein complexes analysed by SEM. In the case of the two VP7/TrVP2 chimeras no flat hexagonal crystals were found as with VP7. A large number of small ball-like structures, which resemble the structures found with mt177, were visible for each chimera (*Figure 4.23*). These structures were much smaller than those observed in the case of mt177, with a diameter of approximately 0.5 to 0.8 μm. The size difference of the structures may be a result of the lower expression levels of the chimeras, although it may also be due to alterations in the protein-protein contacts between VP7 molecules, leading to a greater distortion of the flat-sheet structure that is required to form the hexagonal crystal lattice and morphology.

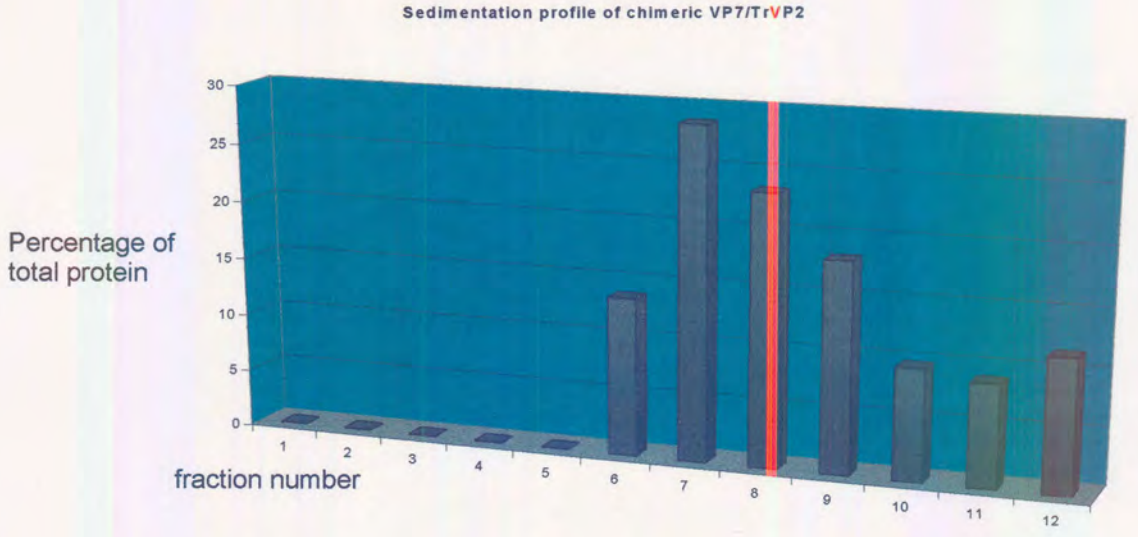

Figure 4.22: A graph representing the sedimentation analysis of the cytoplasmic extracts from Bac-177/TrVP2 infected cells by sucrose density centrifugation. The cells were radioactively labelled 48 h p.i. Prior to centrifugation the cytoplasmic extracts were separated in a soluble and particulate fractions as described in section 4.2.7. The particulate fractions were collected and used for the sedimentation analysis and fractions were collected from the bottom and analysed by autoradiography after resolution by SDS-PAGE. The bands were converted to Boehringer light units (BHU) using the lumi-imager and plotted as a percentage of the total amount of protein in the gradient. A similar profile were acquired from 200/TrVP2.

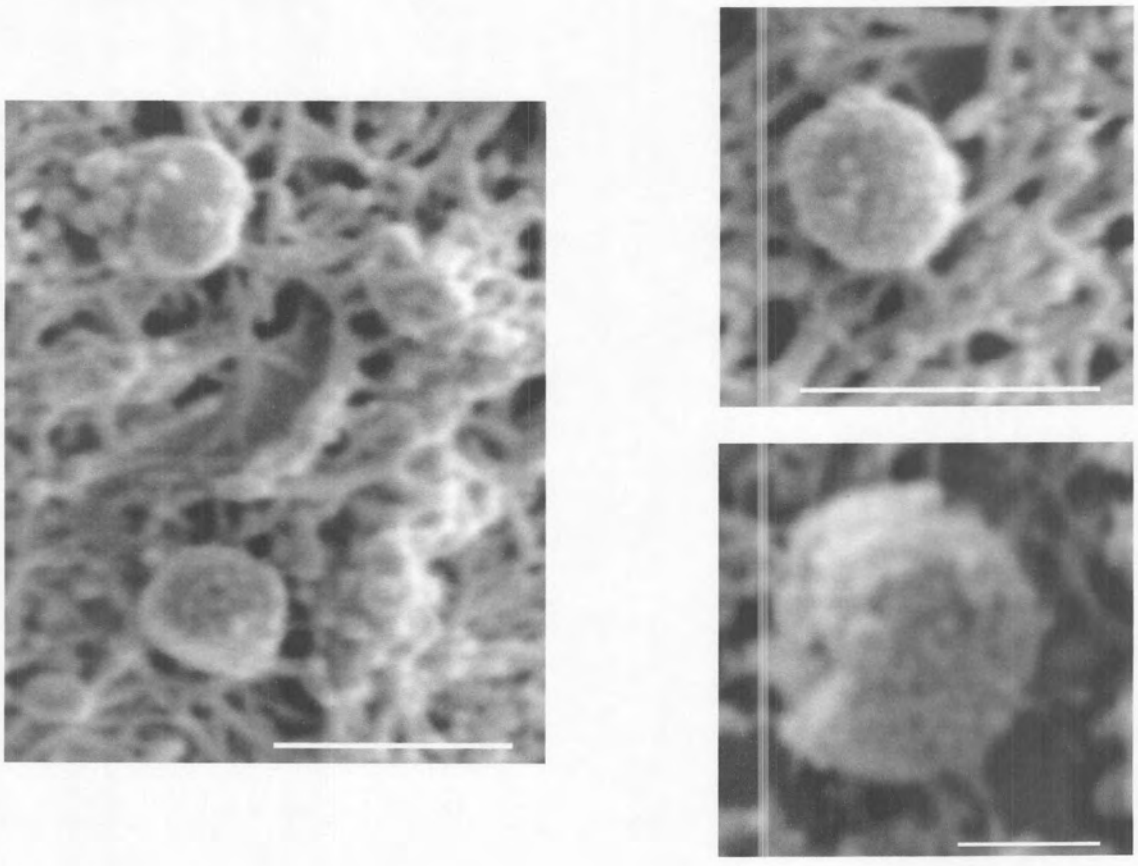

Figure 4.23: Scanning electron micrographs of purified chimeric VP7/TrVP2 ball-like structures. (A) represent structures from 177/TrVP2 and (B) 200/TrVP2. These structures did not show the same intact hexagonal outline as VP7. Bar markers represent 1 um.

4.4. DISCUSSION

In order to evaluate the potential of AHSV VP7 as an antigen delivery system in a subunit vaccine it is necessary to express large quantities of this protein in its native form. The VP7 protein was successfully expressed using an improved baculovirus system. Chuma et al. (1992) reported that AHSV VP7 synthesised in insect cells self-assembled to form disc-shaped crystal structures. When AHSV VP7 is co-expressed with AHSV VP3 in insect cells, it not only aggregate into crystals, but also assembles onto the VP3 scaffold to form CLPs (Maree *et al.*, 1998; chapter 3). The biologically active form of VP7, which is represented by the trimeric molecule, associates with other trimers to form crystals or assembles onto VP3 scaffolds to form CLPs. The availability of the expressed VP7 in its biologically active form will facilitate studies on the immunogenicity of the protein and provide further basis for assessing the suitability of VP7 as a subunit/epitope delivery system.

The large VP7 crystal structures provide an excellent opportunity for presenting antigenic epitopes, since they provide a large surface for epitope display. The disc-shaped crystals are also easily purified. To investigate the use of AHSV-9 VP7 crystals as an antigen delivery system, it was necessary to determine the immune response elicited by these crystals. Semi-purified AHSV-9 VP7 crystals were injected into Macaques and both the antibody and T-cell proliferative responses evaluated. Although a very strong humoral immune response was elicited, only a weak CTL response was detected (personal communication: Wade-Evans, A). This observation confirmed the result that AHSV VP7 crystals, purified from BHK cells infected with AHSV-9, was shown to be highly immunogenic, elicited a strong immune response and is effective as a subunit vaccine in a mouse model (Wade-Evans *et al.*, 1997; Wade-Evans *et al.*, 1998). The passive transfer of antibodies from immunised mice failed to protect syngeneic recipients from AHSV challenge, indicating that an antibody response is unlikely to represent the primary mechanism involved in the protection. Based on this result it was proposed that immunisation with VP7 induces a protective T-cell response in mice. Furthermore, it was found that denatured VP7 crystals resulted in lower levels of protection. The data indicated that the conformation and possibly the assembly of the VP7 into crystals appear to be important in the mechanism of protection against the heterologous serotype challenge. Reports from BTV VP7 indicated that the VP7 protein, contains immunodominant, serotype cross-reactive T-cell epitopes (Angove, 1998). These results imply that VP7 crystals are associated with a strong immune response in animals. The crystals have therefore potential as an antigen presentation system especially if neutralisation relies on a strong humoral immune response.

The use of chimeric AHSV CLPs as vehicles to present immunogenic peptides to the immune system, similar to the chimeric BTV CLPs (Roy *et al.*, 1994) has never been investigated. The main problem with this approach is the low yield of CLPs produced when the two major core proteins of

AHSV, VP3 and VP7, are co-expressed. It is therefore improtant to increase the yield of CLP synthesis in insect cells and secondly to introduce epitope insertion sites into VP7 without disturbing the 3-D structure of VP7. One possible approach to increase the yield of CLP synthesis is to increase VP7 solubility. VP7 crystals are present in insect cells expressing both VP3 and VP7 (chapter 3), which means that VP7 crystal formation compete with the assembly of VP7 trimers onto VP3 scaffolds to form CLPs. In view of this it is therefore possible that an increase in the solubility of VP7 might increase the concentration of free trimers in a cell, which might result in a higher yield of CLPs.

An important component in the development of AHSV VP7 crystals and/or chimeric CLPs as antigen delivery systems is to identify regions in the VP7 molecule, which may act as insertion sites for epitopes. The molecular structure of AHSV VP7, described in chapter 1, formed a basis for deciding which sites were to be exploited for insertion of epitopes, without disrupting the structure. The atomic structure of AHSV VP7 has been found to be very similar to that of the BTV VP7 trimers (described in chapter 1), as expected from the high degree of sequence similarity of the BTV and AHSV VP7 proteins. From the crystallographic data of AHSV VP7 Basak *et al.* (1996) identified properties of the molecular surface of AHSV VP7 which may play a role in the difference in solubilities between AHSV and BTV VP7. These data implicated the upper domain in contributing to the insolubility of AHSV VP7. In other studies it has been reported that single amino acid substitutions can significantly improve protein solubility (Zhao & Sommerville, 1992; Izard *et al.*, 1994). In the AHSV VP7 sequence, amino acid residue 167 is an alanine (A167) while in the comparable sequence of BTV VP7 it is an arginine (Iwata et al., 1992; Basak *et al.*, 1996). At amino acid position 209 in the AHSV VP7 there is a phenylalanine, while in the corresponding sequence of BTV VP7 there is a threonine. The substitution of A167 and F209 by the amino acid residues located in equivalent positions in BTV VP7 (R and T) has been suggested as a means to improve the solubility of AHSV VP7 (Basak *et al.*, 1996). This issue was investigated by Monastyrskaya *et al.* (1997) and it was found that neither mutation improved the solubility of AHSV VP7.

Mapping the hydrophobicity plots to the solvent-accessible surface of AHSV and BTV VP7 trimers has shown the presence of a large hydrophilic area composed of strand βC and η1 (aa 168-178, including the RGD motif of the top domain of one monomer, and the C-terminal helix 9 of the adjoining monomer)(Basak *et al.*, 1996). The A167 forms part of this area. The observation that changing this alanine to arginine did not increase the solubility of AHSV VP7 might reflect the impact of the C-terminal helix 9, as the C-terminus of AHSV VP7 is more hydrophobic with L346 replacing R345 of BTV VP7. Therefore, increasing the solubility of AHSV VP7 may involve mutating a number of amino acids and the factors involved in its solubility may prove to be complicated. The AHSV VP7 crystallographic data also revealed that the N-terminus is situated in the lower domain of VP7, and is likely to be constrained by steric hindrances for the insertion of epitopes. The short C-

terminal arm of VP7 ties the trimers together during capsid or crystal formation and addition of epitopes at the C-terminus may abolish CLP formation as well as aggregation into crystals. The deletion of only 5 amino acids or the in-frame addition of 11 amino acids at the C-terminus of BTV VP7 abolishes CLP formation presumably due to lack of trimer-trimer interaction (Le Blois & Roy, 1993). The absence of trimer-trimer interactions in the case of AHSV VP7 would not only abolish CLP formation but also crystal formation. An extension mutant of BTV VP7 with 11 additional amino acids at the amino terminus of the protein resulted in the assembly of CLPs, which were unstable. The only successful insertion of foreign epitopes in BTV VP7 was at an internal site at position 145 (A145), where 29 amino acids were inserted without inhibiting CLP formation. The site 144-145 is one of the four hydrophilic regions in the top domain of VP7, ideal for the insertion of epitopes.

Accordingly, four internal sites in the top domain of VP7 were identified as hydrophilic regions, located on exposed loops on the surface of the VP7 trimeric molecule. These hydrophilic loops make contact with the surrounding environment in both the VP7 crystals and CLPs. Two of these four hydrophilic sites, Arg177Arg178 and Q200Gly201, were chosen for modification in order to implement the insertion of epitopes. The decision was based on the hydrophilicity and availability of the two sites on the surface of the molecule as analysed by their X-ray crystallographic structure.

Two site-specific insertion mutants of VP7 were prepared through two PCR based strategies. The first is a modification of a strategy reported by Imai *et al.* (1991), while the second, more time consuming method, amplified the gene as two fragments. Both mutational methods, reported in this chapter resulted in the precise introduction of six codons and the creation of three unique restriction sites. The hydrophilicity profile of insertion mutant mt177 demonstrated a significant increase in hydrophilicity for the extended RGD loop. However, the insertion of the same amino acids between amino acids 200-201 resulted in only a small increase in hydrophilicity in that area. This could be explained by the location of the insertions. The exposed region 198-201 is only a small hydrophilic area of 4 amino acids, adjacent to large stretches of hydrophobic residues. The insertion of the extra amino acids adjacent to these hydrophobic regions had a much smaller effect of the hydrophilicity in that region than insertion of the amino acids into the already extensive hydrophilic RGD loop. Computer modelling of the molecular structure of the two insertion mutants indicated that in each case, the extra amino acids would be presented on the surface of the VP7 monomer rather than folding inwards.

For expression in the baculovirus system, the two modified VP7 genes were cloned into the transfer vector pFastbacI. Additional restriction sites, which remained in the multiple cloning site of the vector after the cloning strategy, were also removed to allow easy insertion of foreign sequences at the chosen positions in VP7. One site, *Kpn*I, was retained to enable retrieving of the VP7 gene for future recloning purposes. The recombinant transfer vectors were used to transform *E. coli* cells, containing the bacmid DNA and transposition helper plasmid. Composite bacmid DNA was used to

transfect *S. frugiperda* cells. Both insertion mutants, like unmodified AHSV-9 VP7, were expressed to the same high levels in Sf9 cells infected with the derived baculovirus recombinants. Both modified VP7 proteins migrated as a single distinct band with an electrophoretic mobility slightly slower than wild-type VP7. The distinction in size is approximately 1 kDa and can be accounted for by the six extra amino acids (estimated at approximately 900 daltons) which were introduced into the two modified VP7 proteins. An important question that had to be addressed in the course of this investigation was whether the top domain of VP7 would be flexible enough to allow the insertion of extra amino acids as part of the vector development. Two insertion mutants each containing six extra amino acids between amino acids 177-178 and 200-201 were constructed and expressed. The mutants were analysed for their solubility, crystal formation, antigenic properties and ability to form CLPs with AHSV VP3.

When cytoplasmic extracts of cells infected with either the VP7, mt200 and mt177 recombinant baculoviruses were subjected to low speed centrifugation, almost all the VP7 and mt200 proteins were recovered in the particulate fraction. The mt177 protein was separated into approximate equal amounts of a soluble and a particulate fraction, using differential centrifugation. When the particulate fraction of the three proteins were analysed by sedimentation analysis on sucrose gradients, almost all the VP7 and mt200 proteins migrated at a sedimentation rate of approximately 900 S to the bottom fractions of the gradient. The mt177 protein was present in two different forms on the gradient. Some of the mt177 protein accumulated at the top of the gradient and represents the soluble form of mt177 trimers, while the particulate form of mt177 sedimented at about 900 S to the bottom of the gradient. This indicated that the extra amino acids in the RGD loop of VP7 dramatically increased the solubility of VP7, while no change in solubility was observed when the insertion occurs in Q200G201. The aggregation of VP7 trimers into highly ordered hexagonal lattice of trimeric subunits is an equilibrium process in which the equilibrium is shifted so far to crystal formation that nearly no subunits are present in soluble form. The moment the solubility of VP7 was increased the equilibrium changes and shifted more towards soluble trimers. Therefore the force behind the equilibrium is the hydrophobicity or insolubility of AHSV VP7.

Examination of the gradient purified particulate structures of VP7 and the VP7 insertion mutants by scanning electron microscopy revealed the following. The mt200 protein, like wild-type VP7, aggregated into flat, disc-shaped, usually hexagonal crystals with dimensions of up to 6 μm in diameter and approximately 200 nm thick. These disc-shaped aggregates of expressed AHSV VP7 have previously been observed in recombinant baculovirus-infected insect cells (Chuma et al., 1992) and are also produced in AHSV-infected BHK cells (Burroughs *et al.*, 1994). These crystals are formed of flat sheets of VP7 trimers. Although not proved it can be assumed that each sheet in the crystal represents a double layer of VP7 trimers where the hydrophobic bottom domains of the trimers are located on the inside away from the aqueous surrounding, while the top domains face

the environment. The bottom domains are probably involved in keeping the two layers together by means of hydrophobic interactions, similar to the interaction with the underlying VP3 molecules in the core. In each layer of the crystal the trimers are arranged as hexagonal rings, similar to the rings of VP7 trimers that are observed of the surface of the core particles (Burroughs *et al.*, 1994; Basak et al., 1996; Grimes *et al.*, 1998; Stuart *et al.*, 1998). The mt200 was arranged in the same lattice of trimeric subunits, described for the VP7 crystal lattice (Burroughs *et al.*, 1994). The hexagonal arrangement observed in the VP7 crystal lattice appears to have a direct structural similarity to the segmented, ring-shaped capsomeres that are visible on the outer surface of the AHSV core (Burroughs *et al.*, 1994), which are also composed of VP7 (Hewat *et al.*, 1992). The particulate form of mt177 does not have the characteristic flat, hexagonal crystal appearance of mt200 and VP7, but the particles have a round ball-like structure. The soluble portion of the protein, recovered from the top of the sucrose gradient did not assemble into any recognisable structure, visible by SEM or TEM analysis. This is not unexpected if the top fractions represent soluble trimers. The fine structure of the ball-like structures was further investigated by TEM analysis and showed the same lattice arrangement of trimeric subunits, observed in VP7 and mt200 crystals. A possible explanation for the round, ball-like structures formed by the mt177 protein, is that when the mt177 trimers aggregate into a highly ordered hexagonal lattice structure, the hydrophilic/soluble mt177 trimers resulted in a weaker interactions between adjacent sheets and the crystal appears round and distorted.

Investigation of the CLP formation when co-expressed with AHSV-9 VP3, revealed that both VP7 insertion mutants assembled onto VP3 scaffolds to form CLPs. These CLPs were morphological identical to CLPs formed by the assembly of wild-type VP7 and VP3. Their biophysical character was also identical to that of normal CLPs, since the CLPs produced by the insertion mutants of VP7 appeared to be equally stable in the same ionic strengths and pH conditions as normal CLPs. However, one unique characteristic about the yield of CLPs produced, was observed. The yield of CLPs produced by mt200 was as low as in the case of VP7, since most of the mt200 protein, like VP7, aggregated to form crystals. The yield of CLPs produced by mt177 was significantly higher. No crystals were present with the co-expression of VP3, although a small amount of mt177 protein did aggregate in the highly ordered lattice described in the previous paragraph. These data indicate that mt177 is indeed more soluble than VP7 and that it still forms the trimeric structure necessary for assembly on theVP3 scaffold and that more trimers are available for CLP formation.

The data observed can be summarised as shown in *Figure 2.23*. The VP7 crystals have no known functional significance in the replication cycle of AHSV and are only a by-product in the viral morphogenesis. The assembly of the trimers (B) into hexagonal crystals (D) is forced by the hydrophobic nature of the protein. This resulted in a low yield of CLPs (C) synthesised when co-expressed with VP3, since only a limited quantity of soluble VP7 trimers is available for CLP formation. When the solubility of VP7 is increased (E), the equilibrium shifts towards more soluble

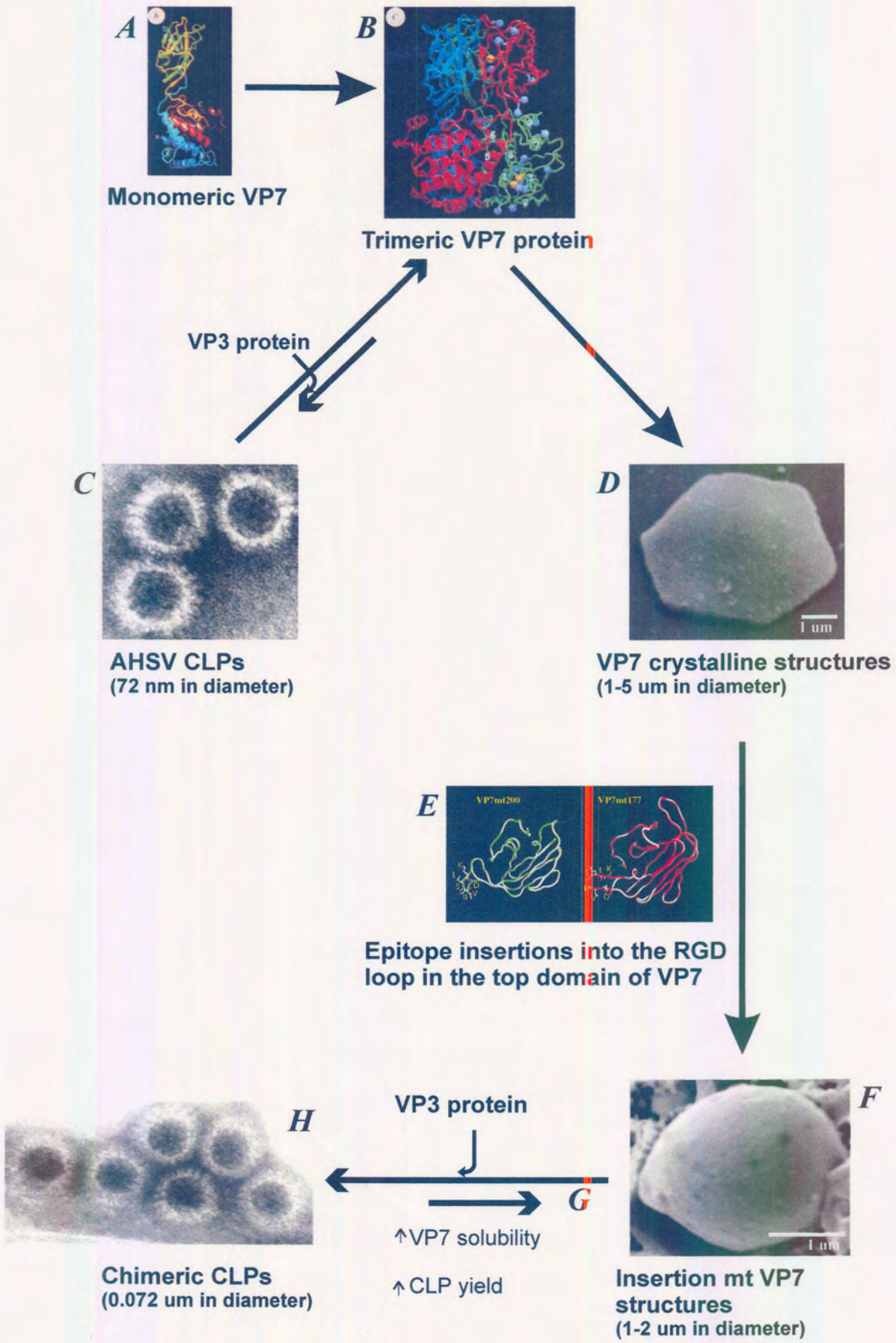

Figure 4.24: Summary of results. See text for details.

trimers. This causes an increase in the effective concentration of the trimers (G) in the cytoplasm of the cell. Therefore, more trimers are available for assembly onto VP3 scaffolds, which resulted in increased yield of CLPs (H) produced.

The next step of the investigation was to determine if the regions chosen for epitope insertion were flexible enough to tolerate additional sequences and what the effect of the insertions will be on the trimerisation and solubility of VP7. The size of the inserts that would be accommodated by the VP7 3-D structure also has be determined. To address these questions two chimeric VP7 mutants were constructed, utilising the restriction enzyme sites introduced into the two specified regions of the VP7 gene. VP7 chimeras with an additional 105 amino acids were prepared, by inserting a region of AHSV-9 VP2, containing at least two neutralising epitopes of the protein. The two VP7/TrVP2 chimeric genes were expressed in insect cells

The chimeric proteins were analysed for their ability to form crystals and their solubility. The two chimeric VP7 proteins (mt177/TrVP2 and mt200/TrVP2) were recovered from the sucrose gradient as a heterogeneous complex with a maximum sedimentation rate of approximately 400 S. The data indicates that the chimeras were present as multiprotein structures, which are larger than the trimeric structures observed in the case of mt177, but also much smaller than the crystals formed by VP7. Examination by SEM revealed small ball-like structures of diameters of approximately 0.5 μm. Since the proteins were more than 90% pure, as analysed by protein gel electrophoresis, it was assumed that these structures represent aggregates of the chimeric proteins.

Data obtained by Roy *et al.* (1997) suggested that the insertion of a number of foreign epitopes into the BTV VP7 at site Gln238 abrogated CLP formation, despite the fact that this site is located on an exposed loop of VP7. Successful insertion of sequences of up to 29 nucleotides could be achieved in the Ala145 site without inhibiting CLP formation. Although CLP formation was not analysed for the chimeras constructed in the study, the successful insertion of a foreign domain into AHSV VP7 resulted in a multimeric protein structure, which resembles structures from highly ordered arrays of protein. Whether the chimeric proteins in this structures are folded correctly and retained the epitopes of the inserted domain, remains to be resolved.

CHAPTER 5

CONCLUDING REMARKS AND FUTURE PROSPECTS

The development of particulate vector systems for the presentation of immunogenic epitopes provides a powerful approach for the delivery of antigens. Some existing particulate vector systems are based on linking an epitope to a carrier protein capable of assembly into a multimeric structure. Examples include hepatitis B particles (Clarke *et al.*, 1987), poliovirus particles (Evans *et al.*, 1989) and yeast Ty-particles (Adams *et al.*, 1987). AHSV is associated with three characteristic structures that could be used as particulate delivery systems. The NS1 tubules were found to be effective carriers for foreign epitopes, in the case of BTV (Mikhailov *et al.*, 1996). The VP7 crystals elicit a strong humoral immune response in an animal model (Wade-Evans *et al.*, 1997; Wade-Evans *et al.*, 1998). Empty virions or particles that simulate the virion surface should also provide a safe way of stimulating protective immunological memory.

The objective of this study was not only to investigate the morphology and assembly of these structures, but also to investigate their use as delivery systems for neutralizing epitopes. Three specific aims were identified and accomplished. The first aim involved the cloning, characterization and expression of the NS1 gene, followed by biochemical and morphological analysis of the NS1 tubules, as well as the identification of potential epitope insertion sites. The second aim was to co-express different combinations of the AHSV genes that encode the four major structural proteins to investigate particle morphogesis in the absence of the other viral components. The last aim involved the identification of epitope insertion sites in VP7 that are not essential for trimer-trimer interactions or CLP formation. The academical and practical value of the results are briefly highlighted and discussed here.

A full-length cDNA copy of the dsRNA segment 5 of AHSV-6 that encodes NS1, was cloned and sequenced. Bioinformatics is the key to understanding the properties and function of AHSV proteins. DNA and protein sequences are amenable to computer analysis, since they can be represented by strings of letters. The NS1 gene contains the conserved terminal hexanucleotides, proposed by Mizukoshi *et al.* (1993), with segment-specific inverted terminal repeats reported for other orbivirus segments. A hydrophilic region, displaying significant antigenicity, was identified in the C-terminus of NS1 and it was postulated that this region may be exposed on the surface of the AHSV NS1 tubules. This was indeed found to be true for BTV NS1 (Du Plessis *et al.*, 1995; Mikhailov *et al.*, 1996). The cloned NS1 gene was epressed *in vitro* and yielded a NS1 protein of the expected size thereby confirming that the ORF was full-length and did not contain any stop codons. Evidence was obtained that the *in vitro* synthesised NS1 protein of AHSV assembled spontaneously to form small tubular structures. This indicates that the ability to form tubules is self-primed and as

such a function of the amino acid sequence of the NS1 protein.

The NS1 gene was expressed to high levels, using a novel Bac-to-Bac™ baculovirus expression system. The use of this expression system has facilitated the rapid and convenient expression of NS1, since the entire recombinant baculovirus genome could be constructed in *E. coli* and did not involve *in vivo* homologous recombination. Heterologous expression of this gene enabled the first assembly studies regarding the AHSV tubule. The baculovirus expressed NS1 assembled into tubular structures in the insect cells with similar morphology to authentic tubules found in AHSV-infected cells (Huismans & Els, 1979). An important finding was that the morphology and biophysical properties differed in many respects from those described for other orbiviruses such as BTV, EHDV and BRDV. The purified tubules reacted in an immuno-labelling assay with anti-AHSV-6 antiserum, as well as with heterologous antiserum. This not only confirmed the AHSV origin of the protein, but also the antigenicity of these multimeric structures.

The subsequent approach for the development of AHSV NS1 tubules as a particulate antigen delivery system is to construct a panel of insertional mutants, by introducing several foreign antigenic sequences of different lengths into the proposed antigenic site of NS1. This would provide the means to identify the maximum length of a foreign peptide that could be inserted into NS1 without disrupting tubule formation. Deletions, point and domain switching analysis of the NS1 protein can be used to identify certain sequences in the NS1 protein that are essential for assembly into tubules. The use of multiple baculovirus gene expression vectors could also enable the formation of multiple epitope tubules, by co-expressing chimeric NS1 proteins with different epitopes. NS1 tubules have many advantages over CLPs as epitope carriers. They are composed of a single protein, in cotrast to CLPs, which consist of VP3 and VP7. In addition, the expression level of recombinant NS1 is generally high (ca. 20% of the proteins synthesised in infected Sf cells) and tubules are easy to purify. Therefore, tubules could provide an efficient and inexpensive system for the presentation of single or multiple foreign epitopes. The tubules are also highly immunogenic and elicit a strong humoral immune response without the use of standard adjuvants.

Using the novel Bac-to-Bac™ baculovirus expression system, dual-gene vectors co-expressing various combinations of AHSV genes under control of either the polh or p10 promoters, were constructed. Co-expression of the VP3 and VP7 genes resulted in the intracellular formation of CLPs, which structurally resembled AHSV cores and reacted strongly with VP7 monoclonal antibodies. In contrast to virus-derived cores, the CLPs were empty, since they lacked the genome and minor core proteins. The problem found with the previous co-infection of VP3 and VP7, regarding the variation in the ratio of VP3 to VP7, which correlates with the variation in the multiplicity of infection of each recombinant virus from cell to cell (Maree *et al.*, 1998) was overcome using this co-expression strategy. The CLPs produced were uniform in structure and the molar

ratios of the two proteins were si VP7 derived from infectious AHSV. However, the yield of CLPs were low, which made the large scale purification of these particles for vaccination purposes or use in high resolution structural studies, very difficult. It should be noted that VP7 aggregates into large distinctive crystals in infected cells, which could impede incorporation into particles. Furthermore, low yields of proteins are generally obtained when AHSV genes are expressed using the baculovirus system in comparison to BTV or EEV genes. These two factors downregulated the assembly of particles.

To investigate the structure and assembly of AHSV VLPs, two dual recombinant baculovirus vectors were used, the one expressing AHSV-9 VP5 and VP7, the other AHSV-9 VP3 and either AHSV-9 or AHSV-3 VP2. The expressed proteins assembled into double capsid particles with a diffuse surface structure. The formation of VLPs in the absence of other AHSV encoded structural or non-structural proteins implies that these proteins are not necessary for the assembly of VLPs in insect cells. The particles, however, were not homogenous, but contained different amounts of the outer capsid proteins and the yield of VLPs was extremely low. This may be due to variable amount of VP7 incorporated during intracellular assembly as a direct result of the variation in the ratio of VP3 to VP7 expression in insect cells co-infected with the two dual recombinant baculoviruses (French *et al.*, 1990; Maree *et al.*, 1998). It is possible that the absence of VP7 capsomeres in partially assembled CLPs resulted in the failure of VP2 or VP5 to associate with the CLPs or in some cases resulted in partial association. This problem could be resolved by constructing a quadruple gene expression vector, which allows the simultaneous expression of all four major structural proteins of AHSV. However, this will not solve the problem of the low expression levels of AHSV proteins. At this stage no information is available on the regulation of AHSV transcription and translation. Dual expression of AHSV genes seems to decrease the expression levels even further, compared to single expression. Quadruple expression could result in even lower expression levels. A large fraction of most of the heterologous expressed AHSV proteins also seems to be insoluble and could also impede the assembly process.

AHSV comprises multiple protein components in non-equimolar ratios, each of which is encoded by a discrete gene (mRNA species). These factors make the mechanism of virus assembly a challenge to unravel. Synthesis of subviral particles in eukaryotic cells by a heterologous expression system, opens up the opportunity to investigate the protein-protein interactions involved in the assembly process, the stages of viral assembly and the contribution of the individual components to that process. An increased understanding of viral morphogenesis may aid the development of antiviral agents, which specifically interfere with the assembly process. The information on the assembly is also important regarding the future development of a recombinant subunit vaccine, utilising the AHSV CLPs and VLPs. For example, by manipulating the structure of various viral proteins, it will be possible to develop particulate antigen delivery systems for the presentation of

immunogenic epitopes against other infectious diseases. Furthermore, it has been reported that BTV VLPs fully protect sheep against BTV, while BTV CLPs induce partial protection not involving neutralising antibodies, implicating a role for cell-mediated immunity. No such information is yet available for AHSV. If this holds true for AHSV VLPs, these particles will not only provide safe and effective vaccination, but also allow differentiation between vaccinated and infected horses, thereby simplifying the international movement of horses.

Another important application is the use of CLPs and VP7 crystals as antigen delivery systems. The VP7 protein, associated with both the CLPs and crystals, was manipulated to receive foreign immunogenic epitopes. The functional significance of two hydrophilic amino acid regions in the structure, trimerisation and solubility of VP7 was subsequently investigated by analysing two insertion mutants of AHSV-9 VP7. A cloning site comprising three unique restriction sites was introduced into two chosen antigenic or hydrophilic regions in the top domain of AHSV-9 VP7, respectively, using the convenient PCR methods for mutagenesis. These cloning sites facilitated the easy insertion of epitopes, for example a truncated fragment of the VP2 protein containing a previously identified immunodominant epitope of VP2, responsible for neutralisation. The effects of inserting as little as 6 amino acids or as much as 105 amino acids in the two chosen sites on protein solubility, folding and trimerisation were investigated. Insertion of six amino acids in the flexible RGD loop located in the top domain of VP7 increased the solubility of VP7, although the protein was still able to form its trimeric structure and to assemble into CLPs. Unlike normal VP7 and insertion mutant mt200, mt177 did not aggregate into highly ordered hexagonal crystals but formed ball-like structures, that could rapidly dissociate into trimers when required by equilibrium. As a result of the increased solubility of the VP7mt177 trimers, the yield of CLPs produced, when co-expressed with VP3, was significantly higher than with normal VP7 or mt200. Preliminary studies indicated that the VP7 structure in this highly flexible loop is able to accommodate up to 105 amino acids without losing the ability to assemble into trimers and ultimately into CLPs. This approach represents a novel strategy and is important for the development of future subunit vaccines, since it was the first report on increased VP7 solubility, as well as on the incorporation of up to 105 amino acids (1/3 of the size of VP7) without obstructing CLP production.

Several contributions regarding the protein-protein interaction in virus assembly, the solubility of VP7, the yield of CLP production and the use of CLPs and VP7 crystals as vehicles for foreign immunogens have been made during this investigation. Subsequent work, following on from that described in this thesis, has been performed on the AHSV-9 VP7 gene and insertion mutants constructed. Firstly, a third insertion mutant of VP7 has been constructed, with three unique restriction enzyme sites in the nucleotide sequence encoding amino acids 144 to 145 (Joanne Riley). Preliminary data indicated that the insertion at 144-145, like mt200, did not influence the solubility of VP7 and that mt144 also forms hexagonal crystals and CLPs. Secondly, three other

chimeric VP7 proteins were also constructed, two of which contained smaller truncated fragments of 33 amino acids of AHSV-9 VP2 inserted in each of the constructed sites, respectively (Lineo Motopi), and a third containing 12 amino acids from NS3 in site 200-201 (Tracey Meiring). These studies have shown that the VP7 chimeras, containing 33 amino acids, remain in a trimeric form that assemble into ball-like structures, similar to those found in this study. This data confirm the results obtained in this study. The insertion of 12 amino acids at position 200-201 (mt200) did not influence the ability of the protein to assemble into hexagonal crystals. The assembly of these chimeras with VP3 is still under investigation.

The immune response elicited by the chimeric VP7 crystals, chimeric CLPs and VLPs will be evaluated in the near future to determine the application of these systems as subunit vaccines. The VP7 crystal and chimeric CLPs may provide the ideal candidate subunit vaccine capable of inducing antibodies against many AHSV serotypes as well as serogroup protection provided by VP7. It is possible that in the future even more elaborate experiments where different sites or domains could be manipulated in a single VP7 protein could result in the expression of more than one epitope onto the VP7 surface. This can also lead to the application of an antigen presentation system for epitopes of a variety of human and animal important viruses.

PAPERS PUBLISHED AND CONGRESS CONTRIBUTIONS

Articles published:

Maree, F.F. and Huismans, H. (1997). Characterisation of tubular structures composed of non-structural protein NS1 of African horsesickness virus expressed in insect cells. *Journal of General Virology* **78**, 1077-1082.

V. Van Staden, C.C. Smit, M.A Stoltz, F.F. Maree and H. Huismans (1998). Characterisation of two African horsesickness virus non-structural proteins, NS1 and NS3. *Archives of Virology* **14**, 251-258.

Maree, S., S. Durbach, F.F. Maree, Vreede, F and H. Huismans. 1998. Expression of the major core structural protiens VP3 and VP7 of African horse sickness virus, and production of core-like particles. *Archives of Virology* **14**, 203-209.

Articles submitted:

Maree, F.F., Riley, J., Meyer, Q. & Huismans, H. Effects of site directed insertion mutagenesis on the crystal formation, solubility and CLP formation of African horsesickness virus VP7. Submitted to *Journal of Virology*.

Maree, F.F., Maree, S., Huismans, H. & Van Dijk, A. The assembly of African horsesickness virus capsids facilitate structural studies and the development of recombinant vaccines. Submitted to *Virology*.

Conferences:

F.F. Maree and H. Huismans: Characterisation of the structure of African horsesickness virus-specific tubules synthesised in insect cells. South African Microbiology Society (S.A.M.S.) congress, Microbiology for Africa, June 1996.

Huismans, H. & Maree, F.F. Afrivan horsesickness virus-specific tubules produced in insect cells by means of a recombinant baculovirus. 10th International Congress of Virology. Jerusalem, Israel, 11-16 August 1996.

F.F. Maree, A. Hall, C. van der Merwe and H. Huismans Investigation of the structure of African horsesickness virus-specific tubules using electron microscopy. Electron microscopy society of South Africa (E.M.M.S.S.A.) congress, November 1996.

Huismans, H., Van Staden, V., Stoltz, M., Maree, F.F. & Smit, C.C. Characterization of two African horsesickness virus non-structural proteins, NS3 and NS1. International meeting

on African horsesickness, Rabat, Morocco, 2-4 April 1997.

Huismans, H., Maree, S., Durbach, S., Maree, F.F. and Vreede, F. Intracellular production of African horsesickness virus core-like particles by expression of the two major core-proteins VP3 and VP7. International meeting on African horsesickness, Rabat, Morocco, 2-4 April 1997.

F.F. Maree and H.Huismans: Assembly of core-like particles of African horsesickness virus by co-expression of the two major core proteins, VP3 and VP7, in insect cells. South African Genetics Society (S.A.G.S.) XVIth Genetics congress, July 1998.

Huismans, H. & Maree, F.F. African horsesickness virus VP7 crystals as presentation systems for antigens. South African Microbiology Society (S.A.M.S.) congress, August 1998.

Maree, F.F. & Huismans, H. The development of Afrivan horsesickness virus VP7 crystals as well as core-like and virus-like particles as delivery systems for antigenic determinants. 11th International Congress of Virology, Sydney, Australia, 9-13 August 1999.

REFERENCES

Altschul, S.F, Gish, W., Miller, W., Meyers, E.W. and Lipman, D.W. (1990). Basic local alignment search tool. *J Mol Biol* **215(3)**, 403-10

Anzola, J.V., Xu, Z., Asamizu, T. and Nuss, D.L. (1987). Segment-specific inverted repeats found adjacent to conserved terminal sequences in wound tumor virus genome and defective interfering RNAs. *Proc Natl Acad Sci USA* **84**, 350-357.

Ausubel, F. M., Brent, R., Kingston, R. E., Moore, D. D., Seidman, J. G., Smith, J. A. and Struhl, K. (1988). Current protocols in molecular biology. John Wiley and Sons, USA.

Bairoch, A., Bucher, P., and Hofmann, K. (1996). The PROSITE database, its status in 1995. *Nucleic Acids Res* **24**(1), 189-196.

Bairoch, A., Bucher, P., and Hofmann, K. (1997). The PROSITE database, its status in 1997. *Nucleic Acids Res* **25**(1), 217-221.

Barnard, B. J. (1993). Circulation of African horsesickness virus in zebra (Equus burchelli) in the Kruger National Park, South Africa, as measured by the prevalence of type specific antibodies. *Onderstepoort J Vet Res* **60**(2), 111-117.

Barnard, B. J. (1997). Antibodies against some viruses of domestic animals in southern African wild animals [published erratum appears in *Onderstepoort J Vet Res* 1998 65(3):101-3]. *Onderstepoort J Vet Res* **64**(2), 95-110.

Barnard, B. J., Bengis, R., Keet, D., and Dekker, E. H. (1994). Epidemiology of African horsesickness: duration of viraemia in zebra (Equus burchelli). *Onderstepoort J Vet Res* **61**(4), 391-393.

Barnard, B. J., Bengis, R. G., Keet, D. F., and Dekker, E. H. (1995). Epidemiology of African horsesickness: antibodies in free-living elephants (Loxodonta africans) and their response to experimental infection. *Onderstepoort J Vet Res* **62**(4), 271-275.

Basak, A. K., Gouet, P., Grimes, J., Roy, P., and Stuart, D. (1996). Crystal structure of the top domain of African horse sickness virus VP7: comparisons with bluetongue virus VP7. *J Virol* **70**(6), 3797-3806.

Basak, A. K., Grimes, J. M., Gouet, P., Roy, P., and Stuart, D. I. (1997). Structures of orbivirus VP7: implications for the role of this protein in the viral life cycle. *Structure* **5**(7), 871-883.

Basak, A. K., Stuart, D. I., and Roy, P. (1992). Preliminary crystallographic study of bluetongue virus capsid protein, VP7. *J Mol Biol* **228**(2), 687-689.

Belyaev, A. S., and Roy, P. (1992). Presentation of hepatitis B virus preS2 epitope on bluetongue virus core-like particles. *Virology* **190**(2), 840-844.

Belyaev, A. S., and Roy, P. (1993). Development of baculovirus triple and quadruple expression vectors: co- expression of three or four bluetongue virus proteins and the synthesis of bluetongue virus-like particles in insect cells. *Nucleic Acids Res* **21**(5), 1219-1223.

Belyaev, A. S., Hails, R. S., and Roy, P. (1995). High-level expression of five foreign genes by a single recombinant baculovirus. *Gene* **156**(2), 229-233.

Birnboim, H. C., and Doly, J. (1979). A rapid alkaline extraction procedure for screening recombinant plasmid DNA. *Nucleic Acids Res* **7**(6), 1513-1523.

Bishop, D.H.L. (1992). Baculovirus expression vectors. Seminars in *Virology* **3**: 253-264.

Borden, E. C., Shope, R. E., and Murphy, F. A. (1971). Physicochemical and morphological relationships of some arthropod-borne viruses to bluetongue virus--a new taxonomic group. Physiocochemical and serological studies. *J Gen Virol* **13**(2), 261-271.

Borden, E. C., Shope, R. E., and Murphy, F. A. (1971). Physicochemical and morphological relationships of some arthropod-borne viruses to bluetongue virus--a new taxonomic group. Electron microscopic studies. *J Gen Virol* **13**(2), 273-283.

Bowne, J. G., and Ritchie, A. E. (1970). Some morphological features of bluetongue virus. *Virology* **40**(4), 903-911.

Bremer, C. W., du Plessis, D. H., and van Dijk, A. A. (1994). Baculovirus expression of non-structural protein NS2 and core protein VP7 of African horsesickness virus serotype 3 and their use as antigens in an indirect ELISA. *J Virol Methods* **48**(2-3), 245-256.

Bremer, C. W. (1976). A gel electrophoretic study of the protein and nucleic acid components of African horsesickness virus. *Onderstepoort J Vet Res* **43**(4), 193-199.

Bremer, C. W., Huismans, H., and Van Dijk, A. A. (1990). Characterization and cloning of the African horsesickness virus genome. *J Gen Virol* **71**(4), 793-799.

Brookes, S. M., Hyatt, A. D., and Eaton, B. T. (1993). Characterization of virus inclusion bodies in bluetongue virus-infected cells. *J Gen Virol* **74**(3), 525-530.

Brown, F. 1992. New approaches to vaccination against foot-and-mouth disease. *Vaccine* **10**, 1022-1026.

Brown, C.C. and Dardiri, A.H. (1990). African horsesickness: A continuing menace. *J Am Vet Med Assoc* **196**, 2019-2021.

Brown, C. C., Meyer, R. F., and Grubman, M. J. (1994). Identification of African horse sickness virus in cell culture using a digoxigenin-labeled RNA probe. *J Vet Diagn Invest* **6**(2), 153-155.

Brown, N. and Faulkner, P. (1977). A plaque assay for nuclear polyhedrosis virus using a solid overlay. *J Gen Virol* **36**, 361-364.

Brown, S.E., Morrison, H.G., Karabatsos, N. and Knudson D.L. (1991). Genetic relatedness of two new Orbivirus serogroups: Orungo and Lebombo. *J Gen Virol* **72**, 1065-1072.

Brown, S. E., Gonzalez, H. A., Bodkin, D. K., Tesh, R. B., and Knudson, D. L. (1988). Intra- and inter-serogroup genetic relatedness of orbiviruses. II. Blot hybridization and reassortment in vitro of epizootic haemorrhagic disease serogroup, bluetongue type 10 and Pata viruses. *J Gen Virol* **69**(1), 135-147.

Burrage, T. G., and Laegreid, W. W. (1994). African horsesickness: pathogenesis and immunity. *Comp Immunol Microbiol Infect Dis* **17**(3-4), 275-285.

Burrage, T. G., Trevejo, R., Stone-Marschat, M., and Laegreid, W. W. (1993). Neutralizing epitopes of African horsesickness virus serotype 4 are located on VP2. *Virology* **196**(2), 799-803.

Burroughs, J. N., Grimes, J. M., Mertens, P. P., and Stuart, D. I. (1995). Crystallization and preliminary X-ray analysis of the core particle of bluetongue virus. *Virology* **210**(1), 217-220.

Burroughs, J. N., O'Hara, R. S., Smale, C. J., Hamblin, C., Walton, A., Armstrong, R., and Mertens, P. P. (1994). Purification and properties of virus particles, infectious subviral particles, cores and VP7 crystals of African horsesickness virus serotype 9. *J Gen Virol* **75**(8), 1849-1857.

Calisher, C.H. and Mertens, P.P.C. (1998). Taxonomy of African horse sickness viruses. In: Mellor, P.S., Baylis, M., Hamblin, C., Calisher, C.H., Mertens, P.P.C. (eds) African horsesickness. *Arch Virol Suppl* **14**, 3-11.

Cashdollar, L. W., Chmelo, R., Esparza, J., Hudson, G. R., and Joklik, W. K. (1984). Molecular cloning of the complete genome of reovirus serotype 3. *Virology* **133**(1), 191-196.

Cashdollar, L.W., Esparza, J., Hudson, G.R., Chmelo, R., Lee, P.W.K. and Joklik, W.K. (1982). Cloning the double-stranded RNA genes of reovirus: Sequence of the cloned S2 gene. *Proc Natl Acad Sci USA* **79**, 7644-7648.

Casper, D.L.D. and Klug, A. (1962). Physical principle in the construction of regular viruses. *Cold Spring Harb Symp Quant Biol* **27**, 1-24.

Chuma, T., Le Blois, H., Sanchez-Vizcaino, J. M., Diaz-Laviada, M., and Roy, P. (1992). Expression of the major core antigen VP7 of African horsesickness virus by a recombinant baculovirus and its use as a group-specific diagnostic reagent. *J Gen Virol* **73**(4), 925-931.

Chung, C.T. and Miller, R.H. (1988). A rapid and convenient method for the preparation and storage of competent bacterial cells. *Nucleic Acids Res.* **16**(8), 3580.

Cloete, M., du Plessis, D. H., van Dijk, A. A., Huismans, H., and Viljoen, G. J. (1994). Vaccinia virus expression of the VP7 protein of South African bluetongue virus serotype 4 and its use as an antigen in a capture ELISA. *Arch Virol* **135**(3-4), 405-418.

Coetzer, J. A. W. and Erasmus, B. (1994). African horsesickness virus. In: Infectious disease of Lifestock with special reference to Southern Africa. (Eds) Els, J. A. W. Coetzer, C. R. Thomson and R. C. Tustin. Oxford University Press, Cape Town, pp 460-475.

Cohen, S., Chang, A. and Hsu, L. (1972). Nonchromosomal antibiotic resistance in bacteria: genetic transformation of *Escherichia coli* by R-factor DNA. *Proc Natl Acad Sci USA* **69**, 2110.

Cowley, J. A., and Gorman, B. M. (1987). Genetic reassortants for identification of the genome segment coding for the bluetongue virus hemagglutinin. *J Virol* **61**(7), 2304-2306.

Cowley, J. A., and Gorman, B. M. (1989). Cross-neutralization of genetic reassortants of bluetongue virus serotypes 20 and 21. *Vet Microbiol* **19**(1), 37-51.

Cowley, J. A., and Gorman, B. M. (1990). Effects of proteolytic enzymes on the infectivity, haemagglutinating activity and protein composition of bluetongue virus type 20. *Vet Microbiol* **22**(2-3), 137-152.

Cromack, A. S., Blue, J. L., and Gratzek, J. B. (1971). A quantitative ultrastructural study of the development of bluetongue virus in Madin-Darby bovine kidney cells. *J Gen Virol* **13**(2), 229-244.

Dales, S. (1963). Association between the spindle apparatus and Reovirus. *Proc Natl Acad Sci*

USA **50**, 268-275.

Davis, R.A., and Borchardt, R.A (1986). Phosphorylation-dephosphorylation of apolipoprotein B. *Meth Enzymol* **129**, 536-542

Davies, A. H. (1994). Current methods for manipulating baculoviruses. *Biotechnology (N Y)* **12**(1), 47-50.

Davies, A. H. (1995). Advances in the use of recombinant baculoviruses for the expression of heterologous proteins. *Curr Opinion in Biotechnol.* **6**, 543-547.

Davies, F. G. and Otieno, S. (1977). Elephants and zebras as possible reservoir hosts for African horsesickness virus. *Vet. Rec.* **100**, 291-292.

Deléage, G., Clerc, F.F. and Roux, B. (1989). ANTHEPROT: IBM PC and Apple Macintosh versions. *Cabios* **5**, 159-160.

Deléage, G., Clerc, F.F., Roux, B. and Gautheron, D.C. (1988). ANTHEPROT: A package for protein sequence analysis using a microcomputer. *Cabios* **4**, 351-356.

Deng, G., and Wu, R. (1981). An improved procedure for utilizing terminal transferase to add homopolymers to the 3' termini of DNA. *Nucleic Acids Res* **9**(16), 4173-4188.

Devaney, M. A., Kendall, J., and Grubman, M. J. (1988). Characterization of a nonstructural phosphoprotein of two orbiviruses. *Virus Res* **11**(2), 151-164.

Devi, R., Burroughs, J.N., Mertens, P.P.C. and Roy, P. (1998). Transmethylase 1 and transmethylase 2 activities associated with the Cap protein (VP4) of BTV, in native cores, core-like particles and as a purified baculovirus expressed protein. *Proc Natl Acad Sci USA*

Du Plessis, D. H., Romito, M., and Jordaan, F. (1995). Identification of an antigenic peptide specific for bluetongue virus using phage display expression of NS1 sequences. *Immunotechnology* **1**(3-4), 221-230.

Du Plessis, D. H., Wang, L. F., Jordaan, F. A., and Eaton, B. T. (1994). Fine mapping of a continuous epitope on VP7 of bluetongue virus using overlapping synthetic peptides and a random epitope library. *Virology* **198**(1), 346-349.

Du Plessis, M., Cloete, M., Aitchison, H., and Van Dijk, A. A. (1998). Protein aggregation complicates the development of baculovirus- expressed African horsesickness virus serotype 5 VP2 subunit vaccines. *Onderstepoort J Vet Res* **65**(4), 321-329.

Du Plessis, M., and Nel, L. H. (1997). Comparative sequence analysis and expression of the M6 gene, encoding the outer capsid protein VP5, of African horsesickness virus serotype nine. *Virus Res* **47**(1), 41-49.

Du Toit, R.M. (1944). The transmission of bluetongue and horsesickness by *Cullicoides*. *Onderstepoort J Vet Sci* **19**, 7-16.

Eaton, B. T., and Crameri, G. S. (1989). The site of bluetongue virus attachment to glycophorins from a number of animal erythrocytes. *J Gen Virol* **70**(12), 3347-3353.

Eaton, B. T., and Hyatt, A. D. (1989). Association of bluetongue virus with the cytoskeleton. *Subcell Biochem* **15**, 233-273.

Eaton, B. T., Gould, A. R., Hyatt, A. D., Coupar, B. E., Martyn, J. C., and White, J. R. (1991). A

bluetongue serogroup-reactive epitope in the amino terminal half of the major core protein VP7 is accessible on the surface of bluetongue virus particles. *Virology* **180**(2), 687-696.

Eaton, B. T., Hyatt, A. D., and Brookes, S. M. (1990). The replication of bluetongue virus. *Curr Top Microbiol Immunol* **162,** 89-118.

Eaton, B. T., Hyatt, A. D., and White, J. R. (1987). Association of bluetongue virus with the cytoskeleton. *Virology* **157**(1), 107-116.

Eaton, B. T., Hyatt, A. D., and White, J. R. (1988). Localization of the nonstructural protein NS1 in bluetongue virus- infected cells and its presence in virus particles. *Virology* **163**(2), 527-537.

Els, H. J. (1973). Electron microscopy of bluetongue virus RNA. *Onderstepoort J Vet Res* **40**(2), 73-75.

Els, H. J. and Verwoerd, D. W. (1969). Morphology of bluetongue virus. *Virology* **38**, 213-219.

Emr, S. D. (1991). Expression in yeast. *Meth Enzymol* **185**, 231-233.

Erasmus, B. J. (1972). The pathogenesis of African horsesickness. *Proc 3rd Int Conf Equine Inf disease,* 208-213.

Erasmus, B. J. (1975). The control of bluetongue in an enzootic situation. *Aust Vet J* **51**(4), 209-210.

Erasmus, B. J. (1976). A new approach to polyvalent immunization against African horsesickness. *Proc 4th Int Conf Equine Inf disease,* 401-403, Veterinary publications, Inc, Princeton, N.Y.

Erasmus, B. J. (1977). Bluetongue and African horsesickness viruses. *Int Symp Reoviridae,* 209-210.

Erasmus, B. J., Young, E., Pieterse, L. M., and Boshoff, S. T. (1978). The susceptibility of zebra and elephants to African horsesickness virus. *J Equine Med Surg* **1**(Supplement), 409-413.

Felgner, P. L., Gadek, T. R., Holm, M., Roman, R., Chan, H. W., Wenz, M., Northrop, J. P., Ringold, G. M. and Danielsen, M. (1987). Lipofection: a highly efficient, lipid-mediated DNA-transfection procedure. *Proc Natl Acad Sci USA* **84**, 7413-7417.

Francki, R.I.B., Fauquet, C.M., Knudson, D.L. and Brown, F. (Eds). (1991). Classification and Nomenclature of Viruses: Fifth report of the International Committee on Taxonomy of Viruses. *Arch Virol Suppl* **2**. Springer-Verlag, Wien.

French, T. J., and Roy, P. (1990). Synthesis of bluetongue virus (BTV) corelike particles by a recombinant baculovirus expressing the two major structural core proteins of BTV. *J Virol* **64**(4), 1530-1536.

French, T. J., Inumaru, S., and Roy, P. (1989). Expression of two related nonstructural proteins of bluetongue virus (BTV) type 10 in insect cells by a recombinant baculovirus: production of polyclonal ascitic fluid and characterization of the gene product in BTV-infected BHK cells. *J Virol* **63**(8), 3270-3278.

French, T. J., Marshall, J. J., and Roy, P. (1990). Assembly of double-shelled, viruslike particles of bluetongue virus by the simultaneous expression of four structural proteins. *J Virol* **64**(12), 5695-5700.

Fu, H., Bland, A.P., Wade-Evans, A.M., Mertens, P.P.C. and Mellor, P.S. (1999). Ultrastructural

comparison of bluetongue virus replication in mammalian cells and *Culicoides* cells. *J Gen Virol*

Fukusho, A., Ritter, G. D., and Roy, P. (1987). Variation in the bluetongue virus neutralization protein VP2. *J Gen Virol* **68**(11), 2967-2973.

Fukusho, A., Yu, Y., Yamaguchi, S., and Roy, P. (1989). Completion of the sequence of bluetongue virus serotype 10 by the characterization of a structural protein, VP6, and a non-structural protein, NS2. *J Gen Virol* **70**(7), 1677-1689.

Furuichi, Y., Morgan, M., Muthukishnan, S. and Shatkin, A.J. (1975). Reovirus messenger RNA contains a methylated blocked 5' terminal structure: 7mGpppGpCp, *Proc Natl Acad Sci USA*, **72**, 362.

Furuichi, Y., Muthukishnan, S. Tomasz, S. and Shatkin, A.J. (1975). Mechanism of formation of reovirus mRNA 5'-terminal blocked and methylated sequence, 7mGpppGpCp. *J Biol Chem* **251**, 5043-5053.

Geourjon, C., and Deleage, G. (1995). ANTHEPROT 2.0: a three-dimensional module fully coupled with protein sequence analysis methods. *J Mol Graph* **13**(3), 209-12, 199-200.

Geourjon, C., Deleage, G., and Roux, B. (1991). ANTHEPROT: an interactive graphics software for analyzing protein structures from sequences. *J Mol Graph* **9**(3), 188-190, 167.

Ghiasi, H., Fukusho, A., Eshita, Y., and Roy, P. (1987). Identification and characterization of conserved and variable regions in the neutralization VP2 gene of bluetongue virus. *Virology* **160**(1), 100-109.

Ghiasi, H., Purdy, M. A., and Roy, P. (1985). The complete sequence of bluetongue virus serotype 10 segment 3 and its predicted VP3 polypeptide compared with those of BTV serotype 17. *Virus Res* **3**(2), 181-190.

Goeddel, D. V. (1991). Systems for heterologous gene expression. *Meth Enzymol* **185**, 3-7.

Gold, L. (1991). Expression in *Escherichia coli. Meth Enzymol* **185**, 11-14.

Gonzalez, H. A., and Knudson, D. L. (1988). Intra- and inter-serogroup genetic relatedness of orbiviruses. I. Blot hybridization of viruses of Australian serogroups. *J Gen Virol* **69**(1), 125-134.

Gorman, B. M., Taylor, J., Brown, K and Meltzer, A.J. (1977). Laboratory studies of arboviruses. Structure and genetics of orbiviruses. *Annu. Rep. Qld Inst Med Res* **32**, 15.

Gorman, B. M. (1978). Susceptibility of orbiviruses to low pH and to organic solvents. *Aust J Exp Biol Med Sci* **56**, 359.

Gorman, B. M., Taylor, J., Walker, P.J. and Young, P.R. (1978). The isolation of recombinants between related orbiviruses. *J Gen Virol* **41**, 333.

Gorman, B. M. (1979). Variation in Orbiviruses. *J Gen Virol* **44**, 1-15.

Gorman, B. M., Taylor, J., Walker, P. J., Davidson, W. L., and Brown, F. (1981). Comparison of bluetongue type 20 with certain viruses of the bluetongue and Eubenangee serological groups of orbiviruses. *J Gen Virol* **57**(2), 251-261.

Gorman, B. M. (1983). On the evolution of Orbiviruses. *Intervirology* **20**, 169-180.

Gorman, B. M. (1985). Molecular structure of bluetongue and related orbiviruses. *Prog Clin Biol Res* **178,** 329-336.

Gorman, B. M. (1985). Speciation in orbiviruses. *Prog Clin Biol Res* **178,** 275-278.

Gorman, B. M. and Taylor, J. (1985). Orbiviruses. In: *Virology,* (Eds) B.N. Fields et al., 275-278. Raven Press, New York.

Gorman, B. M. (1990). The bluetongue viruses. In: *Current Topics in Microbiology and Immunology*, **162**. Springer-Verlag, Berlin.

Gorman, B. M. (1992). An overview of orbiviruses. In: *Bluetongue, African horsesickness and related orbiviruses.* Proceedings of the second international symposium. T.E. Walton and B.I. Osburn (Eds), 335-348. CRC Press, London.

Gouet, P., Diprose, J. M., Grimes, J. M., Malby, R., Burroughs, J. N., Zientara, S., Stuart, D. I., and Mertens, P. P. (1999). The highly ordered double-stranded RNA genome of bluetongue virus revealed by crystallography. *Cell* **97**(4), 481-490.

Gould, A. R. (1988). Conserved and non-conserved regions of the outer coat protein, VP2, of the Australian bluetongue serotype 1 virus, revealed by sequence comparison to the VP2 of North American BTV serotype 10. *Virus Res* **9**(2-3), 145-158.

Gould, A. R., and Eaton, B. T. (1990). The amino acid sequence of the outer coat protein VP2 of neutralizing monoclonal antibody-resistant, virulent and attenuated bluetongue viruses. *Virus Res* **17**(3), 161-172.

Gould, A. R., and Pritchard, L. I. (1988). The complete nucleotide sequence of the outer coat protein, VP5, of the Australian bluetongue virus (BTV) serotype 1 reveals conserved and non- conserved sequences. *Virus Res* **9**(4), 285-292.

Gould, A. R., Hyatt, A. D., and Eaton, B. T. (1988). Morphogenesis of a bluetongue virus variant with an amino acid alteration at a neutralization site in the outer coat protein, VP2. *Virology* **165**(1), 23-32.

Gould, A. R., Martyn, J. C., and Stevenson, L. (1994). Expression of the non-structural protein NS1 of bluetongue virus in bacteria and yeast: identification of two antigenic sites at the amino terminus. *Virus Res* **31**(3), 291-303.

Gould, A. R., Pritchard, L. I., and Tavaria, M. D. (1988). Nucleotide and deduced amino acid sequences of the non-structural protein, NS1, of Australian and South African bluetongue virus serotype 1. *Virus Res* **11**(2), 97-107.

Grimes, J. M., Burroughs, J. N., Gouet, P., Diprose, J. M., Malby, R., Zientara, S., Mertens, P. P., and Stuart, D. I. (1998). The atomic structure of the bluetongue virus core. *Nature* **395**(6701), 470-478.

Grimes, J. M., Jakana, J., Ghosh, M., Basak, A. K., Roy, P., Chiu, W., Stuart, D. I., and Prasad, B. V. (1997). An atomic model of the outer layer of the bluetongue virus core derived from X-ray crystallography and electron cryomicroscopy. *Structure* **5**(7), 885-893.

Grimes, J., Basak, A. K., Roy, P., and Stuart, D. (1995). The crystal structure of bluetongue virus VP7. *Nature* **373**(6510), 167-170.

Grubman, M. J. (1990). Expression of bluetongue virus serotype 17 NS1 protein from a cloned

gene. *Virus Res* **18**(1), 21-8.

Grubman, M. J., and Lewis, S. A. (1992). Identification and characterization of the structural and nonstructural proteins of African horsesickness virus and determination of the genome coding assignments. *Virology* **186**(2), 444-51.

Grubman, M. J., and Samal, S. (1989). Nucleotide and deduced amino acid sequence of the nonstructural protein, NS1, of the US bluetongue virus serotype 17. *Nucleic Acids Res* **17**(24), 10498.

Grubman, M. J., Appleton, J. A., and Letchworth, G. J. d. (1983). Identification of bluetongue virus type 17 genome segments coding for polypeptides associated with virus neutralization and intergroup reactivity. *Virology* **131**(2), 355-366.

Hall, S. J., Van Dijk, A. A., and Huismans, H. (1989). Complete nucleotide sequence of gene segment 8 encoding non-structural protein NS2 of SA bluetongue virus serotype 10. *Nucleic Acids Res* **17**(1), 457.

Hanahan, D. (1983). Studies on transformation of *Escherichia coli* with plasmids. *J Mol Biol* **166**, 557-580.

Hanahan, D., Jessee, J. and Bloom, F.R. (1991). Plasmid transformation of *Escherichia coli* and other bacteria. *Meth Enzymol* **204**, 63-113.

Hatton, M. and Sakaki, Y. (1986). Dideoxy sequencing method using denatured plasmid templates. *Anal Biochem* **152**, 232-238.

Hayama, E., and Li, J. K. (1994). Mapping and characterization of antigenic epitopes and the nucleic acid- binding domains of the VP6 protein of bluetongue viruses. *J Virol* **68**(6), 3604-3611.

Hewat, E. A., Booth, T. F., and Roy, P. (1992). Structure of bluetongue virus particles by cryoelectron microscopy. *J Struct Biol* **109**(1), 61-69.

Hewat, E. A., Booth, T. F., and Roy, P. (1994). Structure of correctly self-assembled bluetongue virus-like particles. *J Struct Biol* **112**(3), 183-191.

Hewat, E. A., Booth, T. F., Loudon, P. T., and Roy, P. (1992). Three-dimensional reconstruction of baculovirus expressed bluetongue virus core-like particles by cryo-electron microscopy. *Virology* **189**(1), 10-20.

Hewat, E. A., Booth, T. F., Wade, R. H., and Roy, P. (1992). 3-D reconstruction of bluetongue virus tubules using cryoelectron microscopy. *J Struct Biol* **108**(1), 35-48.

Higgins, D. G., Thompson, J. D., and Gibson, T. J. (1996). Using CLUSTAL for multiple sequence alignments. *Methods Enzymol* **266**, 383-402.

Higgins, D. G., Bleasby, A.J. and Fuchs, R. (1992). CLUSTAL V: improved software for multiple sequence alignments. *CABIOS* **8**, 189-191.

Higgins, D.G. and Sharp, P.M. (1988). CLUSTAL - a package for performing multiple sequence alignments on a microcomputer. *Gene* **73**, 237-244.

Higuchi, R., Krummel, B., and Saiki, R. K. (1988). A general method of in vitro preparation and specific mutagenesis of DNA fragments: study of protein and DNA interactions. *Nucleic Acids Res* **16**(15), 7351-7367.

Holmes, I. H. (1991). Family *Reoviridae*. In *Classification and Nomenclature of Viruses. Arch Virol* (Supplementum **2)**, 188-189.

Holmes, I. H., Boccardo, G., Estes, M.K., Furuichi, M.K., Hoshino, Y., Yoklik, W.K., McCrae, M., Mertens, P.P.C., Milne, R.G., Samal, K.S.K., Shiata, E., Winton, J.R. and Uyeda, I. (1995). Family *Reoviridae.* In: Murphy, F. A., Fauquet, C.M., Bishop, D.H.L., Ghabrial, S.A., Jarvis, A.W., Martelli, G.P., Mayo, M.A., Summers, M.D. (eds). Virus Taxonomy. Classification and Nomenclature of Viruses. Sixth report of the international committee on Taxonomy of Viruses. Springer, Wien New York. *Arch Virol* [Supplementum **10**], 208-237.

Hopp, T. P., and Woods, K. R. (1981). Prediction of protein antigenic determinants from amino acid sequences. *Proc Natl Acad Sci U S A* **78**(6), 3824-3828.

Hopp, T. P., and Woods, K. R. (1983). A computer program for predicting protein antigenic determinants. *Mol Immunol* **20**(4), 483-489.

House, J. A. and House, C. (1989). Immunization studies on African horsesickness. *Proceedings of the USAHA Ninety-third Meeting*, 356-365.

House, C., House, J. A., and Mebus, C. A. (1992). A review of African horse sickness with emphasis on selected vaccines. *Ann N Y Acad Sci* **653,** 228-232.

House, J. A., Lombard, M., House, C., Dubourger, P. and Mebus, C. A. (1992). Efficacy of an inactivated vaccine for African horsesickness virus serotype 4 In: *Bluetongue, African horsesickness and related orbiviruses.* Proceedings of the second international symposium. T.E. Walton and B.I. Osburn (Eds), 335-248. CRC Press, London.

House, J. A. (1993). African horse sickness. *Vet Clin North Am Equine Pract* **9**(2), 355-364.

House, J. A. (1993). Recommendations for African horse sickness vaccines for use in nonendemic areas. *Rev Elev Med Vet Pays Trop* **46**(1-2), 77-81.

House, J. A., Lombard, M., Dubourget, P., House, C., and Mebus, C. A. (1994). Further studies on the efficacy of an inactivated African horse sickness serotype 4 vaccine. *Vaccine* **12**(2), 142-4.

House, J. A. (1998). Future international management of African horse sickness vaccines. *Arch Virol Suppl* **14,** 297-304.

Howell, P. G. (1962). The isolation and identification of further antigenic types of African horsesickness virus. Onderstepoort *J. Vet. Res.* **29**, 139-149.

Howell, P. G. (1963). African horsesickness. In: *Emerging diseases of Animals.* 73-108. Rome: Food and Agricultural organisation.

Huang, I. J., Hayama, E., Jeong, Y. J., and Li, J. K. (1993). Conservation of the segment 4 gene sequence and of a leucine zipper motif in VP4 among five US bluetongue viruses. *Virology* **195**(2), 772-9.

Huang, I. J., Hwang, G. Y., Yang, Y. Y., Hayama, E., and Li, J. K. (1995). Sequence analyses and antigenic epitope mapping of the putative RNA-directed RNA polymerase of five U.S. bluetongue viruses. *Virology* **214**(1), 280-8.

Huismans, H. (1970). Macromolecular synthesis in bluetongue virus infected cells. I. Virus- specific ribonucleic acid synthesis. *Onderstepoort J Vet Res* **37**(4), 191-7.

Huismans, H., and Verwoerd, D. W. (1973). Control of transcription during the expression of the bluetongue virus genome. *Virology* **52**(1), 81-8.

Huismans, H. (1979). Protein synthesis in bluetongue virus-infected cells. *Virology* **92**(2), 385-96.

Huismans, H., and Els, H. J. (1979). Characterization of the tubules associated with the replication of three different orbiviruses. *Virology* **92**(2), 397-406.

Huismans, H., Bremer, C. W., and Barber, T. L. (1979). The nucleic acid and proteins of epizootic haemorrhagic disease virus. *Onderstepoort J Vet Res* **46**(2), 95-104.

Huismans, H., and Erasmus, B. J. (1981). Identification of the serotype-specific and group-specific antigens of bluetongue virus. *Onderstepoort J Vet Res* **48**(2), 51-8.

Huismans, H., van der Walt, N. T., Cloete, M., and Erasmus, B. J. (1983). The biochemical and immunological characterization of bluetongue virus outer capsid polypeptides. In: Compans, R.W., Bishop, D.H.L (eds). Double-stranded RNA viruses. Elsevier , New York.

Huismans, H., and Cloete, M. (1987). A comparison of different cloned bluetongue virus genome segments as probes for the detection of virus-specified RNA. *Virology* **158**(2), 373-80.

Huismans, H., Cloete, M., and le Roux, A. (1987). The genetic relatedness of a number of individual cognate genes of viruses in the bluetongue and closely related serogroups. *Virology* **161**(2), 421-8.

Huismans, H., van der Walt, N. T., Cloete, M., and Erasmus, B. J. (1987). Isolation of a capsid protein of bluetongue virus that induces a protective immune response in sheep. *Virology* **157**(1), 172-9.

Huismans, H., van Dijk, A. A., and Bauskin, A. R. (1987). In vitro phosphorylation and purification of a nonstructural protein of bluetongue virus with affinity for single-stranded RNA. *J Virol* **61**(11), 3589-95.

Huismans, H., van Dijk, A. A., and Els, H. J. (1987). Uncoating of parental bluetongue virus to core and subcore particles in infected L cells. *Virology* **157**(1), 180-8.

Huismans, H., and Van Dijk, A. A. (1990). Bluetongue virus structural components. *Curr Top Microbiol Immunol* **162**, 21-41.

Huismans, H., Van Staden, V. and Nel, L. (1992). Molecular comparison of the cognate genes of Bluetongue, Afrivan horsesickness and Epizootic haemorrhagic disease viruses which encode nonstructural proteins NS2 and NS3. In: *Bluetongue, African horsesickness and related orbiviruses.* Proceedings of the second international symposium. T.E. Walton and B.I. Osburn (Eds), 358-365. CRC Press, London.

Hyatt, A. D., and Eaton, B. T. (1988). Ultrastructural distribution of the major capsid proteins within bluetongue virus and infected cells. *J Gen Virol* **69**(4), 805-15.

Hyatt, A. D., Brookes, S. M., Gould, A. R., and Eaton, B. T. (1992). Morphogenesisof bluetongue viruse: development of a model for the site of virus synthesis, translocation and release from infected tissue culture cells. In: *Bluetongue, African horsesickness and related orbiviruses.* Proceedings of the second international symposium. T.E. Walton and B.I. Osburn (Eds), 358-365. CRC Press, London.

Hyatt, A. D., Eaton, B. T., and Brookes, S. M. (1989). The release of bluetongue virus from infected

cells and their superinfection by progeny virus. *Virology* **173**(1), 21-34.

Hyatt, A. D., Gould, A. R., Coupar, B., and Eaton, B. T. (1991). Localization of the non-structural protein NS3 in bluetongue virus- infected cells. *J Gen Virol* **72**(9), 2263-7.

Hyatt, A. D., Zhao, Y., and Roy, P. (1993). Release of bluetongue virus-like particles from insect cells is mediated by BTV nonstructural protein NS3/NS3A. *Virology* **193**(2), 592-603.

Inumaru, S., and Roy, P. (1987). Production and characterization of the neutralization antigen VP2 of bluetongue virus serotype 10 using a baculovirus expression vector. *Virology* **157**(2), 472-9.

Inumaru, S., Ghiasi, H., and Roy, P. (1987). Expression of bluetongue virus group-specific antigen VP3 in insect cells by a baculovirus vector: its use for the detection of bluetongue virus antibodies. *J Gen Virol* **68**(6), 1627-35.

Iwata, H., Chuma, T., and Roy, P. (1992). Characterization of the genes encoding two of the major capsid proteins of epizootic haemorrhagic disease virus indicates a close genetic relationship to bluetongue virus. *J Gen Virol* **73**(4), 915-24.

Iwata, H., Hirasawa, T., and Roy, P. (1991). Complete nucleotide sequence of segment 5 of epizootic haemorrhagic disease virus; the outer capsid protein VP5 is homologous to the VP5 protein of bluetongue virus. *Virus Res* **20**(3), 273-81.

Iwata, H., Yamagawa, M. and Roy, P. (1992). Evolutionary relationships among the gnat-transmitted orbiviruses that cause African horse sickness, bluetongue, and epizootic hemorrhagic disease as evidenced by their capsid protein sequences. *Virology* **191**(1), 251-61.

Izard, J., Parker, M.W., Chartier, M., Duche, D. and Baty, D. (1994) A single amino acid substitution can resolve solubility of aggregated colicin A mutants in Escherisia coli. *Prot Eng.* **7**, 1495-1500.

Johnson, J. E., and Speir, J. A. (1997). Quasi-equivalent viruses: a paradigm for protein assemblies. *J Mol Biol* **269**(5), 665-75.

Kahlon, J., Sugiyama, K., and Roy, P. (1983). Molecular basis of bluetongue virus neutralization. *J Virol* **48**(3), 627-32.

Katz, J.B., Henderson, L.M., Erickson, G.A. 1990. Recombination in vivo of pseudorabies vaccine strains to produce new virus strains. *Vaccine* **8**, 286-288.

Kelly, D.C. (1982). Baculovirus replication. *J Gen Virol* **63**, 1-13.

Kimura, T. and Murakami, T. (1977). Tubular structures associated with acute nonbacterial gastro-enteritis in young children. *Infect Immun* **17**, 157-160.

King, L. A. and Posse, R. D. (1992). In: The baculovirus expression system: a laboratory guide. 1-229 London, Chapman and Hall.

Kit, S., Kit, M., Di Marchi, R.D., Little, S.P. and Gale, C. 1991. Modified-live infectious bovine rhinotracheitis virus vaccine expressing monomer and dimer forms of foot-and-mouth disease capsid protein epitopes on surface of hybrid virus particles. *Arch Virol* **120**, 1-7.

Kitts, P. A., and Possee, R. D. (1993). A method for producing recombinant baculovirus expression vectors at high frequency. *Biotechniques* **14**(5), 810-7.

Kitts, P. A., Ayres, M. D., and Possee, R. D. (1990). Linearization of baculovirus DNA enhances the recovery of recombinant virus expression vectors. *Nucleic Acids Res* **18**(19), 5667-72.

Knudson, D. L. and Monath, T. P. (1990). Orbiviruses. In: *Virology* **2**(2). B.N. Fields and D.M Knipe (Eds), 1405-1433. Raven Press, New York.

Knudson, D. L. and Shope, R. E. (1985). Overview of the orbiviruses. In*: Progress in Clinical and Biological Research.* **178***: Bluetongue and related orbiviruses.* T.L. Barber and M.M. Jochim (Eds). 255-266. Alan R Liss, New York.

Knudson, D. L., Tesh, R.B., Main, A.J., St George, T.D. and Digoutte, J.P. (1984). Characterization of the Palyam serogroup viruses (reoviridae: Orbivirus). *Intervirology* **22**, 41-49.

Kowalik, T. F., and Li, J. K. (1989). Sequence analyses and structural predictions of double-stranded RNA segment S1 and VP7 from United States prototype bluetongue virus serotypes 13 and 10. *Virology* **172**(1), 189-95.

Kowalik, T. F., and Li, J. K. (1991). Bluetongue virus evolution: sequence analyses of the genomic S1 segments and major core protein VP7. *Virology* **181**(2), 749-55.

Kowalik, T. F., Li, J. K., Chuang, R. Y., Doi, R. H., and Osburn, B. I. (1990). The complete nucleotide and deduced amino acid sequence of the gene encoding the major inner capsid protein, VP7 of US bluetongue virus serotype 17. *Nucleic Acids Res* **18**(17), 5302.

Kowalik, T. F., Yang, Y. Y., and Li, J. K. (1990). Molecular cloning and comparative sequence analyses of bluetongue virus S1 segments by selective synthesis of specific full-length DNA copies of dsRNA genes. *Virology* **177**(2), 820-3.

Kozak, 1981, M. (1981). Possible role of flanking nucleotides in recognition of the AUG initiation codon by eukaryotic ribosomes. *Nucleic Acid Res.* **9**, 5233-5252.

Kozak, M. (1987). An analysis of 5'-noncoding sequences from 699 vertebrate messenger RNAs. *Nucleic Acids Research* **15**, 8125-8148.

Kraft, R., Tardiff, J., Krauter, K. S. and Leinwand, L. A. (1986). Using mini-prep plasmid DNA for sequencing double-stranded templates with Sequenase. *BioTechniques* **6**, 544-547.

Kusari, J. and Roy, P. (1986). Molecular and genetic comparisons of two serotypes of epizootic heamorrhagic disease of deer virus. *Am J Vet Res* **47**, 1713-17.

Kyte, J., and Doolittle, R. F. (1982). A simple method for displaying the hydropathic character of a protein. *J Mol Biol* **157**(1), 105-32.

Laegreid, W. W. (1996). African horse sickness. In: Horzinek, M.C. (ed). Virus infections of vertebrates, vol 6: Studdert, M.J. (ed). Virus infections of equines. Elsevier, New York, pp101-123.

Laegreid, W. W., Skowronek, A., Stone-Marschat, M. and Burrage, T. (1993). Characterzation of virulence variants of African horsesickness virus. *Virology* **195**, 836-839.

Laegreid, W. W., Burrage, T. G., Stone-Marschat, M., and Skowronek, A. (1992). Electron microscopic evidence for endothelial infection by African horsesickness virus. *Vet Pathol*

29(6), 554-6.

Laemmli, U. K. (1970). Cleavage of structural proteins during the assembly of the head of bacteriophage T4. *Nature* **227**(259), 680-5.

Laviada, M. D., Arias, M., and Sanchez-Vizcaino, J. M. (1993). Characterization of African horsesickness virus serotype 4-induced polypeptides in Vero cells and their reactivity in Western immunoblotting. *J Gen Virol* **74**(1), 81-7.

Le Blois, H., and Roy, P. (1993). A single point mutation in the VP7 major core protein of bluetongue virus prevents the formation of core-like particles. *J Virol* **67**(1), 353-9.

Le Blois, H., Fayard, B., Urakawa, T., and Roy, P. (1991). Synthesis and characterization of chimeric particles between epizootic haemorrhagic disease virus and bluetongue virus: functional domains are conserved on the VP3 protein. *J Virol* **65**(9), 4821-31.

Le Blois, H., French, T., Mertens, P. P., Burroughs, J. N., and Roy, P. (1992). The expressed VP4 protein of bluetongue virus binds GTP and is the candidate guanylyl transferase of the virus. *Virology* **189**(2), 757-61.

Lecatsas, G. (1968). Electron microscopic study of the formation of bluetongue virus. *Onderstepoort J Vet Res* **35**(1), 139-49.

Lecatsas, G., and Gorman, B. M. (1972). Visualization of the extracapsid coat in certain bluetongue-type viruses. *Onderstepoort J Vet Res* **39**(4), 193-6.

Lee, J. W., and Roy, P. (1986). Nucleotide sequence of a cDNA clone of RNA segment 10 of bluetongue virus (serotype 10). *J Gen Virol* **67**(12), 2833-7.

Lee, J., and Roy, P. (1987). Complete sequence of the NS1 gene (M6 RNA) of US bluetongue virus serotype 10. *Nucleic Acids Res* **15**(17), 7207.

Leusch, M. S., Lee, S. C., and Olins, P. O. (1995). A novel host-vector system for direct selection of recombinant baculoviruses (bacmids) in Escherichia coli. *Gene* **160**(2), 191-4.

Levinson, A. D. (1991). Expression in mammalian cells. *Meth Enzymol* **185**, 485-487.

Lewis, S. A., and Grubman, M. J. (1990). Bluetongue virus: surface exposure of VP7. *Virus Res* **16**(1), 17-26.

Liddington, R. C., Yan, Y., Moulai, J., Sahli, R., Benjamin, T. L., and Harrison, S. C. (1991). Structure of simian virus 40 at 3.8-A resolution. *Nature* **354**(6351), 278-84.

Liljas, L. (1996). Viruses. *Curr Opin Struct Biol* **6**(2), 151-6.

Liu, H. M., Booth, T. F., and Roy, P. (1992). Interactions between bluetongue virus core and capsid proteins translated in vitro. *J Gen Virol* **73**(10), 2577-84.

Loudon, P. T., and Roy, P. (1991). Assembly of five bluetongue virus proteins expressed by recombinant baculoviruses: inclusion of the largest protein VP1 in the core and virus-like proteins. *Virology* **180**(2), 798-802.

Loudon, P. T., and Roy, P. (1992). Interaction of nucleic acids with core-like and subcore-like particles of bluetongue virus. *Virology* **191**(1), 231-6.

Loudon, P. T., Hirasawa, T., Oldfield, S., Murphy, M., and Roy, P. (1991). Expression of the outer

capsid protein VP5 of two bluetongue viruses, and synthesis of chimeric double-shelled virus-like particles using combinations of recombinant baculoviruses. *Virology* **182**(2), 793-801.

Lubroth, J. (1988). African horse sickness and the epizootics in Spain. *Equine Prac* **10**, 26-33.

Lubroth, J. (1992). The complete epidemiological cycle of African horsesickness: our incomplete knowledge. In: Walton, T.E and Osburn B.I. (eds). Bluetongue, African horsesickness and related orbiviruses. CRC Press, Baco Raton, pp 982-989.

Luckow, V. A. and Summers, M. D. (1988). Trends in the development of baculovirus expression vectors. *BioTechnology* **6**, 47-55.

Luckow, V. A., Lee, S. C., Barry, G. F. and Olins, P. O. (1993). Efficient generation of infectious recombinant baculoviruses by site-specific transposon mediated insertion of foreign genes into a baculovirus genome propagated in Escherichia coli. *J Virol* **67**, 4566-4579.

Luckow, V.A. (1991). Cloning and expression of heterologous genes in insect cells with baculovirus vectors. In: *Recombinant DNA Tecnology and Application*, pp 97-152. Prokop, A., Bajpai, K. and Ho, C. (Eds), New York, McGraw Hill.

Maeda, S. (1989). Expression of foreign genes in insects using baculovirus vectors. *Annu Rev Entomol* **34,** 351-72.

Maree, F. F., and Huismans, H. (1997). Characterization of tubular structures composed of nonstructural protein NS1 of African horsesickness virus expressed in insect cells. *J Gen Virol* **78**(5), 1077-82.

Maree, S., Durbach, S., and Huismans, H. (1998). Intracellular production of African horsesickness virus core-like particles by expression of the two major core proteins, VP3 and VP7, in insect cells. *J Gen Virol* **79**(2), 333-7.

Maree, S., Durbach, S., Maree, F. F., Vreede, F., and Huismans, H. (1998). Expression of the major core structural proteins VP3 and VP7 of African horse sickness virus, and production of core-like particles. *Arch Virol Suppl* **14,** 203-9.

Marshall, J. J., and Roy, P. (1990). High level expression of the two outer capsid proteins of bluetongue virus serotype 10: their relationship with the neutralization of virus infection. *Virus Res* **15**(3), 189-95.

Marshall, J. J., Fayard, B., and Roy, P. (1990). Biophysical studies on the morphology of baculovirus-expressed bluetongue virus tubules. *J Gen Virol* **71**(8), 1839-44.

Martin, S. A., and Zweerink, H. J. (1972). Isolation and characterization of two types of bluetongue virus particles. *Virology* **50**(2), 495-506.

Martin, S. A., Pett, D. M., and Zweerink, H. J. (1973). Studies on the topography of reovirus and bluetongue virus capsid proteins. *J Virol* **12**(1), 194-8.

Martinez-Torrecuadrada, J. L., and Casal, J. I. (1995). Identification of a linear neutralization domain in the protein VP2 of African horse sickness virus. *Virology* **210**(2), 391-9.

Martinez-Torrecuadrada, J. L., Diaz-Laviada, M., Roy, P., Sanchez, C., Vela, C., Sanchez-Vizcaino, J. M., and Casal, J. I. (1996). Full protection against African horsesickness (AHS) in horses induced by baculovirus-derived AHS virus serotype 4 VP2, VP5 and VP7. *J Gen Virol* **77**(6), 1211-21.

Martinez-Torrecuadrada, J. L., Iwata, H., Venteo, A., Casal, I., and Roy, P. (1994). Expression and characterization of the two outer capsid proteins of African horsesickness virus: the role of VP2 in virus neutralization. *Virology* **202**(1), 348-59.

Martyn, J. C., Gould, A. R., and Eaton, B. T. (1991). High level expression of the major core protein VP7 and the non- structural protein NS3 of bluetongue virus in yeast: use of expressed VP7 as a diagnostic, group-reactive antigen in a blocking ELISA. *Virus Res* **18**(2-3), 165-78.

Martyn, J. C., Gould, A. R., and Yu, M. (1994). Expression of the outer capsid proteins VP2 and VP5 of bluetongue virus in Saccharomyces cerevisiae. *Virus Res* **33**(1), 11-25.

Matsuura, Y., Possee, R. D., Overton, H. A. and Bishop, D. H. L. (1987). Baculovirus expression vectors: the requirements for high level expression of proteins, including glycoproteins. *J Gen Virol* **68**, 1233-1250.

Matthews, R.E.F. (1982). Classification and nomenclature of viruses. Fourth report of the International Committee on Taxonomy of viruses. *Intervirology* **17**, 1-200.

McIntosh, B. M. (1958). Immunological types of horsesickness virus and their significance in immunization. *Onderstepoort J Vet Res* **27**, 465-538.

Mecham, J. O., and Dean, V. C., (1988). Protein coding assignment for the genome of epizootic haemorrhagic disease virus. *J Gen Virol* **69**(12), 1259-1262.

Mecham, J. O., and Jochim, M. M. (1990). Monoclonal antibodies to bluetongue virus define two neutralizing epitopes and a hemagglutinating epitope. *Viral Immunol* **3**(2), 161-70.

Mecham, J. O., Dean, V. C., and Jochim, M. M. (1986). Correlation of serotype specificity and protein structure of the five U.S. serotypes of bluetongue virus. *J Gen Virol* **67**(12), 2617-24.

Mellor, P. S. (1993). African horsesickness: transmission and epidemiology. *Vet Res.* **24**, 199-212.

Mellor, P. S. (1994). Epizootiology and vectors of African horsesickness virus. *Comparative Immunology, Microbiology and Infectious diseases* **17**, 287-296.

Mellor, P. S. and Boorman, J. (1995). The transmission and geographical spread of African horse sickness and bluetongue viruses. *Annals of Tropical Medicine and Parasitology*, **89**, 1-15.

Mertens, P. P. and Sangar, D. V. (1985). Analysis of the terminal sequences of the genome segments of four orbiviruses. *Virology* **140**(1), 55-67.

Mertens, P. P., Brown, F., and Sangar, D. V. (1984). Assignment of the genome segments of bluetongue virus type 1 to the proteins which they encode. *Virology* **135**(1), 207-17.

Mertens, P. P., Burroughs, J. N., and Anderson, J. (1987). Purification and properties of virus particles, infectious subviral particles, and cores of bluetongue virus serotypes 1 and 4. *Virology* **157**(2), 375-86.

Mertens, P. P., Burroughs, J. N., Walton, A., Wellby, M. P., Fu, H., O'Hara, R. S., Brookes, S. M., and Mellor, P. S. (1996). Enhanced infectivity of modified bluetongue virus particles for two insect cell lines and for two Culicoides vector species. *Virology* **217**(2), 582-93.

Mertens, P. P., Pedley, S., Cowley, J., and Burroughs, J. N. (1987). A comparison of six different bluetongue virus isolates by cross- hybridization of the dsRNA genome segments. *Virology*

161(2), 438-47.

Mertens, P. P., Pedley, S., Cowley, J., Burroughs, J. N., Corteyn, A. H., Jeggo, M. H., Jennings, D. M., and Gorman, B. M. (1989). Analysis of the roles of bluetongue virus outer capsid proteins VP2 and VP5 in determination of virus serotype. *Virology* **170**(2), 561-5.

Mikhailov, M., Monastyrskaya, K., Bakker, T., and Roy, P. (1996). A new form of particulate single and multiple immunogen delivery system based on recombinant bluetongue virus-derived tubules. *Virology* **217**(1), 323-31.

Miller, L. K. (1988). Baculoviruses as gene expression vectors. *Annu Rev Microbiol* **42**, 177-99.

Miller, L. K. (1988). Baculoviruses for foreign gene expression in insect cells. *Biotechnology* **10**, 457-65.

Miller, L. K. (1989). Insect baculoviruses: powerful gene expression vectors. *Bioessays* **11**(4), 91-5.

Miller, L. K. (1993). Baculoviruses: high-level expression in insect cells. *Curr Opin Genet Dev* **3**(1), 97-101.

Mizukoshi, N., Sakamoto, K., Iwata, A., Tsuchiya, T., Ueda, S., Apiwatnakorn, B., Kamada, M., and Fukusho, A. (1993). The complete nucleotide sequence of African horsesickness virus serotype 4 (vaccine strain) segment 4, which encodes the minor core protein VP4. *Virus Res* **28**(3), 299-306.

Mizukoshi, N., Sakamoto, K., Iwata, A., Tsuchiya, T., Ueda, S., Watanabe, T., Kamada, M., and Fukusho, A. (1992). The complete sequence of African horsesickness virus serotype 4 (vaccine strain) RNA segment 5 and its predicted polypeptide compared with NS1 of bluetongue virus. *J Gen Virol* **73**(9), 2425-8.

Monastyrskaya, K., Booth, T., Nel, L., and Roy, P. (1994). Mutation of either of two cysteine residues or deletion of the amino or carboxy terminus of nonstructural protein NS1 of bluetongue virus abrogates virus-specified tubule formation in insect cells. *J Virol* **68**(4), 2169-78.

Monastyrskaya, K., Gould, E. A., and Roy, P. (1995). Characterization and modification of the carboxy-terminal sequences of bluetongue virus type 10 NS1 protein in relation to tubule formation and location of an antigenic epitope in the vicinity of the carboxy terminus of the protein. *J Virol* **69**(5), 2831-41.

Monastyrskaya, K., Staeuber, N., Sutton, G., and Roy, P. (1997). Effects of domain-switching and site-directed mutagenesis on the properties and functions of the VP7 proteins of two orbiviruses. *Virology* **237**(2), 217-27.

Morris, T. D. and Miller, L. K. (1992). Promoter influence on baculovirus-mediated gene expression in permissive and nonpermissive insect cell lines. *J Virol* **66**, 7397-7405.

Moss, S. R., Fukusho, A., and Nuttall, P. A. (1990). RNA segment 5 of broadhaven virus, a tick-borne orbivirus, shows sequence homology with segrnent 5 of bluetongue virus. *Virology* **179**(1), 482-4.

Moss, S. R., Jones, L. D., and Nuttall, P. A. (1992). Comparison of the major structural core proteins of tick-borne and Culicoides-borne orbiviruses. *J Gen Virol* **73**(10), 2585-90.

Moss, S. R., Jones, L. D., and Nuttall, P. A. (1992). Comparison of the nonstructural protein, NS3,

of tick-borne and insect- borne orbiviruses. *Virology* **187**(2), 841-4.

Moss, S. R., and Nuttall, P. A. (1994). Subcore- and core-like particles of Broadhaven virus (BRDV), a tick- borne orbivirus, synthesized from baculovirus expressed VP2 and VP7, the major core proteins of BRDV. *Virus Res* **32**(3), 401-7.

Moss, S. R., and Nuttall, P. A. (1995). Comparison of the non-structural protein, NS1, of tick-borne and insect- borne orbiviruses. *Virus Res* **36**(2-3), 287-92.

Moyer, S., Baker, S. and Lessard, J. (1986). Tubuli: a factor necessary for the synthesis of both Sendai virus and vesicular stomatitis virus RNAs. *Proc Natl Acad Sci USA* **83**, 5405-5409.

Murphy, C., Bikel, I. and Livingston, D. (1986). Cellular proteins which can specifically associate with Simian virus SV40 small t antigen. *J Virol* **59**, 692-702.

Murphy, F. A., Borden, E. C., Shope, R. E., and Harrison, A. (1971). Physicochemical and morphological relationships of some arthropod-borne viruses to bluetongue virus--a new taxonomic group. Electron microscopic studies. *J Gen Virol* **13**(2), 273-88.

Murphy, F.A., Fauquet, C.M., Bishop, D.H.L., Ghabrial, S.A., Farvis, A.W., Martelli, G.P., Mayo, M.A. and Summers, M.D. (1995). Virus Taxonomy: The Classification and Nomenclature of Viruses. The Sixth Report of the International Committee on Taxonomy of Viruses. Springer-Verlag, Wien.

Nel, L. H., and Huismans, H. (1990). A chomparison of different cloned genome segments of epizootic haemorrhagic disease virus as serogroup-specific probes. *Arch. Virol* **110**, 103-112.

Nel, L. H., and Huismans, H. (1991). Synthesis of the virus-specified tubules of epizootic haemorrhagic disease virus using a baculovirus expression system. *Virus Res* **19**(2-3), 139-52.

Nel, L. H., Picard, L. A., and Huismans, H. (1990). A characterization of the nonstructural protein from which the virus-specified tubules in epizootic haemorrhagic disease virus-infected cells are composed. *Virus Res* **18**(2-3), 219-30.

Nel, L. H., Picard, L. A., Roy, P. and Huismans, H. (1992). Studies on the nucleic acid sequence and expression of African horsesickness virus and Epizootic haemorrhagic diease virus NS1 encoding genes. In: *Bluetongue, African horsesickness and related orbiviruses.* Proceedings of the second international symposium. T.E. Walton and B.I. Osburn (Eds), 335-248. CRC Press, London.

Oberst, R. D., Stott, J. L., Blanchard-Channell, M., and Osburn, B. I. (1987). Genetic reassortment of bluetongue virus serotype 11 strains in the bovine. *Vet Microbiol* **15**(1-2), 11-8.

Oellerman, R. A. (1970). Plaque formation by African horsesickness virus and characterization of its RNA. *Onderstepoort J vet Res* **37**, 137-144.

Oellermann, R. A., Els, H. J., and Erasmus, B. J. (1970). Characterization of African horsesickness virus. *Arch Gesamte Virusforsch* **29**(2), 163-74.

O'Hara, R. S., Burroughs, J. N., and Mertens, P. P. C. (1993). A generalized genome coding assignment for the African horsesickness serogroup, genus Orbivirus. *Ninth International Congress of Virology*, Glasgow, Scotland.

Oldfield, S., Adachi, A., Urakawa, T., Hirasawa, T., and Roy, P. (1990). Purification and

characterization of the major group-specific core antigen VP7 of bluetongue virus synthesized by a recombinant baculovirus. *J Gen Virol* **71**(11), 2649-56.

Oldfield, S., Hirasawa, T., and Roy, P. (1991). Sequence conservation of the outer capsid protein, VP5, of bluetongue virus, a contrasting feature to the outer capsid protein VP2. *J Gen Virol* **72**(2), 449-51.

O'Reilly, D. R., Miller, L. K. and Luckow, V. A. (1992). An overview of baculoviruses, choosing a transfer plasmid and parent virus, methods for vector construction and gene expression. In: Baculo expression vectors: a laboratory manual. (Eds) D. R. O'Reilly, L. K. Miller and V. A. Luckow. New York, W.H. Freemanand Company. 1-36.

Paeratakul, U, De Stasio, P.R., Taylor, M.M. 1988. A fast and sensitive method for detecting specific viral RNA in mammalian cells. *J Virol* **62**, 1132-1135.

Pearson, L. D., and Roy, P. (1993). Genetically engineered multi-component virus-like particles as veterinary vaccines. *Immunol Cell Biol* **71**(5), 381-9.

Pedley, S., Mohamed, M. E., and Mertens, P. P. (1988). Analysis of genome segments from six different isolates of bluetongue virus using RNA-RNA hybridisation: a generalised coding assignment for bluetongue viruses. *Virus Res* **10**(4), 381-90.

Pelham, H.R.B. and Jackson, R.J. (1976). An efficient mRNA-dependent translation system from reticulocyte lysates. *Eur J Biochem* **56**, 829-852.

Possee, R. D. and Howard, S. C. (1987). Analysis of the polyhedrin gene promoter of the *Autographa californica* nuclear polyhedrosis virus. *Nucleic Acids Res.* **15**, 10233-48.

Prasad, B. V., Yamaguchi, S., and Roy, P. (1992). Three-dimensional structure of single-shelled bluetongue virus. *J Virol* **66**(4), 2135-42.

Prasad, B.V., Rothnagel, R., Zeng, C.Q.Y., Jakana, J., Lawton, J.A., Chiu, W. and Estes, M.K. (1996). Visualisation of ordered genomic RNA and localisation of transcriptional complexes in rotavirus. *Nature* **382**, 471-473.

Purdy, M., Petre, J., and Roy, P. (1984). Cloning of the bluetongue virus L3 gene. *J Virol* **51**(3), 754-9.

Purdy, M. A., Ghiasi, H., Rao, C. D., and Roy, P. (1985). Complete sequence of bluetongue virus L2 RNA that codes for the antigen recognized by neutralizing antibodies. *J Virol* **55**(3), 826-30.

Purdy, M. A., Ritter, G. D., and Roy, P. (1986). Nucleotide sequence of cDNA clones encoding the outer capsid protein, VP5, of bluetongue virus serotype 10. *J Gen Virol* **67**(5), 957-62.

Ramadevi, N., and Roy, P. (1998). Bluetongue virus core protein VP4 has nucleoside triphosphate phosphohydrolase activity. *J Gen Virol* **79**(10), 2475-80.

Ramadevi, N., Burroughs, N. J., Mertens, P. P., Jones, I. M., and Roy, P. (1998). Capping and methylation of mRNA by purified recombinant VP4 protein of bluetongue virus. *Proc Natl Acad Sci USA* **95**(23), 13537-42.

Ramadevi, N., Rodriguez, J., and Roy, P. (1998). A leucine zipper-like domain is essential for dimerization and encapsidation of bluetongue virus nucleocapsid protein VP4. *J Virol* **72**(4), 2983-90.

Ranz, A.I., Miguet, J.G., Anaya, C., Venteo, A., Cortes, E., Vela, C. and SanZ, A. (1992). Diagnostic methods for African horsesickness virus using monoclonal antibodies to structural and non-structural proteins. *Vet Microbiol* **33**, 243-273.

Rao, C. D., Kiuchi, A., and Roy, P. (1983). Homologous terminal sequences of the genome double-stranded RNAs of bluetongue virus. *J Virol* **46**(2), 378-83.

Richards, R. G., MacLachlan, N. J., Heidner, H. W., and Fuller, F. J. (1988). Comparison of virologic and serologic responses of lambs and calves infected with bluetongue virus serotype 10. *Vet Microbiol* **18**(3-4), 233-42.

Rigby, P. W., Dieckmann, M., Rhodes, C., and Berg, P. (1977). Labeling deoxyribonucleic acid to high specific activity in vitro by nick translation with DNA polymerase I. *J Mol Biol* **113**(1), 237-51.

Riley, D. E. (1989). Very rapid nucleotide sequence analysis of improved double-stranded minipreps. *Gene* **75**, 193-196.

Ritter, D. G., and Roy, P. (1988). Genetic relationships of bluetongue virus serotypes isolated from different parts of the world. *Virus Res* **11**(1), 33-47.

Roy, P. (1989). Bluetongue virus genetics and genome structure. *Virus Res* **13**(3), 179-206.

Roy, P. (1990). Use of baculovirus expression vectors: development of diagnostic reagents, vaccines and morphological counterparts of bluetongue virus. *FEMS Microbiol Immunol* **2**(4), 223-34.

Roy, P. (1991). Towards the control of emerging bluetongue disease. Oxford Virology Publications, London, 71pp.

Roy, P. (1992). Bluetongue virus proteins. *J Gen Virol* **73**(12), 3051-64.

Roy, P. (1992). From genes to complex structures of bluetongue virus and their efficacy as vaccines. *Vet Microbiol* **33**(1-4), 155-68.

Roy, P. (1993). Dissecting the assembly of orbiviruses. *Trends Microbiol* **1**(8), 299-305.

Roy, P. (1996). Genetically engineered particulate virus-like structures and their use as vaccine delivery systems. *Intervirology* **39**(1-2), 62-71.

Roy, P. (1996). Multiple gene expression in baculovirus system. Third generation vaccines for bluetongue disease and African horsesickness disease. *Ann N Y Acad Sci* **791**, 318-32.

Roy, P. (1996). Orbivirus structure and assembly [published erratum appears in Virology 1996 Apr 1;218(1):296]. *Virology* **216**(1), 1-11.

Roy, P., Adachi, A., Urakawa, T., Booth, T. F., and Thomas, C. P. (1990). Identification of bluetongue virus VP6 protein as a nucleic acid- binding protein and the localization of VP6 in virus-infected vertebrate cells. *J Virol* **64**(1), 1-8.

Roy, P., and Sutton, G. (1998). New generation of African horse sickness virus vaccines based on structural and molecular studies of the virus particles. *Arch Virol Suppl* **14**, 177-202.

Roy, P., Bishop, D. H., Howard, S., Aitchison, H., and Erasmus, B. (1996). Recombinant baculovirus-synthesized African horsesickness virus (AHSV) outer-capsid protein VP2 provides protection against virulent AHSV challenge. *J Gen Virol* **77**(9), 2053-7.

Roy, P., Bishop, D. H., LeBlois, H., and Erasmus, B. J. (1994). Long-lasting protection of sheep against bluetongue challenge after vaccination with virus-like particles: evidence for homologous and partial heterologous protection. *Vaccine* **12**(9), 805-11.

Roy, P., French, T., and Erasmus, B. J. (1992). Protective efficacy of virus-like particles for bluetongue disease. *Vaccine* **10**(1), 28-32.

Roy, P., Fukusho, A., Ritter, G. D., and Lyon, D. (1988). Evidence for genetic relationship between RNA and DNA viruses from the sequence homology of a putative polymerase gene of bluetongue virus with that of vaccinia virus: conservation of RNA polymerase genes from diverse species. *Nucleic Acids Res* **16**(24), 11759-67.

Roy, P., Hirasawa, T., Fernandez, M., Blinov, V. M., and Sanchez-Vixcain Rodrique, J. M. (1991). The complete sequence of the group-specific antigen, VP7, of African horsesickness disease virus serotype 4 reveals a close relationship to bluetongue virus. *J Gen Virol* **72**(6), 1237-41.

Roy, P., Marshall, J. J., and French, T. J. (1990). Structure of the bluetongue virus genome and its encoded proteins. *Curr Top Microbiol Immunol* **162**, 43-87.

Roy, P., Mertens, P. P., and Casal, I. (1994). African horse sickness virus structure. *Comp Immunol Microbiol Infect Dis* **17**(3-4), 243-73.

Roy, P., Mikhailov, M., and Bishop, D. H. (1997). Baculovirus multigene expression vectors and their use for understanding the assembly process of architecturally complex virus particles. *Gene* **190**(1), 119-29.

Roy, P., Urakawa, T., Van Dijk, A. A., and Erasmus, B. J. (1990). Recombinant virus vaccine for bluetongue disease in sheep. *J Virol* **64**(5), 1998-2003.

Saiki, R.K., Gelfand, D.H., Stoffel, S., Scharf, S.J., Higuchi, R., Horn, G.T., Mullis, K.B. and Erlich, H.A. (1988). Primer directed enzymatic amplification of DNA with a thermostable DNA polymerase. *Science* **2**, 487-491.

Sali, A. and Blundell, T.L. (1993). Comparative protein modelling by satisfaction of spatial restraints.
J Mol Biol **234**(3), 779-815.

Samal, S. K., el-Hussein, A., Holbrook, F. R., Beaty, B. J., and Ramig, R. F. (1987). Mixed infection of Culicoides variipennis with bluetongue virus serotypes 10 and 17: evidence for high frequency reassortment in the vector. *J Gen Virol* **68**(9), 2319-29.

Samal, S. K., Livingston, C. W., Jr., McConnell, S., and Ramig, R. F. (1987). Analysis of mixed infection of sheep with bluetongue virus serotypes 10 and 17: evidence for genetic reassortment in the vertebrate host. *J Virol* **61**(4), 1086-91.

Sambrook, J., Fritch, E.F. and Maniatis, T. (1989). Molecular cloning: a laboratory manual. Second edition. Cold Spring Harbor laboratory Press.

Sanger, F., Nicklen, S. and Coulson, A. R. (1977). DNA sequencing with chain-terminating inhibitors. *Proc Natl Acad Sci USA* **74** (12), 5463-5467.

Schnagl, R.D and Holmes, I.H. (1975). Polyacrylamide gel electrophoresis of the genomes of two orbiviruses: D'Aguilar and Eubenangee. *Intervirology* **5**, 300.

Spence, R. P., Moore, N. F., and Nuttall, P. A. (1984). The biochemistry of orbiviruses. Brief review.

Arch Virol **82**(1-2), 1-18.

Stanley, N.F (1967). Reoviruses. *Br. Med. Bull.* **23**, 50.

Stauber, N., Martinez-Costas, J., Sutton, G., Monastyrskaya, K., and Roy, P. (1997). Bluetongue virus VP6 protein binds ATP and exhibits an RNA-dependent ATPase function and a helicase activity that catalyze the unwinding of double-stranded RNA substrates. *J Virol* **71**(10), 7220-6.

Steockle, M.Y., Shaw, M.W., and Choppin, P.W. (1987). Segment-specific and common nucleotide sequences in the noncoding region of influenza B virus genome RNA. *Proc Natl Acad Sci USA* **84**, 2703-2707.

Stone-Marschat, M. A., Moss, S. R., Burrage, T. G., Barber, M. L., Roy, P., and Laegreid, W. W. (1996). Immunization with VP2 is sufficient for protection against lethal challenge with African horsesickness virus Type 4. *Virology* **220**(1), 219-22.

Stott, J. L., Barber, T. L., and Osburn, B. I. (1985). Immunologic response of sheep to inactivated and virulent bluetongue virus. *Am J Vet Res* **46**(5), 1043-9.

Stott, J. L., Oberst, R. D., Channell, M. B., and Osburn, B. I. (1987). Genome segment reassortment between two serotypes of bluetongue virus in a natural host. *J Virol* **61**(9), 2670-4.

Stuart, D. I., Gouet, P., Grimes, J., Malby, R., Diprose, J., Zientara, S., Burroughs, J. N., and Mertens, P. P. (1998). Structural studies of orbivirus particles. *Arch Virol Suppl* **14**, 235-50.

Summers, M.D. and Smith, G.E. (1987). A manual of methods for Baculovirus vectors and insect cell culture procedures. *Texan Agricultural Experiment Station Bulletin* No. **1555**. Texas Agricultural Experiment Station, College Station, Tex.

Swanepoel, R., Erasmus, B. J., Williams, R., and Taylor, M. B. (1992). Encephalitis and chorioretinitis associated with neurotropic African horsesickness virus infection in laboratory workers. Part III. Virological and serological investigations. *S Afr Med J* **81**, 458-461.

Tabor, S. and Richardson, C. C. (1987). DNA sequence analysis with a modified bacteriophage T7 DNA polymerase. *Proc Natl Acad Sci USA* **84**, 4076-4080.

Tanaka, S., Mikhailov, M., and Roy, P. (1995). Synthesis of bluetongue virus chimeric VP3 molecules and their interactions with VP7 protein to assemble into virus core-like particles. *Virology* **214**(2), 593-601.

Tanaka, S., and Roy, P. (1994). Identification of domains in bluetongue virus VP3 molecules essential for the assembly of virus cores. *J Virol* **68**(5), 2795-802.

Taylor, M.B., van der Meyden, C.H., Erasmus, B.J., Reid, R., Labuschagne, J.H., Dreyer, L. and Prozesky, O.W. (1992). Enchephalitis and chorioretinitis associated with neurotropic African horsesickness virus infection in laboratory workers. Part IV. Experimental infection of the vervet monkey. *S Afr Med J* **81**, 462-467.

Theiler, A. 1921. African horsesickness. *Science Bulletin* **19**, Department of Agriculture. S.A. Pretoria.

Theron, J., and Nel, L. H. (1997). Stable protein-RNA interaction involves the terminal domains of bluetongue virus mRNA, but not the terminally conserved sequences. *Virology* **229**(1), 134-42.

Theron, J., Huismans, H., and Nel, L. H. (1996). Identification of a short domain within the non-structural protein NS2 of epizootic haemorrhagic disease virus that is important for single strand RNA-binding activity. *J Gen Virol* **77**(1), 129-37.

Theron, J., Huismans, H., and Nel, L. H. (1996). Site-specific mutations in the NS2 protein of epizootic haemorrhagic disease virus markedly affect the formation of cytoplasmic inclusion bodies. *Arch Virol* **141**(6), 1143-51.

Theron, J., Uitenweerde, J. M., Huismans, H., and Nel, L. H. (1994). Comparison of the expression and phosphorylation of the non-structural protein NS2 of three different orbiviruses: evidence for the involvement of an ubiquitous cellular kinase. *J Gen Virol* **75**(12), 3401-11.

Thomas, C. P., Booth, T. F., and Roy, P. (1990). Synthesis of bluetongue virus-encoded phosphoprotein and formation of inclusion bodies by recombinant baculovirus in insect cells: it binds the single-stranded RNA species. *J Gen Virol* **71**(9), 2073-83.

Thompson, J. D., Higgins, D. G., and Gibson, T. J. (1994). CLUSTAL W: improving the sensitivity of progressive multiple sequence alignment through sequence weighting, position-specific gap penalties and weight matrix choice. *Nucleic Acids Res* **22**(22), 4673-80.

Tomori, O., Baba, S., Adu, F. and Adeniji, J. (1992). An overview and perspective on orbivirus disease prevalence and occurrence of vectors in Africa. In: Bluetongue, African horse sickness and related orbiviruses. Proceedings of the 2nd international symposium. T.E. Walton and B.I. Osburn (eds), CRC Press, London, pp 23-33.

Turnbull, P. J., Cormack, S. B., and Huismans, H. (1996). Characterization of the gene encoding core protein VP6 of two African horsesickness virus serotypes. *J Gen Virol* **77**(7), 1421-3.

Uitenweerde, J. M., Theron, J., Stoltz, M. A., and Huismans, H. (1995). The multimeric nonstructural NS2 proteins of bluetongue virus, African horsesickness virus, and epizootic hemorrhagic disease virus differ in their single-stranded RNA-binding ability. *Virology* **209**(2), 624-32.

Urakawa, T., and Roy, P. (1988). Bluetongue virus tubules made in insect cells by recombinant baculoviruses: expression of the NS1 gene of bluetongue virus serotype 10. *J Virol* **62**(11), 3919-27.

Urakawa, T., French, T. J., Adachi, Y., Fukusho, A., LeBlois, H., Flamand, M., Mertens, P., and Roy, P. (1994). Synthesis of recombinant baculoviruses expressing the outer capsid protein VP2 of five BTV serotypes and the induction of neutralizing antibodies to homologous and heterologous BTV serotypes [published errata appear in Virus Res 1994 Oct;34(1):93 and 1994 Nov;34(2):187]. *Virus Res* **31**(2), 149-61.

Urakawa, T., Ritter, D. G., and Roy, P. (1989). Expression of largest RNA segment and synthesis of VP1 protein of bluetongue virus in insect cells by recombinant baculovirus: association of VP1 protein with RNA polymerase activity. *Nucleic Acids Res* **17**(18), 7395-401.

Van Dijk, A. A. (1993). Development of recombinant vaccines against bluetongue. *Biotech Adv* **11**, 1-12.

Van Dijk, A. A., and Huismans, H. (1980). The in vitro activation and further characterization of the bluetongue virus-associated transcriptase. *Virology* **104**(2), 347-56.

Van Dijk, A. A., and Huismans, H. (1982). The effect of temperature on the in vitro transcriptase reaction of bluetongue virus, epizootic haemorrhagic disease virus and African

horsesickness virus. *Onderstepoort J Vet Res* **49**(4), 227-32.

Van Dijk, A. A., and Huismans, H. (1987). The identification of factors capable of reversing the core-mediated inhibition of the bluetongue virus transcriptase. *Onderstepoort J Vet Res* **54**(4), 629-33.

Van Dijk, A. A., and Huismans, H. (1988). In vitro transcription and translation of bluetongue virus mRNA. *J Gen Virol* **69**(3), 573-81.

Van Drunen Little van den Hurk, S., Parker, M.D., Massie, B., Van den Hurk, J.V., Harland, R., Babiuk, L.A. and Zamb, T.J. 1993. Protection of cattle from BHV-1 infection by immunization with recombinant glycoprotein gIV. *Vaccine* **11**, 25-35.

Van Staden, V., and Huismans, H. (1991). A comparison of the genes which encode non-structural protein NS3 of different orbiviruses. *J Gen Virol* **72**(5), 1073-9.

Van Staden, V., Smit, C. C., Stoltz, M. A., Maree, F. F., and Huismans, H. (1998). Characterization of two African horse sickness virus nonstructural proteins, NS1 and NS3. *Arch Virol Suppl* **14**, 251-8.

Van Staden, V., Stoltz, M. A., and Huismans, H. (1995). Expression of nonstructural protein NS3 of African horsesickness virus (AHSV): evidence for a cytotoxic effect of NS3 in insect cells, and characterization of the gene products in AHSV infected Vero cells. *Arch Virol* **140**(2), 289-306.

Van Staden, V., Theron, J., Greyling, B. J., Huismans, H., and Nel, L. H. (1991). A comparison of the nucleotide sequences of cognate NS2 genes of three different orbiviruses. *Virology* **185**(1), 500-4.

Van Wyngaard, W., Du Plessis, D. H., Van Wyngaard, S. and Verschoor, J. A. (1992). Production and properties of monoclonal antibodies against African horsesickness virus, serotype 3. *Onderstepoort J Vet Res* **59**,129-133.

Venter, E. H., Huismans, H., and Van Dijk, A. A. (1995). Detection of bluetongue virus and African horsesickness virus in co- infected cell cultures with NS1 gene probes. *Onderstepoort J Vet Res* **62**(4), 217-22.

Venter, E. H., van der Lugt, J. J., and Gerdes, G. H. (1993). Detection of bluetongue virus RNA in cell cultures and in the central nervous system of experimentally infected mice using in situ hybridization. *Onderstepoort J Vet Res* **60**(1), 39-45.

Venter, E. H., Viljoen, G. J., Nel, L. H., Huismans, H., and van Dijk, A. A. (1991). A comparison of different genomic probes in the detection of virus- specified RNA in Orbivirus-infected cells. *J Virol Methods* **32**(2-3), 171-80.

Venter, M., Napier, G. and Huismans, H. (1999). Cloning, sequencing and expression of the gene that encodes the major neutralisation specific antigen of African horsesickness virus serotype 9. *J Virol Methods*.

Verwoerd, D. W. (1969). Purification and characterisation of bluetongue virus. *Virology* **38**, 203-212.

Verwoerd, D. W., and Huismans, H. (1969). On the relationship between bluetongue, African horsesickness and reoviruses: hybridization studies. *Onderstepoort J Vet Res* **36**(2), 175-9.

Verwoerd, D. W., and Huismans, H. (1972). Studies on the in vitro and the in vivo transcription of

the bluetongue virus genome. *Onderstepoort J Vet Res* **39**(4), 185-91.

Verwoerd, D. W., Els, H. J., De Villiers, E. M., and Huismans, H. (1972). Structure of the bluetongue virus capsid. *J Virol* **10**(4), 783-94.

Verwoerd, D. W., Huismans, H and Erasmus, B. J. (1979). Orbiviruses. In: Comprehensive Virology **14**, H. Fraenkel-Conrat and R.R Wagner (Eds) 285-345. Plenum Press, New York.

Verwoerd, D. W., Louw, H. and Oellerman, R. A. (1970). Characterization of bluetongue virus ribonucleic acid. *J Virol* **5**, 1-7.

Viljoen, G. J. and Huismans H. (1989). The characterzation of equine encepholosis virus and the development of genomic probes. *J Gen Virol* **70**, 2007-2015.

Vreede, F. T., and Huismans, H. (1994). Cloning, characterization and expression of the gene that encodes the major neutralization-specific antigen of African horsesickness virus serotype 3. *J Gen Virol* **75**(12), 3629-33.

Vreede, F. T., and Huismans, H. (1998). Sequence analysis of the RNA polymerase gene of African horse sickness virus. *Arch Virol* **143**(2), 413-9.

Wade-Evans, A. M. (1990). The complete nucleotide sequence of genome segment 7 of bluetongue virus, serotype 1 from South Africa. *Nucleic Acids Res* **18**(16), 4919.

Wade-Evans, A. M., and Mertens, P. P. (1990). Expression of the outer capsid protein, VP2, from a full length cDNA clone of genome segment 2 of bluetongue serotype 1 from South Africa, using both Sp6 and vaccinia expression systems and a comparison of the nucleic acid sequence of this segment with those of other serotypes. *Virus Res* **15**(3), 213-29.

Wade-Evans, A. M., Mertens, P. P., and Belsham, G. J. (1992). Sequence of genome segment 9 of bluetongue virus (serotype 1, South Africa) and expression analysis demonstrating that different forms of VP6 are derived from initiation of protein synthesis at two distinct sites. *J Gen Virol* **73**(11), 3023-6.

Wade-Evans, A. M., Pan, Z. Q., and Mertens, P. P. (1988). Sequence analysis and in vitro expression of a cDNA clone of genome segment 5 from bluetongue virus, serotype 1 from South Africa. *Virus Res* **11**(3), 227-40.

Wade-Evans, A. M., Pullen, L., Hamblin, C., O'Hara, R. S., Burroughs, J. N., and Mertens, P. P. (1998). VP7 from African horse sickness virus serotype 9 protects mice against a lethal, heterologous serotype challenge. *Arch Virol Suppl* **14**, 211-9.

Wade-Evans, A. M., Pullen, L., Hamblin, C., O'Hara, R., Burroughs, J. N., and Mertens, P. P. (1997). African horsesickness virus VP7 sub-unit vaccine protects mice against a lethal, heterologous serotype challenge. *J Gen Virol* **78**(7), 1611-6.

Wade-Evans, A. M., Romero, C. H., Mellor, P., Takamatsu, H., Anderson, J., Thevasagayam, J., Fleming, M. J., Mertens, P. P., and Black, D. N. (1996). Expression of the major core structural protein (VP7) of bluetongue virus, by a recombinant capripox virus, provides partial protection of sheep against a virulent heterotypic bluetongue virus challenge. *Virology* **220**(1), 227-31.

Wade-Evans, A. M., Woolhouse, T., O'Hara, R., and Hamblin, C. (1993). The use of African horse sickness virus VP7 antigen, synthesised in bacteria, and anti-VP7 monoclonal antibodies in a competitive ELISA. *J Virol Methods* **45**(2), 179-88.

Wang, L. F., Doi, R. H., Chuang, L. F., Osburn, B. I., Maisonnave, J., Benjamini, E., and Chuang, R. Y. (1989). Bluetongue virus-17 fusion protein ns1 expressed in Escherichia coli by pUC vectors. *Biochem Biophys Res Commun* **162**(2), 892-9.

Wang, L. F., Doi, R. H., Osburn, B. I., and Chuang, R. Y. (1989). Complete sequence of the NS1 gene (S6 RNA) of US bluetongue virus serotype 17. *Nucleic Acids Res* **17**(19), 8002.

Wang, L. F., Hyatt, A. D., Whiteley, P. L., Andrew, M., Li, J. K., and Eaton, B. T. (1996). Topography and immunogenicity of bluetongue virus VP7 epitopes. *Arch Virol* **141**(1), 111-23.

Welling, G. W., Weijer, W. J., van der Zee, R., and Welling-Wester, S. (1985). Prediction of sequential antigenic regions in proteins. *FEBS Lett* **188**(2), 215-8.

Whistler, T., and Swanepoel, R. (1988). Characterization of potentially foetotropic Palyam serogroup orbiviruses isolated in Zimbabwe. *J Gen Virol* **69**, 2221-27.

Whistler, T., and Swanepoel, R. (1990). Proteins of Palyam serogroup orbiviruses isolated in Zimbabwe. *J Gen Virol* **69**, 2221-7.

White, J. R., and Eaton, B. T. (1990). Conformation of the VP2 protein of bluetongue virus (BTV) determines the involvement in virus neutralization of highly conserved epitopes within the BTV serogroup. *J Gen Virol* **71**(6), 1325-32.

Wilson, I.A., Skehel, J.J. and Willey, D.C. (1981). *Nature* **289**, 366-373.

Wilson, W. C. (1990). Development and optimization of a hybridization assay for epizootic hemorrhagic disease viruses. *J Virol Methods* **30**(2), 173-81.

Wilson, W. C., Fukusho, A., and Roy, P. (1990). Diagnostic complementary DNA probes for genome segments 2 and 3 of epizootic hemorrhagic disease virus serotype 1. *Am J Vet Res* **51**(6), 855-60.

Wu, X., Chen, S. Y., Iwata, H., Compans, R. W., and Roy, P. (1992). Multiple glycoproteins synthesized by the smallest RNA segment (S10) of bluetongue virus. *J Virol* **66**(12), 7104-12.

Xu, G., Wilson, W., Mecham, J., Murphy, K., Zhou, E. M., and Tabachnick, W. (1997). VP7: an attachment protein of bluetongue virus for cellular receptors in Culicoides variipennis. *J Gen Virol* **78**(7), 1617-23.

Yancey, R.J., 1993. Recent advances in bovine vaccine technology. *J Dairy Sc* **76**, 2418-2436.

Yu, Y., Fukusho, A., Ritter, D. G., and Roy, P. (1988). Complete nucleotide sequence of the group-reactive antigen VP7 gene of bluetongue virus. *Nucleic Acids Res* **16**(4), 1620.

Yu, Y. D., Fukusho, A., and Roy, P. (1987). Nucleotide sequence of the VP4 core protein gene (M4 RNA) of US bluetongue virus serotype 10. *Nucleic Acids Res* **15**(17), 7206.

Zao, G.P. and Sommerville, R.L. (1992). Genetic and biochemical characterization of the trpB8 mutation of Escherichia coli thryptophane synthase: An amino acid switch at the sharp turn of the trpsin-sensitive hinge region diminishes binding and alters solubility. *J Biol Chem* **267**, 526-541.

Zuidema, D., Schouten, A., Usmany, M., Maule, A. J., Belsham, G. J., Roosien, J., Klinge-Roode,

E. C., van Lent, J. W., and Vlak, J. M. (1990). Expressio ı of cauliflower mosaic virus gene I in insect cells using a novel polyhedrin-based baculovi us expression vector. *J Gen Virol* **71**(10), 2201-9.